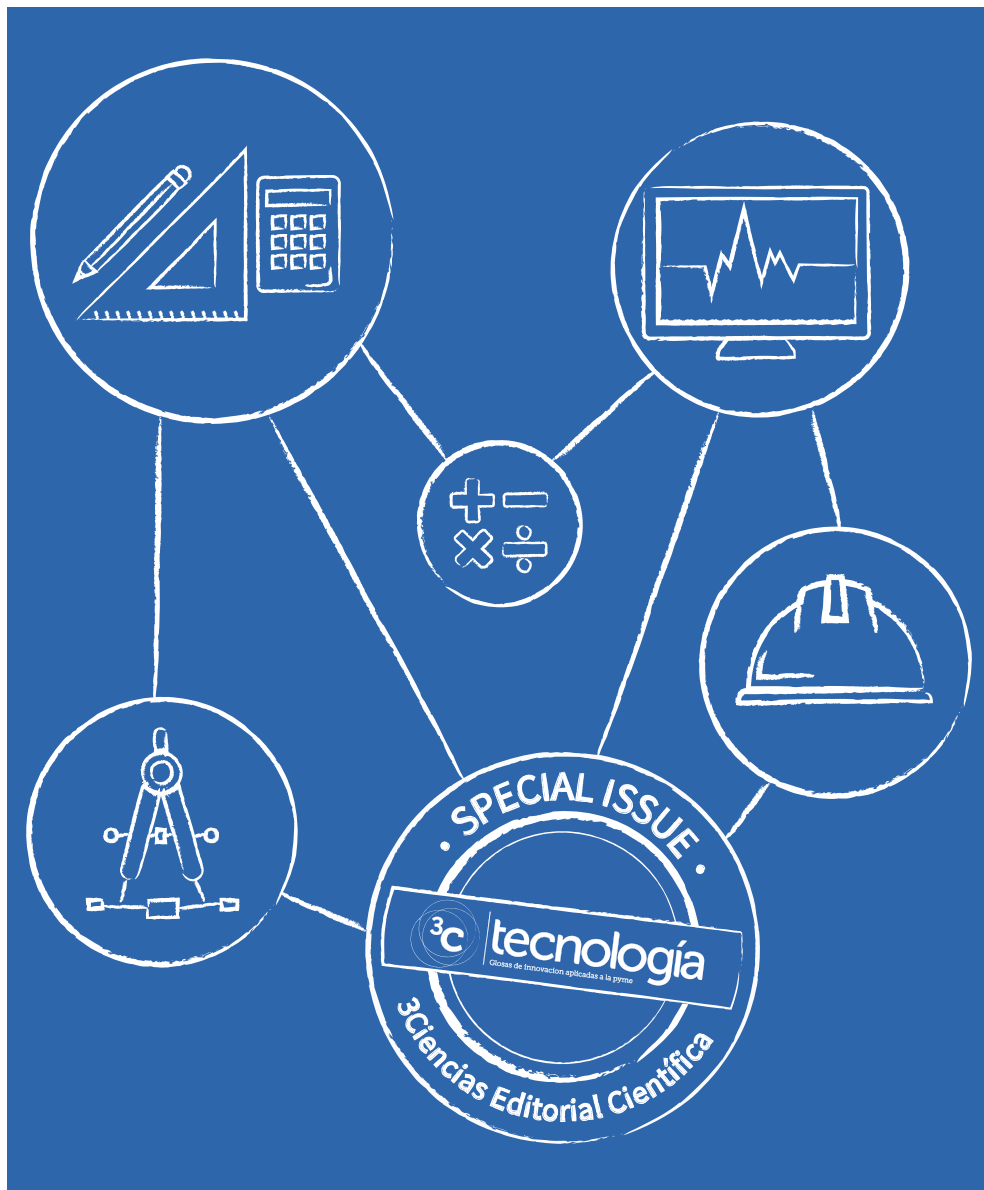"RECENT TRENDS IN COMPUTER SCIENCE AND ENGINEERING (RTCSE)"
FACULTY OF INFORMATION TECHNOLOGY, UNIVERSITAS YARSI, JAKARTA, INDONESIA.

"Recent Trends in Computer Science and Engineering (RTCSE)"

Faculty of Information Technology, Universitas YARSI, Jakarta, Indonesia.

Glosas de innovacion aplicadas a la pyme

CONSEJO EDITORIAL EDITORIAL BOARD

POLÍTICA EDITORIAL

OBJETIVO EDITORIAL

La Editorial científica 3Ciencias pretende transmitir a la sociedad ideas y proyectos innovadores, plasmados, o bien en artículos originales sometidos a revisión por expertos, o bien en los libros publicados con la más alta calidad científica y técnica.

COBERTURA TEMÁTICA

3C Tecnología es una revista de carácter científico-social en la que se difunden trabajos originales que abarcan la Arquitectura y los diferentes campos de la Ingeniería, como puede ser Ingeniería Mecánica, Industrial, Informática, Eléctrica, Agronómica, Naval, Física, Química, Civil, Electrónica, Forestal, Aeronáutica y de las Telecomunicaciones.

NUESTRO PÚBLICO

- Personal investigador.
- Doctorandos.
- Profesores de universidad.
- Oficinas de transferencia de resultados de investigación (OTRI).
- Empresas que desarrollan labor investigadora y quieran publicar alguno de sus estudios.

AIMS AND SCOPE

PUBLISHING GOAL

3Ciencias wants to transmit to society innovative projects and ideas. This goal is reached thought the publication of original articles which are subdue to peer review or thorough the publication of scientific books.

TEMATIC COVERAGE

3C Tecnología is a scientific-social journal in which original works that cover Architecture and the different fields of Engineering are disseminated, such as Mechanical, Industrial, Computer, Electrical, Agronomic, Naval, Physics, Chemistry, Civil, Electronics, Forestry, Aeronautics and Telecommunications.

OUR TARGET

- Research staff.
- PhD students.
- Professors.
- Research Results Transfer Office.
- Companies that develop research and want to publish some of their works.

NORMAS DE PUBLICACIÓN

3C Tecnología es una revista arbitrada que utiliza el sistema de revisión por pares de doble ciego (*double-blind peer review*), donde expertos externos en la materia sobre la que trata un trabajo lo evalúan, siempre manteniendo el anonimato, tanto de los autores como de los revisores. La revista sigue las normas de publicación de la APA (American Psychological Association) para su indización en las principales bases de datos internacionales.

Cada número de la revista se edita en versión electrónica (e-ISSN: 2254 – 4143), identificándose cada trabajo con su respectivo código DOI (Digital Object Identifier System).

PRESENTACIÓN TRABAJOS

Los artículos se presentarán en tipo de letra Baskerville, cuerpo 11, justificados y sin tabuladores. Han de tener formato Word. La extensión será de no más de 6.000 palabras de texto, incluidas referencias.

Los trabajos deben ser enviados exclusivamente por plataforma de gestión de manuscritos OJS:

https://ojs.3ciencias.com/

Toda la información, así como las plantillas a las que deben ceñirse los trabajos se encuentran en:

https://www.3ciencias.com/normas-de-publicacion/

SUBMISSION GUIDELINES

3C Tecnología is an arbitrated journal that uses the double-blind peer review system, where external experts in the field on which a paper deals evaluate it, always maintaining the anonymity of both the authors and of the reviewers. The journal follows the standards of publication of the APA (American Psychological Association) for indexing in the main international databases.

Each issue of the journal is published in electronic version (e-ISSN: 2254 − 4143), each work being identified with its respective DOI (Digital Object Identifier System) code.

PRESENTATION WORK

The papers will be presented in Baskerville typeface, body 11, justified and without tabs. They must have Word format. The extension will be no more than 6.000 words of text, including references. Papers must be submitted exclusively by OJS manuscript management platform:

https://ojs.3ciencias.com/

All the information, as well as the templates to which the works must adhere, can be found at:

https://www.3ciencias.com/normas-de-publicacion/

ESTRUCTURA

Los trabajos originales tenderán a respetar la siguiente estructura: introducción, métodos, resultados, discusión/conclusiones, notas, agradecimientos y referencias bibliográficas.

Es obligatoria la inclusión de referencias, mientras que notas y agradecimientos son opcionales. Se valorará la correcta citación conforme a la 7.ª edición de las normas APA.

RESPONSABILIDADES ÉTICAS

No se acepta material previamente publicado (deben ser trabajos inéditos). En la lista de autores firmantes deben figurar única y exclusivamente aquellas personas que hayan contribuido intelectualmente (autoría). No se aceptan artículos que no cumplan estrictamente las normas.

INFORMACIÓN ESTADÍSTICA SOBRE TASAS DE ACEPTACIÓN E INTERNACIONALIZACIÓN

- Número de trabajos aceptados publicados: 17.
- Nivel de aceptación de manuscritos en este número: 85%.
- Nivel de rechazo de manuscritos: 15%.
- Internacionalización de autores: 8 países (Rusia, Estados Unidos, Iraq, Pakistán, Perú, Arabia Saudita, Sudáfrica, Reino Unido).

Normas de publicación: https://www.3ciencias.com/normas-de-publicacion/instrucciones/

STRUCTURE

The original works will tend to respect the following structure: introduction, methods, results, discussion/conclusions, notes, acknowledgments and bibliographical references. The inclusion of references is mandatory, while notes and acknowledgments are optional. The correct citation will be assessed according to the 7th edition of the APA standards.

ETHICAL RESPONSIBILITIES

Previously published material is not accepted (they must be unpublished works). The list of signatory authors should include only and exclusively those who have contributed intellectually (authorship). Articles that do not strictly comply with the standards are not accepted.

STATISTICAL INFORMATION ON ACCEPTANCE AND INTERNATIONALIZATION FEES

- Number of accepted papers published: 17.
- Level of acceptance of manuscripts in this number: 85%.
- Level of rejection of manuscripts: 15%.
- Internationalization of authors: 8 countries (Russia, United States, Iraq, Pakistan, Perú, Saudi Arabia, South Africa, United Kingdom).

Guidelines for authors: https://www.3ciencias.com/en/regulations/instructions/

INDEXACIONES INDEXATIONS

INDEXACIONES INDEXATIONS

/SUMARIO/
/SUMMARY/

/PRÓLOGO/
/PROLOGUE/

RECENT TRENDS IN COMPUTER SCIENCE AND ENGINEERING (RTCSE)

Jason Levy

University of Hawaii, (USA).

E-mail: jlevy@hawaii.edu ORCID: https://orcid.org/0000-0002-9978-5412

Bishwajeet Pandey

Gyancity Research Consultancy, (India).

E-mail: gyancity@gyancity.com ORCID: https://orcid.org/0000-0001-5593-8985

Bhawani Shankar Chowdhry

Mehran University of Engineering and Technology (MUET), (Pakistan).

E-mail: bhawani.chowdhry@faculty.muet.edu.pk ORCID: https://orcid.org/0000-0002-4340-9602

Ciro Rodriguez

Universidad Nacional Mayor de San Marcos, (Perú).

E-mail: crodriguezro@unmsm.edu.pe ORCID: https://orcid.org/0000-0003-2112-1349

This set of distinguished seventeen papers strengthens interdisciplinary linkages between the fields of engineering decision making, emerging computer science technologies and pandemic planning. Rather than separating the engineering and computer science technologies from their 'real world' impact, those contributing to this special issue have demonstrated attention to the engineering decision making issues that their work informs. Accordingly, this special issue helps engineering and computer science academics and practitioners to better understand the complex relationships related to intertwined and complex topics ranging from engineering reliability, environmental risk and health crises. In summary, this distinguished, cross-disciplinary, valuable, timely and international collection of seventeen papers examines the most challenging societal-technologic dilemmas facing society in light of the recent black swan events facing society. The papers have a special emphasis on crafting comprehensive, sustainable and intelligent solutions to effectively transform technologic challenges with the power of Recent Trends in Computer Science and Engineering (RTCSE). It should be noted that these papers constitute a sample of the leading papers published in recent Gyancity conferences.

In the first paper Ezzy *et al.* (2020) discuss a solution to the problem of warehouse automation for transferring goods. To meet the demands of large scale material movement in warehouses, an automated system is proposed in lieu of a manual workforce to automate the warehouse picking process using an Automated Guided Vehicle (AGV). The system is designed such that the robot can operate on a known 'map' laid out on the warehouse floor. The system proposed is a prototype of a large-scale system and demonstrates proof of concept of the overall AGV system for warehouse management. The system performance is measured in a straight-line movement and once the robot turns at specific degrees. A metal track was built via metal strips and was then detected by the proximity sensors. This process is also very robust and can withstand the demands of an industrial setting.

In the second paper, Urooj *et al.* (2020) provides a discussion of water crises: they note that one large amount of residential and industrial are wasted every year. They created a Kivy application for the user in which they can control the fluid waste problem with the integration of hardware that includes Microcontrollers, Ultrasonic sensors, Relay shields, node MCU 8266, and a contactor. With their designed application, users can control the water level status, motor accessibility (on/off), the status of water consumption, and

message alerts. In future work, they seek to enhance the water model and apply it to the agriculture sectors.

In the third paper, Talha *et al.* (2020) put forward a unique turbine that provides optimal electrical output. The authors note that a water turbine is one of the key technologies used in producing green energy which benefits both the environment and society. The design of the turbine is such that when water encounters the blade, the turbine begins to rotate to generate electricity. It is proposed that the model can be improved if the joint resistance is addressed by adding a ball bearing that will increase the motion. Future designs of the turbine can be improved by fully submerging the turbine instead of partial submersion without the detriment of ease in installation and maintenance. The design can further be implemented on other water systems such as rivers and canals by changing the size of the turbine.

In the fourth paper, Tiwari, Kumar and Sharan (2020) examines the concept of the reversible logic: it depends on the dominant modules of a processor. The authors note that the shift register can be studied with the use of the reversible logic which can shift the bits of the information towards both side i.e. left and right. In order to analyze the quantum processor, the Quantum Computational Automata (QCA) as well as Verilog software is used to simulate the parameters of the device and then obtain the characteristics of the device. The authors take a reversible logical computing based approach that can be used in the ALU of a quantum processor with the help of D-type FFs. This circuit is designed and analyzed for key parameters such as the size of the cell, the number of cells used, delay, temperature dependency, power dissipation, etc. The proposed circuit acts as an alternative to the CMOS technology, and is analyzed for a typical range of power dissipation ($650 - 750$ meV) and temperature ($1^oK - 10^oK$).

In the fifth paper, Memon *et al.* (2020 provide an overview of buck-boost converter technologies.

The authors note that the buck-boost converter operating in critical conduction mode (CRM) is commonly utilized in various applications. The system has a number of advantages: protection against short circuiting, minimum component count, low operating duct-cycles, and low voltage, MOSFETs. Etc. A new control scheme of variable on-time

control (VOTC) is proposed in this paper. The VOTC can be implemented by modulating the turn-on time of the buck-boost switch.

Simulation results are presented to verify the effectiveness of the proposed control strategy.

In the sixth paper, Shah and Abosaq (2020) discuss a novel approach: the concept of powering systems wirelessly. The authors note that in the 19th century, Nikola developed 'Tesla Tower' in hope of transferring power wirelessly. The authors discuss WPT using Inductive Coupling which falls under the domain of NFWPT: a transmitter coil is used to transmit power to the receiver coil via a magnetic field. Inductive coupling is an efficient way to transmit power through short distances and make its way in smartphones and the health industry. This paper discusses the theoretical foundation of Inductive coupling and presents results of an experimental work done on WPT via Inductive Coupling.

In the seventh paper Hertzog and Swart (2020) propose a revolutionary technology for fishermen. The purpose of this paper is to present a cost-effective and innovative test jig that may be used to determine the reliability and consistency of operation of various fishing-bait release mechanisms. The main components of the system are a HX711 instrumentation amplifier, a load cell and an Arduino Mega microcontroller. The accuracy of the system was determined to be 99.879%. Reliability values for a Gannet Sport mechanism with a 0.55 mm Kingfisher line ranged from 599 g to 642 g, giving a maximum deviation of 43 g.

The results provide evidence that the system is both reliable and valid.

In the eighth paper, Lehloka, Swart and Hertzog (2020) discuss issues of energy supply. The purpose of this paper is to empirically validate the optimum tilt for PV modules in the Highveld of South Africa. Three fixed-axis PV modules installed at optimum tilt angles of Latitude minus 10°, Latitude, and Latitude plus 10° serve as the basis of this study. These optimum tilt angles are utilized based on the recommendations by Heywood and Chinnery. A key recommendation is that PV modules should be mounted at Latitude minus 10° for the summertime period in the Highveld region of South Africa. Energy supply is a major problem in today's world due to an increase in demand, fossil fuel challenges and increase in global warming due to carbon emissions. It is shown that the efficiency of Photovoltaic (PV)

systems is affected not only by varying environmental conditions but also by the installation of its PV modules.

In ninth, Ali *et al.* (2020) examine the effectiveness of tumor diagnoses. This paper facilitates radiologists in diagnosing lung tumors and helps differentiate between the types of tumor. Computed Tomography (CT)-scan images in Digital Imaging and Communications in Medicine (DICOM) format are used to identify the lung tumor (benign or malignant) using a learning algorithm. The proposed diagnostic software provides accurate results with bright CT scans: different orientations can help to increase the efficiency and accuracy of the diagnostic procedure. The proposed computer aided diagnosis can help the radiologists to detect tumors at an early stage, decrease the false positive rate, and reduce the overall cost of the diagnostic procedure.

The tenth paper involves the design of an automated pizza cutting machine in the food industry. The objective of this paper authored by Saeed, Sattar and Ferguson (2020) involves the design of a machine that would cut a pizza into even slices by a single press. The need of the product has been determined by surveys that were collected from various pizza vendors. This machine is designed to cut a pizza of any size in less than 30 seconds; increasing the overall productivity. The pneumatic system and round cutting tools are used to get the pizza cuts into even slices with better precision and more accurate shape. The stress and motion analysis conducted as part of the design procedure and their results are also discussed.

The eleventh paper, authored by Steenekamp and Swart (2020), discuss premature bearing failures due to Electrical Current Discharge (ECD). The purpose of this paper is to present an innovative jig that may be used to expose mechanical bearings to ECD, in order to clarify its associated effects on the bearing that need to be understood before any mitigating techniques can be proposed. An experimental design is used in this study. A method is presented using an ignition coil wiring harness of a vehicle to safely induce ECD across a specific bearing. Three samples were used and analyzed with an optical and electron scanning microscope. The used ball bearing exposed to ECD showed micro-cratering, a result of electric current passage. A few deep scratches and indentations were observed on the raceway surface. This is due to abrasive wear particles embedded in the raceway surface

sliding between the major bearing components. A recommendation is made to use this innovative jig to test the impact of ECD on bearings from other suppliers.

Twelfth, Ujjan *et al.* (2020) note that robust and accurate adhesion level identification is crucial for proper operation of railway vehicles. In this research a solid axle Wheel-set was modeled along with different adhesion conditions and a dataset was prepared for the training of Deep Neural Networks (DNNs) in Python. Furthermore, it explored the potential of DNNs and various data driven algorithms on our noisy sequential dataset for classification tasks and achieved 91% accuracy in identification of adhesion condition with the final model.

In the thirteenth paper, in this special issue, Huapaya, Rodriguez and Esenarro (2020) describes the most prominent algorithms of Supervised Machine Learning (SML), their characteristics, and comparatives in the way of treating data. The Heart Disease dataset obtained from Kaggle was used to determine and test its highest percentage of accuracy. To achieve the objective, Python sklearn libraries were used to implement the selected algorithms, evaluate and determine which algorithm is the one that obtains the best results, applying decision tree algorithms achieved the best prediction results.

In the fourteenth paper, the effect of the COVID-19 epidemic on research activities in Engineering universities in Pakistan, are discussed by Massan, Dahri and Shaikh (2020). Their solutions via technology are also emphasized. It is shown that invasive quarantines and adept social distancing are required to mitigate the effects of the Coronavirus COVID-19 pandemic. The goal of this paper is to ensure good practices, effective command, and clear and lucid communication in order to defeat the pandemic and prevent the rise of future disasters

In the fifteenth paper, the Usability of eGovernance for the citizens of Pakistan is discussed by Dahri, Massan and Maitlo (2020). The study findings show that most of the users had good perceived usability satisfaction and only one-third of the users were rated as possessing little or poor usability. The objectivity of the results indicates the need to bridge the mismatch between the developer's perception and the user experience.

In the sixteen paper, an extended Kalman filter is discussed. Mal *et al.* (2020) use this model to estimate contact forces at the wheel-rail interface. The wheel-track interface is the most significant part in the railway dynamics because the forces produced at wheel-track interface governs the dynamic behavior of entire vehicle. This contact force is complex and highly non-linear function of creep and affected with other railway vehicle parameters. The real knowledge of creep force is necessary for reliable and safe railway vehicle operation. This paper proposed model-based estimation technique to estimate non-linear wheelset dynamics. In this paper, non-linear railway wheelset is modeled and estimated using Extended Kalman Filter (EKF). Both wheelset model and EKF are developed and simulated in Simulink/MATLAB.

In the seventeenth paper, Ivanov *et al.* (2020) note that digital technologies are transforming the field of medical training, simulation and modeling. Advances in the field of virtual Augmented Reality (AR) and virtual simulation are described in detail, particularly as they relate to medical education and training. An overview of key medical simulation tools is provided in order provide foundational knowledge about this rapidly growing field. A timely and valuable original Augmented Realty system is put forward.

/01/

AUTOMATED LOGISTIC SYSTEMS: NEEDS AND IMPLEMENTATION

Abbas Shabbir Ezzy

Faculty of Shaheed Zulfiqar Ali Bhutto Institute of Science and Technology
Karachi, (Pakistan).
E-mail: abbas.shabbir@szabist.edu.pk ORCID: https://orcid.org/0000-0002-8565-3718

Farhan Zafar Khan

Senior R&D Engineer, Mywater PVT. Ltd
Karachi, (Pakistan).
E-mail: farhanzafark@gmail.com ORCID: https://orcid.org/0000-0003-0305-6950

Moiz Akram

Student of Shaheed Zulfiqar Ali Bhutto Institute of Science and Technology
Karachi, (Pakistan).
E-mail: moizakram@hotmal.co.uk ORCID: https://orcid.org/0000-0002-1539-0449

Janib Agha

Student of Shaheed Zulfiqar Ali Bhutto Institute of Science and Technology
Karachi, (Pakistan).
E-mail: janibagha@gmail.com ORCID: https://orcid.org/0000-0002-6920-9617

Atif Saeed

Faculty of Shaheed Zulfiqar Ali Bhutto Institute of Science and Technology
Karachi, (Pakistan).
E-mail: m.atif@szabist.edu.pk ORCID: https://orcid.org/0000-0003-1551-4314

ABSTRACT

In this paper, a solution to the problem of warehouse automation for transferring goods is discussed. To meet the demands of large scale material movement in warehouses, an automated system is proposed in lieu of a manual workforce to automate the warehouse picking process using an Automated Guided Vehicle (AGV). Such a vehicle can operate in an industrial setting with minimal human intervention. The system is designed such that the robot can operate on a known 'map' laid out on the warehouse floor.

When starting and ending coordinates are provided, it can calculate the shortest path to its destination and guide itself along the path avoiding obstacles.

The system proposed is a prototype of a large-scale system and demonstrates proof of concept of the overall AGV system for warehouse management. The document is centered on developing the hardware model of automatic guide vehicle (AGV) system and group it with metal detection detector. The system performance is measured in a straight-line movement and once the robot turns at specific degrees. A metal track was built via metal strips and was then detected by the proximity sensors. This is a cheap process and an alternative to magnetic strip and infrared sensors. This process is also very robust and can withstand the demands of an industrial setting.

Furthermore, control software was implemented using Robot Operating System (ROS) and interfacing for all the sensors was done using python scripts. Central processing was carried out for the data from all sensors and movement decisions were made based on the status of the sensors. Through this project, the concept of a small scale AGV produced using locally available materials, was proven. All the objectives for this project were met successfully and the product performed according to its intended design criteria.

KEYWORDS

Industry 4.0, Automated Systems, Mechatronics, Productivity, Shortest Path, Localization.

1. INTRODUCTION

1.1. PROBLEM STATEMENT

This robot is designed mainly to tackle the need of moving goods from one point in a warehouse to another and has a large demand in warehouse usage like for example in ALI BABA, DHL and TCS. A large workforce of human operators is required to fulfill order processing as there is not a lot of robotics involved in a warehouse environment. Also it has many features like obstacle avoidance and line following which makes it even more efficient. There is pressing need for automation of warehouse management processes. This includes the introduction of robots to automate the picking process to increase efficiency, reduce costs and provide a scalable solution. In Pakistan this system is not currently implemented and warehouses here are mostly being run on human operators. This increases its demand in the country to save cost and improve efficiency.

Path planning algorithms like A* and Dijkstra (Zhang & Zhao, 2014) for navigation are readily available in theory form, but their practical applications are limited. Major goal of the research work was to implement A* algorithm for navigation in a warehouse environment and to demonstrate proof of concept.

1.2. SYSTEM OVERVIEW

The system design has two type of sensors used that are ultrasonic and RFID sensor and both sensors are connected to an Arduino Uno module which is then connected to a raspberry pi. The proximity sensors which are directly connected to a raspberry pi are used for metal detection or line detection process. The raspberry pi is then connected to a motor driver which actuates the motors.

1.3. CURRENT STATE OF ART

Advanced path planning algorithms such as Dijkstra and A* are being applied to select routes, these are operating software of path planning. Path planning on a floor of a warehouse is usually done using these algorithms which are used to design specified path on the floor and then the nodes and the routes need to be taken by a robot are decided while using these algorithms.

A wide range of navigation technologies such as laser/vision/ contour/wire/magnetic tape are available, all of these technologies are being used in the path planning purposes of an Automated guided vehicle, all these methods have their own advantages and disadvantages but the ones which are cheapest and efficient are implemented to save cost and improve efficiency.

Robust systems implement multiple AGV'S with intelligent traffic management and obstacle avoidance, multiple AGV's are also being implement and traffic control management system is being used to control the movement of these multiple robots plus the coordination and communication of multiple robots is very important.

AGV systems minimize operator input and increases efficiency. This has also changed the dynamics of a warehouse management industry.

1.4. LITERATURE REVIEW

The problem of designing an Automated Guided Vehicle (AGV) can be broken down into three main aspects. Path planning involves algorithms for calculation of shortest path to a given destination in the environment. Navigation provides methods for establishing mobility of the robot. It mainly involves design for the mechanism the AGV will use to determine path to follow. Finally, localization is third important aspect of AGV operation. It defines how the AGV will update its current location in real time. Very important for decision making regarding path to follow going forward. Also, an integral part of multiple AGV systems where location of each robot determines path and movement of other robots through the environment.

Path Planning is the most important aspect of an autonomous guided vehicle's operation. Given a map, the robot must plan shortest path on its own. This makes the robot independent of human input apart from start and end points. Different algorithms exist to implement shortest path planning with respect to mobile robots. One very common and widely used algorithm is Dijkstra's algorithm. It provides an effective implementation for calculation of shortest path, and routing flexibility in an AGV (Vale *et al.*, 2017) including the remote handling operations of transportation performed by automated guided vehicles (AGV).

Furthermore, the algorithm can be modified to accommodate multiple AGVs in the same environment, as well as account path planning around obstacles. Dijkstra's algorithm provides an effective method of calculating shortest path to a destination. However, it does not account for heuristic costs and takes extra time finding all shortest paths through the map. To account for heuristic costs, A-star (A*) and improved A* algorithms are implemented. It can be demonstrated that the A* algorithm can be effectively utilized to return the smoothest and shortest time path (Wang *et al.*, 2015) flexible manufacture systems (FMS. Using this technique, the path selected for an AGV considers the least number of turns that the AGV must make to reduce movement time.

Furthermore, multiple AGVs can be handled by such a system, by eliminating the path already being utilized by an AGV and calculating the second shortest path for the next vehicle. The A* algorithm can also be demonstrated to solve complex problems such as parking of multiple cars automatically in an urban environment (Shaikh & Dhale, 2013) hence they are frequently applied in automated warehouses, sea ports and airports to optimize the transportation tasks and, consequently, to reduce costs. Developed countries are using automation for performing several tasks in warehouses, storages and products distribution center in order to decrease costs of transportation and distribution of goods. It is important to emphasize that its productivity is highly dependent on the adopted route. Consequently, it is essential to use efficient routes schemes. Hence in this research , the AGV routing decision is one of the main issues to be solved. This research proposes an algorithm that produces optimal routes for AGV (Automated Guided Vehicles. In this case, a smart parking system utilizes an AGV to park cars in a multi storied environment. The algorithms calculate shortest paths while accounting for static and dynamic obstacles and result in an efficient system that can handle multiple robots moving through the environment at the same time. In industrial, specifically warehouse settings, the map for an AGV is often pre-defined topologically. In these situations, it has been found that using an improved Dijkstra's algorithm along with an A* algorithm provides a high level of automation when calculating shortest paths for multiple AGVs (Walenta *et al.*, 2017). In this approach, Dijkstra's algorithm can be utilized for global path planning, whereas A* algorithm can be used to carry out localized path planning. This method has been proved to work with multiple AGVs in the same environment, as well as local obstacles that may occur in the path of the AGVs.

Navigation of AGVs is a problem that yields multiple solutions, each with its own merits and demerits. Many different approaches have been proposed over the years, and each has its own area of application (Guo, Yang, & Yan,, 2012). There are two broad categories of technologies that can enable navigation in a mobile robot: those based on physical path, and those based on virtual path. For many industrial applications, technologies based on physical path prove to be more robust and simpler to implement. Two of the most prevalent technologies in the industry over the last 20 years are wire guided navigation and magnetic strip navigation. Magnetic strips have certainly been proposed as an efficient, low cost solution for the navigation problem. Commonly available hardware, such as a magnetometer can be used to detect configurations of magnetic strips as landmarks (Han, Kuo, & Chang, 2016).

Not only does this system demonstrate the ability to navigate using magnetic strips, it also shows that such systems can be effectively used to localize AGVS on a map. Modern AGV systems are exploring virtual path-based technologies for navigation. These types of systems do not rely on any physical object to lay out a path. Instead systems such as a vision-based range finder can be implemented for free-ranging AGVs in industrial environments (Surer, 2018). A line shaped laser transmitter is used to transmit a line which is detected by a receiver. Based on the vertical height of the line detected by the sensor, the distance to the obstacle can be estimated. Another novel system implements magnetic spots on the floor and hall effect sensors to navigate the AGV (Marin-Plaza *et al.*, 2018). By continuously measuring the x, y and z components of magnetic field emitted by the magnet spot, an effective driving system can be implemented which follows the 'line' of maximum flux along the floor. It is even possible to use PID control and allow the AGV to self-correct its course if it strays of the path.

Localization of the AGV can be done in a number of ways. However, a low cost, yet efficient method is required within the scope of this project. A simple RFID sensor and transmitter can be used to provide effective localization of an AGV (Škrabánek & Vodička, 2016). RFID tags placed on the floor contain unique location information. As the sensor on the AGV passes over the tag, it reads the information on the tag and updates its location based on the information.

2. METHODOLOGY

2.1. HARDWARE METHODOLOGY

After finalizing the design and selecting the sensor, all the resources were being implemented in AGV in their respective order. The chassis was purchased from an online vendor but needed modifications for the motors and sensors to be mounted.

Before integrating the hardware into the final product, it was important to test each component individually. This was done to ensure that each component was operating properly, and to catch any errors in its performance or implementation. This step allowed us to thoroughly investigate the working of the hardware components. The benefit of doing individual testing were that it was easier to pinpoint system failures after integration. Had all the sensors and hardware modules been implemented straight away on to the final product, sources of errors would have been very hard to identify. Knowing beforehand how each component performed, and what caused it to fail allowed us to quickly debug any issues that arose during construction and operation of the AGV.
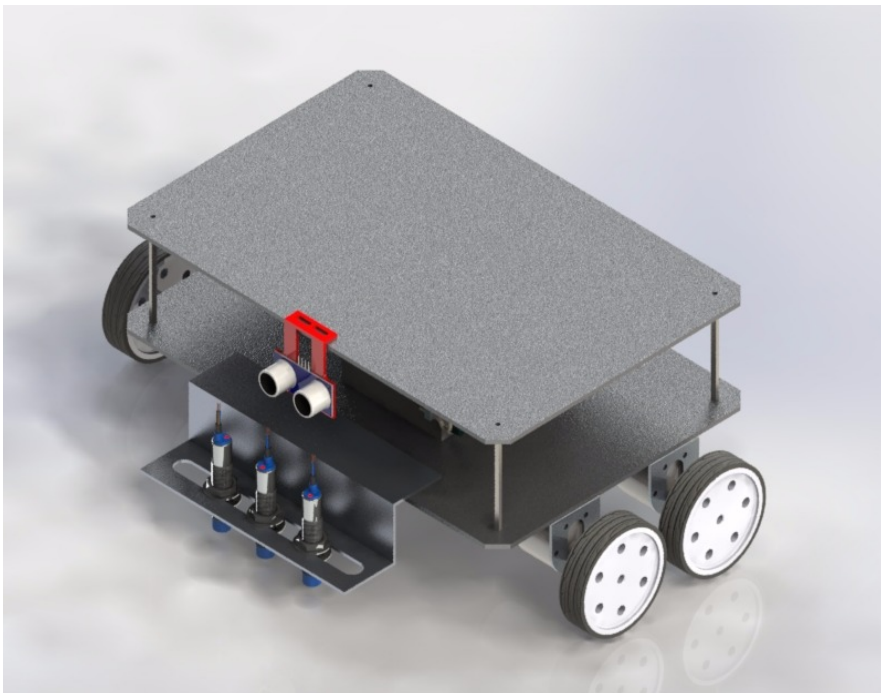
Figure 1. CAD Design of chassis.

3. SOFTWARE METHODOLOGY

In this section the software design for the AGV is presented. The operating system used for programming is discussed, and then the software design principals as well as logic is described.

3.1. SOFTWARE DESIGN

3.1.1. REQUIREMENTS

A large part of this project depends upon the software implementation of various concepts and algorithms correctly so that the robot can perform all its functions optimally. Therefore, a lot of deliberation was put towards conceptualizing the best possible software solution for this project.

The requirements for this project could be broken down into a few major categories.

The most important task that the software would be required to carry out would be to calculate the shortest path between two nodes on a given map. For this purpose, an efficient and suitable shortest path algorithm would need to be implemented. To enable this algorithm to operate, the topological layout of the environment would have to be implemented as a graph. Using features on the graph, the algorithm would then take in the starting and ending nodes and calculate the optimum path between them.

Once the shortest path is calculated the robot would need to commence movement. To achieve this, line following code would need to be integrated into the code. Based on inputs from the hardware, decisions would have to be made on whether the robot should go straight or move left or right. Another layer of complexity would be at intersections. Based on given map, the robot would have to decide on which path to take if given a choice between multiple directions.

In order to localize the robot within the physical environment, code would have to be added to interface with the RFID reader (Gupta *et al.*, 2014). This would enable the robot to read tags placed throughout the map. Values of these tags would be tallied against the shortest path calculated by the algorithm. Based on the value of the latest tag, the software would

have to check which direction on the path would need to be taken. It would also allow the program to terminate once the end node was reached and detected.

Obstacles are a huge part of any dynamic environment. Any number of obstacles can occur in the robot's path at any moment. In the hardware, an ultrasonic sensor would detect and send signals based on the presence of any obstacles. The software would have to reflect that by interfacing with the hardware and safely stopping the robot whenever any obstacle was detected.

Finally, code for all the hardware modules including the sensors and the motor drive system would have to implemented.

It was an important requirement that all these modules be working in parallel at the same time and the code should be able to handle these operations in real time without any delay and with minimum errors.

3.1.2. DESIGN

Based on the requirements discussed in the previous section the software was required to communicate with a number of sensors. Each sensor would send its data continuously and the data would need to be handled in parallel and real time. Furthermore, it was required that decisions be made based on the readings from each sensor and based on those readings control signals be sent to the motors to control movement. To facilitate this, a central processing node would need to be implemented. This central node would take in information from the sensors and make decisions for the robot's movement. It would also send signals to the drive system so that the motors could carry out the correct motion. However, the central processor would not directly communicate with any of the sensors. To do that, separate nodes would be used. Each node would be dedicated to a single sensor and would communicate its data to the central processor. A similar approach would be applied to the graph and shortest path calculations. A separate node would initialize the graph and based on user input, calculate the shortest path. Once the calculation was complete the shortest path would be sent to the central processor.
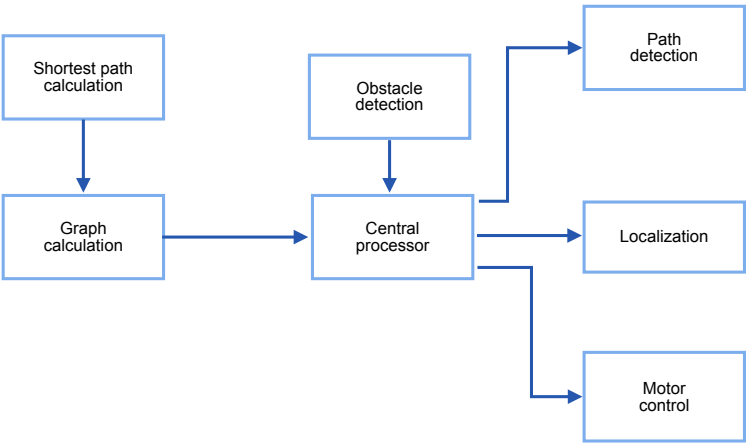
Figure 2. Overview of Software Design.

Using ROS as the platform for this robot allowed for the implementation of parallel processing for the sensor inputs. In ROS, a node could be defined for each sensor. This node would be responsible for setting up communication with the sensor and reading data from it. Then using the concept of topics and messages, the data would be published to an individual topic. Since ROS operates as an operating system, all these nodes would be operating at the same time. Hence, data would be coming in from multiple sensors in parallel. The individual topics also operate in isolation from one another so there would be no lag between the time when the data is published and the time when it is received by the central processor. The central processor would be listening to all available topics and would be able to discern which data was coming from each topic. Upon receiving the data, the decision-making process would then be carried out and commands sent to the motors to control movement.

Flowchart

An in-depth representation of the logic for the software is shown in the figure below. There are a few critical steps that need to be taken to ensure that the flow of the program is sound and performs according to the specifications.

To begin processing, the robot needs the start and end coordinates for locations on the map. Without these, shortest path calculations cannot be carried out and movements cannot be made. Once received, the software calculates the shortest path to the destination and

sends the outcome of calculations to the central processor. The first thing to check before moving, is whether there is an obstruction in the robot's path. This is done through the ultrasonic sensor. The input of the ultrasonic sensor supersedes any other sensor input and all movement is stopped immediately if any obstacle appears in the robot's path. If there is no obstacle in the path, line following protocols can be followed. The robot utilizes the proximity sensors to detect the presence of the metallic strip. Depending on the sensor that detects the path, movement decisions can be made. If during this process an RFID tag is detected, the robot updates its position based on the information stored on the tag. This will also allow the robot to know when the destination is reached. In case the destination tag is detected, the robot can stop all movement, and await further instructions.
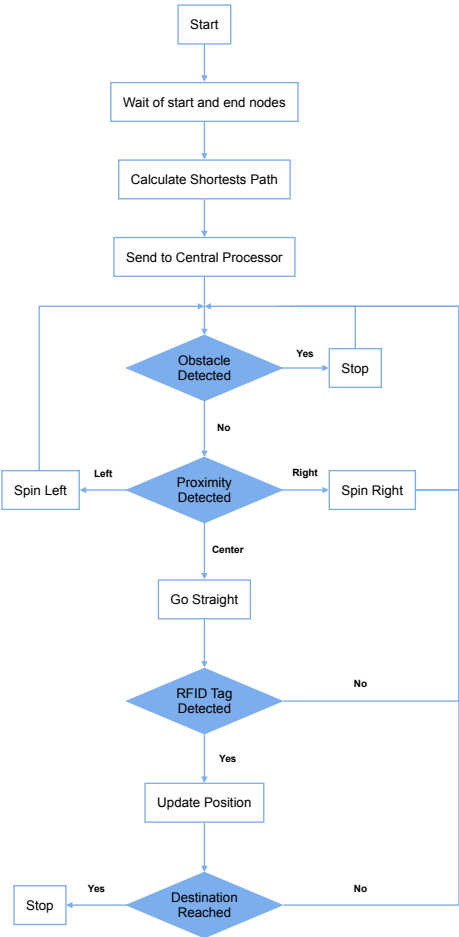
Figure 3. Software Flowchart.

3.1.3. IMPLEMENTATION

Once the design phase was complete and the algorithms finalized the implementation phase was commenced. In this phase the coding was carried out based on the algorithms and decisions made in the design phase.

In addition to separate nodes for each sensor, there was a central processor node that took in the information from each node. The purpose of the central processor was to carry out all the decision making for the robot and control the motors accordingly. The data from the sensors was passed to this node using custom messages. Multiple functions were added and conditions for each sensor were monitored. Based on the decision flowchart shown in the previous section, the code could then decide what action to take and the movement of the robot was controlled accordingly.

There were a few performance metrics that needed to be evaluated to define the performance of the system. The main concern was the time it would take for the system to return the shortest path for any given set of locations. The shortest path calculation needed to be accurate and the prompt for this to be a successful implementation of the theory. The following chart highlights the time it takes for the A* algorithm to run the shortest path calculations and return the results.

Currently the map consists of only 10 nodes. This is based on the current needs. Further simulations were carried out with a larger number of nodes and the performance was evaluated for eventual scalability of the systems. The results are shown in the table below.

Another metric was the overall performance of the system. As can be seen in the decision flowchart in the previous section, the realization of the system would be complex. A multitude of processes and scripts running in parallel were utilized to enable communications between the sensors and the actuators. Hence it was important to ensure that the software ran smoothly and there were no delays in the processing of inputs from the sensors, the decisions made based on those inputs and the outputs to the actuators. To that end, the overall time from input to the system and the robot to reach its destination was recorded. The results can be seen in the table below.
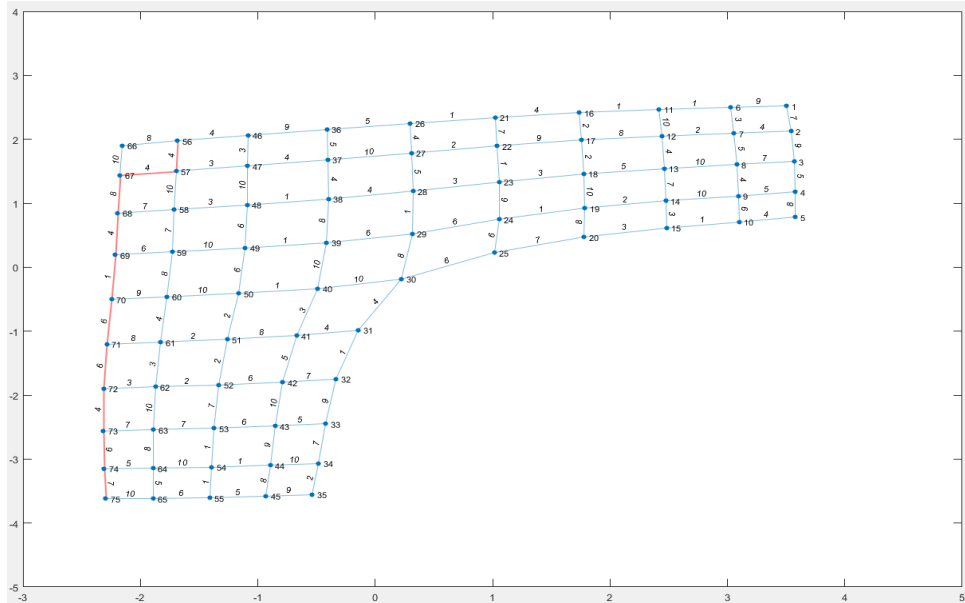
Figure 4. Implementation of Shortest Path Algorithm on Auto Generated Graph.

4. RESULTS

The purpose of this project was to design and develop an Autonomous Guided Vehicle prototype with the objective of demonstrating its usefulness in the warehouse picking process. The performance of the AGV was to be measured based on three major criteria: path planning, navigation and localization. Results for each criterion are discussed in the following sections.

4.1. PATH PLANNING

For path planning, a graph data structure was implemented in python and using starting and ending nodes as input, the shortest path was calculated using A-star algorithm. This process was found to be a very efficient and quick method of calculating the shortest paths of a given map. The environment was mapped beforehand, and the distances and nodes designated cartesian coordinates. It was found that the algorithm was implemented to a high degree of accuracy and the results were providing shortest paths correctly every time. Some of the results are shown below:
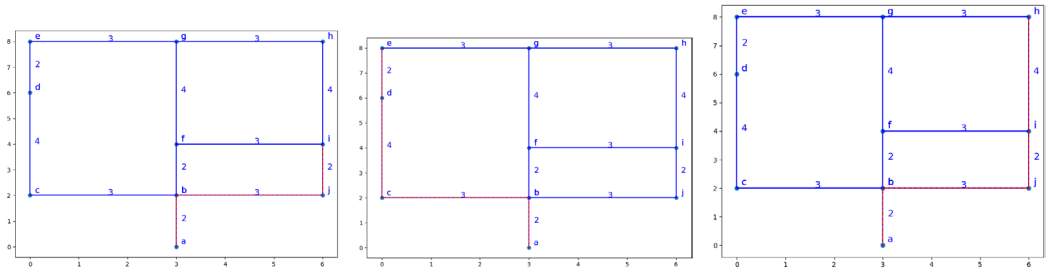
Figure 5. Shortest Path Calculated from a) A to I; b) A to E; c) A to H.

As shown in the results, for this map the shortest path calculation yielded correct results each time. This map is fairly simple and straightforward, and easy to calculate for. However, the algorithm is capable of handling much more complex maps with multiple intersections and can be used to figure out shortest paths in very complicated environments as well.

4.2. NAVIGATION

For the line following part of navigation, testing was carried out extensively on different sections of the path and the algorithms and hardware were fine tuned to perform as efficiently as possible. This resulted in very smooth movement of the robot in a straight line and very good error correction every time it went away from the central sensor (Lee & Yang, 2012).

A complex mathematical solution had to be implemented for intersections. In this case, based on the RFID tag being read before the intersection, a direction of travel (left, right or straight) was selected and stored. When the intersection was detected the robot stopped, and then turned in the required direction. When the turn was complete and the path detected again, the robot would then begin to move according to the line following algorithm. This was also successfully implemented and tested on the hardware, and the robot was performing reasonably well with a very small percentage of errors.

4.3. LOCALIZATION

Localization on the AGV was carried out using RFID tags as nodes on the map and an RFID reader module on the robot itself. Every time a tag was detected by the reader it would update the robot's position based on the information stored on the tag. This would also trigger the mathematical calculation to tell the robot which direction to take at the

next intersection. Overall the performance of this module and its code was found to be satisfactory and the tags were detected with a high degree of accuracy. During testing it was discovered that the reader was not able to detect tags if they were placed very close to each other and were moved too quickly near the reader. To avoid this during operation, the tags on the map were placed sufficiently far away from each other and the speed of the robot was kept at a slower pace. This resulted in accurate operation of this module and errors were not seen during operation and testing.

5. CONCLUSIONS

With the help of an AGV we will be able to find the shortest path for number of AGV's to carry load from one point to another. This will increase the efficiency, save time and lot of cost in a warehouse environment as the whole process of moving objects from one point to another is now automated. The A* algorithm will be able to calculate the shortest path by each AGV to reach from the starting point to the final position. The AGV has also a feature of obstacle avoidance and it will recalculate the shortest path if an obstacle comes in between and it will avoid the obstacle and will then start to move again recalculating the shortest path via the A* algorithm between two nodes. Depending upon the load the nearest AGV will be chosen and the shortest path will be taken to reach the destination to save time. We will be able to save a lot of time by calculating the shortest path for the AGV to travel between any 2 nodes. The use of a single AGV in a warehouse has reduced 4-5 human operators which were moving things from one point to another which has made this process more efficient, time saving and economical as the whole process in now automated.

In this project we have chosen proximity sensors to detect the metal line which is also following the metal line. The sensors can work in any kind of environment that is greasy, dusty and non-greasy metal lines. It was proven that these sensors are no influenced by any environmental factor and are way better than any other black and white lines which are influenced by other environmental factors such as light intensity and battery conditions.

We used RFID tags to mark the nodes from A to I and gave specific initial and final nodes via algorithm for the AGV to move, when the RFID sensor passed over these tags it detected the command from the specific tag and took the direction specified by those tags. This

was a very distinct process which helped for the AGV to move from node to node taking the shortest path with the help of A* algorithm which help to take the shortest route via calculations.

While doing this research we had different options to use for example use of magnetic tape and its sensors was much more expensive and motors of high efficiency and torque were much too expensive so we came to an alternate solution of using metal strips which was a very cheap and reliable approach and which brought the cost down to almost a quarter and made this system more reliable, easy to implement and cheap for using on a large scale in a warehouse management system.

Thus by implementing this system in Pakistan where this technology is not in use at this moment of time we can change the dynamics of a ware house industry in Pakistan where there is lot of need to make the system automated , save time and cost is very important where many people are unaware of modern changing dynamics of this world and keeps them up to date to a country which is not much moving towards the Automated technology, it will be a huge step for the industry in Pakistan to Automate the warehouse management system.

6. FUTURE WORK

This project was meant to act as a prototype and proof of concept for an AGV that could be implemented in Pakistan using locally available components and materials. The major upgrade that can be done to this project is to scale up the size and capacity of the robot to handle industrial scale loads. Upgrading the design to match industry standards, an AGV that can easily carry up to 50 kg of weight can be easily implemented.

Using the lessons learned with the implementation of this system, the software can also be upgraded. In the future, the system can be expanded to accommodate multiple AGVs working in the same environment. The system would then handle the path planning for all the vehicles, making sure to include the current whereabouts of each robot and planning accordingly. Furthermore, communications between the AGVs can also be implemented to increase the autonomy of each individual robot.

Finally, to monitor and control the entire system, an IOT based interface can be implemented. This would allow users to monitor the system very quickly and would provide ample information regarding the status of each robot and the tasks that it has been assigned.

REFERENCES

Guo, L., Yang, Q., & Yan, W. (2012). Intelligent path planning for automated guided vehicles system based on topological map. In *Proceedings of 2012 IEEE Conference on Control, Systems and Industrial Informatics, ICCSII 2012*. https://doi.org/10.1109/CCSII.2012.6470476

Gupta, N., Singhal, A., Rai, J. K., & Kumar, R. (2014). Path tracking of Automated Guided Vehicle. In *2014 7th International Conference on Contemporary Computing, IC.* https://doi.org/10.1109/IC3.2014.6897183

Han, M. J., Kuo, C. Y., & Chang, N. Y. C. (2016). Vision-based range finder for automated guided vehicle navigation. In *Proceedings of IEEE Workshop on Advanced Robotics and Its Social Impacts, ARSO.* https://doi.org/10.1109/ARSO.2016.7736272

Lee, S. Y., & Yang, H. W. (2012). Navigation of automated guided vehicles using magnet spot guidance method. *Robotics and Computer-Integrated Manufacturing, 28*(3), 425-436. https://doi.org/10.1016/j.rcim.2011.11.005

Marin-Plaza, P., Hussein, A., Martin, D., & De La Escalera, A. (2018). Global and Local Path Planning Study in a ROS-Based Research Platform for Autonomous Vehicles. *Journal of Advanced Transportation,* Article ID 6392697. https://doi.org/10.1155/2018/6392697

Shaikh, A., & Dhale, A. (2013). AGV Path Planning and Obstacle Avoidance Using Dijkstra's Algorithm. *International Journal of Application or Innovation in Engineering & Management (IJAIEM)*.

Škrabánek, P., & Vodička, P. (2016). Magnetic strips as landmarks for mobile robot navigation. In *International Conference on Applied Electronics, Pilsen, Czech Republic*. https://doi.org/10.1109/AE.2016.7577279

Surer, E. (2018). Smart Objects and Technologies for Social Good. In *Third International Conference, GOODTECHS 2017, Pisa, Italy*. Part of the *Lecture Notes of the Institute for Computer Sciences, Social Informatics and Telecommunications Engineering* book series (LNICST, vol. 233). https://doi.org/10.1007/978-3-319-76111-4

Vale, A., Ventura, R., Lopes, P., & Ribeiro, I. (2017). Assessment of navigation technologies for automated guided vehicle in nuclear fusion facilities. *Robotics and Autonomous Systems, 97,* 153-170. https://doi.org/10.1016/j.robot.2017.08.006

Walenta, R., Schellekens, T., Ferrein, A., & Schiffer, S. (2017). A decentralised system approach for controlling AGVs with ROS. *2017 IEEE AFRICON: Science, Technology and Innovation for Africa, AFRICON 2017, Cape Town, South Africa*. https://doi.org/10.1109/AFRCON.2017.8095693

Wang, C., Wang, L., Qin, J., Wu, Z., Duan, L., Li, Z., Cao, M., Ou, X., Su, X., Li, W., Lu, Z., Li, M., Wang, Y., Long, J., Huang, M., Li, Y., & Wang, Q. (2015). Path planning of automated guided vehicles based on improved A-Star algorithm. *2015 IEEE International Conference on Information and Automation, ICIA 2015, Lijiang, China*. https://doi.org/10.1109/ICInfA.2015.7279630

Zhang, Z., & Zhao, Z. (2014). A multiple mobile robots path planning algorithm based on a-star and dijkstra algorithm. *International Journal of Smart Home, 8*(3), 75-86. https://doi.org/10.14257/ijsh.2014.8.3.07

/02/

IOT BASED FLUID MANAGEMENT AUTOMATION SYSTEM USING RASPBERRY PI AND ULTRASONIC SENSORS

Ayesha Urooj

Sir Syed University of Engineering and Technology. Karachi, (Pakistan).

E-mail: aurooj161@yahoo.com ORCID: https://orcid.org/0000-0002-6985-3269

Sallar Khan

Sir Syed University of Engineering and Technology. Karachi, (Pakistan).

E-mail: sallarkhan_92@yahoo.com ORCID: https://orcid.org/0000-0001-8988-3388

Sana Shafiq

Sir Syed University of Engineering and Technology. Karachi, (Pakistan).

E-mail: sanashafiq2001@gmail.com ORCID: https://orcid.org/0000-0003-1873-7425

Bilal Ahmed

Sir Syed University of Engineering and Technology. Karachi, (Pakistan).

E-mail: bilal-ahmed007@hotmail.com ORCID: https://orcid.org/0000-0002-4360-2103

Abdul Basit

Sir Syed University of Engineering and Technology. Karachi, (Pakistan).

E-mail: basit.rr123@gmail.com ORCID: https://orcid.org/0000-0003-4044-8590

Shaheer Mustafa Ansari

Sir Syed University of Engineering and Technology. Karachi, (Pakistan).

E-mail: shaheer1234@gmail.com ORCID: https://orcid.org/0000-0001-9470-9368

ABSTRACT

Water crises is one of the most important problem of current era, as a huge amount of water wasted every year especially in residential and industrial. Improper timings and extensive electric consumption are one of the hectic issues faced by the society. We have successfully created a Kivy application for the user in which they can control the fluid wastage problem with the integration of hardware that includes (Microcontrollers, Ultrasonic sensors, Relay shield, node MCU 8266, and contactor). Through the help of our designed application, user can control: Water level status, Motor accessibility (on/off), status of water consumption, message alert facility of fluid. In future work, we focus to enhance the water model and will try to promote it to immense water plants as well as it can be adopted by agriculture sectors.

KEYWORDS

Crises Extensive, Kivy, Relay Shield, Consumption, Accessibilities, Immense.

1. INTRODUCTION AND RELATED WORK

The water level administration has been a noteworthy issue so new strategies must be embraced to control the water level. Here are the expected framework works superior to the current framework. The current framework works along these lines that we make UI (User Interface) for the association of the client so the client can handle equipment through application so it will construct enthusiasm of client and furthermore manufacture cooperation as we probably are aware nowadays there is a great deal of wastage of water issue so we can attempt to make equipment and programming thusly that they control water from over streaming and it assumes a crucial job for client when they use Proposed framework: Here we will display the fundamental thought of our proposition. This proposed framework works beneath computerization and contains components like Raspberry pie, ultrasonic sensor, engine pump, transfer, driven, buzzer and LCD in which each component has its claim usefulness, but Arduino looks like the heart of the venture as all the components are interfaces with Arduino. The ultrasonic sensor plays a major part in determining the water level display within the tank. This sensor is fitted for both tanks upper and lower which is utilized for receiving flag and work concurring to the given condition and motor close at that time when they receive flag conjointly it can do tight clamp versa it can be on and works agreeing to client prerequisite. We have structured a code that at whatever point the tank is getting low the engine naturally turns over and stops when the tank spans to the client required level so the engine will consequently shut so here nobody required for controlling to engine this is the principle bit of leeway of proposed framework. Since no segment contacts the water, there is no possibility of harm to the parts while in the current framework there are water verification ultrasonic sensors which can works quick as contrast with without water confirmation sensors (Varun, Kumar, Chowdary, & Raju, 2018). Water is one of most precious and invaluable the natural resources on our planet researches observed that the scarcity of water become constantly increasing this result will be a globally shortage of water and there will not enough water to fulfil our basic needs. This major issue provokes us design a methodology to serve water wherever and whenever it is needed our methodology not just saving water, we make it usage efficient and measurable. We take two tanks one is basement tank and another is roof tank these are generally build in any residential, industrial, and commercial sectors couple of distance sensors are fixed into

the tanks that reads water levels and transfer signals to microcontroller that will trigger the motor pump on or off when the tanks need to be filled or controlling overflowing of water.

Through this perception we will tend to control and monitor water usage and consumption water monitoring parameters helps in saving of water. If in case they are inappropriate the model and its deployment area required audit or inspection by our team, our skilled workers and developers diagnose the different parameters such as hardware software and field area. On the other hand, hardware models (motors) are automate by android application through the cloud service that make this project smart and IoT based (Rao *et al.*, 2018). Inserted structure is presently a day's assuming an important job in engineering configuration process for productive examination process and successful activity. Because of time unpredictability in electronic viewpoints installed structure have turned into a noticeable piece of our everyday life. So hence, with the assistance of installed structure we have monitored a venture which can quantify the water level of a capacity tank and show it on the LCD (Shetty, Wagh, & Dudwadkar, 2018). Web of Things (IoT) can be characterized as a system of gadgets which are interconnected. It involves a lot of sensors, correspondence arrange just as programming empowered electronic gadgets that empowers end clients to procure precise information occasionally, through the correspondence channel, what's more, considers information trade among clients and the associated gadgets. This framework can be utilized to automatize the control of dams, industrial zones and so forth without human obstruction. This can likewise be utilized to accumulate data on the degree of water all through the nation. Internet of thing works faster build connection and focusses on making the sensors works more and more efficiently. Collecting the data regarding the failed sensors and provide a more reliable way to optimize and provide reliability (Siddula, Babu, & Jain, 2018).

There have been many hydrological studies and theories have been proposed by the experts around the globe which highlight our environment changes our ecosystems mainly for the ecological role of water in our colonies, dams and powerhouses, furthermore many other researches, and experiments have also been made in recent years related to safety precautions for the usage of water and prevent it from wastage. Our study related to water resource management depends on the consumption of water by the population where water is essential to use and in what quantity? the rapid increase of population

and an unaccountable supply and usage would be the root cause of water crises. We use ultrasonic sensors and microcontrollers on water supplies those are co-related with user mobile interface as it is observed that in the local residencies their determining the locations where schedule or unscheduled load shedding of electricity effectuate the human time and cost that will cause to uncertain water wastage and shortage, major polluting sources that contribute to water savage and its tributaries, an analysis has been made in order to evaluate the two major water storage in every house should using the water this Fluid Management Automation (F.M.A) methodology comes under the section, which is one of the most reliable management systems of the water and other fluids (Dunca, 2018).

Water may be a rare normal asset, fundamental for life and to carry out the endless larger part of economic activities. It is crucial, non-expandable by the unimportant will of man, unpredictable in its way of presenting itself in time and space, effectively defenseless and helpless of progressive employments (Durán-Sánchez, Álvarez-García, & del Río-Rama, 2018). The fluid water management system present in the application which is used by the client and application stores previous records of water level information. We don't allow any user to get access on that, but admins have only the excess to check information of clients, but client can reset the password and entertain with application. The real water level present in the application shown on the application-based interface. Application-based interface stores the records of the water level data (Patil *et al.*, 2017).

An IoT framework is made for this framework to test the capacities notice in the venture and it can likewise control the water stream and offer help as well, customer (Narendran, Pradeep, & Ramesh, 2017). Systematically interest in new enhance has brought about higher water prices, however, without picking up the maximum capacity benefits through water competence (Levidow *et al.*, 2014). The framework will mechanize the method by putting a single sensor unit within the tank that will occasionally take estimations of the water level and will control the tool naturally. This framework disposes of the try of individuals for everyday filling of the tank and checks for overflow. The issue like flood of water within the tank of intrigued, filter tank condition and tool overheating due to persistent utilization is method (Ahmadloo, Sobhanifar, & Hosseini, 2014).

This paper planned for advertise our venture in installing a control structure into a programmed water pump controller. One of the inspirations for this analysis was the need to carry an answer for the issue of water lack in different spots wiping out the significant offender misuse of water. A lot of water is misused and wasted. It will help the conditions and water cycle which thus guarantees that we spare water for our future (Patil & Singh, 2014).

2. RESEARCH METHODOLOGY

As we know that the water is one of the most important and most essential natural resources for living beings, until it is used in an accountable manners this organized system Undertaking dependent on both equipment and programming where as shown in Figure 2 we can utilize distinctive equipment like distance sensors (Ultrasonic sensors HC-or JSN-SR04T) Microcontrollers (Node MCU, Raspberry Pi, Relay shield, Contactors) and made equipment as indicated by the prerequisites (Ahmadloo *et al.*, 2014). Furthermore our proposed system of Fluid water management automation that work on some fluid and water level measurements its consumption utilization and its wastage controlling these all functionalities could be achieved by the use of programming and instructions to develop the user interactive interface an mobile application so any client can interact with the interface and cause their need to satisfy, some basic method and description of components are explained under.

2.1. MICROCONTROLLERS
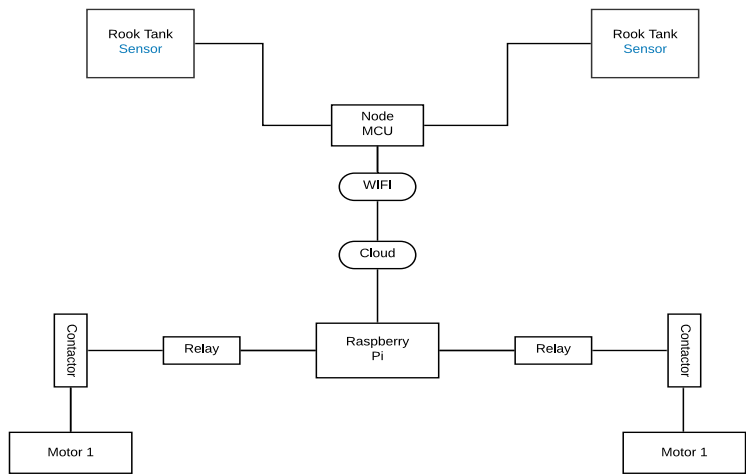
Figure 1. Structure diagram

2.1.1. RASPBERRY PI

Raspberry pi as shown in Figure 2 is a credit card size board micro PC and the least expensive chip utilized by understudies. The raspberry pi is programmed to perform several operations according to our project purposes like controlling automation monitoring sequencing and displaying. Due to its size and portability, we can fix it to the desired location here we are fixing it near to motor-pump and switching board, thus our model saves time, space and cost. Raspberry pi transfers the instructions to sensors and motor pumps when the user wants, or it could automate the motors and sensors as per designed algorithm by the programmer.

Figure 2. Raspberry Pi module 3B+.

2.1.2. NODE MCU ESP8266

ESP8266 is a WI-FI chip having all-inclusive TCP/IP stack and microcontroller capability as shown in Figure 3, Moreover Node MCU is an open-source platform majorly used in internet of things (IoT) based project and relevant purposes, basically ultrasonic sensors which are used in this project are not able to connect to the internet on its own because they don't have their built-in setup we use Node MCU ESP8266 to do so, we programmed with an Arduino Integrated Development Environment (IDE) and setting the connection with sensors and raspberry pie in order to perform wireless communication to an extended distance in this way both the sensors can send the readings to Raspberry Pie which performs further actions accordingly.

Figure 3. Node MCU 8266.

2.2. ULTRASONIC SENSOR

As shown in Figure 4, Ultrasonic sensor detects the object and calculates the distance of the object. The sensor head to generate an ultrasonic wave and receives the wave back after hitting the object and make some readings (Shetty, Wagh, & Dudwadkar, 2018). Ultrasonic sensors have four pins (GND, VCC, ECHO, and TRIGGER. We have already defined levels of tanks in our system. User can check live status of water the levels of the tanks. We utilize ultrasonic sensor for both upper and lower tank so water level can distinguish for the two tanks and this work water level engine will naturally close everything should be possible since raspberry pi offers sign to ultrasonic sensor and it will close when arrived at that level (Varun *et al.*, 2018).

Figure 4. Receiving Signal through Ultrasonic Sensors

2.3. CLOUD SERVER

Firebase included a task so we can make database effectively and store data most assuredly and by guaranteeing that all data keep private and discharge so a client can undoubtedly be enrolled with an email with no dread, Firebase would offer help and communicate client by its highlights. Here some important code for firebase as follow, as shown in below Figure 5.
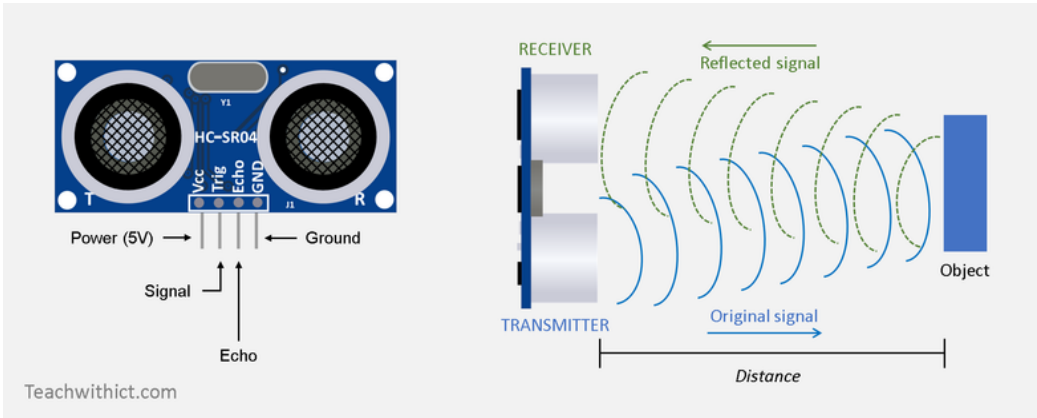
2.3.1. CODING

```
1  #:include firebaseloginscreen.kv
2  #:import FirebaseLoginScreen firebaseloginscreen.FirebaseLoginScreen
3  #:import utils kivy.utils
4  FloatLayout:
5      canvas.before:
6          Color:
7              rgb: 1,1,1
8          Rectangle:
9              size: self.size
10             pos: self.pos
11
12     FirebaseLoginScreen:
13         canvas.before:
14             Rectangle:
15                 size: self.size
16                 pos: self.pos
17                 source: "welcome2.jpg"
18         size_hint: 1,1
19         pos_hint: {"top": 1, "right": 1}
20         web_api_key: "AIzaSyAuNBIBxkzOicmEFLqeyAZcr0xjxguKdP8"
21         primary_color: utils.get_color_from_hex("#001c5d")
22         secondary_color: utils.get_color_from_hex("#ebfff5")
23         tertiary_color: utils.get_color_from_hex("#7cc992")
24
25         on_login_success:
26             print("Successfully logged in")
27
```

Figure 5. Firebase Coding

2.3.2. EXPLANATION

We can use firebase coding because it can provide support to client and also give security to admin to make client data secrete and allow client to recover security if hacked.

3. EXPERIEMENTAL RESULTS AND DISCUSSIONS

3.1. USER INTERFACE (KIVY PLATFORM)

This application is created using the software Kivy which is a python cross platform of android this all above screens are made by using the tool Spyder as we know people in society not aware with Kivy software but Kivy also use to makes interactive applications Kivy is a free and open-source Python library for creating versatile applications and another multi touch application programming with a characteristic (UI) Kivy platform also support all platform including IOS, Android and many others etc.

3.2. ACCESS PAGE

Access page made so client can sign in as indicated by given ID and login secret key and login id and secret phrase spared in database. As shown in figure 6, All client should be enrolled to utilize the application and his engine data all information would save money on database and our application additionally gives the intelligent and simple interface so all sort of client can undoubtedly deal with if any client overlooked secret key so it can reset by getting email on enlisted email ID.
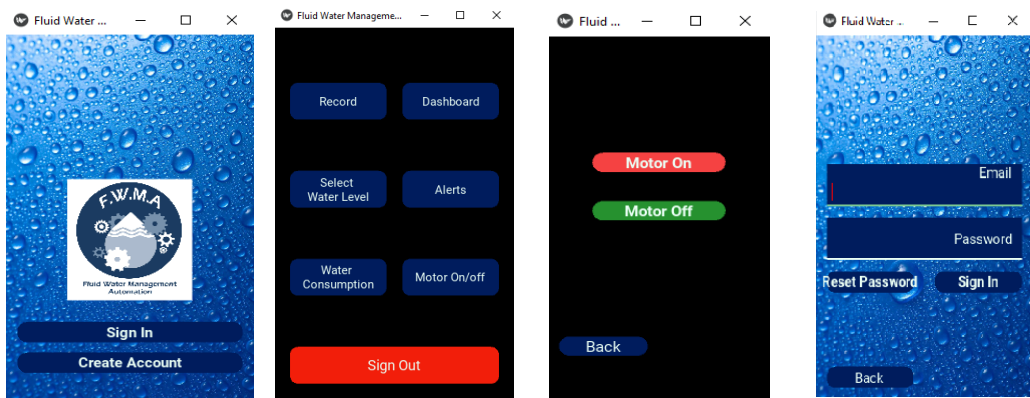
Figure 6. Mobile Application Interface

After login page, this page shows up where a client can see all capacities which incorporate into UI and client can utilize capacities like on the off chance that they, at that point need to see record or on the other hand, need to see history so a client can log in and can see the history and furthermore engage with every single given capacity.

3.3. ALERTS

In this capacity cautions can be sent to utilize this alarm created by an application which gets ready which stores in the database. For Ex: IF client set the engine condition 5 gallons so when arrived at that level engine will naturally be shut and produces an alert in a client mobile phone, however, there is a condition that client must sign in to utilize application capacities.

3.4. WORKING

Here we can talk about the trial and dialogs which we have done and make mindful about our research paper to other individuals. The water level information is Raspberry to the microcontroller board through the WIFI (Ebere & Francisca, 1970). The degree of water from both the tanks are gotten in a steady progression at the microcontroller. In the event that the volume is expanding, at that point, the level of water increasing and when it is going to arrive at the maximum limit of a sign is sent to the motor (Pudasaini *et al.*, 2014). When we are implementing our system first, we measure the roof tank measurement in terms of size, volume or capacity, volume could be calculated by multiplying all three dimensions height, breadth, width. If the tank is cylindrical diameter height and pi would be multiplied, further we are scaling the tank in percentage as shown in Figure 7.
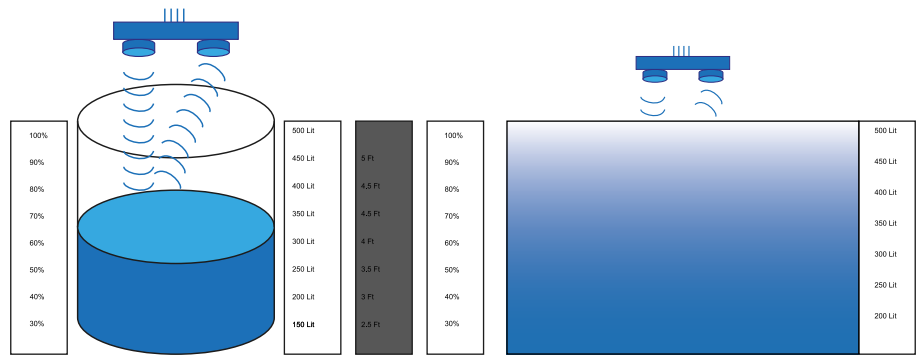
Figure 7. Cylindrical Shape Tank & Rectangular Shape Tank

An average cylindrical and rectangular tank in residential areas are about five feet in height and have a capacity of 500 Liters of water. After measuring tanks its specification will be sent to user cloud server and microcontroller so the system will show the following attributes. The second phase of implementation or experiment user can control motors. In this utilization case outline it is simple for the client to comprehend our prerequisites plainly initially if client need to utilize our proposed framework so they should be login by making account else they can't get access of our application, when client makes get to so then one screen shows up which is essentially the UI which can be constrained by the client can check water level, water status, choice of water and furthermore they advise by our application when water arrived at that level.

3.4.1. USES AND APPLICATIONS

The above administration proposed framework facilitate the procedure of water level administration. We can settle numerous related issues which we face by individuals this proposed framework works consequently as indicated by client necessity by diminishing the labor and furthermore diminished flaws.

- If there should arise an occurrence of crisis if client neglect to close the engine p==3 physically this application closes when water came to at given level.

- It can use in the dams for check of fluid and water.

- It can likewise help in water system where is wastage of water is more.

The proposed system is visualized and monitored by using the mobile application and some hardware's used two ultra-sonic sensors, one Raspberry pi, Micro SD card jumper wires, a breadboard, node MCU 8286, Raspberry relay shield, power supply etc. Raspberry pi is connected to the 5v Dc current through power supply. The voltage up and down are controlling with Raspberry relay shield. All the programming is set to the pins of Raspberry pi and get the result on user interface.

4. CONCLUSION

Human life's and world development growth are fully dependent on water .As we can see now a days water problem become common day by day so we proposed solution to overcome from wastage of water problem so user can save water in daily manner so it can help for user to avail this facility as much as they can . We made an app by which user can control water system through application in application there are different functionalities so user can entertain through different manner and save water as much as possible. Water is crucial for all of us so we can make this type of more project to overcome this problem.

5. ACKNOWLEDMENTS

like to express my gratitude towards Professors, Lab assistant and to our Computer Science department, Sir Syed University of Engineering and Technology for providing us resources.

REFERENCES

Ahmadloo, E., Sobhanifar, N., & Hosseini, F. S. (2014). Computational Fluid Dynamics Study on Water Flow in a Hollow Helical Pipe. *Open Journal of Fluid Dynamics*, *4*(02), 133–139. https://doi.org/10.4236/ojfd.2014.42012

Dunca, A. M. (2018). Water pollution and water quality assessment of major transboundary rivers from Banat (Romania). *Journal of Chemistry*, *2018*. https://doi.org/10.1155/2018/9073763

Durán-Sánchez, A., Álvarez-García, J., & del Río-Rama, M. de la C. (2018). Sustainable water resources management: A bibliometric overview. *Water (Switzerland)*, *10*(9), 1–19. https://doi.org/10.3390/w10091191

Ebere, E. V., & Francisca, O. O. (1970). Microcontroller based Automatic Water level Control System. *International Journal of Innovative Research in Computer and Communication Engineering*, *2013*, 1390–1396.

Rao, K., Srinija, S., Bindu, K. H., & Kumar, D. S. (2018). IOT based water level and quality monitoring system in overhead tanks. *International Journal of Engineering & Technology*, *7*(2.7), 379. https://doi.org/10.14419/ijet.v7i2.7.10747

Levidow, L., Zaccaria, D., Maia, R., Vivas, E., Todorovic, M., & Scardigno, A. (2014). Improving water-efficient irrigation: Prospects and difficulties of innovative practices. *Agricultural Water Management*, *146*, 84–94. https://doi.org/10.1016/j.agwat.2014.07.012

Narendran, S., Pradeep, P., & Ramesh, M. V. (2017). An Internet of Things (IoT) based sustainable water management. *GHTC 2017 - IEEE Global Humanitarian Technology Conference, Proceedings*, *2017-Janua* (October), 1–6. https://doi.org/10.1109/GHTC.2017.8239320

Patil, K. N., Tushar, K., Swaranjali, M. S., & Shreya, M. A. (2017). IOT Based Water Level Monitoring System For Lake. *International Research Journal of Engineering and Technology(IRJET)*, *4*(2), 1425–1427. https://irjet.net/archives/V4/i2/IRJET-V4I2278.pdf

Patil, Y., & Singh, R. (2014). Smart Water Tank Management System for Residential Colonies Using Atmega128A Microcontroller. *International Journal of Scientific & Engineering Research*, *5*(6), 355–357. https://www.ijser.org/researchpaper/Smart-Water-Tank-Management-System-For-Residential-Colonies.pdf

Pudasaini, S., Pathak, A., Dhakal, S., & Paudel, M. (2014). Automatic Water Level Controller with Short Messaging Service (SMS) Notification. *International Journal of Scientific & Technology Research 4*(9), 1-2250. https://www.researchgate.net/publication/299825981_Automatic_Water_Level_Controller_with_Short_Messaging_Service_SMS_Notification

Shetty, T., Wagh, P., & Dudwadkar, A. (2018). Water level monitoring system. *International Research Journal of Engineering and Technology (IRJET), 05*(08), 1712–1714. https://www.irjet.net/archives/V5/i8/IRJET-V5I8295.pdf

Siddula, S. S., Babu, P., & Jain, P. C. (2018). Water Level Monitoring and Management of Dams using IoT. *Proceedings - 2018 3rd International Conference On Internet of Things: Smart Innovation and Usages, IoT-SIU 2018*, (February), 1–5. https://doi.org/10.1109/IoT-SIU.2018.8519843

Varun, K. S., Kumar, K. A., Chowdary, V. R., & Raju, C. S. K. (2018). Water Level Management Using Ultrasonic Sensor (Automation). *International Journal of Computer Sciences and Engineering*, *6*(6), 799–804. https://doi.org/10.26438/ijcse/v6i6.799804

/03/

DESIGN AND ANALYSIS OF INLINE PIPE TURBINE

Muhammad Talha

Student, Department of Mechatronics Engineering, SZABIST, (Pakistan).

E-mail: talhapacifer@gmail.com ORCID: https://orcid.org/0000-0003-4369-2388

Atif Saeed

Faculty, Department of Mechatronics Engineering, SZABIST, (Pakistan).

E-mail: m.atif@szabist.edu.pk ORCID: https://orcid.org/0000-0003-1551-4314

Mustafa Jaffer

Student, Department of Mechatronics Engineering, SZABIST, (Pakistan).

E-mail: mustafa.jafferxp@gmail.com ORCID: https://orcid.org/0000-0001-8364-8619

Hayyan Yousuf Khan

Student, Department of Mechatronics Engineering, SZABIST, (Pakistan).

E-mail: hayyankhan1@live.com ORCID: https://orcid.org/0000-0002-4441-6863

Ali Haider

Student, Department of Mechatronics Engineering, SZABIST, (Pakistan).

E-mail: alihyder10005.ah@gmail.com ORCID: https://orcid.org/0000-0003-4961-4882

Wajahat Ali

Student, Department of Mechanical Engineering, QUEST, (Pakistan).

E-mail: wajahatqureshi281@gmail.com ORCID: https://orcid.org/0000-0003-3345-6461

ABSTRACT

In this current smart era, electricity is considered a necessity for development as almost all of machinery and circuitry runs on electrical power. Therefore, the production of electricity is a must for attaining progress. But nowadays, there is a constant struggle for access to large fossil reservoirs and the development for renewable resources is slow. There have been innovative inventions such as the wind turbines, water turbines, solar cells and many other renewable sources. These resources have slowed down the depletion of fossil fuels to a certain extent, but these inventions do have their shortcomings and most areas where energy harnessing is possible, are left unanswered. One such area where energy conversion is possible is in the water transportation system. To harness electrical energy from this system, a small turbine generator can be installed onto the pipelines to harness the kinetic energy of the flowing water in them. Hence forth by applying this research, another renewable energy resource is developed.

KEYWORDS

Electricity, Pipe turbine, Design, Joint resistance.

1. INTRODUCTION AND LITERATURE REVIEW

In the continuous growth of technology and society, many issues rise from the demands of progress. Some refer to the changes in climate due to pollution, to the shear lack of utilities. One such problem that we are still currently facing is the shortage of electricity. The world is in thorough search for renewable resources of electrical energy, and there has been substantial increase in green energy but with many shortcomings. Among these renewable resources are tidal generators, solar cells, wind turbines, geothermal generators and water turbines. But the shortcomings are that these resources are dependent on multiple factors such as lack of proper reservoir spacing for dams, weather anomalies, time dependencies of solar generators and tide dependencies of wave generators. Although these problems can be reduced to a minimum, other dependencies will still exist. Therefore we are constructing this project to further reduce the generated loses within mainly household and infrastructures. One such area where energy loses are not being addressed to, is found within the water transportation systems. These systems are in fact powered by the green energy projects such as dams, but the outcome of its use is still quite usable. Another place where the energy loses are not addressed is the water pipelines in houses and buildings which require an electric motor to pump water around multiple parts of the area (Breeze, 2005; Sthel, Tostes, & Tavares, 2013; Das, 2015; Junejo, Saeed, & Hameed, 2018). The flowing water in these lines runs at a high velocity at downward bends. Our solution to this problem is to install a small turbine with correspondence to the cross sectional area of the pipe (Lamfon, Najjar, & Akyurt, 1998: Hajmohammadi *et al.*, 2013; Samora *et al.*, 2016).

The water turbine is one of the key technologies used in producing green energy which is beneficial to both, the environment and the society. The turbine uses the flow of water to generate electricity. The design of the turbine is such that when water encounters the blade, the turbine begins to rotate. The continuous force exerted by the water allows the turbine at a tremendously high amount of speed. This rotation is then utilized by a generator, whose rotating shaft is connected to the center of the turbine. Due to this connection the rotary mechanical movement of the turbine is transformed into electrical energy which is used to provide power to other areas. This turbine is only used as generating tools within large reservoirs, but other running water systems are still unaddressed hence there is a loss of

kinetic energy which can be utilized by transforming it into electrical energy (Bauer, Marx, & Drück, 2014; Saeed *et al.*, 2018a; Saeed et al, 2018b).

The utilization of this flow of water is essential, therefore projects over how it can be done is not uncommon. There have been many experimentations of in-pipe water turbine therefore we are taking reference from the research of Oladosu and Koya (2018) from the Department of Mechanical engineering at Obafemi Awolowa University, Nigeria. Their research provided us with ample numerical data on the flow within pipes showing us the coordinates of maximum flow velocity, which is located at the center point of the pipe's diameter. Another research of Jiyun *et al.* (2018) of The Hong Kong Polytechnic University, China, has also been taken into consideration. This research describes the optimal turbine design for the highest efficiency. In their research, they have performed a simulation using a generator connected to a DN-100T-joint turbine to gather energy when placed inside a horizontal pipe in a vertical manner. The blade designs are shown to be more cup-shaped to allow contact with a larger volume of water. The results show that the turbine is giving a maximum efficiency of 55% upon nozzle adjustments. Another inspiration for our design is accredited to the research of Joel Titus and Bakthavatsalam of the National Institute of Technology, Tiruchirappalli, India. Their semi-submerged design is considerably easier to construct and install in remote locations and is extremely viable in irrigation systems (Jiyun, 2017). However their simplistic design the turbine itself hinders the efficiency of energy production. By further widening and cupping the blades of the turbine, a larger volume of water can encounter the blades thus giving a higher angular acceleration and producing more electrical power. The research performs by Jiyun *et al.* (2018) of The Hong Kong Polytechnic University has also helped in designing our project. Their work on the outer angle of the turbine blade shows that the blade must be curved enough so that the inner wall of the turbine blade is parallel to the flow of water, but the outer wall of the blade does not receive first contact with the flowing water. This will allow the water to apply a larger force onto the blade of the turbine while decreasing the velocity of the water for short period of time to allow the other blade to sink into the water.

2. METHODOLOGY

We have divided this research into three phases:

1. Designing

2. Construction

3. Testing

For the designing phase, we make our design on the SolidWorks software. On it we created the parts necessary for the construction of the turbine. We created a metal disk of thickness 0.5 inches and a diameter of 6 inches. We then constructed the spoon for the turbine. The outer diameter of the cup of the spoons is of 0.47 inches whereas the inner diameter is of 0.4 inches. These spoons will act as the blades of the turbine and the cup of these spoons will be placed at the center of the pipe where the fluid velocity is at its highest. The two parts, disk and spoons are then assembled together after the spacing for the spoons is cut into the turbine disk. We then constructed and attached a shaft of 0.3 inches diameter into the center of the turbine disk. This shaft is a part of the DC output motor that will be connected to the turbine for electricity production. We then created a prototype pipeline of three parts which's center piece is cut halfway. We then placed the turbine on to the pipeline accordingly in the assembly. Finally, we then constructed a cover box for the turbine so that water may not leak from the system out into the surrounding.

For the construction phase, we decided on using a thin metal sheet for the disk because if turbine becomes too heavy, much larger force will be required to rotate the turbine at high speed, thus hampering the efficiency of the output. This sheet is then mechanically cut into a circular shape of a diameter 6 inches. Small cuts for the joining of the spoons are applied onto the metallic disk at 45° intervals.

For the testing phase we will apply a certain amount of external loading through simulations using SolidWorks onto the cup of the spoon while keeping the handle of the spoon fixed as it will be joined with the turbine disk. By applying a distributed loading on the cup of the spoon we can mimic the effects of the water pressure exerted onto the spoon. Motion analysis of the assembly will also be performed on the software to understand the movement output of the assembled turbine (Song, Ni, & Tan, 2011).

3. ANALYSIS AND OBSERVATION

Wireless by performing static analysis on the spoon using SolidWorks, we observe that the highest amount of stress is acting on the area between the cup and handle due to which there will be a small amount of displacement of the cup hence giving a low factor of safety of the entire spoon. However, since this is a static analysis, the rotatory motion of the turbine disk has not been considered. If the rotation of the turbine would be considered, the stress on the critical region of the spoon would substantially decrease therefore a higher factor of safety can be attained without the requirement of a stronger and more expensive material.
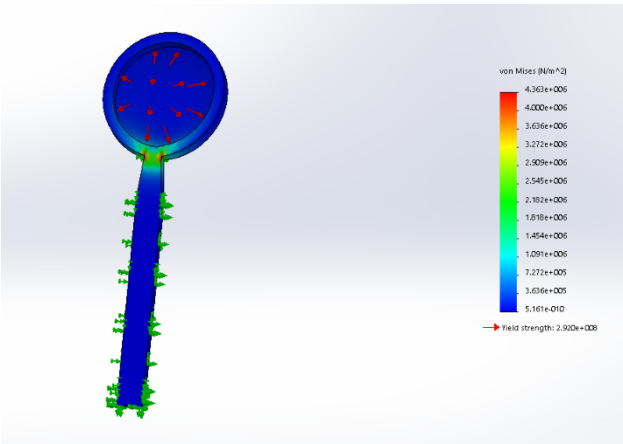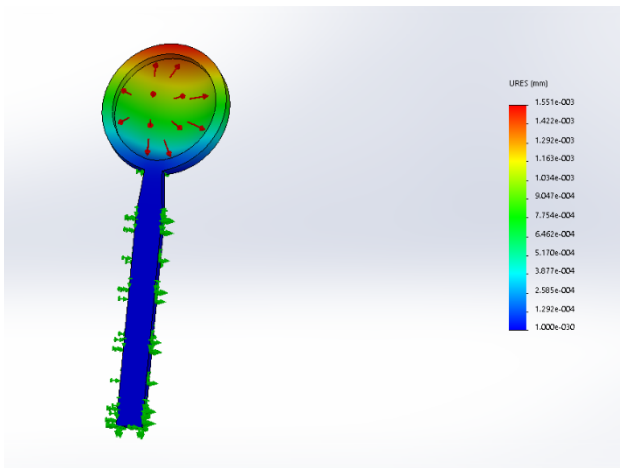

Figure 1. Stress Diagram.
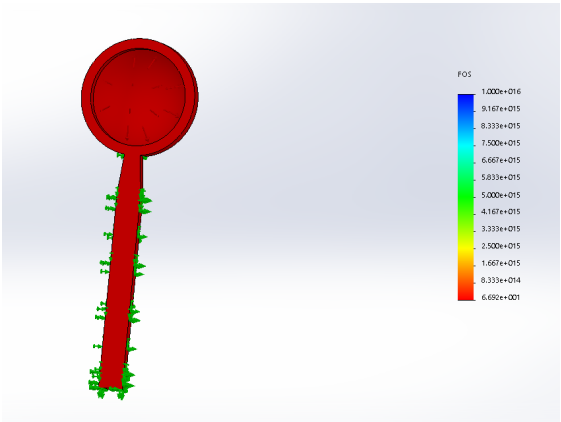

Figure 2. Strain Diagram.

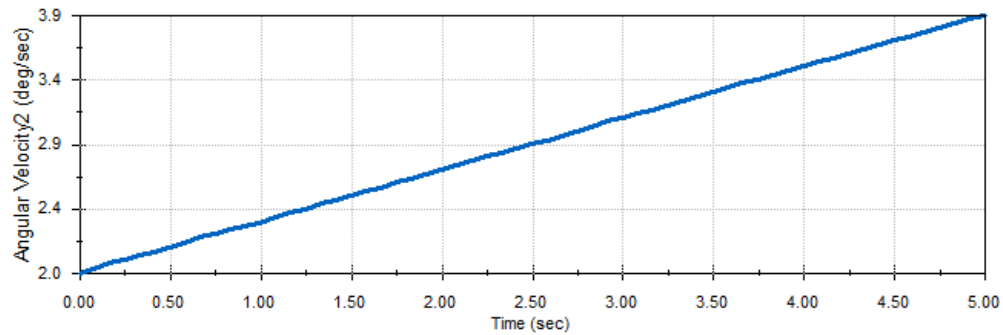**Figure 3.** Factor-of-Safety Diagram.

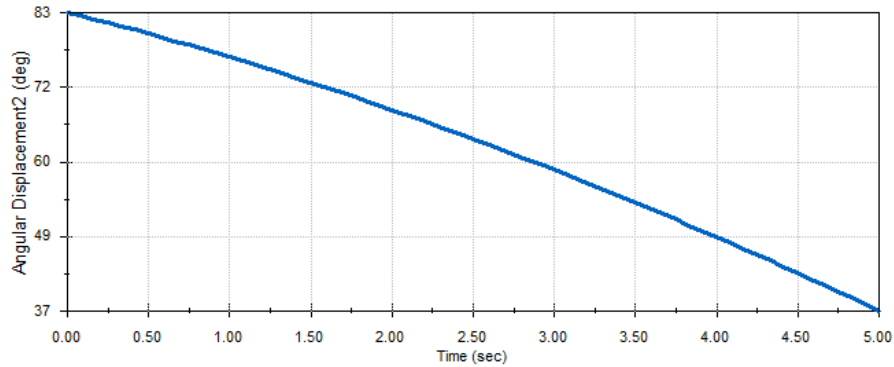
Figure 4. Angular velocity against time.

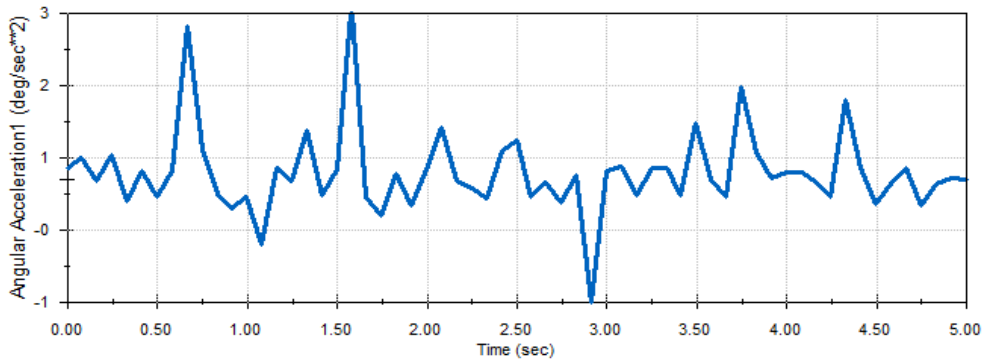**Figure 5.** Angular displacement against time.

Figure 6. Angular acceleration against time.

The angular acceleration graph of the turbine displays ecstatic as there is a small amount of resistance in the joints of the cover therefore there is a reverse acceleration. This resistance may be due to the changes in the applied pressure of the water flowing within the pipes or if the spoon is touching the edges of the wall.

4. CONCLUSION

The turbine shows a good amount of electrical output but can further be improved if the joint resistance is addressed by adding a ball bearing that will increase the motion. A better design of the turbine can also be achieved by fully submerging the turbine instead of partial submersion without the detriment of ease in installation and maintenance.

The design can further be implemented on other flowing bodies of water such as rivers and canals by increasing and decreasing the size respectively of the turbine as this design can be applied over multiple flowing bodies of water.

REFERENCES

Bauer, D., Marx, R., & Drück, H. (2014). Solar District Heating for the Built Environment-Technology and Future Trends within the European Project EINSTEIN. *Energy Procedia*, *57*, 2716-2724. https://doi.org/10.1016/j.egypro.2014.10.303

Breeze, P. (2005). *Power Generation Technologies*. Elsevier. https://doi.org/10.1016/C2012-0-00136-6

Das, G. (2015). Advantages of green technology. *International Journal of Research - GRANTHAALAYAH, 3*(9), 1-5. https://www.researchgate.net/publication/306402862_ADVANTAGES_OF_GREEN_TECHNOLOGY

Hajmohammadi, M. R., Eskandari, H., Saffar-Awal, M., & Campo, A. (2013). A new configuration of bend tubes for compound optimization of heat and fluid flow. *Energy, 62*, 418-424. https://doi.org/10.1016/j.energy.2013.09.046

Jiyun, D., Hongxing, Y., Zhicheng, S., & Xiadong, G. (2017). Micro hydro power generation from water supply system in high rise buildings using pump as turbines. *Energy, 137*, 431-440. https://doi.org/10.1016/j.energy.2017.03.023

Jiyun, D., Hongxing, Y., Zhicheng, S., & Xiadong, G. (2018). Development of an inline vertical cross-flow turbine for hydropower harvesting in urban water supply pipes. *Renewable Energy, 127*. https://doi.org/10.1016/j.renene.2018.04.070

Junejo, F., Saeed, A., & Hameed, S. (2018). 5.19 Energy Management in Ocean Energy Systems. *Comprehensive Energy Systems, 5*, 778-807. https://doi.org/10.1016/B978-0-12-809597-3.00539-3

Lamfon, N. J., Najjar, Y. S. H., & Akyurt, M. (1998). Modeling and simulation of combined gas turbine engine and heat pipe system for waste heat recovery and utilization. *Energy Conversion and Management, 39*(1-2), 81-86. https://doi.org/10.1016/S0196-8904(96)00175-6

Oladosu, T. L., & Koya, O, A. (2018). Numerical analysis of lift-based in-pipe turbine for predicting hydropower harnessing potential in selected water distribution networks for waterlines optimization. *Engineering Science and Technology, an International Journal, 21*(4), 672-678. https://doi.org/10.1016/j.jestch.2018.05.016

Saeed, A., Mithaiwala, H. M., Hussain, A. I., Kukda, M. F., & Shoukat, M. H. (2018a). Enhancement of Efficiency through optimization of flywheel. In *7th International Conference on Renewable Energy Research and Applications (ICRERA),* 124-129. https://doi.org/10.1109/ICRERA.2018.8566986

Saeed, A., Zubair, M., Khan, F. A., Mairaj, F., Siddique, M., & Shiwanli, A. (2018b). Energy Savings through Ammonia Based Absorption Chiller System: A proposed Strategy. In *7th International Conference on Renewable Energy Research and Applications (ICRERA)*, 168-173. https://doi.org/10.1109/ICRERA.2018.8566805

Samora, I., Hasmatuchi, V., Münch-Alligné, C., Franca, M. J., Schleiss, A. J., & Ramos, H. M. (2016). Experimental characterization of a five blade tubular propeller turbine for pipe inline installation. *Renewable Energy, 95*, 356-366. https://doi.org/10.1016/j.renene.2016.04.023

Song, F., Ni, Y., & Tan, Z. (2011). Optimization design,modeling and dynamic analysis for composite wind turbine blade. *Procedia Engineering, 16*, 369-375. https://doi.org/10.1016/j.proeng.2011.08.1097

Sthel, M., Tostes, J. G. R., & Tavares, J. R. (2013). Current energy crisis and its economic and environmental consequences: Intense human cooperation. *Natural Science, 05*(02), 244-252. https://www.researchgate.net/publication/276492317_Current_energy_crisis_and_its_economic_and_environmental_consequences_Intense_human_cooperation

/04/

PERFORMANCE ANALYSIS OF THE QUANTUM PROCESSOR: BASED ON REVERSIBLE SHIFT REGISTER USING QCA

Rajinder Tiwari

Research Scholar, Department of ECE, ASET, Amity University, Lucknow (India).

Associate Professor, Department of ECE, Model Institute of Engineering and Technology (MIET), Jammu, (India).

E-mail: trajan@rediffmail.com ORCID: https://orcid.org/0000-0003-1734-5892

Anil Kumar

Asst. Pro VC and Director, ASET, Amity University, Lucknow, (India).

E-mail: akumar3@lko.amity.edu ORCID: https://orcid.org/0000-0001-8976-3642

Preeta Sharan

Professor, Department of ECE, The Oxford College of Engineering and Technology, Bengaluru, (India).

E-mail: sharan.preeta@gmail.com ORCID: https://orcid.org/0000-0002-3549-7147

ABSTRACT

The concept of the reversible logic depends on the dominant modules of a processor that has motivated to obtain the performance analysis of the quantum based processors. In continuation to this discussion, the shift register can be studied with the use of the reversible logic which is capable of shifting the bits of the information towards both side i.e. left and right. In this process of the analysis of the quantum processor, the Quantum Computational Automata (QCA) as well as Verilog, software has been used so as to simulate the parameters of the device and then obtain the characteristics of the device. In this discussion, a reversible logical computing based approach has been mentioned that can be used in the ALU of a quantum processor with the help of D-type FFs or its combination that act as an inevitable and the most crucial basic building block in the design of quantum processor. This circuit has been designed and analyzed for the most dominant parameters, say, size of cell, number of cells used, delay, temperature dependency, power dissipation, etc. This proposed circuit which acts as an alternative to the CMOS technology, has been analyzed for a typical range of the power dissipation $(650 - 750 \text{ meV})$, temperature range $(1^{o}K - 10^{o}K)$.

KEYWORDS

QCA, CMOS, Power Dissipation, QCA Well, Shift Register, Reversible Logic Computation, Quantum Processor.

1. INTRODUCTION

The QCA is the foremost and potentially promising technology which has been accepted for the typical Nano range of the frequency in the device implementations. In other words, we can say that this QCA has been emerged as the solution to the limitations of the CMOS Technology existing in the range of microns or micro of the frequency i.e. in terms of speed or delay of the data transmission, density or area in terms of the number of quantum cell used, etc. Due to this unique feature of the quantum computing with the help of QCA has emerged as a fantastic approach in the design and implementation of the device that provides the desired characteristics and performance. The demonstration of the QCA technology has been done simply by implementing it with Quantum Dots i.e. metal dots at quite predominant range of the parameters, say, temperature, pressure, etc. (Tiwari, Kumar, & Sharan, 2018).

It means that these metal dots have been used in the design of various basic blocks or modules of this system such as QCA based wires, logic gates, memories, and reversible gates. As per Moore's law, it has been seen that after every ten years the density of the components fabricated on the chip gets almost doubled that becomes the most significant limitations of the CMOS Technology. In other words, it has been observed that size and area of the fabricated board keeps on increasing that in turn increases the overall size of the processor. Due to this reason, the power dissipation i.e. loss of energy is quite large in this technology, delay is also quite huge. All these limitations are taken care by simply making use of QCA tools that operate in the range of nanoscale. In this technology, the fabrication techniques of the chips played quite dominant role with the desired performance such as preparation of dyes for the ICs which includes quite complex structure and resistant to various degradation methods. The fabrication process of the ICs includes the standard techniques as compared to the conventional methods of separating the impurities such as oxidation, membrane separation, precipitation, etc. (Tiwari *et al.*, 2018).

An important problem of the design and implementation of reversible logic based universal shift register for a quantum processor, especially, the ALU of desired bit. In the context of designing the highly efficient ALU, one must formulate the study and implementation of the important modules of the ALU such as comparator, shift register, logic gates, memories, etc.

with the help of the reversible computing. In this discussion, the problem has been based on designing and implementing a reversible logic based shift register that is bidirectional in nature. Now in order to obtain the understanding of this technique, one must obtain the comparative analysis of this concept with the prevailing technology i.e. CMOS Technology. For the proper understanding of this technology, one must discuss the development process of this technique with the help of ITRS in the scale of 45nm (Tiwari *et al.*, 2017).

2. QUANTUM CELLULAR AUTOMATA (QCA)

With the development of this technology in the nano scale range, various devices have been designed and implemented which in turn becomes the basic building blocks of most of the system, say, ALU which is designed for quantum processors. Few of the most commonly used devices based on this system are discussed below with help of figures. It is commonly used in the circuits based on nano technology i.e. in nanometer scale with an innovative feature of bonding the charge carriers in more than one dimension. In this topology, the charges are contained in this circuit due to its potential energy. The typical examples of the quantum dots are shown in the below Figure 1 (b) (Tiwari *et al.*, 2018).

The basic logical unit which behaves as the most commonly used element in the quantum computational automata (QCA) as shown in below Figure 1 (a). On the basis of the performances and results obtained with the use of this device i.e. QCA in nanoscale of the frequency of the input signal as compared to the 45 nm CMOS technology. This technology has proved to be the best alternative of the devices like the transistors, silicon, and CMOS paradigm with the quantum elements i.e. QCA well of quantum energy (Tiwari, 2019).
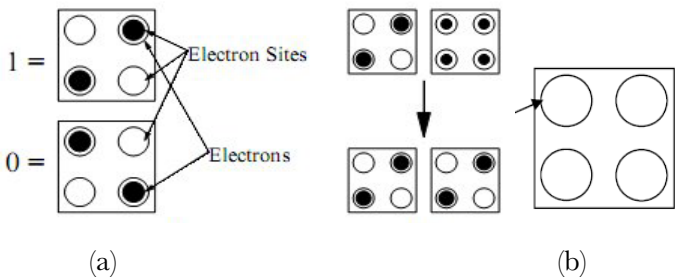
Figure 1. (a) QCA (b) Single Cell. Source: (Tiwari *et al.*, 2018).

The quantum computing is implemented simply by controlling the tunneling phenomenon of the charges with the help of four phase clock signal of the cell that has been used in the development of the system as shown in the below Figure 2 (Singh, & Pandey, 2016).
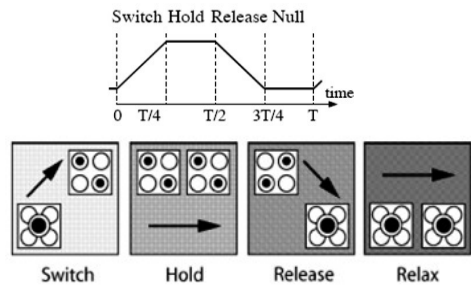
Figure 2. QCA Clockwise Sequencing. Source: (Tiwari *et al.*, 2018).

QCA Wires as shown in below Figure 3.
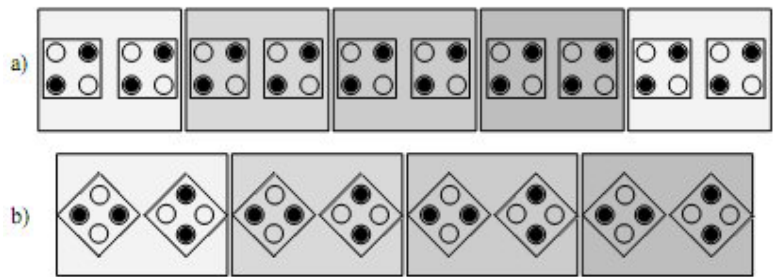
Figure 3. (a) 90° Orientation (b) 45° Orientation of the Cell. Source: (Tiwari *et al.*, 2018).

Majority gate i.e. a three inputs A, B and C device using fours quantum cells as shown in below Figure 4. These cells are oriented with the charge orientation based logic values i.e. 0 and 1with the corresponding input and out terminals. The operational behavior of this majority has been explained with the help of below given equation 1 (Thapliyal, Ranganathan, & Kotiyal, 2013).
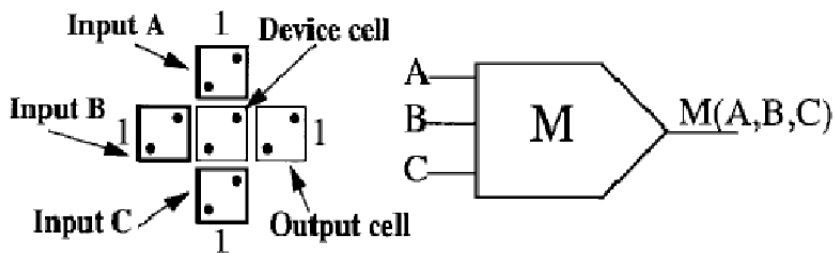
Figure 4. M-Gate. Source: (Rajmohan, & Ranganathan, 2011).

$$M(A,B,C) = AB + AC + BC \qquad (1)$$

Logical gates as shown in below Figure 5.
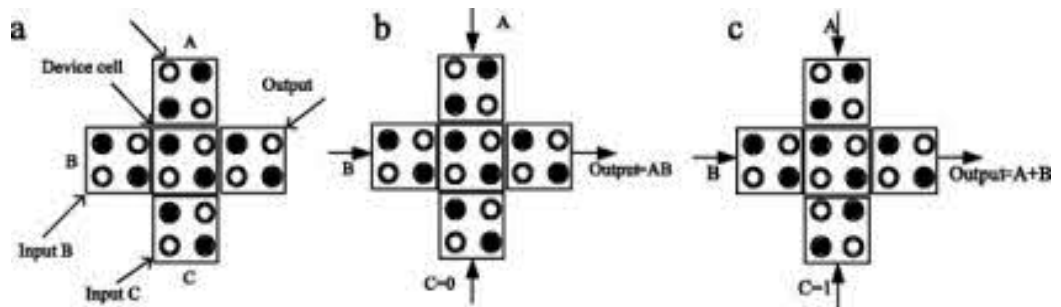
Figure 5. Logic Gates using QCA. Source: (Ganesh, Kishore, & Rangachar, 2008).

QCA Based Memories as shown in the below given Figure 6.
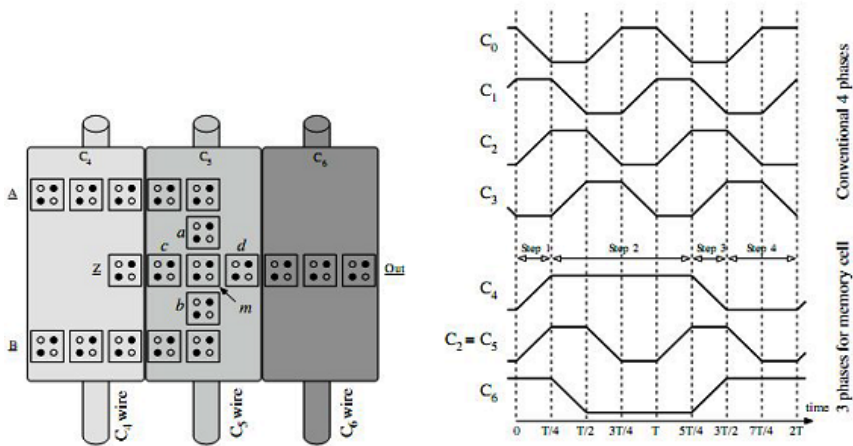
Figure 6. Line based QCA Memory. Source: (Ganesh *et al.*, 2008).

These gates operating on reversible computing have equal number of inputs and outputs as compared to the traditional gates and have bi-mappings between input vectors and output vectors; consequently the input data can be recreated from the output vector states. A reversible gate with n inputs and n output is known as n * n gate as shown in below Figure 7. Feynman Gate is a 2 * 2 reversible gate as shown in the below Figure 7 which is also known as CNOT, i.e., controlled NOT Gate. The input (A, B) and output (P, Q) relation is as follows i.e. (Roohi & Khaemol, 2014).

$$P = A \tag{2}$$

$$Q = A \oplus B \tag{3}$$

On the contrary, Fredkin gate is a (3 * 3) conservative reversible gate as shown in the below Figure 8. The relation between input vectors and its output vectors is as follows (Walus *et al.*, 2004).

$$P = A \tag{4}$$

$$Q = {}^-AB + AC \tag{5}$$

$$R = AB + {}^-AC \tag{6}$$
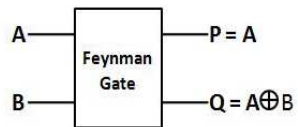
Figure 7. Feynman Gate. Source: (Ali, Hossin, & Ullah 2011).
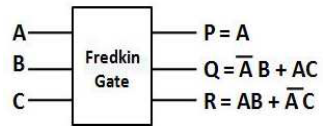
Figure 8. Fredkin Gate. Source: (Ali, Hossin, & Ullah 2011).

3. REVERSIBLE COMPUTING BASED SHIFT REGISTER MEMORY

Based on the above discussion about the performance of the reversible logic based gates as compared to the traditional gates, there are ample circuits that have been implemented for the quantum system. Out of these, the author has discussed the behavior of the shift register based memory cell which proves to be the most valuable module of the quantum processors. The typical design of the memory cell i.e. shift register is shown in the above given Figure 9 (Tiwari *et al.*, 2017).
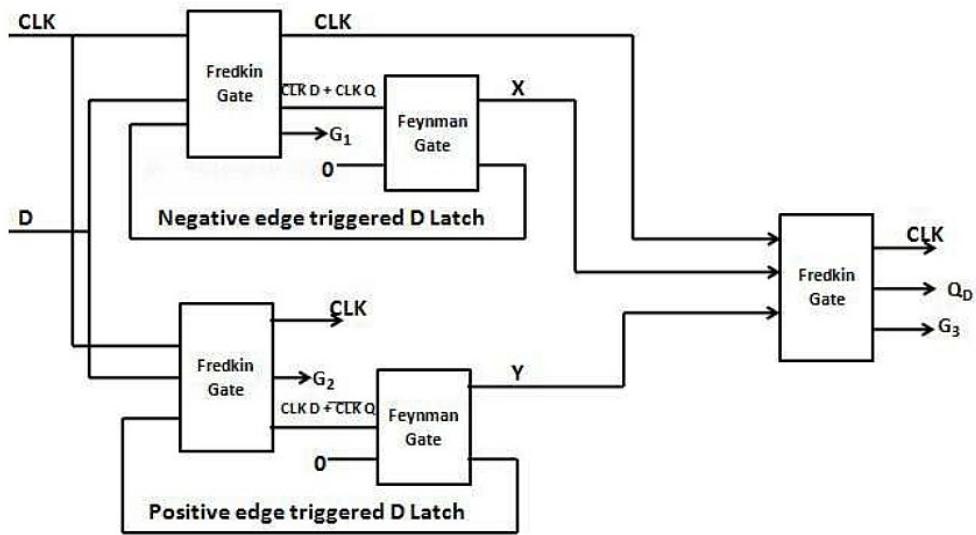
Figure 9. Basic Diagram of Shift Register Memory. Source: (Das & De, 2013).

$$X = \left(\left(\frac{R}{W} \right)' . D + \left(\frac{R}{W} \right) D' \right) = X \odot D \qquad (7)$$

$$Y = D \qquad (8)$$

4. PROPOSED UNIVERSAL SHIFT REGISTER MODEL FOR QUANTUM PROCESSORS

Reversible Universal Shift Register for Quantum Processor (ALU):

In this discussion, the author has extended the above discussion of designing and implementing the shift registers which is capable of rotating in both left and right direction with the reversible logic gates. In this discussion, reversible computing based Delay Flip Flop and 4:1 multiplexer has been used to obtain the circuit design. The efficiency of this proposed circuit has been evaluated using QCA and an analysis can be obtained with the reference circuit based on the number of cell i.e. density of the circuit, data transferring speed i.e. delay, etc. The below given 10 and 11 shows the design of the circuit using the QCA tool. Here the Figure 10 shows 4-bit shift register which has been design by making use of 4:1 MUX and four stages of the Delay Flip Flop with the PIPO data flow. Similarly, the below given Figure 11 provides us an alternative approach of the design of

the proposed circuit with the help of the reversible gates i.e. 8:1 MUX and eight stages of Delay Flip Flops.
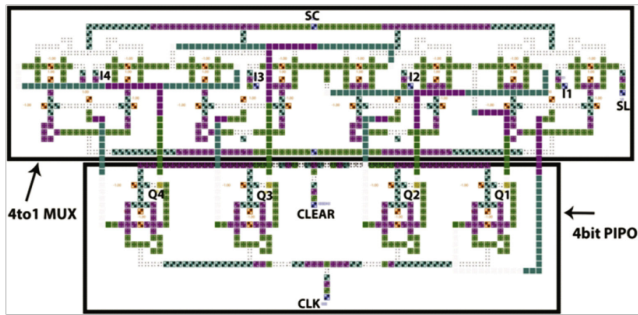
Figure 10. Proposed Circuit (Universal Shift) PIPO-4-Bit.

Figure 11. Proposed Circuit (Universal Shift) PIPO-8-Bit.
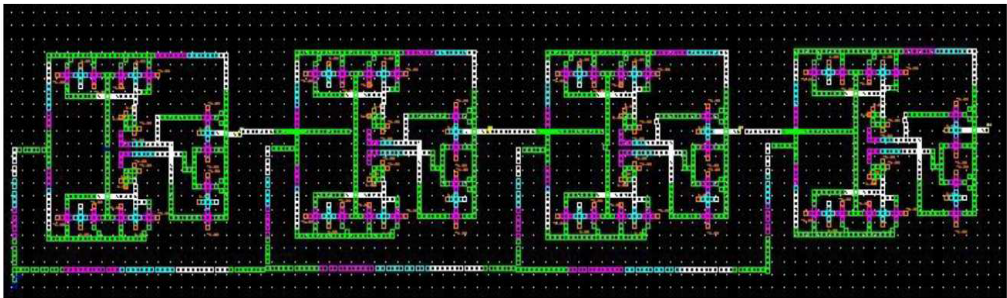
Figure 12. Proposed Circuit (Universal Shift) SIPO 4-Bit.

The above Figure 12 shows another configuration of designing the proposed model with SIPO data flow tendency with the use of Delay Flip Flops.

Reversible Logic Gates Based D Flip Flop:

Another technique of designing the circuit of Delay Flip Flop has been considered for the quantum processors, especially, the modules which are dominant for the design of ALU. The below given Figure 13 shows the Delay Flip Flop using the QCA Designer Tool 2.0.
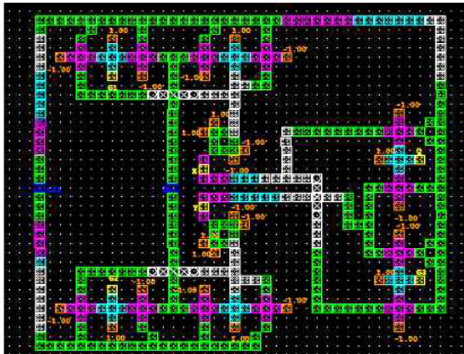
Figure 13. QCA Implementation of D Flip Flop used in Proposed Circuit.

Reversible 4:1 Multiplexer Using QCA Tool:

The below given Figure 14 (a) and 14 (b) shows the schematic arrangement of the 4:1 MUX so as to obtain the desired performance in terms of switching the desired input at the output of the circuit. This circuit has been proven to the most predominant module of the shift register of the ALU designed primarily for the quantum processors.
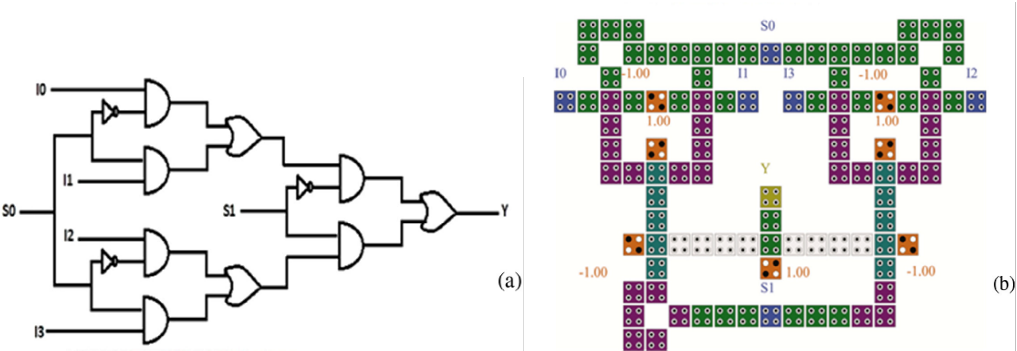
Figure 14. Schematic Circuit & QCA Implementation of 4: 1 MUX used in Proposed Circuit.

5. SIMULATION RESULTS & DISCUSSIONS

The performance of the proposed model discussed based on the most pre-dominant parameters of the reversible logic based shift register i.e. area of the cell, number of cells used, delay i.e. speed of the data transmission between output and input of the circuit. Thus, based on the behavior of these parameters, using QCA Designer Tool 2.0, writing the codes for the structure behavior of the proposed model using VHDL and Verilog codes. In this proposed circuit, the author has made the use of the reversible gates with best

3C Tecnología. Glosas de innovación aplicadas a la pyme. ISSN: 2254 – 4143   Edición Especial Special Issue Abril 2020

efficiency i.e. Fredkin & Feynman gates. From this simulation as shown in Figure 15, it has been observed that the power dissipation or the loss of information of these two reversible gates is quite less as compared to others. Due to this reason, these gates are quite common in use for the development of various modules of the quantum processors. These reversible gates have got a limitation due to tunneling effect of the energy which in turn causes the increase in the power dissipation. This discussion of the author has been supported with the help of below give Table 1 and Figure 16 that gives the information of the power dissipation of the proposed model with respect to the circuits of the reference work done by others.
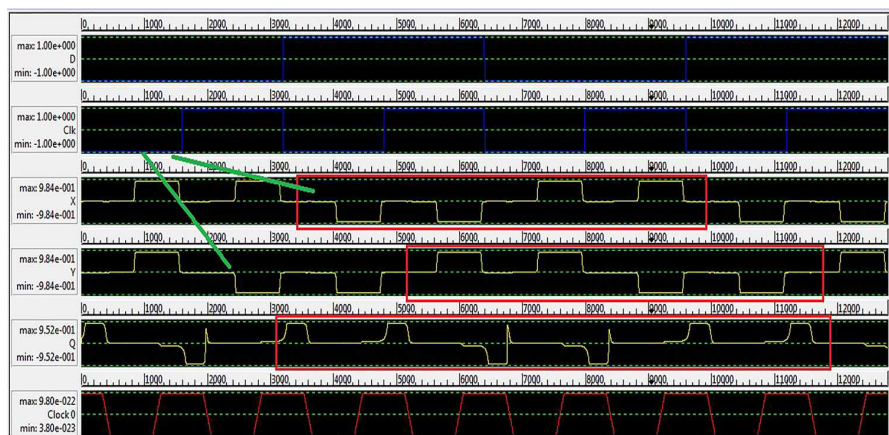
Figure 15. Simulation results of the Proposed Circuit using QCA Designer Tool.
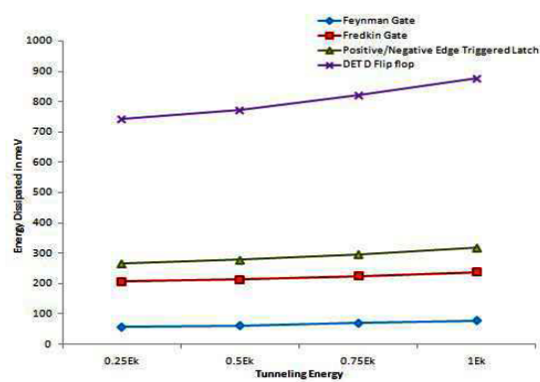
Figure 16. Power & Energy Analysis of the Proposed Model.

This discussion based on the performance of the proposed circuit of universal shift register has been carried out based on the delay comparison, cell count comparison, area comparison has been simulated with the use of some suitable software as shown in below Figure 17.

Table 1. Power Dissipation in Proposed Model using Reversible Logic Gates.

Proposed QCA Based Model	Power Dissipated at T=2°K (meV)			
	0.25Ek	0.5Ek	0.75Ek	1Ek
Feynman Gate	58.4	63.4	70.9	79.6
Fredkin Gate	208.6	215.6	226.6	239.6
Reversible 4:1 MUX	267	279	297.5	318.8
Reversible D Flip flop	742.6	773.6	821.6	876.8
Reversible Universal Shift Register	651.2	648.2	676.2	688.2

The below given Figure 17 fives the behavior of the universal circuit with the reference work carried out by other researchers in terms of the temperature with a mean polarization of the quantum cells i.e. XE-001 neV.
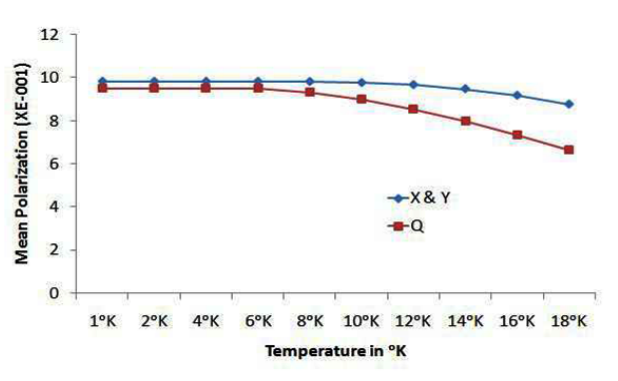
Figure 17. Comparison of the Proposed Model with Reference Model in terms of Temperature.

From the above discussions, it has been found that the power dissipation and the loss of energy of the proposed circuit using majority gates using the reversible computing ability. On this basis of these all, the author has concluded with the simulated result supported by Table 1 providing the comparative analysis based on the considered parameters.
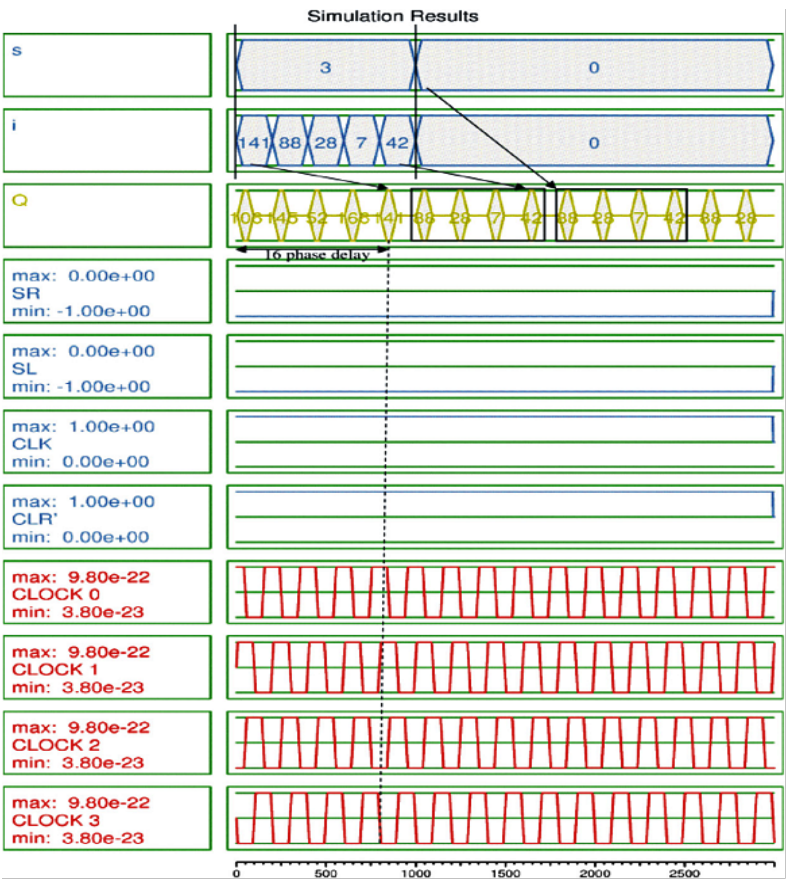
Figure 18. Overall Performance Based Simulation Results of the Proposed Model.

The above Figure 18 shows the overall performance of the proposed model of the universal shift register for the quantum processor, i.e. the ALU which is using the reversible logic based computing as compared to the 45 nm CMOS Technology.

6. CONCLUSION

In this paper, the authors has undergone with a non-exhaustive literature survey to obtain the problem enunciation of this problem. In this process, the author has taken the most dominant parameters i.e. number of cells, delay and area of the quantum cells of the reversible gates to design and implement an innovative circuit of universal shift register that can be used for the design of ALU of the quantum processor. In this context, the author has made the use of the circuit of 4:1 multiplexer in addition to the reversible gate based D

flip flop in order to design and implement the 4-bit as well as 8-bit shift register with SIPO and PIPO based data transmission. This proposed circuit which acts as an alternative to the CMOS technology, has been analyzed for a typical range of the power dissipation (650-750 meV), temperature range (1°K-10°K).

ACKNOWLEDGEMENTS

REFERENCES

Ali, M. B., Hossin, M. M., & Ullah, M. E. (2011). Design of Reversible Sequential Circuit using Reversible Logic Synthesis. *International Journal of VLSI Design & Communication Systems (VLSICS)*, *2*(4), 37-45. https://www.researchgate.net/publication/276200730_Design_of_Reversible_Sequential_Circuit_Using_Reversible_Logic_Synthesis

Das, J. C., & **De, D.** (2013). Reversible binary to grey and grey to binary code converter using QCA. *IETE Journal of Research, 61*(3), 223–229. https://doi.org/10.1080/03772063.2015.1018845

Ganesh, E. N., Kishore, L., & Rangachar, M. J. S. (2008). Implementation of quantum celular automata combinational and sequential circuits using Majority Logic reduction method, *International Journal Nanotechnology and Applications, 2*(1), 89-106. https://www.academia.edu/8038090/Implementation_of_Quantum_cellular_automata_combinational_and_sequential_circuits_using_Majority_logic_reduction_method

Rajmohan, V., & Ranganathan, V. (2011). Design of Counters using Reversible Logic. In *3ʳᵈ IEEE International Conference on Electronics Computer Technology,* 138-142. https://doi.org/10.1109/ICECTECH.2011.5941973

Roohi, A., Khademolhosseini, H., Sayedsalehi, S., & Navi, K. (2011). A Novel Architecture for Quantum-Dot Cellular Automata Multiplexer. *International Journal of Computer Science Issue (IJCSI), 8*(6), 55-60. https://www.ijcsi.org/papers/IJCSI-8-6-1-55-60.pdf

Shamsabadi, A. S., Ghahfarokhi, B. S., Zamanifar, K., & Movahedinia, N. (2009). Applying inherent capabilities of quantum-dot cellular autómata to design: D flip flop Case Study. *Journal of System Architectecture, 55*(3), 180–1877. https://doi.org/10.1016/j.sysarc.2008.11.001

Singh, R., & Pandey, M. K. (2016). Design and Optimization of Sequential Counters using a Novel Reversible Gate. In *International Conference on Computing, Communication and Automation, (ICCCA), Noida, India.* https://doi.org/10.1109/CCAA.2016.7813936

Thapliyal, H., Ranganathan, N., & Kotiyal, S. (2013). Design of Testable Reversible Sequential Circuits. *IEEE Transactions on Very Large Scale Integration (VLSI) Systems,* 21(7), 1201-1209. https://doi.org/110.1109/TVLSI.2012.2209688

Tiwari, R. (2019). A Novice Approach to Implementation of System on Chip Based Smart CMOS Sensor for Quantum Computing Based Applications. In *2ⁿᵈ International Conference on Microelectronics, Computing and Communication Systems (MCCS 2017), 476, 563-574.* https://www.researchgate.net/publication/330222760_A_Novice_Approach_to_Implementation_of_System_on_Chip_Based_Smart_CMOS_Sensor_for_Quantum_Computing_Based_Applications

Tiwari, R., Bastawade, D., Sharan, P., & Kumar, A. (2017). Performance Analysis of Reversible ALU in QCA. *Indian Journal of Science & Technology, 10*(29), 01-05. https://www.researchgate.net/publication/319466556_Performance_Analysis_of_Reversible_ALU_in_QCA

Tiwari, R., Kumar, A., & Sharan, P. (2018). Design and Implementation of 4:1 Multiplexer for Reversible ALU using QCA. In *2nd International Conference Microelectronics and Telecommunication Engineering (ICMETE 2018), Ghaziabad, India,* 191-196. https://doi.org/10.1109/ICMETE.2018.00050

Tiwari, R., Kumar, A., & Sharan, P. (2018). Performance Analysis of Universal Circuit for Reversible ALU using QCA & CMOS Technology. *International Journal of Engineering & Technology (UAE)*, *7*(4.38), 732-736. https://doi.org/10.14419/ijet.v7i4.38.25775

Walus, K., Dysart, T. J., Jullien, G. A., & Budiman, R. A. (2004). QCADesigner: a rapid design and Simulation tool for quantum-dot cellular autómata. *IEEE Transactions on Nanotechnology, 3*(1), 26-31. https://doi.org/10.1109/TNANO.2003.820815

/05/

AC/DC CRITICAL CONDUCTION MODE BUCK-BOOST CONVERTER WITH UNITY POWER FACTOR

Abdul Hakeem Memon

IICT, Mehran UET, Jamshoro, Sindh, (Pakistan).

E-mail: hakeem.memon@faculty.muet.edu.pk ORCID: https://orcid.org/0000-0001-8545-3823

Fazul Muhammad Noonari

IICT, Mehran UET, Jamshoro, Sindh, (Pakistan).

E-mail: fazulmuhammad@gmail.com ORCID: https://orcid.org/0000-0003-4252-2782

Zubair Memon

IICT, Mehran UET, Jamshoro, Sindh, (Pakistan).

E-mail: zubair.memon@faculty.muet.edu.pk ORCID: https://orcid.org/0000-0001-5967-3152

Ahmar Farooque

IICT, Mehran UET, Jamshoro, Sindh, (Pakistan).

E-mail: dahri.ahmar@outlook.com ORCID: https://orcid.org/0000-0003-0015-482X

Mohammad Aslam Uqaili

IICT, Mehran UET, Jamshoro, Sindh, (Pakistan).

E-mail: aslam.uqaili@faculty.muet.edu.pk ORCID: https://orcid.org/0000-0002-6102-3623

ABSTRACT

The buck-boost converter operating in critical conduction mode (CRM) is commonly utilized in various applications because of many advantages like protection against short circuit, minimum component count, low operating duct-cycle, and low voltage on MOSFETs. However, its input power factor (PF) is not high while operating in constant on-time control. To attain unity PF for universal input voltage range, a new control scheme of variable on-time control (VOTC) is proposed in this paper. The VOTC can be implemented by modulating the turn-on time of the buck-boost switch. The working principle and performance comparison of the converter is discussed with both types of control scheme. The input PF the converter is high in case of VOTC than the COTC. Simulation results are presented to verify the effectiveness of the proposed control strategy).

KEYWORDS

Buck-boost converter, Power factor, Critical conduction mode.

1. INTRODUCTION

Power electronic technology is employed in various sorts of modern equipment's which has made our life, simpler, easier and comfortable. However, with this comfort and easiness this technology brings power quality issues because it is centered on solid-state devices. These issues introduce harmonic contained current or distorted current which has several drawbacks like more power loss, voltage distortion and EMI compatibility issues etc. Therefore, the standards are set by various industrious like IEC61000-3-2 limit and IEEE 519 (IEC 61000-3-2:2014, 2014; Langella, Testa, & Alii, 2014) to limit these harmonics. In order to meet relevant harmonic standard and reducing input current distortion, power factor correction (PFC) converter has been widely applied (García *et al.*, 2003; Singh *et al.*, 2011; Memon *et al.*, 2017; Memon *et al.*, 2018; Memon *et al.*, 2019). Generally, conventional power converter topologies, such as boost, buck-boost and buck converters, can be used to achieve low cost single-stage PFC, and each converter topology has its own characteristics. The traditional boost PFC converter, with advantages of low input current ripple, high efficiency and inherent current shaping ability, is a good choice for PFC application. However, it cannot maintain high efficiency at universal input voltage. Buck converter can maintain high efficiency at all input voltages. However, there is no input current when the output voltage is less than input voltage (Memon *et al.*, 2018). The traditional buck-boost topology, with advantages of inherent current shaping ability, low cost, step-down and step-up voltage conversion, is a good choice compared with flyback, CUK and SEPIC converters. It is used in many applications such as wind energy control, Adaptive control applications, and power amplifier applications etc. However, when the on-time is constant, the power factor (PF) of buck-boost PFC converter is low.

For modifying the performance of buck/boost converter, various researchers have proposed various techniques and control schemes. In Ghanem, Al-Haddad, and Roy, (1996), a new control mechanism is presented to increase the PF near to unity for a cascaded buck-boost converter for the high-power application in continuous conduction mode (CCM). Comparative analysis between single stage buck converter and the single buck-boost converter in discontinuous conduction mode is given in Moschopoulos and Zheng (2006). The work in Wei *et al.* (2008) has done the comparative study between the bridged buck-boost PFC converter and bridgeless buck/boost PFC converter and proposed the bridgeless

buck-boost PFC topology for improving the efficiency. In Jayahar and Ranihemamalini (2011), inductor average current control strategy is proposed for improving PF of CCM buck-boost converter. The work in Jayahar, Ranihemamalini, and Rathnakannan (2016) has given the solution to improve PF for CCM buck converter. The bridgeless buck-boost converter with switched capacitor for low power applications is put forward in Saifullah *et al.* (2017) for reducing the conduction losses and improving the efficiency.

In this paper, an improved control scheme for buck-boost converter operating under critical conduction mode (CRM) is proposed to realize unity PF.

This paper is divided into six sections. In section 2, the operation states of CRM buck-boost PFC converter are analyzed with traditional control. The proposed control scheme is introduced in section 3 to realize unity PF. Then the comparative analysis is discussed in section 4 in terms of input PF. In section 5, the effectiveness of proposed topology is evaluated by simulation results. Finally, some conclusions are drawn in section 6.

2. OPERATING PRINCIPLE OF THE CONVERTER

Figure 1 illustrates the power circuit of buck-boost converter in CRM mode. It comprises of bridge diode rectifier, a buck-boost switch (Q_{b-b}), a freewheeling diode (D_{fw}), an inductor (L) and an output capacitor (Co), etc.
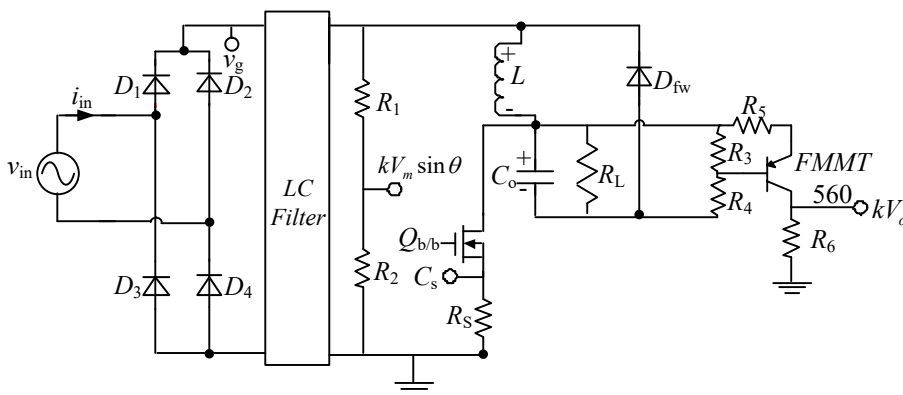
Figure 1. Power circuit of a buck-boost converter.

The instantaneous and rectified input voltage during half line cycle can be given as:

$$v_{in} = v_a = V_{pk} \sin \theta \tag{1}$$

Whereas ''V_{pk}'' represent the input voltage amplitude, θ represent the input voltage angle.

There are two switching cycles when buck-boost converter works in critical conduction mode (CRM). In case of first switching cycle, switch (Q_{b-b}) is ON, the inductor is charged as shown in Figure 2 and the value is given as
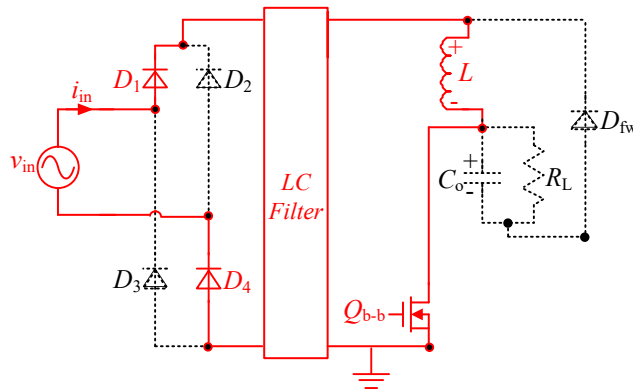
Figure 2. The Operation of converter during switching pattern 1.

$$\frac{di_L}{dt} = \frac{V_{pk} \sin \theta}{L} \tag{2}$$

$$i_{L\_pk} = \frac{t_{on} V_{pk} \sin \theta}{L} \tag{3}$$

During second switching cycle, (Q_{b-b}) is OFF; the inductor will discharge through load and output capacitor as indicated in Figure 3.

The expression for discharge time is:

$$t_{off} = \frac{V_{pk} \sin \theta}{L} t_{on} \tag{4}$$

Also,

$$t_s = t_{on} + t_{off} \tag{5}$$
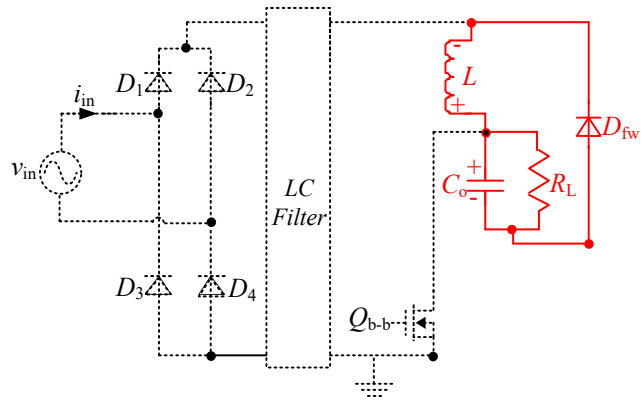
Figure 3. The Operation of converter during switching pattern 2.

The inductor and switch current waveforms are shown in Figure 4.
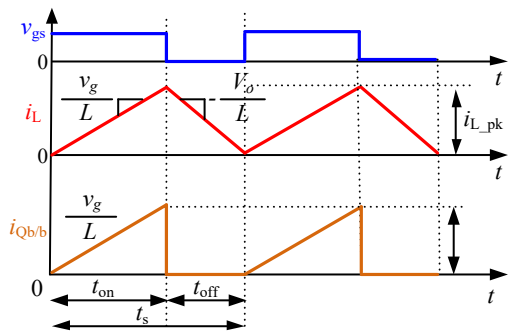
Figure 4. The inductor and switch current waveforms.

From (4) and (5), following relation is obtained:

$$t_s = \frac{t_{on}}{V_o}\left(V_o + V_{pk}\sin\theta\right) \tag{6}$$

The duty-cycle of buck-boost switch is expressed as:

$$D_{b\_b} = \frac{V_o}{V_o + V_{pk}\sin\theta} \tag{7}$$

With traditional control the input current of buck-boost converter is given as:

$$i_{in(b\_b\_COTC)} = \frac{V_o V_{pk} \sin\theta}{2L\left(V_{pk}\sin\theta + V_o\right)} t_{on} \tag{8}$$

The expression of average input power is derived as:

$$P_{in\_COTC} = \frac{V_{pk}^2 V_o t_{on}}{2\pi L} \int_0^\pi \frac{\sin^2\theta}{\left(V_{pk}\sin\theta + V_o\right)} d\theta \tag{9}$$

The value of t_{on} is calculated from '' (9)'' by assuming 100% efficiency:

$$t_{on} = \frac{2\pi L P_o}{V_{pk}^2 V_o \int_0^\pi \dfrac{\sin^2\theta}{\left(V_{pk}\sin\theta + V_o\right)} d\theta} \tag{10}$$

The input PF with traditional control scheme can be got by joining (1) and (8-10).

$$PF_{COTC} = \sqrt{\frac{2}{\pi}} \frac{\displaystyle\int_0^\pi \frac{\sin^2\theta}{\left(V_{pk}\sin\theta + V_o\right)} d\theta}{\sqrt{\displaystyle\int_0^\pi \frac{\sin^2\theta}{\left(V_{pk}\sin\theta + V_o\right)^2} d\theta}} \tag{11}$$

The table of input PF with traditional control is drawn in Table 1 with the help of equation (11) and the specification of the converter. It indicates low PF at high input voltage.

Table 1. Input PF with traditional control.

S.NO	VRMS	PF(COTC)
1	90	0.968
2	110	0.963
3	130	0.96
4	150	0.956
5	170	0.954
6	190	0.951
7	210	0.949
8	230	0.947
9	250	0.945
10	264	0.945

Through Fourier analysis, the harmonics of the input current is calculated as:

$$I_n = \frac{2}{\pi} \int_0^\pi i_{in} \sin n\theta d\theta \qquad (n = 1,3,5.....) \tag{12}$$

Based on (9) and (12), Figure 5 is drawn. It indicates the comparison of measured current harmonic with IEC Class C limits. It can be observed that the 5th and 7th harmonic for converter is unable to meet the limit value. Specially, the 5th harmonic cannot meet the standard for universal input voltage range, while 7th harmonic at high input voltage.
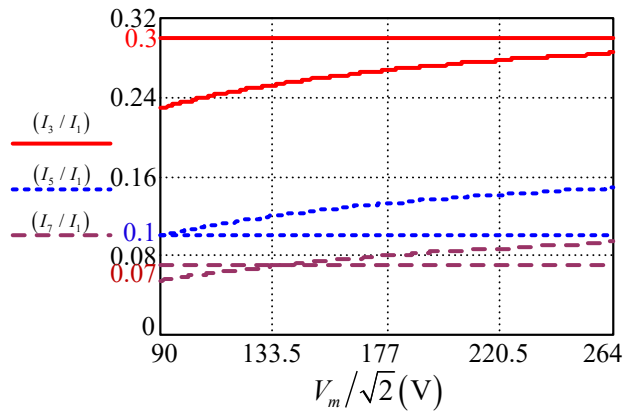
Figure 5. Input current harmonic.

3. PROPOSED VARIABLE ON-TIME CONTROL SCHEME TO IMPROVE INPUT PF

To achieve unity PF, the variation rule for t_{on} should be:

$$t_{on(b\_b)} = k_{on} \left(\frac{V_{pk} \sin\theta + V_o}{V_o} \right) \tag{13}$$

By substituting (13) into (8), we can get average input current with VOTC as:

$$i_{in(b\_b\_VOTC)} = \frac{V_{pk} \sin\theta}{2L} k_{on} \tag{14}$$

It shows shape of average input current is purely sinusoidal at all input voltage. Thus, unity PF can be realized.

From (1) and (15), the average input power is expressed as:

$$P_{in\_VOTC} = \frac{k_{on}V_{pk}^2}{4L} \tag{15}$$

Assuming converter to be 100% efficient, then k_{on} is calculated as:

$$k_{on} = \frac{4P_oL}{V_{pk}^2} \tag{16}$$

4. COMPARATIVE ANALYSIS

From (14), the input PF curve with proposed control scheme is drawn in Table 2, which also includes the PF values with traditional control scheme of Table. It can be concluded that the PF of the converter with proposed control is higher as compared to COTC. The percentage improvement of PF increases as the input rms voltage is increased.

Table 2. Input PF curve with proposed control scheme.

S.NO	VRMS	PF(COTC)	PF(VOTC)	% Improvement
1	90	0.968	1	3.30
2	110	0.963	1	3.84
3	130	0.96	1	4.00
4	150	0.956	1	4.40
5	170	0.954	1	4.82
6	190	0.951	1	5.15
7	210	0.949	1	5.38
8	230	0.947	1	5.60
9	250	0.945	1	5.80
10	264	0.945	1	5.82

5. SIMULATION VERIFICATION

For verifying the effectiveness of VOTC strategy, simulations are carried out. The input voltage range is 90-264VAC, and the output is 24V. For ensuring the current to be in CRM, L6561 IC is used. All the components in the circuit are selected as idea. The Simulation results in Figure 9 and Figure 10 shows that vin, and iin, for proposed converter with COTC and VOTC at 110VAC input, respectively. The input waveform shows that with VOTC

the input current is sinusoidal as compared with COTC. Hence, the near unity PF can be realized by using proposed control scheme.
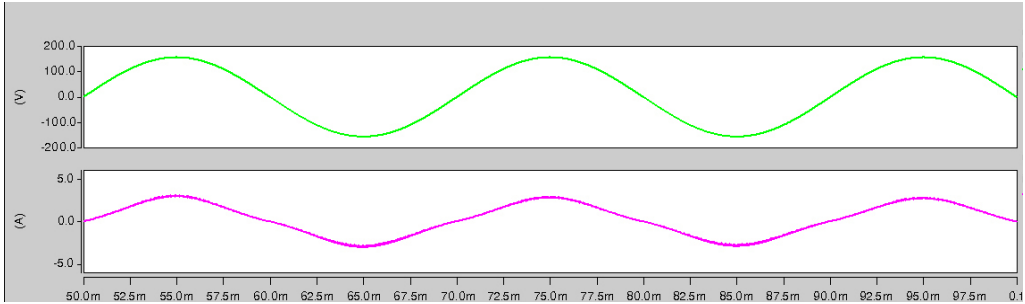
Figure 9. v_{in}, and i_{in}, with COTC.
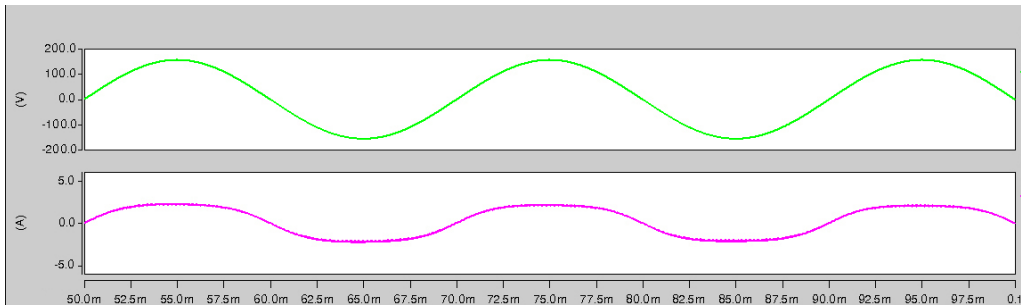
Figure 10. v_{in}, and i_{in}, with VOTC.

5. CONCLUSION

A variable on-time control scheme and the implementation circuit are proposed in this paper to make the shape of average input current purely sinusoidal for the CRM buck–boost PFC converter. The analysis and simulation results are given. Compared with that of the COT control:

1. Input current meets the harmonic standard.

2. PF is high

3. THD is low

REFERENCES

García, O., Cobos, J. A., Prieto, R., Alou, P., & Uceda, J. (2003). Single phase power factor correction: A survey. *IEEE Transactions on Power Electronics, 18*(3), 749-755. https://doi.org/10.1109/TPEL.2003.810856

Ghanem, M. C., Al-Haddad, K., & Roy, G. (1996). A new control strategy to achieve sinusoidal line current in a cascade buck-boost converter. *IEEE Transactions on Industrial Electronics, 43*(3), 441-449. https://doi.org/10.1109/41.499817

IEC 61000-3-2:2014. (2014). Electromagnetic compatibility (EMC) - Part 3-2: Limits - Limits for harmonic current emissions (equipment input current <= 16 A per phase). https://webstore.iec.ch/publication/4149

Jayahar, D., & Ranihemamalini, R. (2011). Inductor average current mode control for single phase power factor correction buck-boost converter. In *2011 International Conference on Emerging Trends in Electrical and Computer Technology, Nagercoil, India, (pp. 274-279).* IEEE. https://doi.org/10.1109/ICETECT.2011.5760128

Jayahar, D., Ranihemamalini, R., & Rathnakannan, K. (2016). Design and Implementation of Single Phase AC-DC Buck-Boost Converter for Power Factor Correction and Harmonic Elimination. *International Journal of Power Electronics and Drive Systems, 7*(3), 1004. https://www.researchgate.net/publication/311986790_Design_and_Implementation_of_Single_Phase_AC-DC_Buck-Boost_Converter_for_Power_Factor_Correction_and_Harmonic_Elimination

Langella, R., Testa, A., & Alii, E. (2014). *IEEE recommended practice and requirements for harmonic control in electric power systems*. IEEE Std. 519-2014. IEEE.

Memon, A. H., & Yao, K. (2018). UPC strategy and implementation for buck–buck/boost PF correction converter. *IET Power Electronics, 11*(5), 884-894. https://doi.org/10.1049/iet-pel.2016.0919

Memon, A. H., Baloach, M. H., Sahito, A. A., Soomro, A. M., & Memon, Z. A. (2018). Achieving High Input PF for CRM Buck-Buck/Boost PFC Converter. *IEEE Access, 6,* 79082-79093. https://doi.org/10.1109/ACCESS.2018.2879804

Memon, A. H., Memon, M. A., Memon, Z. A., & Hashmani, A. A. (2019d). Critical Conduction Mode Buck-Buck/Boost Converter with High Efficiency. *3C Tecnología. Glosas de innovación aplicadas a la pyme. Speciaal Issue, November 2019*, 201-219. http://dx.doi.org/10.17993/3ctecno.2019.specialissue3.201-219

Memon, A. H., Memon, Z. A., Shaikh, N. N., Sahito, A. A & Hashmani, A. A. (2019b). Boundary conduction mode modified buck converter with low input current total harmonic distortion. *Indian Journal of Science and Technology*, *12*(17).

Memon, A. H., Nizamani, M. O., Memon, A. A., Memon, Z. A., & Soomro, A. M. (2019e). Achieving High Input Power Factor for DCM Buck PFC Converter by Variable Duty-Cycle Control. *3C Tecnología. Glosas de innovación aplicadas a la pyme. Special Issue, November 2019,* 185-199. http://dx.doi.org/10.17993/3ctecno.2019.specialissue3.185-199

Memon, A. H., Pathan, A. A., Kumar, M., Sahito, A. A J., & Memon, Z. A. (2019a). Integrated buck-flyback converter with simple structure and unity power factor. *Indian Journal of Science and Technology*, *12*(17).

Memon, A. H., Shaikh, N. N., Kumar, M., & Memon, Z. A. (2019c). buck-buck/boost converter with high input power factor and non-floating output voltage. *International Journal of Computer Science and Network Security*, *19*(4), 299-304. http://paper.ijcsns.org/07_book/201904/20190442.pdf

Memon, A. H., Yao, K., Chen, Q., Guo, J., & Hu, W. (2017). Variable-on-time control to achieve high input power factor for a CRM-integrated buck–flyback PFC converter. *IEEE Transactions on Power Electronics, 32*(7), 5312-5322. https://doi.org/10.1109/TPEL.2016.2608839

Moschopoulos, G., & Zheng, Y. (2006). Buck-boost type ac-dc single-stage converters. In *IEEE International Symposium on Industrial, Montreal, Que., Canada*. IEEE. https://doi.org/10.1109/ISIE.2006.295794

Saifullah, K., Al Hysam, M. A., Haque, M. Z. U., Asif, S., Sarowar, G., & Ferdaous, M. T. (2017). Bridgeless AC-DC buck-boost converter with switched capacitor for low power applications. In *TENCON 2017-2017 IEEE Region 10 Conference, Penang, Malaysia (pp. 1761-1765)*. IEEE. https://doi.org/10.1109/TENCON.2017.8228143

Singh, B., Singh, S., Chandra, A., & Al-Haddad, K. (2011). Comprehensive study of single-phase AC-DC power factor corrected converters with high-frequency isolation. *IEEE transactions on Industrial Informatics*, *7*(4), 540-556. https://doi.org/10.1109/TII.2011.2166798

Wei, W., Hongpeng, L., Shigong, J., & Dianguo, X. (2008). A novel bridgeless buck-boost PFC converter. In *2008 IEEE Power Electronics Specialists Conference, Rhodes, Greece (pp. 1304-1308)*. IEEE. https://doi.org/10.1109/PESC.2008.4592112

/06/

WIRELESS POWER TRANSFER VIA INDUCTIVE COUPLING

Mirsad Hyder Shah

Ex-Fellow, Department of Electrical Engineering, DHA Suffa University. Karachi, (Pakistan).
E-mail: itsmirsadhyder@yahoo.com ORCID: https://orcid.org/0000-0003-2476-5887

Nasser Hassan Abosaq

Assistant Professor, Computer Science and Engineering Department. Yanbu University College, Yanbu Industrial City, (Saudi Arabia).
E-mail: abosaqn@rcyci.edu.sa ORCID: https://orcid.org/0000-0003-1354-3170

ABSTRACT

The concept of transferring electrical power to a load wirelessly is an intimidating and a challenging idea. The genius of powering systems wirelessly has pulled the curtains to a new world. In the 19th century, Nikola developed 'Tesla Tower' in hope to transfer power wirelessly. Since then, the world is trying hard to say goodbye to wires. WPT using Inductive Coupling which falls under the domain of NFWPT, uses a transmitter coil to transmit power to the receiver coil via a magnetic field. Inductive coupling is an efficient way to transmit power through short distances and making its way in smartphones and the health industry. Electric vehicle charging stations are also trending thanks to wireless power transfer. This paper discusses the theoretical foundation of Inductive coupling and presents results of an experimental work done on WPT via Inductive Coupling. In the process above, an efficiency of 72% was achieved.

KEYWORDS

Wireless Power Transfer, Inductive Coupling.

1. INTRODUCTION

Many Engineers and Physicists credit Nikola Tesla for the concept of wireless power transfer, ignoring Faraday being the pioneer of the concept of transferring energy wirelessly when he demonstrated how Electromotive-Force and Current were induced in a conductor when subjected to a changing magnetic field, and hence the concept of Wireless Power Transfer was derived. In 1892, Nikola Tesla believed wireless power transfer was possible and began building what he called the 'Tesla Tower'. This 200 feet high tower was energized with 300kW of power but couldn't prove to succeed because of the long distance approach (Johnson, 1990). The late 19th century saw an attempt to power electric vehicles through electrodynamic induction, but combustion engines proved much more efficient. In 1978, the United States powered an electrical vehicle successfully; while in 1987, Canada successfully flew the first fuel-free airplane model. Commercial use of powering smartphones wirelessly came up on the scene after 2009, when Palm Inc. introduced wireless charging in their smartphones. Samsung and Apple followed the lead and presented wireless charging in 2013 and 2014 respectively.

1.1. RESEARCH SIGNIFICANCE

Wirless power transfer is the dawn of a new age. At present, many companies have introduced commercial use of wireless charging for smartphones, EV cars and other electronic devices. Wireless Power Transfer has even made its mark in the healthcare, especially in the implantable medical devices. This study presents a simple prototype which can be employed for smartphones or cars with an impressive efficiency of 72% when placed in proximity.

1.2. OVERVIEW OF WPT

Wireless power transfer can be classified into two fields; NFWPT (Near Field Wireless power technology) and FFWPT (Far Field Wireless power technology) (Hassan & Elzawawi, 2015).

NFWPT is further classified as electromagnetic induction, as it depends on the coupling of the magnetic-field between the two coils, which explains why it has a short range. The field (range) of NFWPT decreases exponentially. It includes Inductive Power Transfer

(IPT), Resonant Inductive Power Transfer, Capacitive Power Transfer (CPT), Resonant Capacitive Coupling and Magneto-dynamic coupling (Hassan & Elzawawi, 2015).

FFWPT is further classified as electromagnetic radiation. It is most convenient for long range applications. But due to the power losses, it is comparatively less efficient. It includes lasers (radiowaves) and microwaves to transmit power.

Table 1. Classification of WPT technologies.

WPT Technolgies	Range	Frequency	Efficiency	Power transfer via
NFWPT	Short-Medium	Hz-kHz	High	Electric or Magnetic Fields.
FFWPT	Long	MHz	Low	Infrared or Ultraviolet or Microwaves

Source: (Hassan & Elzawawi, 2015).

2. WPT USING INDUCTIVE COUPLING

Any Wireless Power Technology must have two core components for it to work; a transmitter and a receiver. In the case of Inductive Coupling, the transmitter and receiver are two separate coils wound on materials with high permeability. This increases the efficiency of the circuit by increasing the inductance of the coils. The transmitter transfers AC power to the receiver which can then be converted to DC for in use applications. As DC power transfer has higher energy loss hence the model comprises of transferring AC power.

In Inductive power transfer, longitudinally arranged dipole fields are produced. These fields decrease with the cube of distance between the transmitter and the receiver. Hence one of the factors affecting the efficiency is the distance between the two coils. Hence, the closer the receiver and the transmitter, the better the efficiency (Van Schuylenbergh & Puers, 2009).

Inductive coupling solely involves magnetic fields for transferring power and therefore can be referred to as 'Magnetic coupling' as well. It works on the basic principle of faraday's law of induction which explains how a magnetic field will interact with an electrical circuit to produce an electromotive force (EMF) in the secondary coil. The power transfer in Inductive coupling is directly proportional to the frequency as well as the mutual inductance between the coils. The mutual inductance between the transmitter and receiver can be calculated by:

$$M = k \times \sqrt{\left(L_1 \times L_2 \right)} \tag{1}$$

Where, k is the coupling coefficient. It is a dimensionless parameter.

Another factor which affects the efficiency of WPT is misalignment tolerance. Misalignment is the displacement of the receiver coil with respect to the transmitter coil that leads to a decline in both the efficiency and power transfer of the IPT system. Since,

$$\phi_B = \iint_0^A \vec{B}.d\vec{A} \tag{2}$$

For maximum flux, the dot product requires the angle between the flux density ($\vec{B}$) and the area enclosed to be 0 deg [cos 0 =1]. This can be ensured when both the transmitter and receiver coils overlap each other.

Graphic 1 shows the basic model of a complex circuit which transfers power via inductive coupling. The transmitter consists of an AC voltage source (V_p) and a primary coil (L_p) on the left hand side, while the receiver consists of a secondary coil (L_s) and R_{load}. A bridge rectifier and further electronic circuitry are lumped as R_{load} on the right hand side. The transmitter is powered through an AC source (a coil driver) which produces a magnetic flux in the primary coil. This induces a voltage in L_p which in turn produces a flux in the secondary coil L_s. This flux produces a voltage in the secondary coil which can be rectified for further use (Van Schuylenbergh & Puers, 2009).
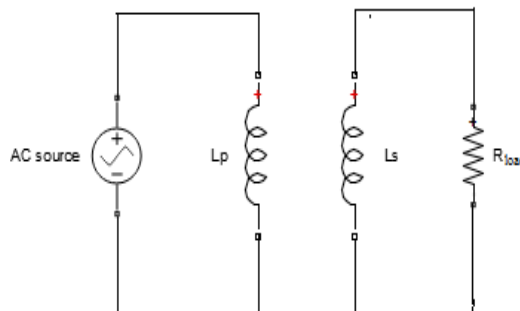
Graphic 1. Basic circuit diagram of WPT using inductive coupling. **Source:** (Van Schuylenbergh & Puers, 2009).

To calculate the link efficiency of the coupling circuit, Graphic 2 is used. Since, Graphic 1 is a generalized block of Graphic 2; it neglects the coil resistances of the receiver and transmitter. From transformer theory, we know that the two coils employ the coupling coefficient (k) and that both the inductances L_p and L_s are affected by k.

From transformer theory we know that, reducing the circuit with respect to primary side will yield:
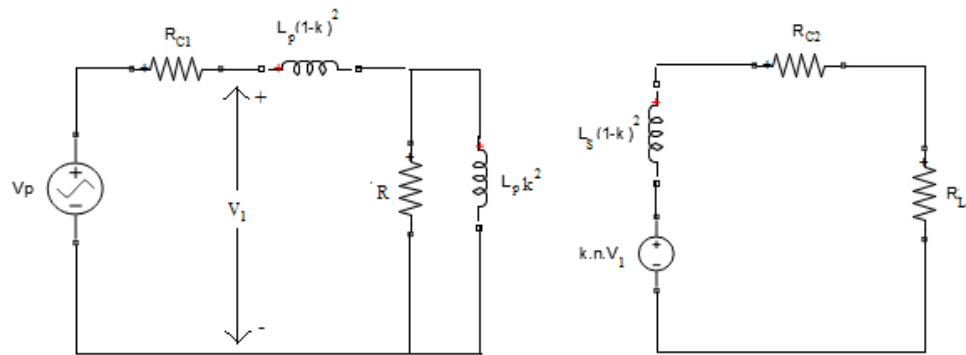
Graphic 2. Inductive circuit referred to the primary side and coil losses included. **Source:** (Van Schuylenbergh & Puers, 2009).

Where,

$$R = \left(\frac{k}{n}\right)^2 \left(R_{load} + R_{c2}\right) \tag{3}$$
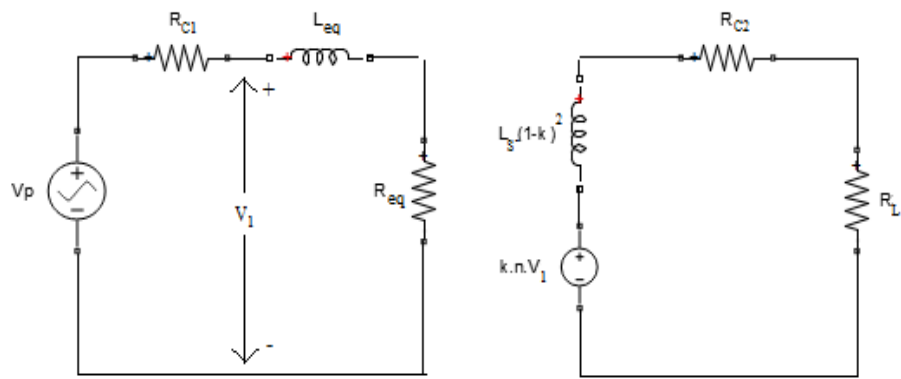
Graphic 3. Equivalent circuit for the calculation of link efficiency. **Source:** (Van Schuylenbergh & Puers, 2009).

And the equivalent resistance and inductance are given by:

$$L_{eq} = L_p \left[\frac{R^2 + \omega^2 L_p^2 k^4 \left(1 - k^2\right)}{R^2 + \omega^2 L_p^2 k^4} \right] \tag{4}$$

$$R_{eq} = R \left[\frac{\omega^2 L_p^2 k^4}{R^2 + \omega^2 L_p^2 k^4} \right] \tag{5}$$

The link efficiency is given by,

$$\eta_{link} = \left(\frac{R_{eq}}{R_{eq} + R_p} \right) \left(\frac{R_{load}}{R_{load} + R_s} \right) \tag{6}$$

$$\eta_{link} = \left(\frac{k}{n} \right)^2 \frac{R_{load} \omega^2 L_p^2 k^4}{\left(R + R_p \right) \omega^2 L_s^2 k^4 + R^2 R_p} \tag{7}$$

It can be observed that one of the factors the link efficiency is dependent on is the square of primary inductance of the coil. A higher value of mutual coupling 'k' is also desirable for better link efficiency (Van Schuylenbergh & Puers, 2009).

3. THEORY OF WPT

According to amperes law, the loop integral of the $\vec{B}$ field equals the net current i enclosed by the loop.

$$\phi \vec{B}.\vec{dl} = \mu i \tag{8}$$

Where $\vec{B}$ is the magnetic flux density, i is the net current and μ is the permeability. $[\mu = \mu_o \mu_r]$

According to Biot-Savart Law,

$$dB = \frac{\mu \times i \times dl \times \sin\theta}{4\pi r^2} \tag{9}$$

Where:

dl: is the infinitesimal length of conductor carrying the electric current i.

r: is the distance from the length element dl to the field point P.

The magnetic flux is given by equation (2):

$$\phi_B = \iint_0^A \vec{B}.d\vec{A} \tag{2}$$

Where, A is the area enclosed in a given loop.

Solving the differential in (9) and then after equating in (2) we get,

$$\phi_B \phi \frac{dl}{\mu A \times l} = i \tag{10}$$

Ampere's law in term of reluctances is given by,

$$\varnothing_B = \frac{i}{Rm} \tag{11}$$

Where,

Rm is the reluctance of the magnetic loop. $\left[\dfrac{A}{W_b}\right] \left[R_m = \phi \dfrac{dl}{\mu A \times l}\right]$

According to faradays law,

$$\phi \vec{E}.d\vec{l} = \frac{d\varnothing_B}{dt} \tag{12}$$

Where, $\vec{E}$ is the emf or the electromotive force, $\varnothing_B$ is the magnetic flux.

The voltage in the coils is given by,

$$v_1(t) = L_p \frac{di_1(t)}{dt} + M \frac{di_2(t)}{dt} \tag{13}$$

$$v_2(t) = L_s \frac{di_2(t)}{dt} + M \frac{di_1(t)}{dt} \tag{14}$$

The coupling coefficient k and inductance ratio are given by

$$k = \frac{M}{\sqrt{L_p L_s}} \qquad (15)$$

$$n = \sqrt{\frac{L_s}{L_p}} \qquad (16)$$

4. EXPERIMENTAL WORK AND RESULTS

For the construction of an inductive coupling circuit, the transmitter has an AC source (V_p) and a coil with inductance (L_p). The input frequency can be adjusted as per the application of usage. The greater the frequency the more the transmission efficiency. The receiver is comprised of a coil of inductance (L_s) which produces an EMF for the power to be delivered to the load. As the coil Ls delivers AC voltage, a bridge rectifier is used to convert AC voltage to DC voltage which is then delivered to the load.
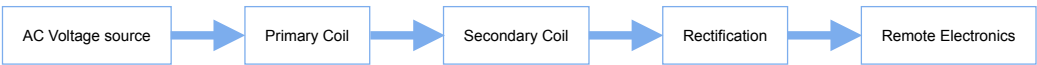
Graphic 4. Block diagram of WPT using inductive coupling. **Source:** (Yahaya *et al.*, 2018).

The proposed model in Graphic 4 was implemented for charging a mobile phone.

Transmitter and receiver coils were wound on plastic forms, both the coils had the same number of turns. The core was made from steel plates and was arranged around each of the coils. The steel plates were held together by a coating of shellac.

The radius of both the coils were 0.07m, while the input voltage provided was 240V. Following results were obtained when a piece of paper was placed between the two coils and consequently the distance between the two coils was increased. A similar approach to the work done in Yahaya *et al.* (2018).

Table 2. Voltage, current and power when distance is changed.

Distance (cm)	Input Voltage (V)	Input Current (A)	Input Power (W)	Output Voltage (V)	Output Current (A)	Output Power (W)	Efficiency (%)
0	208	0.12	24.96	22.087	0.881	19.468	78
1	208	0.12	24.96	17.12	0.816	13.977	56
2	208	0.12	24.96	10.935	0.707	7.737	31

Distance (cm)	Input Voltage (V)	Input Current (A)	Input Power (W)	Output Voltage (V)	Output Current (A)	Output Power (W)	Efficiency (%)
3	208	0.12	24.96	6.12	0.57	3.494	14
4	208	0.12	24.96	2.055	0.242	0.499	2
5	208	0.12	24.96	0.12	0.149	0.0179	0.072

As it was predicted by Akpeghagha *et al.* (2019), the efficiency drops drastically with the increase of distance between the two coils. Here, the input voltage and input current are the voltage and currents of the primary coil (L_p) , while the output voltage and output current are the voltage and currents of the secondary coil (L_s).
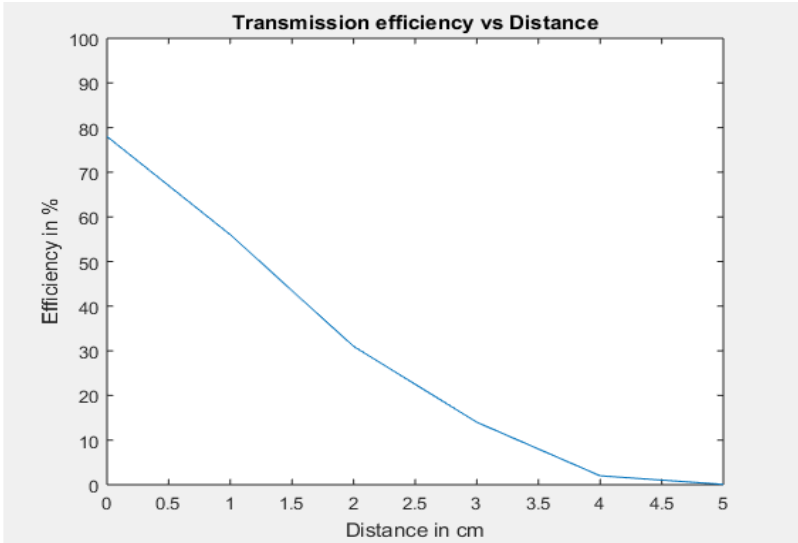
Graphic 5. Graphical representation of Transmission efficiency vs Distance.

REFERENCES

Akpeghagha, O., Iwunna, C. M., Igwele, M. M., & Okoro, H. (2019). Witricity: Design And Implementation Of A Wireless Power Transfer System Via Inductive Coupling. *International Journal of Innovative Research and Advanced Studies (IJIRAS), 6*(4), 16-19. https:// pdfs.semanticscholar.org/508a/5b58b549248fb0c2769e2e10d6dc577ecc39.pdf?_ ga=2.107407746.1668826937.1585911452-626794738.1556264447

Hassan, M. A., & Elzawawi, A. (2015). Wireless Power Transfer through Inductive Coupling. *Recent Advances in Circuits,* 115-118. http://www.inase.org/library/2015/zakynthos/bypaper/CIRCUITS/CIRCUITS-18.pdf

Johnson, G. L. (1990). Building the world's largest Tesla coil-history and theory. In *Proceedings of the Twenty-Second Annual North American Power Symposium, Auburn, AL, USA (pp. 128-135).* IEEE. https://doi.org/10.1109/NAPS.1990.151364

Van Schuylenbergh, K., & Puers, R. (2009). *Inductive powering: basic theory and application to biomedical systems.* Springer Netherlands. https://www.springer.com/gp/book/9789048124114

Yahaya, C. K. H. C. K., Adnan, S. F. S., Kassim, M., Ab Rahman, R., & Bin Rusdi, M. F. (2018). Analysis of Wireless Power Transfer on the Inductive Coupling Resonant. *Indonesian Journal of Electrical Engineering and Computer Science, 12*(2), 592-599. https://www.researchgate.net/publication/327249559_Analysis_of_Wireless_Power_Transfer_on_the_inductive_coupling_resonant

/07/

COST-EFFECTIVE AND INNOVATIVE TEST JIG FOR FISHING-BAIT RELEASE MECHANISMS ATTACHED TO DRONES

Pierre Eduard Hertzog

Department of Electrical, Electronics and Computer Engineering
Central University of Technology, Bloemfontein, (South Africa).
E-mail: phertzog@cut.ac.za ORCID: http://orcid.org/0000-0002-3396-6050

Arthur James Swart

Department of Electrical, Electronics and Computer Engineering
Central University of Technology, Bloemfontein, (South Africa).
E-mail: aswart@cut.ac.za ORCID: http://orcid.org/0000-0001-5906-2896

ABSTRACT

Fishing-bait release mechanisms are used in conjunction with drones to drop bait at a specific fishing location. It is really a revolutionary technology to many fishermen. However, many of these release mechanisms have no real technical data associated with them. Therefore, the purpose of this paper is to present a cost-effective and innovative test jig that may be used to determine the reliability and consistency of operation of various fishing-bait release mechanisms. The main components of the system are a HX711 instrumentation amplifier, a load cell and an Arduino Mega microcontroller. The accuracy of the system was determined to be 99,879%. Reliability values for a Gannet Sport mechanism with a 0.55 mm Kingfisher line ranged from 599 g to 642 g, giving a maximum deviation of 43 g. The results provide evidence that the system is both reliable and valid. It is recommended to use it to clarify technical data regarding the weights at which different fishing-bait release mechanisms operate.

KEYWORDS

Arduino, Load-cell, Electronic measurements.

1. INTRODUCTION

"A few years ago, the city council of Monza, Italy, barred pet owners from keeping goldfish in curved bowls... saying that it is cruel to keep a fish in a bowl with curved sides because gazing out, the fish would have a distorted view of reality. But how do we know we have the true, undistorted picture of reality?" ("Brainy Quote", 2019). These words by the late world-renowned physicist, Stephen Hawking, illustrates that our perception of reality may be distorted, just as the viewpoint of a fish may be distorted in a curved glass bowl. To correct this distortion would require that we obtain accurate knowledge based on facts.

However, we would first need to de-construct our erroneous knowledge and then re-construct it with the accurate knowledge that we have received. De-constructing knowledge must be preceded by an acknowledgement that our knowledge, or perceptions, may be erroneous, or even biased. This is true even of simply things in life, such as fishing.

Fishing is as old as the hills, yet as new as today when it comes to new and innovative equipment and technologies. For example, drones have been used in fishing to identify good fish spots and for bait release purposes. The Internet of Things and fishing drones using an integrated remote camera have been used to target specific fishing spots to enable easier catching of fish (Maksimovic, 2018). Fishing for large fish beyond the breakers by first looking for them and then dropping the bait and a hook in front of them is quite popular in South Africa and can be achieved by using a fishing line dropping drone (SUAS News, 2019). This may also be termed a fishing-bait release mechanism that is attached to the bottom of a drone, which is really a revolutionary technology to many fishermen.

However, with so many different models available for this type of technology, the question may arise "Which release mechanism is more reliable and consistent in operation? Some fishermen may prefer the old tradition of casting the fishing line, while others may have strong opinions about a preferred modernized technology that makes use of a fishing-bait release mechanism. De-constructing erroneous perceptions of which model is best, and then re-constructing knowledge of which model is reliable and consistent would require the use of one or other scientifically accepted test.

The purpose of this paper is to present a cost-effective and innovative test jig that may be used to determine the reliability and consistency of operation of various fishing-bait release mechanisms. The paper starts with a brief history of drone technology and presents some of its many applications. Previous research in the field of release mechanisms are also presented. The design of the jig is then given, followed by the methodology employed to obtain the scientific empirical results. Conclusions end the paper.

2. LITERATURE

Some believe that the first type of drone was used in July 15, 1849 when the Habsburg Austrian Empire launched 200 pilotless balloons armed with bombs against the revolution-minded citizens of Venice (Ferrao, 2016). However, others view this as an erroneous belief, especially when considering the official definition given by The Oxford Dictionary. It defines a drone as "a remote-controlled pilotless aircraft or missile" ("Oxford Dictionary", n.d.). The aspect of remote-control and flight must be factored into the discussion. The Federal Aviation Administration (FAA) of the USA further defines a drone as a small unmanned aircraft system weighing under 55 lb (or 24,9 kg) (Federal Aviation Administration, 2016). The aspect of weight thus needs to be factored into the discussion. Considering the words remote-controlled, flight and weight leads one to conclude that drones were first used towards the end of the 20th century, when newer technologies allowed for the inclusion of these factors into their design and development.

Moreover, the decline in cost due to these technological advancements has allowed drones to become viable options for a diverse range of services, including health services (Wulfovich, Rivas, & Matabuena, 2018), agriculture (Parihar, Bhawsar, & Hargod, 2016), sports (Park, Kim, & Suh, 2018), conservation (Sandbrook, 2015) and in monitoring solar farms (Benatto *et al.*, 2019). Drones have also been used in border patrol, disaster relief, law enforcement, and in the original use of military missions and training (Upchurch, 2015).

A specific research paper, published in 2019, described a novel way to reliably deliver packages using a drone. For years, companies such as Amazon and Google have been hard at work developing a safe and practical way of utilizing the potential of unmanned aerial vehicles to improve upon their current network of delivery services. Transportation

of even large packages has become feasible due to the advances in drone-based robotics. The biggest problem left unanswered is how to best release the package once the drone has arrived at the drop off location. A possible solution details a basket that can hold onto the package until the drone is rapidly flipped upside down in an aerial maneuver (oftentimes called a roll) and the centrifugal force ejects the payload from the basket (Burke *et al.*, 2019). However, this may prove draining to the battery.

Another option that overcomes this challenge involves a mechanism attached to the bottom of a drone that can deploy a payload from air to land using a parachute method. The study that reported on this release mechanism made use of an Arduino UNO microcontroller (Wan, Azrie, & Shuib, 2018). This type of Arduino microcontroller can also be used in a practical test system to determine the reliability and consistency of operation of various release mechanisms relating to fishing-bait.

3. INNOVATIVE TEST JIG DESIGN

The practical test system of the innovative test jig is given in this section. Firstly, an overview of the complete test system is given, where after the load cell, instrumentation amplifier and the 24-bit analogue-to-digital converter is explained. The next step explains the Arduino software as well as the communication between the microcontroller, the SD card and the Nextion touch screen display. The complete block diagram of the tension release measurement system is shown in Figure 1.

The first block is a load cell that is rated for 5 kg. The load cell has a safe overload of 6 kg and will be damaged if the load exceeds 7.5 kg. The load cell has a measurement precision of 0.05%. It is mounted with two x 5 mm bolts onto a fixed structure, while two x 4 mm bolts are used to connect to the load. One of the reasons why this load cell was selected is because of its ease of mounting. The load cell is constructed of four strain gauges that is coupled in a Wheatstone Bridge configuration. As the innovative test jig is custom made for release mechanisms for fish-bait, a 5 kg load cell is adequate. In order to perform accurate weight measurements, an instrumentation amplifier and higher resolution analogue to digital converter is necessary.

The second and third blocks shows the instrumentation amplifier and the high precision 24-bit analogue to digital converter that is part of the HX711 load cell sensor interface module. The HX711 module was chosen for this project and is specially designed to work with strain gauges that is coupled in a Wheatstone Bridge configuration. It was used in load cell project involving a garbage alert system that was developed by the National Institute of Technology in India (Paavan, Sai, & Naga, 2019). The HX711 module can be programmed for a gain of 32, 64 or 128 and it has an input voltage range of 4.8 to 5.5 V DC. The refresh frequency is selectable between 10 and 80 Hz and it has a low operating current of 1.6 mA.

The center block in the diagram is the Arduino Mega microcontroller. It is used to obtain the high-resolution 24-bit data from the HX711 module and to do necessary processing. This process will be explained in the following section with the use of flow charts.
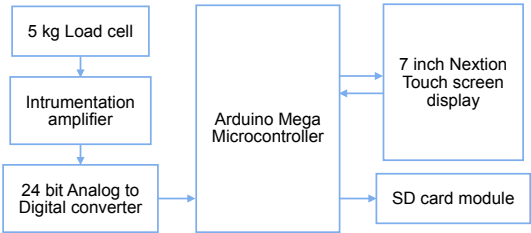
Figure 1. System block diagram.

The Arduino Mega microcontroller also saves the recorded data to a micro SD card that is situated on an SD module that fits as a shield on the Arduino. The microcontroller also connects to a 7-inch Nextion touchscreen display. This display is used as a user interface that shows recorded data while providing a number of push-button functions.

The Arduino program is presented in the form of a simplified flowchart as can be seen in Figure 2. Because of limitations in space, the flowchart only shows the major functions in the Arduino program to give the reader an idea of the general flow of data. After startup, the first block is the initialization bock where the necessary libraries for the display, the SD card and the HX711 module is loaded. After initialization, the weight measurements start and is displayed on the Nextion display. There are three push-button functions that can be selected by the user.
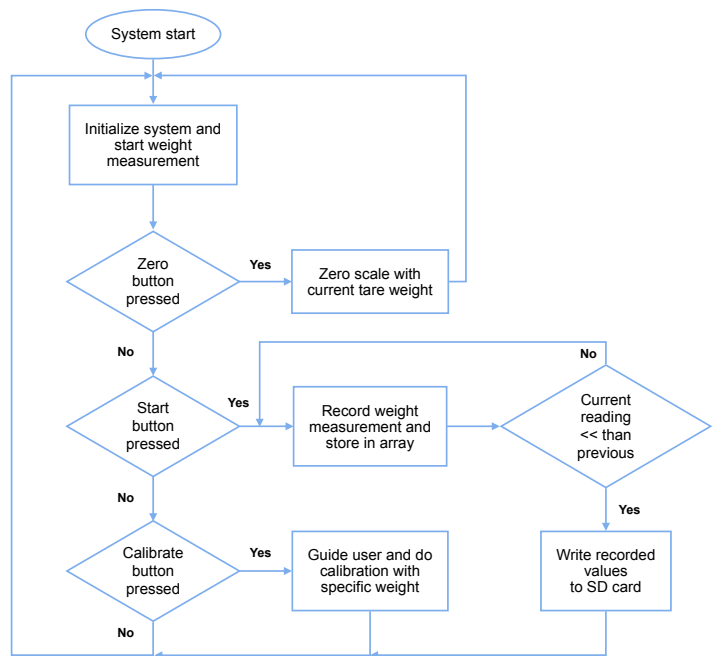
Figure 2. Simplified flow diagram of Arduino Mega program.

The first button is the calibration button that is used to calibrate the scale with a specific weight that is recorded in the program. If this button is pressed, the user must remove the load bucket and dropping mechanism from the load cell and connect a calibrated weight (333.2g) to the scale. The program will then do an automatic calibration to find the best calibration factor. There will also be a message on the screen that will notify the user when the calibration process is completed. Calibration is discussed in more detail later in the paper.

The zero button is used to zero the scale, with or without the tar weight, before the load bucket is connected to the dropping mechanism. The zero button also sets the experiment counter to zero that is used to identify the start of the recorded data that is sent to the SD card.

The next button is the start button and is used to start a test session where all weight measurements are recorded in an array. The weight is increased by allowing more water to flow into the load bucket by means of a water-value. After each measurement, a test is done to determine if the current measurement is smaller than the previous measurement. If not,

then another measurement is done. As soon as the current measurement is smaller than the previous measurement then the system will detect that the release mechanism has activated. It will then display the maximum weight reading on the screen and write all the weight measurements in the array to the SD card. The number and name of the experiment is also recorded that specifies certain parameters about the fishing line that is used with the fishing-bait. The time taken, in milliseconds, to complete a series of measurements for each experiment is also recorded, along with the number of measurement samples and the number of milliliters (ml) per sample. As 1 ml of water is equal 1 g, the number of grams per sample can be used to calculate the accuracy of the measurement. For instance, if the weight increases with 1 g per sample then the maximum accuracy of the measurement cannot exceed 1 g. After all the data is written to the SD card, a message is displayed on the Nextion display to inform the end user that the test system is ready for the next experiment session.

Calibration is done by using a specific calibrated weight. In this test system, a stainless-steel bar of 333.2 g is used. The exact weight of the bar was determined by using a calibrated scale (ADAM 6031) with a resolution of 0.1 gram. Figure 3 shows the flow diagram of the calibration sequence used in the Arduino program. When the zero button on the Nextion display is pushed, the scale is set to zero with the current tar. The user is then required to put the calibrated weight onto the scale, and the program executes a measurement command. If the measured weight is too high, then the calibration factor is decreased, and the measurement is repeated. If the measured weight is too low, then the calibration factor is increased, and the measurement is repeated. As soon as the measured weight is equal to the 333.2 g of the calibrated weight, then a completion message is communicated to the user via the Nextion display.

The Nextion touch screen display is used as a user interface for the test system. A photo of the display is shown in Figure 4. On the display, two measurements can be seen. The first measurement is the current reading from the load cell and the second reading is the last maximum reading recorded by the test system. On the bottom, left-hand corner are messages that have been communicated to the user. The three push-button functions can be seen on the bottom right side of the figure.
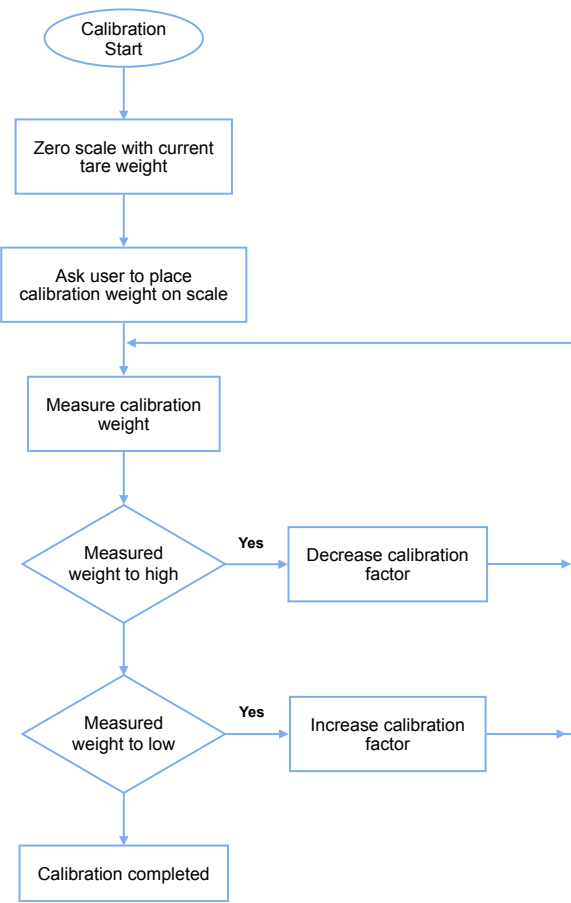
Figure 3. Simplified flow diagram of calibration software.

The calibration button (CAL) is used to calibrate the test system. The zero button (ZERO) is used to zero the scale with the tar weight. The start button (START) is used to start the experiment session. When the start button is pressed, the experiment number will be incremented by a value of 1 (the current value of 3 is shown in the top right-hand corner). The top left-hand corner shows the description of the experiment that can be changed in the Arduino software for each make of and model of the release mechanism. For instance, in Figure 4 it shows that the Gannet Sport release mechanism was used with a dry fishing line having a 0.55 mm diameter. It also shows that the test was concluded at 525 g.
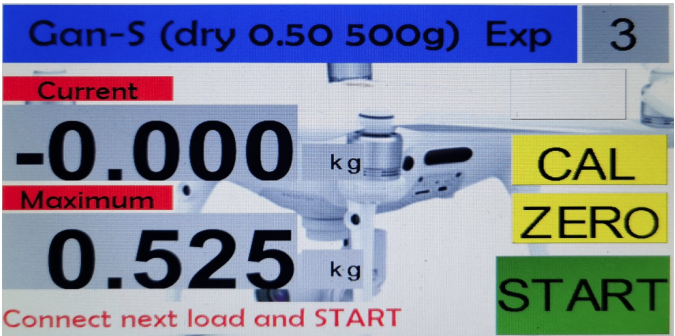
Figure 4. Nextion touch screen display showing the user interface.

Figure 5 shows a typical circuit and internal block diagram of the HX711 microchip. The HX711 load cell model has two analogue input channels (INA and INB). The differential inputs on the channel are coupled directly with the load cell Bridge sensor output. Channel INA can be programmed with a gain of 128 or 64. These large gains are needed to accommodate the very small output signals from the strain gauge sensors. An input voltage of +- 20 mV will result in a full-scale output of 5 volt with the 128 gain setting. Channel INB has a fixed gain of 32 and the input V range is +-80mV for a full-scale output reading.

Figure 6 shows a photo of the completed practical test system. A two-liter water reservoir is located at the top of the system, which is used to increase the weight of the load bucket. The Nextion touch screen display, mounting bracket and dropping mechanism are also visible. Calibration weights are shown at the bottom of the photo.
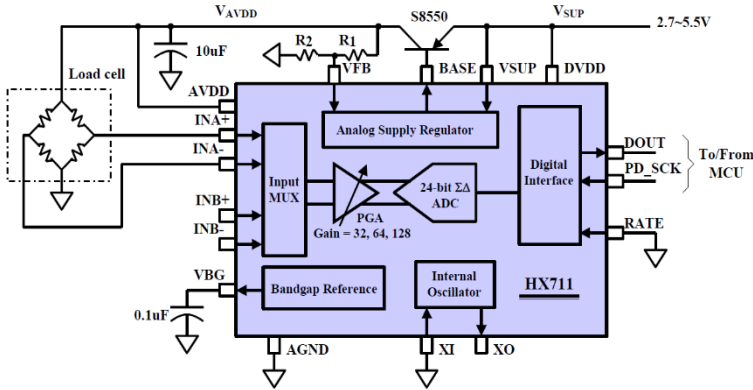
Figure 5. Typical circuit and internal block diagram of the HX711 microchip. **Source:** (Qian, Liu, & Wu, 2019).
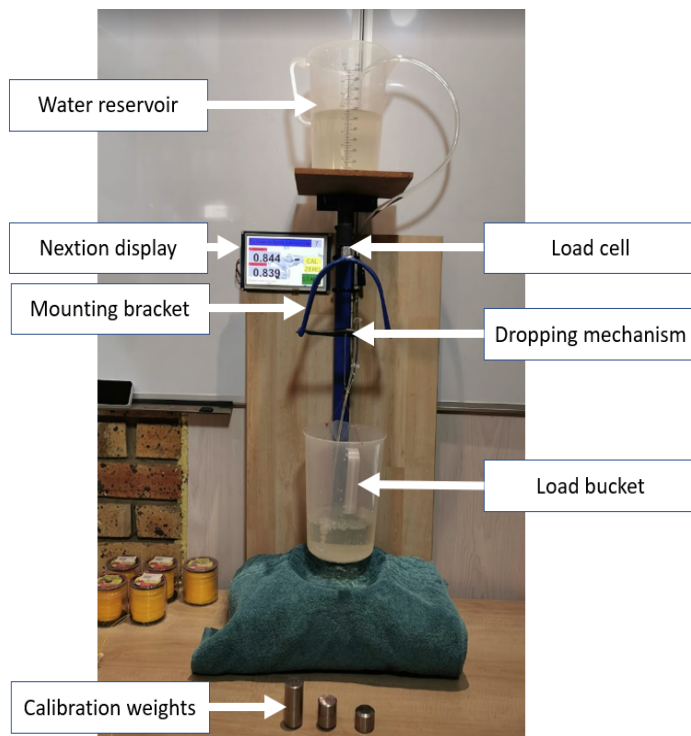
Figure 6. Practical setup of the innovative test jig for fishing-bait release mechanisms.

4. METHOD

In this section, the methodology will be explained. At startup, the system is first calibrated and then set to zero, and it will be reflected on the display. The next step will be to securely attach the release mechanism. Then the bucket is connected that will represent the load. The user then presses the start button on the touch screen display and opens the valve so that the water flows into the load bucket. Data from the load cell is recorded each second until the loading bucket is disconnected by the release mechanism. New readings are compared with previous readings to determine when the measurement process must stop. This occurs when the new readings are more than 10% lower than the previous readings. All sampled data is recorded to an SD card. The user will then empty the bucket and re-start the experiment. This is repeated 10 times for each release mechanism to enhance the validity of the results and reliability of the innovative test jig. Validity usually refers to the degree that a measurement is a true reflection of the measurand (quantity intended to be measured), while reliability (also called precision) usually refers to the repeatability of the

measurements. It must be noted that reliability is not always connected to the accuracy, but accuracy is linked to validity. An instrument may be reliable (measures the same value every time for a given parameter) but not accurate (measured value is repeatedly far off the true value).

5. RESULTS

In order to determine the accuracy of the designed system, the following was done. After the system had performed a self-calibration, three test weights were used to measure the accuracy of the system. The weight of these were measured using an accurate and calibrated scale (ADAM 6031). The resolution of the system was initially set to 0.1 g in the software. Ten consecutive measurements were done with the first test weight (144.6 grams). Recorded measurements ranged between 144.3 to 144.8 grams with a maximum deviation of 0.3 g from the true value. This was repeated for the other two weights. Recorded measurements for the 201.7 g weight ranged from 201.3 to 201.9 g with a maximum deviation of 0.4 g. Recorded measurements for the 333.3 g weight ranged from 332.8 to 333.4 g with a maximum deviation of 0.4 g. The error percentage of the system was calculated to be $\pm 0{,}1\%$ using the 333,5 g weight and its maximum deviation (translates to an accuracy of 99,879%). Given this value, it was not deemed necessary for the system to display fractions of a gram and thus the resolution was set to 1 g. This resolution is more than adequate for this type of experiment as the drone is expected to carry loads around 500 g.

In order to test and demonstrate the practical usability of the innovative test jig, the following results are presented. Figure 7 shows the measurements for one experiment where a Gannet Sport release mechanism was used with a 0.55 mm line. It is evident from Figure 7 that the loading bucket weight was 193 g at the start of the experiment. As the water poured into the bucket at a constant rate, the weight increased to 835 g where the Gannet Sport released the load, and the measured weight drops down to zero. This point is recorded as the weight at which the release mechanism activates.
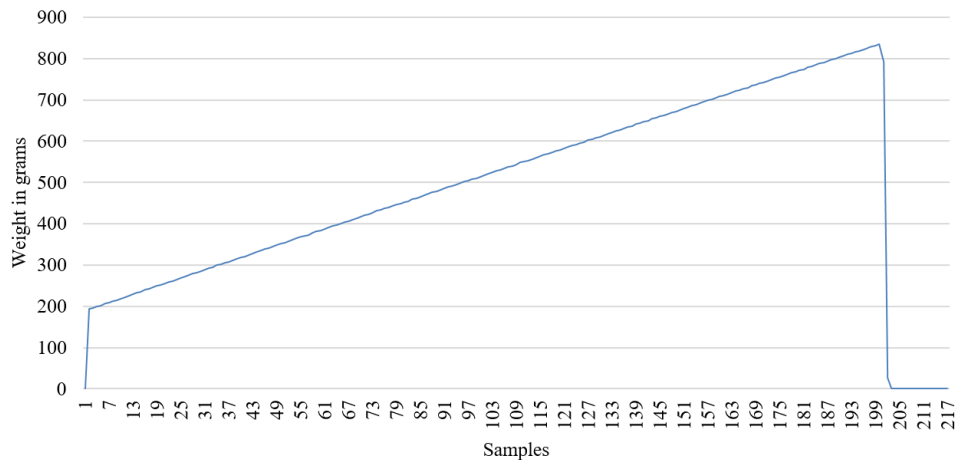
Figure 7. Data for one release experiment for the Gannet Sport with 0.55 mm line.

Figure 8 shows the maximum readings for ten consecutive readings where the Gannet sport was used with a 0.55 mm Kingfisher line. The maximum readings over the ten experiments ranged from 599 (reading no 1) to 642 g (reading no 5). Please note that no technical data is provided regarding the weights at which the release mechanism operates. This innovative jig and measurement system may now be used to clarify this.
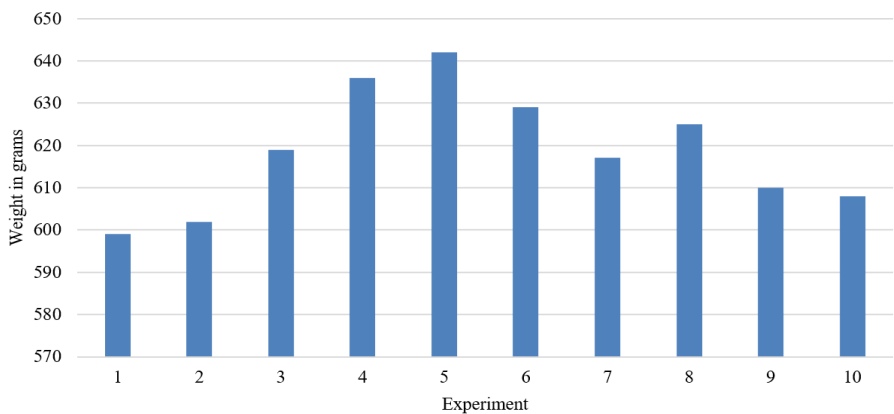
Figure 8. Recorded weights for the Gannet Sport with 0.55 mm line.

6. CONCLUSIONS

The purpose of this paper was to present a cost-effective and innovative test jig that may be used to determine the reliability and consistency of operation of various fishing-bait release mechanisms. The costs associated with the jig amount to $150 where the main

components are a HX711 instrumentation amplifier, a load cell and an Arduino Mega microcontroller. The accuracy of the system was determined to be 99,879%. Reliability values for a Gannet Sport mechanism with a 0.55 mm Kingfisher line ranged from 599 g to 642 g, giving a maximum deviation of 43 g. The results provide evidence that the system can record measured values on an SD card for later use by the researcher. It may now be used to clarify technical data regarding the weights at which different fishing-bait release mechanisms operate.

REFERENCES

Benatto, G. A. D. R., Mantel, C., Riedel, N., Lancia, A. A. S., Thorsteinsson, S., Poulsen, P. B., Forchhammer, S., Parikh, H. R., Spataru, S. V., & Séra, D. (2019). Drone-Based Daylight Electroluminescence Imaging of PV Modules. In *Proceedings of 46th IEEE Photovoltaic Specialist Conference IEEE Press.* https://vbn.aau.dk/en/publications/drone-based-daylight-electroluminescence-imaging-of-pv-modules

Brainy Quote. (2019, 2 January). http://www.brainyquote.com/quotes/

Burke, C., Nguyen, H., Magilligan, M., & Noorani, R. (2019). Study of A Drone's Payload Delivery Capabilities Utilizing Rotational Movement. In *International Conference on Robotics, Electrical and Signal Processing Techniques (ICREST), Dhaka, Bangladesh*, 672-675. https://doi.org/10.1109/ICREST.2019.8644318

Federal Aviation Administration. (2016, 28 June). *Operation and certification of small unmanned aircraft systems. In 81 Federal Register 42063.* https://www.federalregister.gov/documents/2016/06/28/2016-15079/operation-and-certification-of-small-unmanned-aircraft-systems

Ferrao, R. (2016). Drones and the Future of Armed Conflict. In 17 *ISIL Year Book of International Humanitarian and Refugee Law* (vol. 16), p. 270.

Maksimovic, M. (2018). Greening the Future: Green Internet of Things (G-IoT) as a Key Technological Enabler of Sustainable Development. In Dey, N., Hassanien, A., Bhatt, C., Ashour, A., Satapathy, S. (eds) *Internet of Things and Big Data Analytics Toward Next-Generation Intelligence*. Studies in Big Data, (vol. 30). Springer, Cham. https://doi.org/10.1007/978-3-319-60435-0_12

Oxford Dictionary. (n.d.). http://www.oxforddictionaries.com/

Paavan, L. C. S., Sai, T. G., & Naga, M. K. (2019). An IoT based Smart Garbage Alert System. In *3rd International Conference on Trends in Electronics and Informatics (ICOEI)*, Tirunelveli, India, 425-430. https://doi.org/10.1109/ICOEI.2019.8862518

Parihar, P., Bhawsar, P., & Hargod, P. (2016). Design & development analysis of quadcopter. *COMPUSOFT, An international journal of advanced computer technology, 5*(6), 2128. https://www.academia.edu/26483673/Design_and_Development_Analysis_of_Quadcopter

Park, J., Kim, S., & Suh, K. (2018). A comparative analysis of the environmental benefits of drone-based delivery services in urban and rural areas. *Sustainability, 10*(3), 888. https://doi.org/10.3390/su10030888

Qian, H., Liu, J., & Wu, Y. (2019). A Self-Service Scheme of Infant Scale for Height and Weight. In *IEEE MTT-S International Microwave Biomedical Conference (IMBioC)*, Nanjing, China, 1-3. https://doi.org/10.1109/IMBIOC.2019.8777754

Sandbrook, C. (2015). The social implications of using drones for biodiversity conservation. *Ambio, 44*(Suppl 4), 636-647. https://doi.org/10.1007/s13280-015-0714-0

SUAS News. (2019, 27 November). *Gannet Pro fishing drone*. https://www.suasnews.com/2019/10/gannet-pro-fishing-drone/

Upchurch, E. K. (2015). Drone on the Farm: The Benefits and Controversies Surrounding the Future of Unmanned Aircraft Systems in Agriculture. *Drake Journal of Agricultural Law, 20*, 309. https://aglawjournal.wp.drake.edu/wp-content/uploads/sites/66/2016/09/agVol20No2-upchurch.pdf

Wan, W. M., Azrie, M. S., & Shuib, A. (2018). Mechanism For Drones Delivering The Medical First Aid Kits. *Advances in Transportation and Logistics Research, 1,* 303-315. http://proceedings.itltrisakti.ac.id/index.php/ATLR/article/view/33

Wulfovich, S., Rivas, H., & Matabuena, P. (2018). Drones in Healthcare. In Rivas H., Wac K. (eds) *Digital Health. Health Informatics.* Springer, Cham, 159-168. https://doi.org/10.1007/978-3-319-61446-5_11

/08/

VALIDATING THE OPTIMUM TILT ANGLE FOR PV MODULES IN THE HIGHVELD OF SOUTH AFRICA FOR THE SUMMER SEASON

Motlatsi Cletus Lehloka

Department of Electrical and Mining Engineering, University of South Africa, Christiaan de Wet Road and Pioneer Avenue, Florida, Roodeport, (South Africa).

E-mail: lehlomc@unisa.ac.za ORCID: https://orcid.org/0000-0002-0901-9731

Arthur James Swart

Department of Electrical, Electronic and Computer Engineering, Central University of Technology, Bloemfontein, (South Africa).

E-mail: aswart@cut.ac.za ORCID: http://orcid.org/0000-0001-5906-2896

Pierre Eduard Hertzog

Department of Electrical, Electronic and Computer Engineering, Central University of Technology, Bloemfontein, (South Africa).

E-mail: pertzog@cut.ac.za ORCID: http://orcid.org/0000-0002-3396-6050

ABSTRACT

Energy supply is a major problem in today's world due to increase in demand, depleting of fossil fuels and increase in global warming due to carbon emission. The need for an alternate, overall efficient and environment-friendly energy system has ascended globally. Photovoltaic (PV) systems can be used to harness solar energy that is considered to be one of the most promising alternative energy sources. However, its efficiency is affected not only by varying environmental conditions but also by the installation of its PV modules. The purpose of this paper is to empirically validate the optimum tilt for PV modules in the Highveld of South Africa. Three fixed-axis PV modules installed at optimum tilt angles of Latitude minus 10°, Latitude, and Latitude plus 10° serve as the basis of this study. These optimum tilt angles are utilised based on the recommendations by Heywood and Chinnery. A key recommendation is that PV modules should be mounted at Latitude minus 10° for the summertime period in the Highveld region of South Africa.

KEYWORDS

PV module, LabVIEW, Latitude, Tilt angles.

1. INTRODUCTION

Solar photovoltaic (PV) systems are classified as a clean and renewable energy source and therefore, they have been drawing more and more attention, especially in the field of electricity generation due to the shortage and pollution effects of fossil fuels. Solar energy is one of the primary sources of clean, abundant and inexhaustible energy, that not only provides alternative energy resources, but also improves environmental pollution. The use of renewable energy resources to produce electricity is a rising trend in various countries worldwide. This is because these energies do not produce the greenhouse gases; therefore, do not become a destructive factor on the ozone layer and the environment. The effects that fossil fuels have on the environment have led to scientists trying to find more environmentally friendly fuels and cleaner sources of energy (Yao *et al.*, 2014; Lawless & Kärrfelt, 2018).

In order to maximise energy production from PV modules, the latter requires the use of optimum tilt and orientation angle for the location of interest. Optimizing the output power of any PV array or module requires a number of factors to be considered, including the tilt angle, orientation angle and environmental conditions (Yadav & Chandel, 2013; Moghadam *et al.*, 2011). Before the introduction of solar tracking methods, fixed PV modules were positioned with a reasonable tilted angle based on the latitude of the location. A number of studies have been carried out to find the optimum tilt angles of PV modules in various environments (Ferdaus *et al.*, 2014; Moghadam & Deymeh, 2015).

Sunlight incidence angle varies throughout the year due to the rotation of the earth around its own axis and its elliptical orbit. While sunlight falls to the earth with steep (high) angles in summer in the Northern Hemisphere, it falls with shallow (low) angles in winter. Many fixed PV modules are not installed at the suggested tilt angle, for example, true North in South Africa, thereby indicating a non- alignment to the maximum solar radiation available for a given day (Karafil *et al.*, 2015; Swart & Hertzog, 2015). Furthermore, as the sun is not a stationery object it is essential to install the fixed PV modules at optimum tilt and orientation angle for the location of interest. Climate change has also resulted in the rise of atmospheric temperature and a modified pattern of precipitation and evapotranspiration, which has directly led to alteration of regional hydrological cycles. Repetitive testing of key variables associated with renewable energy systems under ever-changing environmental

conditions must be maintained, to either strengthen or reconstruct previously published literature in this field. Repeated testing of any construct in research is just as necessary as it reinforces knowledge, promotes validity and enables its successful use in other applications (Hertzog & Swart, 2018a, 2018b).

The purpose of this paper is to empirically validate the optimum tilt for PV modules in the Highveld of South Africa. The motive behind validating these angles is mainly to establish if the recommendations by Heywood and Chinnery still holds truth in the Highveld of South Africa under ever-changing environmental conditions that are related to climate change. The paper will firstly provide a brief description of tilt angles, and then outline the context of the research site. The experimental setup will then be explained, followed by the research methodology. Quantitative data is then presented in a number of tables and figures along with discussions.

2. LITERATURE STUDY

Efficient operation of PV modules depends on many factors, among which are the installation angles. The optimum installation angles involve placing a fixed PV module at an orientation angle of 0° and changing the angle of tilt to Latitude minus 10°, Latitude and Latitude +10° respectively. These angles are derived from the Heywood and Chinnery equations of Latitude for calculating tilt angles of PV modules in South Africa. The orientation angle is defined as the angle between true South (or true North) and the projection of the normal of the PV module to the horizontal plane. The tilt angle is defined as the angle between the PV module surface and the horizontal plane (Swart & Hertzog, 2015). Figure 1 illustrates both the orientation and tilt angle of PV modules. The PV modules should face "true north" in the northern Hemisphere and "true south" in the southern Hemisphere (Kaldellis & Zafirakis, 2012; Chin, Babu, & McBride, 2011).

Many authors presented models to predict solar radiation received on inclined surfaces from the typically measured global horizontal irradiance and diffuse horizontal irradiance. While the direct beam radiation on a tilted surface can be calculated using geometric relations, the conversion for the diffuse radiation is more complex and has been approached using different models. Studies have been done in South Africa to determine the optimum angles

of fixed solar collectors, but these studies do have some limitations. Like other locations in the world, results were based on mathematical models of solar resource, measured solar data or both. Various other studies on the optimisation of tilt angles have considered the effects of cloudiness, wind speed cooling, maximising radiation on flat plate collectors, Latitude, clearness index, day number and different geographical locations. In line with many theoretical and experimental investigations on optimizing the output power of a PV module by varying its tilt angle, it is essential to empirically validate the results.

Figure 1. The tilt and orientation angles of a PV module. **Source:** (Asowata, Swart, & Pienaar, 2012).

In 2013, a research study was conducted at the Vaal University of Technology (VUT) (subsequently called the VUT study) to determine the fixed PV module tilt angle for optimum power yield throughout the year. A Latitude plus 10º angle was suggested. The research was conducted in an area that was declared an 'airshed priority area' due to the concern of elevated pollutant concentrations within the area, being specifically particulates (Kaddoura, Ramli, & Al-Turki, 2016; Khoo *et al.*, 2013; Hertzog & Swart, 2016). Another study conducted at the Central University of Technology (CUT) (subsequently called the CUT study) was done to validate three different tilt angles for PV modules in a semi-arid region. Results suggest that PV modules need to be installed at a tilt angle of Latitude plus 10º for semi-arid regions during the summer season. Contrary to the VUT and CUT study, the current location of interest is a residential area affected mainly by domestic fuel burning, vehicles emission and it is also known for its thunderstorms.

3. RESEARCH SITE

South Africa is zoned into six regions namely; arid, semi-arid, dry sub-humid, humid and very humid (Gauché, 2016). Arid are regions where a combination of high temperatures and low rainfall causes evaporation that exceeds precipitation (Barakat, 2009). Humidity is a measure of how much moisture is present compared to how much moisture the air could hold at a specific temperature. Figure 2 illustrates the South African map of climate indicators aridity. The current location of interest is the University of South Africa (UNISA), Science campus, Florida with the given coordinates of 26.1586° S and 27.9033° E (classified under the Highveld region of South Africa). From Figure 2, it can be noted that the current study (also called the UNISA study) is in the dry sub-humid region while the CUT study is located in the semi-arid region. Even though the VUT study is also located in the sub-humid region, it was in the area that was declared airshed priority area because of high level of pollution as compared to the UNISA study. With ever-changing environmental conditions, it is important to continue investigating the optimum installation angles for PV modules around the globe. The results of this UNISA study will help in establishing if the VUT and CUT studies recommendations' still hold truth.

Figure 2. The climate indicators aridity. Source: (Gauché, 2016).

4. PRACTICAL SETUP

Three PV modules with the same load profile were used (4 by 0.82 Ω resistors in series with a 1 Ω resistor (100 W)). All the PV modules were set to an orientation angle of 0°. Their tilt angles varied between 16°, 26° and 36°. The angles were derived using Latitude minus 10° (26° - 10°), Latitude (26°) and Latitude plus 10° (26° + 10°) (see Table 1 for mathematical calculations). A reference tilt angle of 26° was used in this study, corresponding to the Latitude value of the installation site at the UNISA, Florida campus, which is lying on the elevated plateau of the interior of South Africa (Highveld).

Table 1. Calculation of tilt angles.

Source	Site Latitude	Equation	Calculation	Tilt angle
Heywood and Chinnery (1971)	26°	Latitude - 10°	26°-10°	16°
	26°	Latitude	26°	26°
	26°	Latitude + 10°	26°+10°	36°

The system block diagram is illustrated in Figure 3 while the practical setup is illustrated in Figure 4. The practical setup has three identical PV modules (a 310 W YL310P-35b polycrystalline PV module with a rated voltage = 36.3 V, open circuit voltage = 45.6 V, rated current = 8.53 A and short circuit current = 8.99 A). The data logging interface circuit provides signal conditioning between the PV module and the data acquisition (DAQ) equipment. Figure 5 illustrates the National Instruments (NI) data acquisition (DAQ) hardware installed inside the control boxes. The DAQ incorporates other PV modules which are not part of this research study. Voltage and current measured from the PV modules are relayed to LabVIEW where the optimum power is calculated. The LabVIEW user interface was used to visualize the measured data. The main function of a signal conditioning circuit (also used as a load) is to scale down signal voltage and add offset voltages (Juhana & Irawan, 2015). It is oriented towards limiting the input voltage to the DAQ system to less than 10 V as the DAQ system can only handle a maximum input of 10 V.

Figure 3. Block diagram of the system.
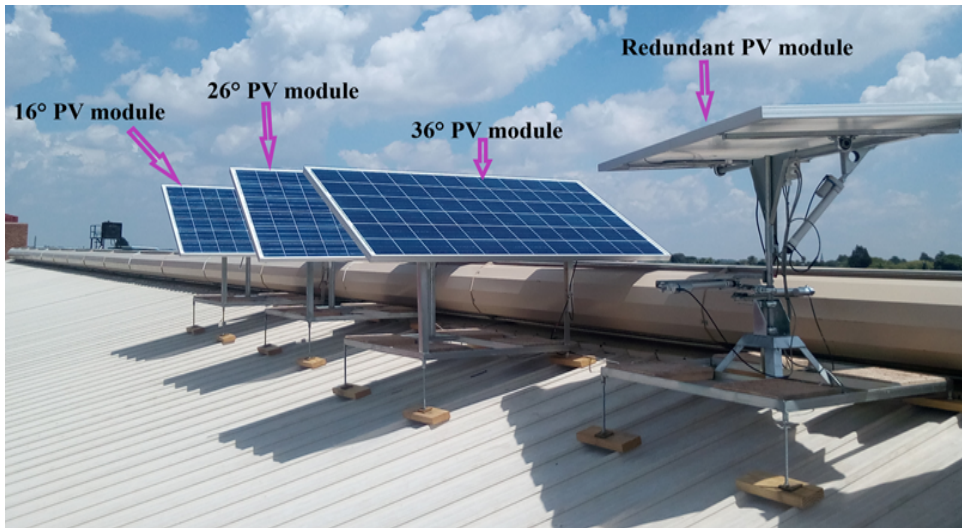
Figure 4. The three PV modules fixed at different tilt angles.

Figure 5. The DAQ system hardware box.

Figure 6 illustrates the load resistance circuit diagram that provides signal conditioning and that is also used as the system load (Figure 7), featuring high power resistors that are chosen to satisfy the voltage divider rule. An economic viable load for considering output power results from identical PV module can include the following:

- Batteries with a solar charger;

- Batteries with a maximum power point tracker (MPPTs);

- Regulated and non-regulated light emitting diode (LED) lamps; and

- Fixed load resistors (Swart & Hertzog, 2016a).
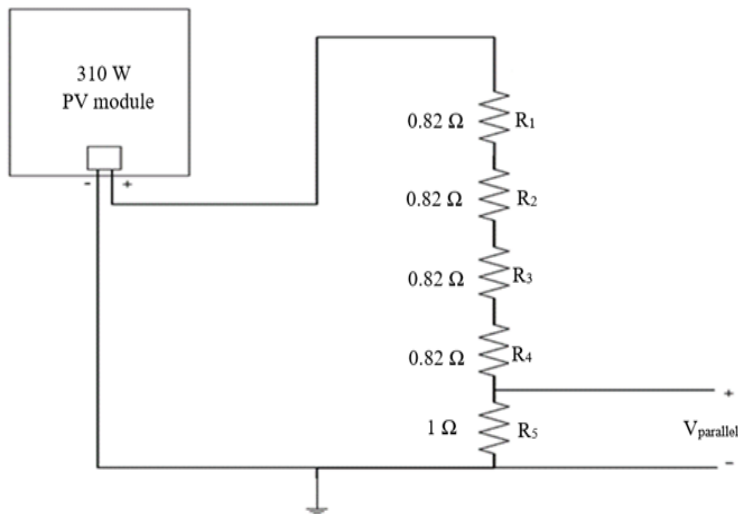
Figure 6. The circuit diagram of the load resistance.

Using fixed load resistance instead of a solar charger or maximum power point tracker (MPPT) was discovered to be an effective and easy method to start loading PV modules located outdoors for measurement purposes and could be a more viable option for monitoring long-term PV module performance. Fixed resistive loads can greatly reduce the test system costs and complexity, however, the disadvantage is that there is no way to implement maximum power tracking (MPT). Fixed load resistors in this study form a typical voltage divider circuit, where five resistors are connected in series across a source voltage. As the source voltage is dropped in successive steps through the series resistors, any desired portion of the source voltage may be "tapped off" to supply individual voltage requirements. The voltage divider circuit provides signal conditioning, as the optimum voltage of the PV module is 36.3 V which is much higher than the allowed input voltage to the NI DAQ unit which is limited to 10 V (eq. 1). Using three 0.82 Ω and 1 Ω resistors (100 W) in series enables the input voltage to the NI DAQ to be less than 10 V. This DAQ is connected directly to a personal computer running the LABVIEW software where measurements are recorded (Swart & Hertzog, 2016b; Tien & Shin, 2016).

$$V_{out} = V_{in}\left(\frac{R_1}{R_T}\right)$$
$$= 36.3\left(\frac{1}{4.28}\right) \tag{1}$$
$$= 8.48 \, V$$

Where: V_{out} = Voltage divider output to the DAQ system

V_{in} = PV module output voltage

R_1 = System 1 Ω resistor where the voltmeter is connected across

R_T = Total resistance of the circuit in series ($R_1 + R_2 + R_3 + R_4 + R_5 = 4.28$ Ω)

Figure 7. The system loads.

5. RESEARCH METHODOLOGY

This section describes the research methodology that was engaged in for the empirical experimental design portion of the study. The outcome was to establish the tilt angle that yields optimal output power from three identical PV modules set at three different tilt angles

in the Highveld region of South Africa during the summer season. This was done by setting the PV modules with the same load profile at Latitude minus 10° (16°), Latitude (26°) and Latitude plus 10° (36°) respectively. For calibration purposes, the three PV modules were set at fixed angles of 0° (orientation) and 26° (tilt) (see Figure 8). The intention of calibrating the system was to eliminate any bias between the systems. Calibration of equipment is of vital importance before measurements can be taken to ensure accuracy and to validate any future measurements as being reliable (Swart & Hertzog, 2019). To check validity of the system, the three PV modules were set to the same tilt angle of 26° for few hours on the 3rd of February 2019. The measurements were taken using a Rish Multi 16S True RMS digital multimeter. The readings on the digital multimeter correlated with the ones on the LabVIEW user interface software resulting with no need for any adjustment. Subsequently, the PV modules were set to their respective tilt angles again.
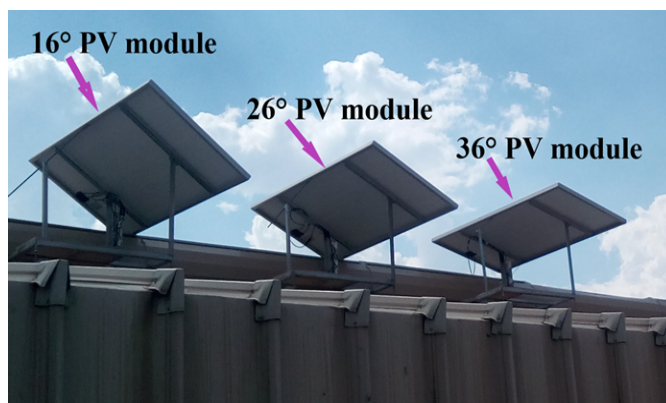
Figure 8. The three PV modules fixed at 0° orientation angle and 26° tilt angle.

The LabVIEW user interface was used to visualize the measured data. It was designed and developed for this research pertaining to the operating parameters of PV modules and linear actuators. The sample interval (measurements taken every 4 seconds from the LabVIEW user interface) and cycle duration of 12 hours (6 am − 6 pm) may be adjusted after each complete cycle, as LabVIEW first needs to close an opened text file on the hard drive of the computer. This text file contains the measurements displayed on the user interface, which are only saved at the end of the complete cycle. The system was let to run for a period of three months being December 2018 to February 2019 which is the summer season in South Africa.

6. THE LABVIEW USER INTERFACE

Figure 9 shows the LabVIEW user interface that was used to display voltage and current readings from the PV modules. The measure voltage and current were used to calculate the output power (P=VI). The LabVIEW user interface provides the following information:

- Analog instantaneous value of voltage for each PV module (point A);

- Digital instantaneous value of voltage for each PV module (point B);

- Analog instantaneous value of current for each PV module (point C);

- Digital instantaneous value of voltage for each PV module (point D);

- Instantaneous value of voltage for each PV module in graph form (point I);

- Instantaneous value of current for each PV module in graph form (point J);

- Date-time string function to start and stop the data recording process at predefined moments of time e.g sunrise time and sunset time (E and F);

- Numeric indicator indicating direction to which the PV modules are taking e.g vertical or horizontal (H-I); and

- The stop button function to control the while loop execution.

Figure 9. The LabVIEW front panel.

7. RESULTS

This section provides results regarding calibration and the different output powers of the three PV modules set at different tilt angles. The calibration readings highlighted on Figure 10 show the physically measured voltage of 34.9 V and current of 8.29 A on the digital multimeters.

Figure 10. The Rish Multi 16S True RMS multimeter.

Table 2. Calibration results.

Name Angle	LabVIEW Current (A)	Module Current (A)	Current Error percentage (%)	LabVIEW Voltage (V)	Module Voltage (V)	Voltage Error percentage (%)
16º	8.27	8.29	0.24	34.7	34.9	0.57
26º	8.27	8.29	0.24	34.4	34.5	0.29
36º	8.27	8.29	0.24	34.7	34.8	0.29

These values correlated well with those shown on the LabVIEW user interface as shown in Table 2. The calibration readings were compared to the available readings in the LabVIEW user interface, so that the instantaneous voltage and current values displayed on the interface equalled the values displayed on the digital multimeter. The system was calibrated between 12:30 noon and 1 pm when the sun was perpendicular to all the PV modules. The measurements were first done on the latitude minus 10° (16°) PV module. Current of 8.29 A from the PV module was measured (physically) while the LabVIEW interface displayed 8.27 A. The readings (currents and voltages) measured physically on the other modules and displayed by the LabVIEW interface within the 30 minutes time are displayed in Table 2. Table 2 further presents the percentage difference between the digital multimeter and LabVIEW readings. The highest error percentage for voltage occurred

for the 16° PV module (being 0,57 %). Results indicate that three identical PV systems can be calibrated to produce the same results, with variability of less than 1 % (Swart & Hertzog, 2019). A consistent percentage (0,24 %) between the multimeter and LabVIEW user interface was established for the current values. The voltage measured for one day was utilised to plot a graph as illustrated in Figure 11 where the three PV modules were fixed at the same tilt and orientation angles (0° and 26°) for calibration purposes.
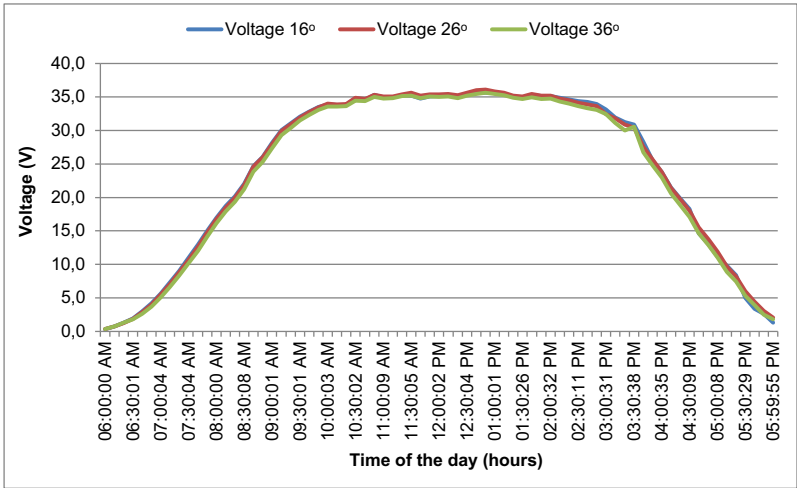
Figure 11. The three PV modules fixed at 0° orientation and 26° tilt angles.

The PV modules continued to behave similarly throughout the day. From 10 am to 15:00 pm the PV modules were aligned to the larger portion of the solar radiation which is normally maximum at 12 noon. The PV modules were producing constant output voltage which was nearly the maximum rated voltage. The purpose of the calibration was to produce the same results from all three PV modules that were orientated similarly. This was achieved, resulting in a valid setup where subsequent measurements or results will be reliable.

Table 3 shows the results of the instantaneous average power for a period of three months, being December 2018, January and February 2019. The results on Table 3 were used to plot a chart as illustrated in Figure 12 and a graph in Figure 13 for further analysis.

Table 3. The three months instantaneous power readings and the total Wh.

Time	16°	26°	36°
Dec '18 Week 1	125,9	121,2	114,1
Dec '18 Week 2	133,0	128,2	120,7

Time	16º	26º	36º
Dec '18 Week 3	153,6	147,9	139,3
Dec '18 Week 4	107,6	103,7	97,6
Jan '19 Week 1	154,6	148,9	140,2
Jan '19 Week 2	139,4	134,2	126,4
Jan '19 Week 3	119,8	115,4	108,6
Jan '19 Week 4	42,0	40,6	38,4
Feb '19 Week 1	123,9	119,4	112,4
Feb '19 Week 2	166,2	160,1	150,7
Feb '19 Week 3	166,6	160,5	151,1
Feb '19 Week 4	157,9	152,1	143,2
Total ave. Wh	266108,8	258424,2	212786,1
Percentage difference	16° > 26° = 5,3 %	26° > 36°= 8,8 %	16° > 36°=14,2 %

From both figures, it is evident that the Latitude minus 10° (16°) PV module outperformed the Latitude (26°) and Latitude plus 10° (36°) PV modules in power harvesting throughout the summer season. Similar research has shown that a PV module with a tilt angle of Latitude minus 10° yields the highest output power for summer months in a semi-arid region of South Africa (Hertzog & Swart, 2018a). The percentage difference between the total Wh produced for the summer season between 16° and 26° PV modules was 5,3 %. The percentage difference between 16° and 36° PV modules was 14,2 %, while the percentage difference between 26° and 36° PV modules was 8,8 %.
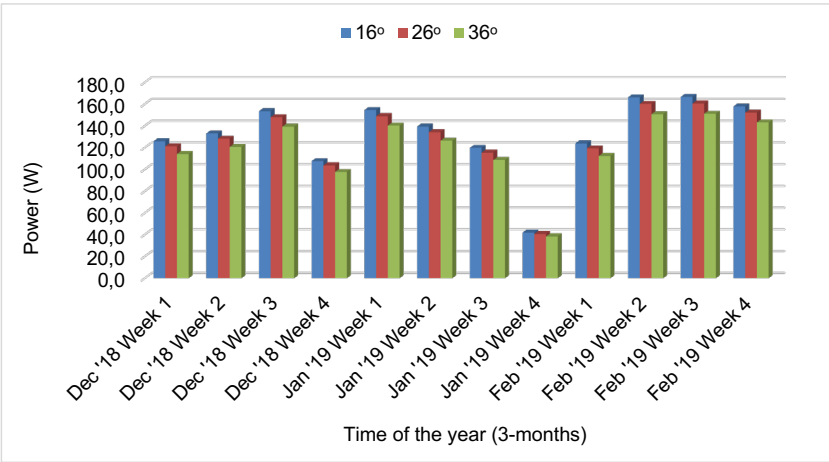

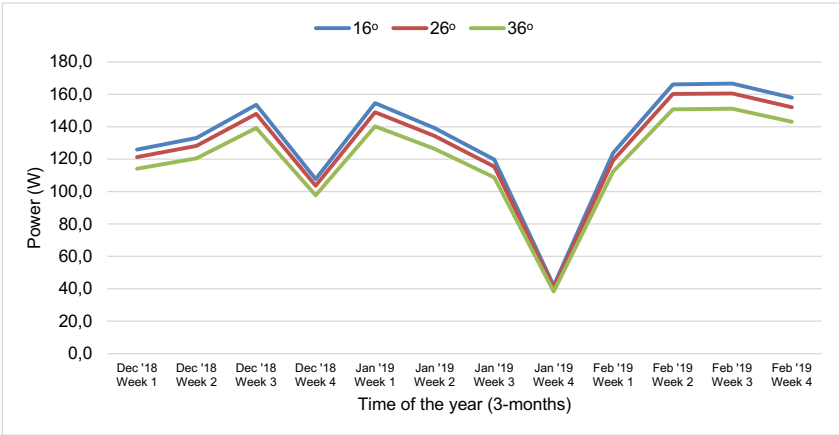**Figure 12.** Number of samples for the three-month period.

Figure 13. The three PV modules fixed at 0° orientation and different tilt angles for three months.

8. CONCLUSIONS

The purpose of this paper was to empirically validate the optimum tilt angle for PV modules in the Highveld of South Africa in the summer season. Three fixed PV modules were set at the same orientation angle of 0°, but at different tilt angles of Latitude minus 10° (16°), Latitude (26°) and Latitude plus 10° (36°). This was done based on a recommendation by Chinnery and Heywood for calculating tilt angles for PV module installations in the Southern Hemisphere. The PV modules were installed at the UNISA Science campus, which lies in the Highveld of South Africa.

Reliability and validity of any results was firstly established by having all three modules set to the same tilt angle. A variability of less than 1 % was established indicating a higher level of similarity between the performances of all three PV modules. The main results then showed that the PV module installed at Latitude minus 10° outperformed the PV module installed at Latitude by 3.48 %. It also outperformed Latitude plus 10° by 10.69 %. This correlates well with literature and previous results obtained in the CUT and VUT studies which recommended that PV modules be placed at a tilt angle of Latitude minus 10° during the summer season in South Africa.

It is important to state that possible limitations of this study include the fact that only one research installation site was used, and that data has not yet been collected for the other

seasons of the year (autumn, winter and spring). It is vital to obtain results for the other seasons of the year to establish any variability in the optimum tilt angle values.

It is recommended to set a fixed-type PV module to an optimum tilt angle value that allows it to harvest the maximum power from the sun. Based on the results in this study, it is recommended to place fixed-type PV modules at a tilt angle of Latitude minus 10º with a 0° orientation angle during the summer season in the Highveld region of South Africa.

ACKNOWLEDGMENT

REFERENCES

Asowata, O., Swart, A. J., & Pienaar, C. (2012). Optimum Tilt Angles for Photovoltaic Panels during Winter Months in the Vaal Triangle, South Africa. *Smart Grid and Renewable Energy, 3*, 119-125. https://www.researchgate.net/publication/258148876_Optimum_Tilt_Angles_for_Photovoltaic_Panels_during_Winter_Months_in_the_Vaal_Triangle_South_Africa

Asowata, O., Swart, A. J., Pienaar, H. C., & Schoeman, R. M. (2013). Optimizing the output power of a stationary PV panel. In *Proceedings of the Southern Africa Telecommunications Networks and Applications Conference (SATNAC), Stellenbosch, South Africa*. https://www.researchgate.net/publication/258148774_Optimizing_the_output_power_of_a_stationary_PV_panel

Asowata, O., Swart, J., & Pienaar, C. (2012). Optimum tilt and orientation angles for photovoltaic panels in the Vaal triangle. In *2012 Asia-Pacific Power and Energy Engineering Conference, Shanghai, China*. https://doi.org/10.1109/APPEEC.2012.6307168

Barakat, H. N. (2009). Arid Lands: Challenges and Hopes. In Cliek, V., Smith, R. H. (eds.) *Earth system: History and natural variability* (Vol. 3). Eols Publishers Co. Ltd.

Bazyari, S., Keypour, R., Farhangi, S., Ghaedi, A., & Bazyari, K. (2014). A Study on the Effects of Solar Tracking Systems on the Performance of Photovoltaic Power Plants. *Journal of Power and Energy Engineering, 02*(04), 718-728. https://www.researchgate.net/publication/273986929_A_Study_on_the_Effects_of_Solar_Tracking_Systems_on_the_Performance_of_Photovoltaic_Power_Plants

Chin, C. S., Babu, A., & McBride, W. (2011). Design, modeling and testing of a standalone single axis active solar tracker using MATLAB/Simulink. *Renewable Energy, 36*(11), 3075-3090. https://doi.org/10.1016/j.renene.2011.03.026

Ferdaus, R. A., Mohammed, M. A., Rahman, S., Salehin, S., & Mannan, M. A. (2014). Energy Efficient Hybrid Dual Axis Solar Tracking System. *Journal of Renewable Energy,* Article ID 629717. https://doi.org/10.1155/2014/629717

Gauché, P. (2016). *Spatial-temporal model to evaluate the system potential of concentrating solar power towers in South Africa* (Thesis PhD). Stellenbosch University. https://scholar.sun.ac.za/handle/10019.1/100151

Hafez, A. Z., Soliman, A., El-Metwally, K. A., & Ismail, I. M. (2017). Tilt and azimuth angles in solar energy applications. *Renewable and Sustainable Energy Reviews, 77,* 147-168. https://doi.org/10.1016/j.rser.2017.03.131

Hertzog, P. E., & Swart, A. J. (2015). Determining the optimum tilt angles for PV modules in a semi-arid region of South Africa for the summer season. *Proceedings of Southern Africa Telecommunication Networks and Applications Conference (SATNAC), Hermanus, South Africa.* https://www.researchgate.net/publication/281810112_Determining_the_optimum_tilt_angles_for_PV_modules_in_a_semi-arid_region_of_South_Africa_for_the_summer_season

Hertzog, P. E., & Swart, A. J. (2016). Validating the Optimum Tilt Angle for PV Modules in the Central Region of South Africa for the Winter Season. In *13th International Conference on Electrical Engineering/Electronics, Computer, Telecommunications and Information Technology (ECTI-CON), Chiang Mai, Thailand.* https://doi.org/10.1109/ECTICon.2016.7561316

Hertzog, P. E., & Swart, A. J. (2018a). Optimum Tilt Angles for PV Modules in a Semi-Arid Region of the Southern Hemisphere. *International Journal of Engineering & Technology, 7*(4.15), 290-297. http://dx.doi.org/10.14419/ijet.v7i4.15.23010

Hertzog, P. E., & Swart, A. J. (2018b). Validating three different tilt angles for PV modules in a semi-arid region. In *IEEE International Conference on Innovative Research and Development (ICIRD), Bangkok, Thailand, 1-6.* https://doi.org/10.1109/icird.2018.8376327

Juhana, T., & Irawan, A. I. (2015). Non-intrusive load monitoring using Bluetooth low energy. In *9th International Conference on Telecommunication Systems Services and Applications (TSSA), Bandung, Indonesia, 1-4.* https://doi.org/10.1109/TSSA.2015.7440454

Kaddoura, T. O., Ramli, M. A. M., & Al-Turki, Y. A. (2016). On the estimation of the optimum tilt angle of PV panel in Saudi Arabia. *Renewable and Sustainable Energy Reviews, 65,* 626-634. https://doi.org/10.1016/j.rser.2016.07.032

Kaldellis, J., & Zafirakis, D. (2012). Experimental investigation of the optimum photovoltaic panels' tilt angle during the summer period. *Energy, 38*(1), 305-314. https://doi.org/10.1016/j.energy.2011.11.058

Karafil, A., Ozbay, H., Kesler, M., & Parmaksiz, H. (2015). Calculation of optimum fixed tilt angle of PV panels depending on solar angles and comparison of the results with experimental study conducted in summer in Bilecik, Turkey. In *9th International Conference on Electrical and Electronics Engineering (ELECO), Bursa, Turkey.* https://doi.org/10.1109/ELECO.2015.7394517

Khatib, T., Mohamed, A., & Sopian, K. (2012). On the monthly optimum tilt angle of solar panel for five sites in Malaysia. In *13th International Power Engineering and Optimization Conference of Institution of Electrical and Electronic Engineering, Melaka, Malaysia.* https://doi.org/10.1109/PEOCO.2012.6230827

Khoo, Y. S., Nobre, A., Malhotra, R., Yang, D., Rüther, R., Reindl, T., & Aberle, A. G. (2013). Optimal orientation and tilt angle for maximizing in-plane solar irradiation for PV applications in Singapore. *IEEE Journal of Photovoltaics, 4*(2), 647-653. https://doi.org/10.1109/JPHOTOV.2013.2292743

Lawless, C., & Kärrfelt, E. (2018). *Sun Following Solar Panel: Using Light Sensors to Implement Solar Tracking* (Bachelor's Thesis at ITM). KTH Royal Institute of Technology. School of Industrial Engineering and Management. http://kth.diva-portal.org/smash/get/diva2:1216641/FULLTEXT01.pdf

Le Roux, W. G. (2016). Optimum tilt and azimuth angles for fixed solar collectors in South Africa using measured data. *Renewable Energy, 96*(Part A), 603-612. https://doi.org/10.1016/j.renene.2016.05.003

Moghadam, H., & Deymeh, S. M. (2015). Determination of optimum location and tilt angle of solar collector on the roof of buildings with regard to shadow of adjacent neighbors. *Sustainable Cities and Society, 14*, 215-222. https://doi.org/10.1016/j.scs.2014.09.009

Moghadam, H., Tabrizi, F. F., & Sharak, A. Z. (2011). Optimization of solar flat collector inclination. *Desalination, 265*(1-3), 107-111. https://doi.org/10.1016/j.desal.2010.07.039

Osterwald, C. R., Adelstein, J., Cueto, J. A. del, Sekulic, W., Trudell, D., McNutt, P., Hansen, R., Rummel, S., Anderberg, A., & Moriarty, T. (2006). Resistive Loading of Photovoltaic Modules and Arrays for Long-Term Exposure Testing. *Progress in Photovoltaics Research and Applications, 14*(6), 567-575. https://doi.org/10.1002/pip.693

Swart, A. J., & Hertzog, P. E. (2015). Validating the acceptance zone for PV modules using a simplified measuring approach. In *13th International Conference on Electrical Engineering/Electronics, Computer, Telecommunications and Information Technology (ECTI-CON), Chiang Mai, Thailand.* https://doi.org/10.1109/ECTICon.2016.7561312

Swart, A. J., & Hertzog, P. E. (2016a). Validating the acceptance zone for PV modules using a simplified measuring approach. In *13th International Conference on Electrical Engineering/Electronics, Computer, Telecommunications and Information Technology (ECTI-CON), Chiang Mai, Thailand.* https://doi.org/10.1109/ECTICon.2016.7561312

Swart, A. J., & Hertzog, P. E. (2016b). Verifying an economic viable load for experimental purposes relating to small scale PV modules. In *Proceedings of the Southern Africa Telecommunications Networks and Applications Conference (SATNAC), 5-10, Fancourt, George, Western Cape, South Africa.* https://www.researchgate.net/publication/310447924_Verifying_an_economic_viable_load_for_experimental_purposes_relating_to_small_scale_PV_modules

Swart, A. J., & Hertzog, P. E. (2019). Regularly calibrating an energy monitoring system ensures accuracy. *WEENTECH Proceedings in Energy, 5*(1), 37-45. http://weentechpublishers.com/paper.aspx?pid=f0679b7d-346c-4098-b359-d19c06ca051b

Tien, N. X., & Shin, S. (2016). A Novel Concentrator Photovoltaic (CPV) System with the Improvement of Irradiance Uniformity and the Capturing of Diffuse Solar Radiation. *Applied Sciences, 6*(9), 251. https://www.researchgate.net/publication/307949696_A_Novel_Concentrator_Photovoltaic_CPV_System_with_the_Improvement_of_Irradiance_Uniformity_and_the_Capturing_of_Diffuse_Solar_Radiation

Wang, L.-M., & Lu, C.-L. (2013). Design and Implementation of a Sun Tracker with a Dual-Axis Single Motor for an Optical Sensor-Based Photovoltaic System. *Sensors (Basel), 13*(3), 3157-3168. https://doi.org/10.3390/s130303157

Yadav, A. K., & Chandel, S. S. (2013). Tilt angle optimization to maximize incident solar radiation. *Renewable and Sustainable Energy Reviews, 23*, 503-513. https://doi.org/10.1016/j.rser.2013.02.027

Yao, Y., Hu, Y., Gao, S., Yang, G., & Du, J. (2014). A multipurpose dual-axis solar tracker with two tracking strategies. *Renewable Energy, 72,* 88-89. https://doi.org/10.1016/j.renene.2014.07.002

/09/

AGGREGATED MODEL FOR TUMOR IDENTIFICATION AND 3D RECONSTRUCTION OF LUNG USING CT-SCAN

Syed Abbas Ali

N.E.D University of Engineering and Technology, Karachi, (Pakistan).

E-mail: saaj@neduet.edu.pk ORCID: https://orcid.org/0000-0001-6014-1559

Nazish Tariq

Dow University of Health and Sciences, Karachi, (Pakistan).

E-mail: nazish.tariq1988@gmail.com ORCID: https://orcid.org/0000-0002-3275-390X

Sallar Khan

Sir Syed University of Engineering and Technology, Karachi, (Pakistan).

E-mail: sallarkhan_92@yahoo.com ORCID: https://orcid.org/0000-0001-8988-3388

Asif Raza

Sir Syed University of Engineering and Technology, Karachi, (Pakistan).

E-mail: asif.raza@ssuet.edu.pk ORCID: https://orcid.org/0000-0002-2340-0627

Syed Muhammad Faza-ul-Karim

Sir Syed University of Engineering and Technology, Karachi, (Pakistan).

E-mail: fkarim15@yahoo.com ORCID: https://orcid.org/0000-0002-9039-8184

Muhammad Rahil Usman

Sir Syed University of Engineering and Technology, Karachi, (Pakistan).

E-mail: usman.rahil@gmail.com ORCID: https://orcid.org/0000-0002-8385-3345

ABSTRACT

This paper facilitates radiologists in diagnosis of lung tumor and provides with a probability to differentiate between the types of tumor through automated analysis and increase in accuracy. The system is aggregated model for tumor identification and 3D reconstruction of lung using (computed Tomography) CT-scan images in Digital Imaging and Communications in Medicine (DICOM) format to identify the lung tumor (Benign or Malignant) using learning algorithm. The proposed system is capable to reconstruct the 3D model of lung tumor using CT-scan medical images and identify tumor (Benign or Malignant) including location of tumor (Attached to wall or parenchyma) with significant accuracy. The proposed diagnostic software provides significant results with bright CT scans to identify lungs tissue with different orientations by rotating it and reduces the enormous false positive rate by increasing the efficiency and accuracy of the diagnostic procedure. Whereas, CT-scan image is below required brightness or if CT-scan is done in a dark room than the module does not shows considerable results of segmentation. The proposed computer aided diagnosis can help the radiologists to detect tumor at early stage, decrease the enormous false positive rate, and the overall cost of the diagnostic procedure; thus, bringing windfall benefits in the field of medical imaging.

KEYWORDS

Medical Imaging, Image Processing, Lung Tumor, Machine learning.

1. INTRODUCTION AND RELATED WORK

Health of an individual is a worldwide issue that implies lots of problems especially where health service may be deficient and unsupervised. Lungs tumor is one of the leading causes of death in both males and females. Smoking is one of risk factors of lung tumor. However, the duration of smoking and number of cigarettes consumed also contribute a lot in the risk of lung tumor. The chances of expanding lung tumor can be lowered if the habit of smoking is dropped to a certain extent. Majorly, both smokers and people are exposed to second-hand smoke. Individuals who were never passive smoker and never exposed to second-hand smoke can have tumor. There might be no apparent cause of lungs tumor in these cases. Doctors believed that lungs tumor damage the cells; when an individual inhales smoke of the cigarette, which is full of substances (carcinogens) that can cause tumor, immediately bring changes in lungs tissue.

Firstly, the body may be able to adjust these changes, but with the continuous exposure, the normal cells that link lungs are damaged increasingly. Afterwards, the damaged cells act abnormally and develop tumor eventually. The occurrence of small lungs tumor is exclusively found in heavy smokers. Small lungs tumor is least common as compared to non-small lungs tumor. Adenocarcinoma, large cell carcinoma, and squamous cell carcinoma are included within on-small cell lung tumors. Scientists currently developing a diagnostic system based on sputum color images. Many algorithms for medical imaging have been suggested. In lung tumor detection method, a robust method of abstraction was proposed in which all the features are transferred through an artificial neural network (ANN) accompanied by training the framework for classification purposes (Miah & Yousuf, 2015).

Previously, an edge system was used to recreate volumes of emphysema in the lungs (McCollough *et al.*, 2006). A limit method was appropriate for dividing each picture. However, a 3D reproduction was not endeavored. The normality or abnormality of the lung is determined by image processing-based identification of lung tumor on CT scanning images. Lung tumor has been optimized through support vector machine (SVM) algorithms and techniques (Abdillah, Bustamam, & Sarwinda, 2017). In this optimization, the function used is relied on gradient-oriented histogram, color moments, texture, and; therefore, is

graded for identifying its medicinal value (Venkataraman & Mangayarkarasi, 2017). A vector-dependent support method was used based on the gray level rivalry matrix and the eight texture characteristics histogram to describe and differentiate objects either without or with nodules (Madero *et al.*, 2015).

No thought was given during the stage of process segmentation. Similarly, lung CT images testing were performed and indicated effective use of predictive computer-aided design (CAD) for lung tumor diagnosis (Tiwari, 2016; Ritika *et al.*, 2011). An enhanced SVM classifier was used for diagnosing leukemia tumor using a fast-correlation-based filter to choose the most influential and non-correlated genes. The picture was transformed to the processing period and provided more accurate results. Lung tumor detection phases in CT scanning pictures use different image processing techniques (Kavitha, Gopinath, & Gopi, 2017).

Picture quality appraisal changes where low pre-preparing strategies were utilized considering Gabor channel inside Gaussian guidelines. Depending on general highlights, a typical correlation was made. In this exploration, the primary identified highlights for exact pictures correlation were pixels rate and mask-labeling (Altarawneh, 2012). Lung tumor detected using the ANN has also low accuracy. It was comparatively easier for abstract or complex issues such as image identification but increase precision to strengthen the scale by several extents (Agarwal, Shankhadhar, & Sagar, 2015; AlZubaidi *et al.*, 2017).

The noteworthy change was noted in previous study conversely of masses alongside the concealment of foundation tissues, which were acquired by tuning the parameters of the proposed change work in a predefined extent (Patil & Kuchanur, 2012). A study was on lung tumor detection using a deep learning approach. A pipeline of pre-processing techniques has been proposed for emphasizing lung regions susceptible for tumor and extracted features through ResNet and UNet models. The element set was assigned into different classifiers through Random Forest and XGBoost. Methods for detecting lung tumor nodule were evaluated, including principal component analysis, support vector machines, Naïve Bayes, decision trees, and artificial neural networks, and K-Nearest neighbors. The study has compared all strategies for pre-processing and without pre-processing. According to the results, the best outcome was obtained from the ANN with approximately 82%

accuracy after image processing. CT images of lungs were examined on a computer-aided classification (Dev *et al.*, 2019).

MATLAB software has been applied to implement all the procedures in the proposed system. Different stages entailed image pre-processing, segmentation, SVM classification, feature extraction, and image acquisition. Firstly, a threshold value was computed, and image was segmented into right and left lung. Secondly, the DICOM format lung CT image was surpassed as input, which undergone pre-processing. Lungs were extracted and passed as input to the SVM after those 33 features of each segmented lungs. Lastly, the CT image was categorized as tumorous or non-tumorous based on the training data. This strategy allows more satisfactory outcomes when compared to other current systems (Dev *et al.*, 2019). Different computer-aided techniques were assessed for investigating the existing technique and for examining their drawbacks and restrictions. In addition, the study has proposed the new model with enhancements in the effective model. Lung tumor detection techniques were listed and sorted based on their detection accuracy.

The techniques were investigated on each step and overall restriction, whereas limitations were pointed out. Some techniques might have higher accuracy and low accuracy, but not closer to 100%. The need of 3D rotatable model was to view lungs from different orientations and other functionalities for detecting lungs tumor including feature extraction nodule detection by learning classifier, active contour-based nodule contour extraction, and nodule connectivity recognition by tissue classification. Detection of tumor using learning algorithm support vector machine (SVM) helps radiologist to diagnose the nature of tumor by performing biopsy. The proposed diagnostic tool detects and classifies lungs tumor as benign or malignant.

Detection was based on extracted features, in comparison with benign and malignant sizes. The objective was to see lungs tissue with different orientations by rotating it and reducing the enormous false positive rate by increasing the efficiency and accuracy of the diagnostic procedure. It not only reduces the overall cost but also creates a better environment for the screening of lung tumor; lessens the duration of diagnosis, and prognosis of the disease.

The significance of this paper is of twofold. Firstly, this study aims to mitigate the variability in order to assess and report the lung tumor risk between interpreting physicians. In fact,

computer assisted approaches have been observed for enhancing consistency between physicians in different clinical contexts such as mammography screening and nodule detection. Secondly, learning classifier can enhance classification performance by stimulating the less experienced or non-experienced clinicians in order to evaluate the risk of a specific nodule being malignant.

2. DESIGN PHASES

This paper has divided its objective in three different phases.

Firstly, this study extracted or selected different features for the 3D construction. Secondly, this study has developed learning classifier. Lastly, the study has designed a tool for integrated solution. In the first phase, personnel from two different areas of expertise took part. Firstly, radiologists help to understand the relative information of the anatomy, physiology of the lung functionality and the symptoms of the tumors, and their types derived from the available CT scans.

Secondly, researchers from engineering discipline analyzed the transformation of the parameters related to lung tumors (disease and their types) in computer understandable parameters, which were used to drive the further stages for developing the tool. The second phase of this paper processed the related information that was transformed from physical results of patients to computer based learning algorithms.

In this paper, one of the significant research oriented tasks was to identify the best or fairly relative feature to transform the actual information of the CT scan result into computer based outcome. Machine learning was used to achieve this goal and the selection of the feature was done from available feature stream and some were derived as new features using in-depth understanding of the physiology of the lung with and without disease. In the next step, the machine learning tool used the derived features from the previous step to select the most appropriate or accurate classifier based on recognition percentage value. These results were used to develop the combination of different classifiers with derived features to select the most accurate classifiers in particular situation. The result of the classifier identified lung tumor with appropriate features and learning classifiers.

In this phase, the CT scan images were segmented to get the mask of images by applying multiple functions of image processing. The masks of these images were combined to get the 3D image, which can be seen over different orientations using Matlab viewer. The lung tissue was used fully for radiologists to identify the tumor by just looking at the 3D reconstructed images. In the third phase of this paper, an integrated application for lung tumor detection was developed.

The results derived were used along with significant features, classifiers, and their combinations. The developed software tool for lung tumor detection was capable of addressing the following aspects:

- Improve the false positive rate of results.

- Software based CT scan Diagnosis.

2.1. FEATURE SELECTION

The following parameters for lung tumor classification, symptoms and nodule classification were Apex, Base, Lobes, surfaces and borders:

Lobes: Lobular structure of both the lungs varies from each other. The left lung comprises of inferior and superior lobes, which were divided by an oblique slit. The right lung was comprised of middle, inferior, and superior lobes. In addition, the lobes were divided from each other by two different fissures.

- Oblique fissure – starting from the inferior border, it grows in the super posterior direction, till it sees the posterior lung border.

- Horizontal fissure: It increases horizontally at the 4th rib level for meeting the oblique fissure from the sternum.

Lung tumor may be caused due to the irregular and uncontrollable growth of cells in lung tissue. Lung nodules were the abnormalities in the lung tissue. They were generally small and approximately spherical masses of tissue, having a size of about 5 millimeters to 30 millimeters. Non-small cell lung tumor and small cell lung tumor were two broad categories of lung tumor.

Hemoptysis, weight loss, shortness or wheezing of breath, fatigue, fever, and coughing were the signs and symptoms of lung tumor. Due to a tumor mass, the symptoms stress on adjacent structures such as superior vena cava obstruction, difficulty swallowing, chest pain, and bone pain. The presence of metastatic disease was recommended within the symptoms, including weight loss, neurological symptoms, and bone pain. The kidney, bone, brain, adrenal glands, liver, pericardium, and opposite lung were included as common sites of spread. There were two major classifications of a tumor. It can either be a benign or a malignant tumor with the following characteristics as shown in Figure 1 and Figure 2.

2.1.1. BENIGN CHARACTERISTICS

- It was not tumorous.

- It was localized in a region and does not invade in other tissues.

- The size was less than 2 cm and does not changes for 2 years.

- It was rounded in shape with smooth edges.

- It has calcium deposits in it and the HU value was near to bone.

2.1.2. MALIGNANT CHARACTERISTICS

- It was tumorous

- It invades in surrounding tissues and may spread in the body.

- Size was more than 2.5cm.

- It has irregular and speculated edges.

- It has no calcium deposits and HU values corresponds to that of fluids and soft tissue

2.2. SELECTED FEATURES

The following features were selected for classification of tumor area, perimeter, diameter, centroid, robustness, smoothness, indentation, and calcification along with pixel value for tumor classification.
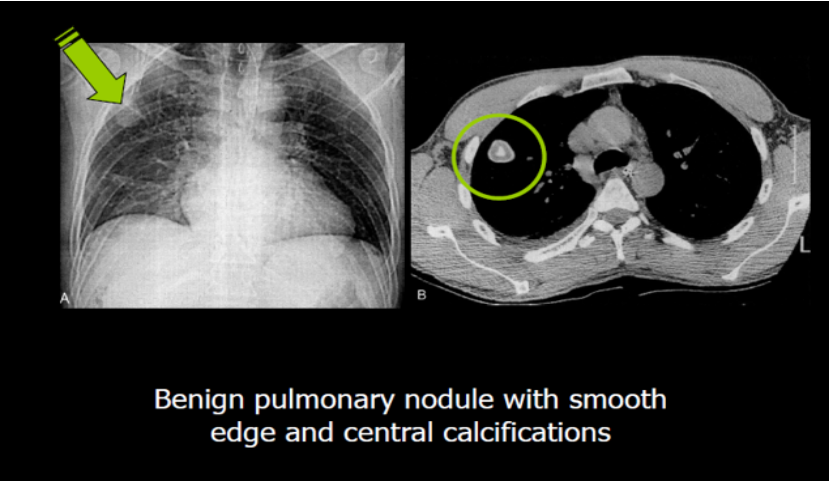
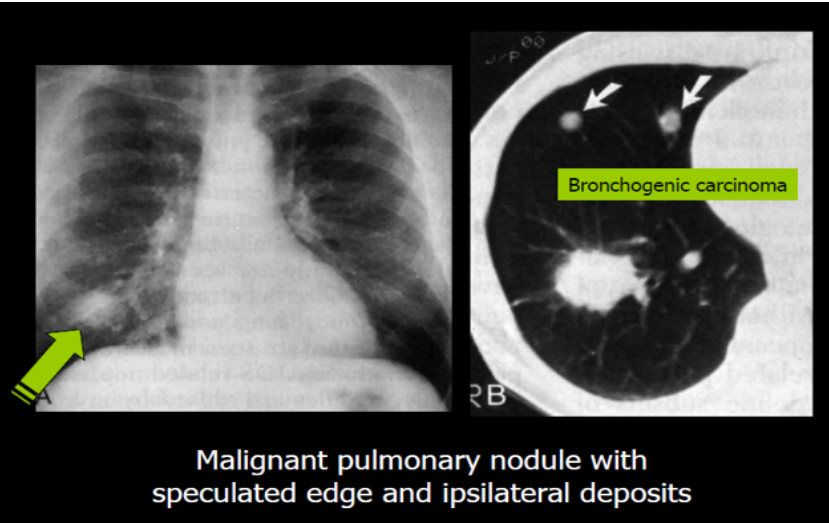**Figure 1.** Benign Pulmonary Nodule with smooth edge and central calcification.

Figure 2. Malignant Pulmonary Nodule with speculated edge and ipsilateral deposits.

2.3. FEATURE EXTRACTION

Feature extraction was used to extract the lung mask from CT-scan images. Dataset was generated using 16 slice machine currently being used in many hospitals in Pakistan. It included many variations in cases. Some were squamous cell carcinoma, adenocarcinoma, and large cell carcinoma. The study has used DICOM image format using 3D Viewers to extract DICOM image features. Segmentation module was used after preprocessing to extract lung mask from CT-scan images in Figure 3. There were different set of tools used to develop the software for 3D reconstruction and identification of lungs tumor. MALAB

tool was used for Graphical User Interface (GUI), image segmentation for getting 3D functionalities, and identification of wall tumor. Figure 4 shows the basic flow of system. In 3D image viewer, function can be used to view 3D image volumes like CT scans. It has maximum Volume Rendering (VR), Slice render or intensity projections (MIP) (Figure 5). Image Segmentation for getting 3D mask functionalities comprises on following steps as shown in Figure 6.
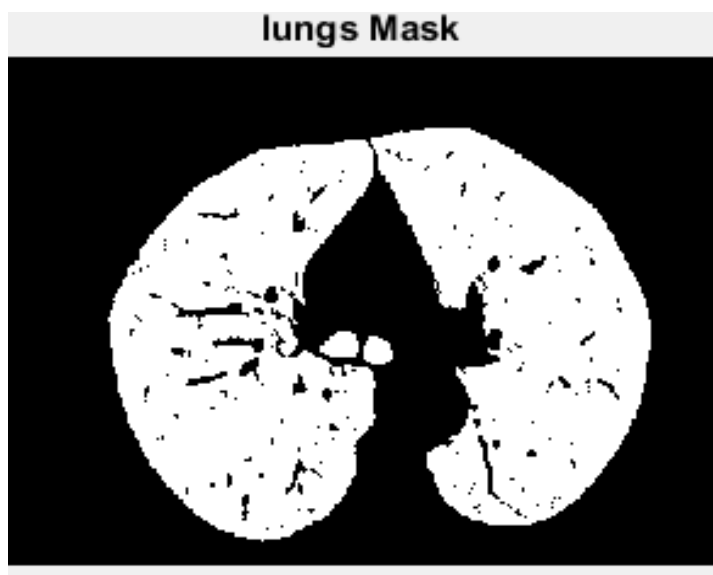
lungs Mask

Figure 3. Lung Mask.

2.4. LEARNING CLASSIFIERS

Machine learning offers systems the competence for getting more appropriate outcome to predict result regardless being comprehensively programmed. Data mining and predictive modeling was the process involved in machine learning. Support Vector machine was an attractive approach for defining decision boundaries, as the idea related about decision planes. Simple technique for finding decision planes that a set of objects separates out between different memberships of class. SVM was used for classifying data analysis and regression analysis. For example, there was a n-dimensional space; the study has plotted each data item in each point that each feature value being the particular coordinate value. By finding the best hyper-plane, the study has performed the classification that differentiates the two classes very well.
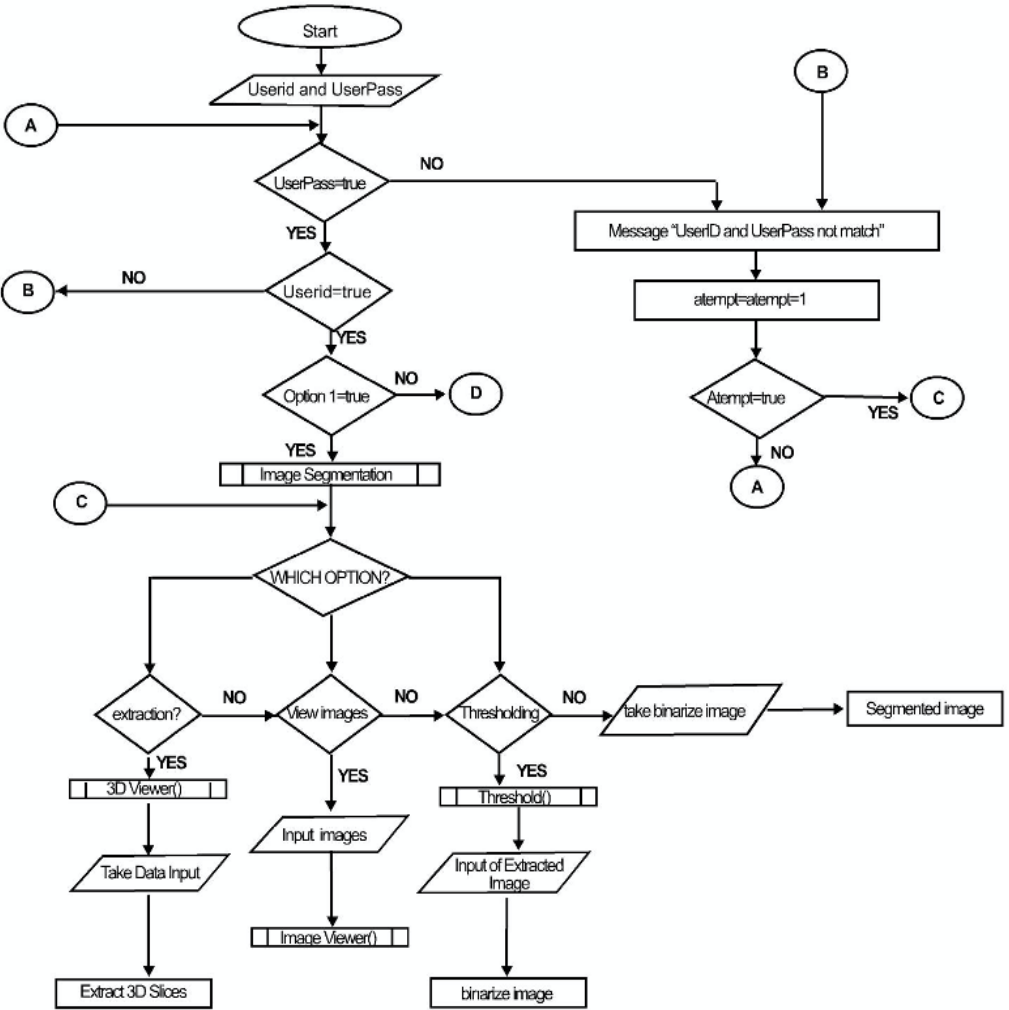
Figure 4. Design Flow Diagram.

3. EXTRACTION OF SLICES AND 3D RECONSTRUCTION

In this module, the tumor was extracted from lungs mask and converted them into object form (Array). The array obtained consists of different ranges of pixels. The number of pixels varies with the CT scan. Some CT scans may have 250 pixels; some may have more than 400 pixels. Different set of tools were used to develop the proposed software for 3D reconstruction and identification of lungs tumor.
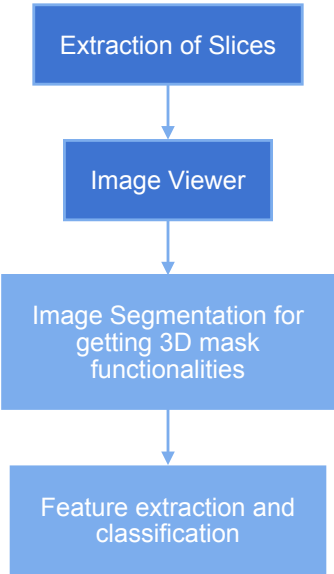
Figure 5. System Flow.

Extraction of slices were performed using 3D viewer. This function was used to view 3D image volumes like CT scans. It has a maximum Volume Rendering (VR), Slice render or intensity projections (MIP). In this window, 'File' has an option for loading medical data, 'Render' has an option viewing 3D slices,'Volume1' indicates that data was loaded and 'save picture' was used for saving slices coronal (XY), sagittal (YZ) and axial (XZ) (Figure 6).

Figure 6. Basic flow of 3D Viewer for extraction of slices.

4. IMAGE SEGMENTATION AND THRESHOLDING

Image segmentation divides the data into adjoining regions elected by individual anatomical objects. The process of image thresholding was to divide an image into a background and a foreground. Objects were isolated from image segmentation and gray scale images to binary images. One of the most influential aspects in images was image thresholding with high

contrast levels. 'Load' option was used for load slices image that applies thresholding, moves the 'Threshold slider' to adjust the segmentation until the lungs appear well-delineated, and simply sets the 'minimum' and 'maximum' properties. The 'save' option was used for saving thresholding slices images individually as shown in Figure 7.
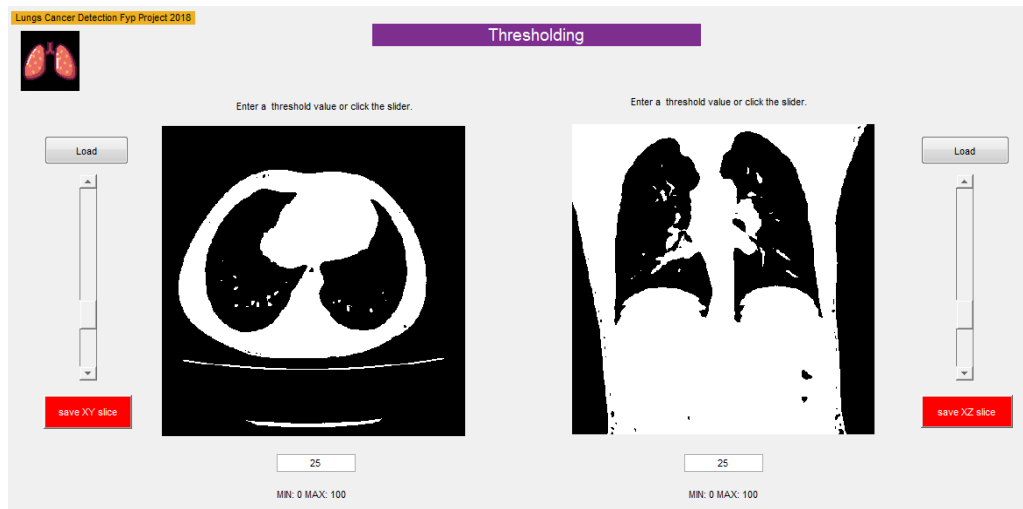

Figure 7. Image Threshold Window.

Image viewer window was used for viewing each slice individually. The following steps were developed to 3D reconstruction of lungs using mask shown in Figure 8.
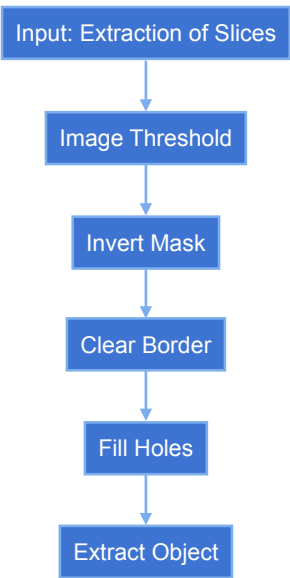
Figure 8. 3D Reconstruction of Lungs Using Mask.

4.1. INVERT MASK

On the segmentation tab, click 'Invert mask' to make the segmented lungs the foreground. 'Imcomplement()' unction was the complement of binary image; black become white and white become black; zeros and ones were reversed.

Figure 9. Invert Mask on Image Segmentation Window.

4.2. CLEAR BORDER

On the segmentation tab, click 'Clear border' removed all the segmented parts that were not the lungs. Since these all touch the edges, use the **'imclearborder()' function to remove** them.

Figure 10. Clear Border on Image Segmentation Window.

4.3. FILL HOLES

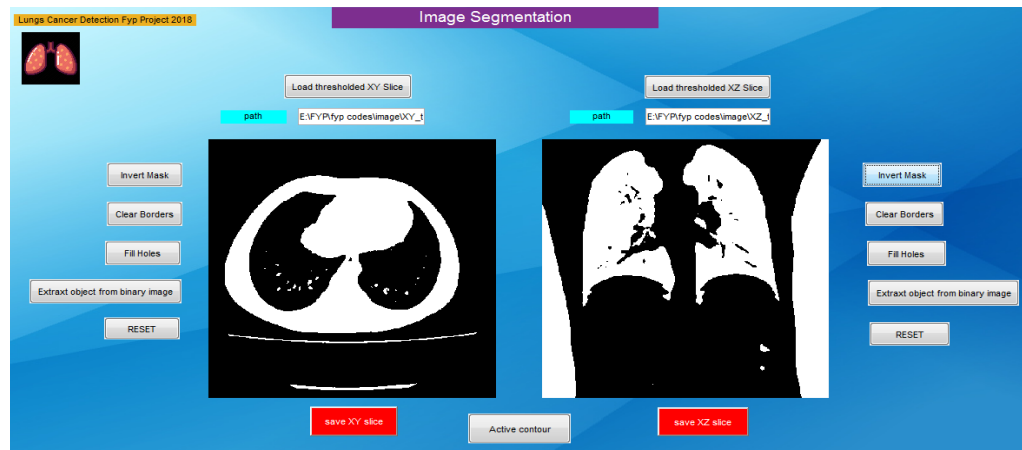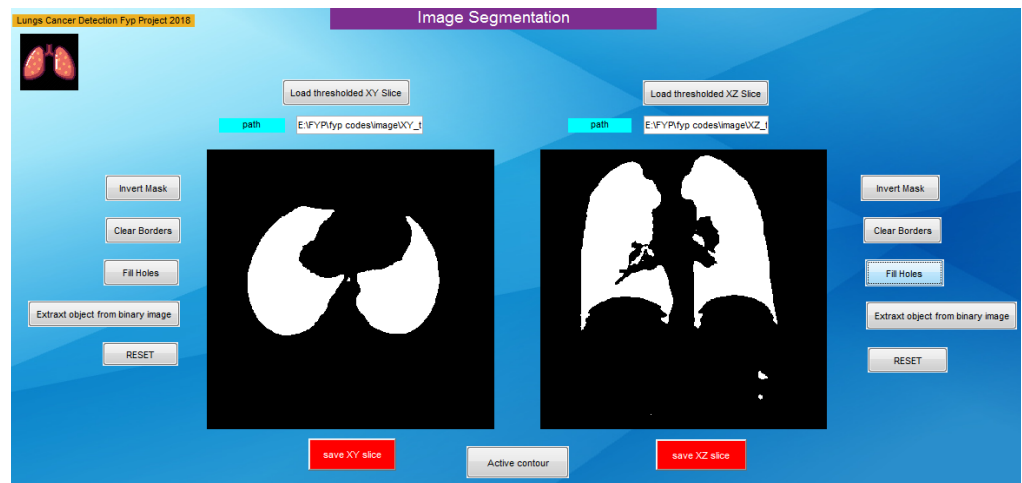On the segmentation tab, click 'Fill holes' means fill the small holes that appear in the lung areas. Use 'imfill(t,'holes')' function means input binary image filled with holes.

4.4. EXTRACT OBJECT

On the segmentation tab, click 'Extract objects' mean extract objects from binary image by size. Use 'bwareafilt(t1,n,keep)' function means it keeps the 'n' largest/smallest objects. If you want to keep n largest object, specify the 'keep' parameter with the value 'largest'.
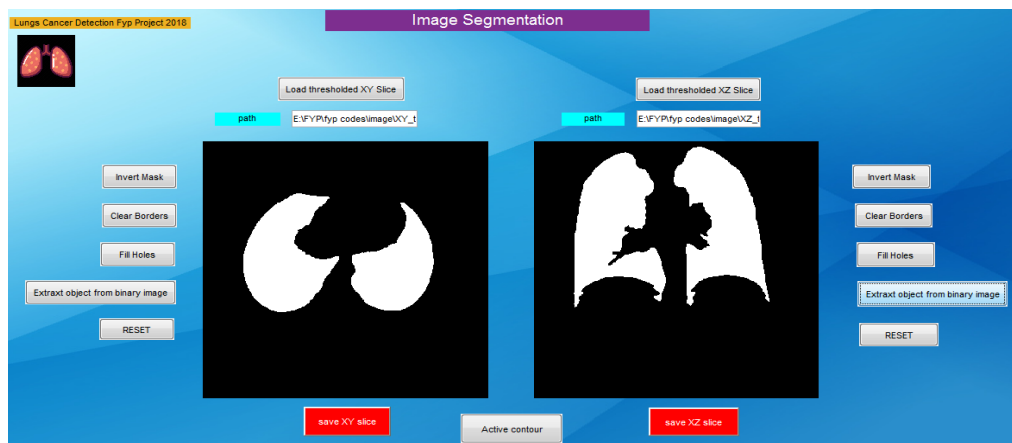
Figure 11. Extract Objects on Image Segmentation Window.

4.5. JPEG, TIFF IMAGE SEGMENTATION

In this module, a JPEG or tiff image was loaded and checked whether it was a grey scale image or not. If not than it was converted into a grey image. Afterwards, the grey image was used as input to draw the histogram of the pixels value in the image. The image was then binaries and fill holes and clear border function was applied to filter the image. A function to extract two lobes of lungs was called and extracted the lungs from the CT scan. Finally the lungs mask was obtained by inverting the lungs using binary image.
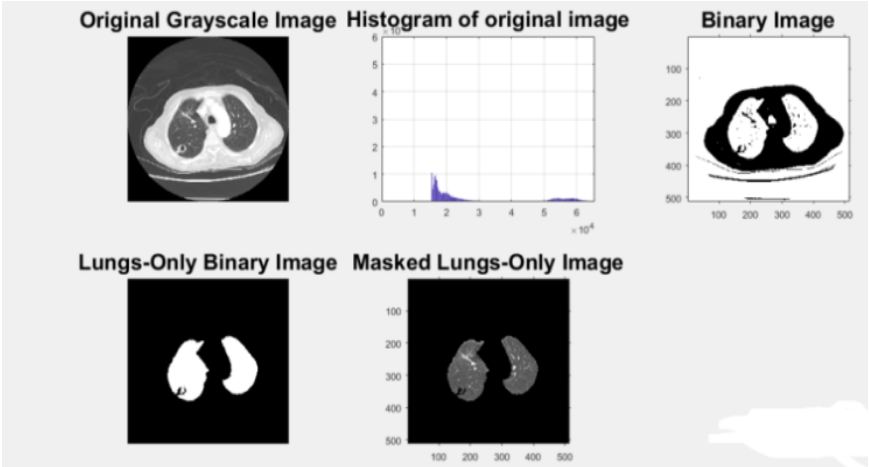
Figure 12. Tiff Image Segmentation.
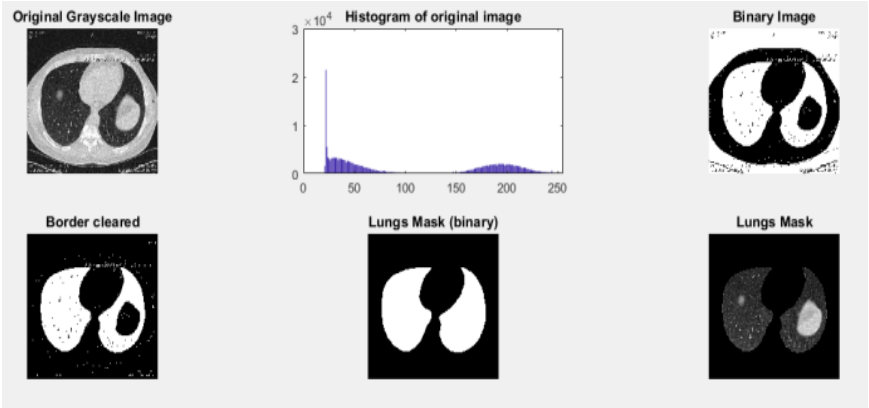
Figure 13. Image Segmentation.

5. RESULTS AND DISCUSSION

To detect the tumor, proposed software methodology was tested on two fronts. Due to the limited amount of data availability, the core focus was on a single image testing. The array obtained from the previous module contains the length of pixel in mm. This data was used to train the SVM algorithm and classified the data into two hyper planes. First, hyper plane was assigned 1 for which the length of the pixel was below 30mm and the other hyper plane consist of the pixels having length more than 30mm and they were assigned as -1. Since the size for malignant tumor was more than 30mm, so basically this algorithm was based on classifying malignant and benign tumor as shown in Figure 14.
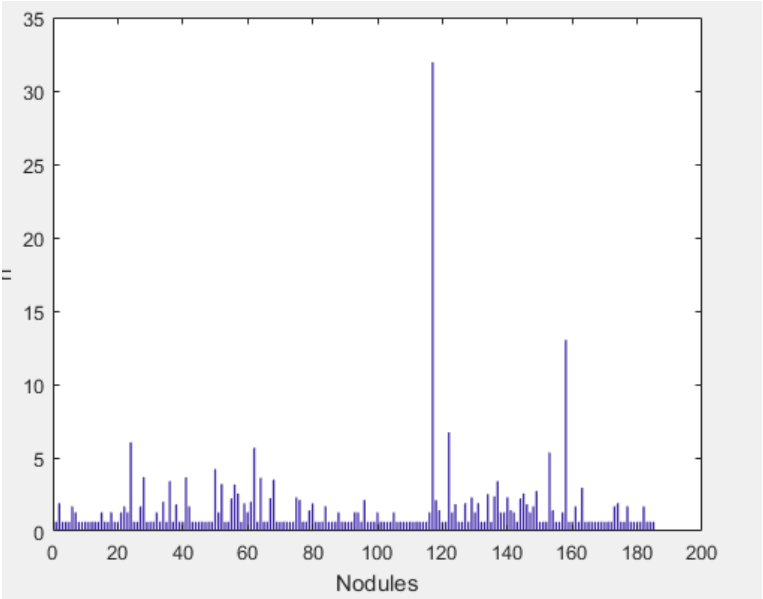
Figure 14. Position of pixel for more than 30mm.

All three modules were tested on single slice data of CT scan. The slice selected for input was on random basis and was manually selected for gaining accurate results. Tumor on selected slice was clearly visible so that the results can be compared, and the accuracy of the module can be found. Two image testing formats were used in this proposed software 1) TIFF format and 2) JPEG format. The input was provided in TIFF format to module and applied segmentation on image, TIFF images having less count than JPEG image. In the output stage, considering JPEG image which were much clear than TIFF image. In the final phase of the system, the extracted tumors were then passed to a machine learning algorithm. The algorithm compares the size of extracted tumor to the learned size and if the size of some pixels exceeds a particular value then malignant tumor was identified. The study has compared the results with the radiologists. If the malignant probability was more for a case of malignant that means that system was working correctly. The study had found no false negative rate in the system.

This study has performed image processing on CT scan image so the quality of image was critical. Experimental output provided significant results with bright CT scans. CT scan image was below required brightness or if CT scan was done in a dark room than the

module cannot do segmentation clearly. Accuracy of machine learning algorithm depends on the data set. The more the data set, the more accurate results will come.

The system's accuracy was currently compromised due to limited data. The accuracy can be improved by training and testing the data on larger amount of data. Furthermore, some other more advanced machine leaning methods can also be used for better performance. Currently, the study was working on supervised learning to switch to unsupervised algorithm, which may prove to be better for the accuracy of the system. The algorithm can be implemented to other imaging techniques like PET scan, MRI, Nuclear Medicine, bioluminescence, mammography, fluorescence etc. so that one can see which technique works well with computer aided diagnosis of lung tumor detection.

6. CONCLUSION

In this study, computer aided diagnosis software was proposed that can detect and classify lungs tumor as benign or malignant. Detection was done based on extracted features, in comparison with benign and malignant sizes. This proposed method incorporated functionalities like segmentation of lungs through threshold and some morphology functions to obtain the mask of lungs and then use these masks to make a 3D model. The need of 3D rotatable model was to view lungs from different orientations and other functionalities for detecting lungs tumor are feature extraction nodule detection by learning classifier (SVM), Active Contour Based Nodule Contour Extraction and Nodule Connectivity Recognition by Tissue Classification. The diagnostic tool was capable for reconstructing the 3D view of lung tumor and classifies the nature of tumor by identifying the location of tumor attached to the wall or parenchyma. Furthermore, diagnostic tool reduces the false positive rate by improving the significant accuracy. Moreover, this application will help in the reduction of the overall cost and create a better environment for the screening of lung tumor using CT scan (Medical Imaging), lessen the duration of diagnosis, and prognosis of the disease using learning algorithm.

REFERENCES

Abdillah, B., Bustamam, A., & Sarwinda, D. (2017). Image processing based detection of lung tumor on CT scan images. *Journal of Physics Conference Series, 893*(1), 012063. https://www.researchgate.net/publication/320687993_Image_processing_based_detection_of_lung_cancer_on_CT_scan_images

Agarwal, R., Shankhadhar, A., & Sagar, R. K. (2015). Detection of Lung Cancer Using Content Based Medical Image Retrieval. In *Fifth International Conference on Advanced Computing & Communication Technologies, Haryana, India.* https://doi.org/10.1109/ACCT.2015.33

Altarawneh, M. (2012). Lung Cancer Detection Using Image Processing Techniques. *Leonardo Electronic Journal of Practices and Technologies, 11*(20). https://www.researchgate.net/publication/265998089_Lung_Cancer_Detection_Using_Image_Processing_Techniques

AlZubaidi, A. K., Sideseq, F. B., Faeq, A., & Basil, M. (2017). Computer aided diagnosis in digital pathology application: Review and perspective approach in lung tumor classification. In *Annual Conference on New Trends in Information & Communications Technology Applications (NTICT), Baghdad, Iraq.* https://doi.org/10.1109/NTICT.2017.7976109

Bhatia, S., Sinha, Y., & Goel, L. (2019). Lung Cancer Detection: A Deep Learning Approach. In Bansal, J., Das, K., Nagar, A., Deep, K., Ojha, A. (eds) *Soft Computing for Problem Solving.* Advances in Intelligent Systems and Computing, vol. 817. Springer, Singapore. https://doi.org/10.1007/978-981-13-1595-4_55

Dev, C., Kumar, K., Palathil, A., Anjali, T., & Panicker, V. (2019). Machine Learning Based Approach for Detection of Lung Cancer in DICOM CT Image. In Hu, YC., Tiwari, S., Mishra, K., Trivedi, M. (eds) *Ambient Communications and Computer Systems. Advances in Intelligent Systems and Computing,* vol. 904. Springer, Singapore. https://doi.org/10.1007/978-981-13-5934-7_15

Günaydin, Ö., Günay, M., & Şengel, Ö. (2019). Comparison of Lung Cancer Detection Algorithms. In *Scientific Meeting on Electrical-Electronics & Biomedical Engineering and Computer Science (EBBT), Istanbul, Turkey*, pp. 1-4. https://doi.org/10.1109/EBBT.2019.8741826

Kavitha, K. R., Gopinath, A., & Gopi, M. (2017). Applying improved svm classifier for leukemia tumor classification using FCBF. In *International Conference on Advances in Computing, Communications and Informatics (ICACCI), Udupi, India.* https://doi.org/10.1109/ICACCI.2017.8125817

Madero, H., Vergara, O. O., Cruz, V. G., Ochoa, H. D. J., & Nandayapa, M. D. J. (2015). Automated system for lung nodules classification based on wavelet feature descriptor and support vector machine. *BioMedical Engineering OnLine, 14*(9). https://doi.org/10.1186/s12938-015-0003-y

Makaju, S., Prasad, P. W. C., Alsadoon, A., Singh, A. K., & Elchouemi, A. (2018). Lung Cancer Detection using CT Scan Images. *Procedia Computer Science, 125,* 107–114. https://doi.org/10.1016/j.procs.2017.12.016

McCollough, C., Zhang, J., Bruesewitz, M., & Bartholmai, B. (2006). Optimization of CT image reconstruction algorithms for the lung tissue research consortium (LTRC). In *Proceedings Volume 6143, Medical Imaging 2006: Physiology, Function, and Structure from Medical Images; 614330.* https://doi.org/10.1117/12.653290

Miah, M. B. A., & Yousuf, M. A. (2015). Detection of lung cancer from CT image using image processing and neural network. In *2015 International Conference on Electrical Engineering and Information Communication Technology (ICEEICT), Dhaka*, pp. 1-6. https://doi.org/10.1109/ICEEICT.2015.7307530

Patil, S. A., & Kuchanur, M. B. (2012). Lung cancer classification using image processing. *International Journal of Engineering and Innovative Technology (IJEIT), 2(*3). https://www.yumpu.com/en/document/read/22587818/lung-cancer-classification-using-image-processing-ijeit

Ritika, S., Meenu, R., Pawan, P., & Saurabh, S. (2011). Fast dissolving drug delivery system-A Review. *International Research journal of Pharmacy, 2*(11), 21-29. https://irjponline.com/admin/php/uploads/671_pdf.pdf

Tiwari, A. K. (2016). Prediction of Lung Tumor Using Image Processing Techniques: A Review. *Advanced Computational Intelligence: An International Journal (ACII), 3*(1), 1−9. http://aircconline.com/acii/V3N1/3116acii01.pdf

Venkataraman, D., & Mangayarkarasi, N. (2017). Support vector machine based classification of medicinal plants using leaf features. In *International Conference on Advances in Computing, Communications and Informatics (ICACCI), Udupi, India.* https://doi.org/10.1109/ICACCI.2017.8125939

/10/

AUTOMATIC PIZZA CUTTING MACHINE

Atif Saeed

Lecturer, Department of Mechatronic Engineering, SZABIST,
Karachi, (Pakistan).
E-mail: m.atif@szabist.edu.pk ORCID: https://orcid.org/0000-0003-1551-4314

Saud Sattar

Postgrad student, MSc Electronics Engineering Management, University of York,
(United Kingdom).
E-mail: saud.sattar@yahoo.com ORCID: https://orcid.org/0000-0003-2477-0838

Andrew Ferguson

Strategic Project Manager/Principal, Careers & Placement, University of York,
(United Kingdom).
E-mail: andrew.ferguson@york.ac.uk ORCID: https://orcid.org/0000-0003-3146-9330

ABSTRACT

The objective of this research is to determine the need of an automated pizza cutting machine in food industry and to design a machine that would cut a pizza into even slices by a single press. The need of the product has been determined by the surveys that were collected from various pizza vendors. From the survey it was concluded that market will welcome the product as it would overcome several issues like unequal slice cut and lower productivity.

This machine is designed to cut a pizza of any size in less than 30 seconds; increasing the overall productivity. The pneumatic system and round cutting tools are used to create basic structure in this project to get the pizza cuts into even slices with better precision and accurate shape. The stress and motion analysis conducted as part of design procedure and their results are also discussed.

KEYWORDS

Mechatronics System, Pizza Industry, Productivity, Sustainability, Reliability, CAD Simulations.

1. INTRODUCTION

In today's world as many new technologies have overshadowed mankind's work and as population is increasing day by day. Our needs for products and usage is increasing and everyone wants to get the best of everything as quick as possible. The mission of this project is to design an automatic pizza cutter which cuts pizza into equal number of slices. Optimally each pizza will cut in less than 30 seconds. The aim of this design is to provide an automatic machine in households and in restaurants. As an actuator, pneumatic system is used with a round cutting tool. The cutting tool contains blades, this tool works as a die to cut a pizza.

Knifes and rollerblades often used for cutting purposes in households, industries and meat shops. The process of cutting uses multiple tools, that are operated manually or automatically. The cutting process which uses hands or non-motorized are manually operated tools and the one which are motorized, electrically, hydraulically or pneumatically driven cutting tools are known as automatic or machined tools. There are different types of knives which are available in the market. Daggers of different lengths, width, sizes and weight are available depending on which type of materials or properties we want to cut. Simple single dagger is used in cutting pizza linearly. Multiple dagger can be used to cut pizzas in equal divisions in one single process. This will ensure highest cutting precision. Cutting can be done by round multiple stainless blades (Astakhov & Davim, 2008).

Metal cutting instruments often have two cutting edges, both oriented to the cutting direction and the tilt continually differs in round-necked instruments. In right-angled cutting, the cutting edge of the work piece is always at the correct angles. When the blade is in the direction of motion it is known as oblique cutting. The slice-push ratio of the blade's velocity or displacement is parallel to the cutting corner displacement and velocity is perpendicular to the cutting corner which makes the cutting easier. The ratio of slice-push is achieved when right-angled blade is driven obliquely as well as inferior (Atkins, 2006; Kurin & Surdu, 2017).

Automated cutting devices are commonly used in the processing of various sheets and rolling materials. The materials are cut by a knife, laser, waterjet, plasma or ultrasound controlled by a computer. The most efficient means of cutting textiles are fully automated knife cutting systems. For single-ply and multiply cutting procedures, they guarantee adequately high quality and precision (Deokar *et al.*, 2017; Gracia *et al.*, 2009).

This product aims to increase the speed and efficiency of preparing takeaway and restaurant pizzas globally.

In an article by The Guardian, at the end of 2019 it was noted that Dominos generated a revenue of 339.5 million pounds i.e. 5.5% more than their sales in 2018. the average market analysis, since 2010 till 2019, shows that this market has an upward trend in turnover and profit (Jolly, 2019). Another article suggested that on average every American spends 23 pounds each year just on Pizza (Links, 2019). Same article on The Guardian quoted that Dominos sold 500,000 pizza solely in UK on Christmas Eve 2019 (Jolly, 2019). In another article it is statistically forecasted that North American pizza market would grow to 10% in the next 5 years (Littman, 2018). The Economist in an article discussing the pizza industry gave statistics that 83% of consumers eats pizza at least once a month and as per 2018 industry census, 60.47% of the respondents reported to increase in sales comparing to their sales of previous year. It also forecasted the growth of 10.7% in upcoming 5 years (The Economist, 2015). So, any business analyst or entrepreneur can clearly see the potential of this growing market and could readily opt for the machines that could help making things easier for customer facing staff charged with supplying ever increasing numbers of pizzas to customers with increasingly demanding tastes.

The goal of this project is to design and fabricate the automated pizza cutting machine that would function on specific design goals. These design goals were:

- to cut the large pizza up to 12n into 8 equal slices within 20 seconds,

- to cut the 21-inch pizza into 12 equal slices,

- to implement the safety mechanism on blades so that it shall stop functioning if something is near the blades.

The project was specifically designed to complete its task in a timely manner and to ensure that slices were of equally distribution so that both the productivity could be increased, and human error of not cutting the slices equally can be overcome. Also, the blades were designed to be covered with butter paper to assure that none of the harmful substances of carbon plated steel could harm food. This coating needs to be replaced after specified cycles in order to assure proper hygiene.

2. MATERIALS & METHODS

2.1. TURNING IDEAS INTO REALITY

Firstly the sense, feeling, plans, concept and design have been delivered on the piece of paper. It is the main process in which the whole idea and the theme of the project is based on and hence it takes ample amount of time in getting everything on the right track.

2.2. RUGGED DRAFT INTO ENGINEERING DESIGN

Once the rugged drafts and basic designs have been finalized, the whole project goes into the engineering territory and solid modeling have been made. The basic positions, calculation, dimension and placements are considered and get completed in this area of territory.

2.3. CHOOSING THE RIGHT MATERIAL

Different shops and markets are there to purchase the specific and appropriate materials for the structure and components of the project. Choosing the right kind of material depends on the application of the material, the environment in which the prototype is tested and the factor of safety of the device.

2.4. DESIGNING STRUCTURE

The wooden sheets are carefully dimensioned, cutout, holed and surface is smoothed. The joining of parts has been done by screws

2.5. MAKING OF BLADE

The long metals sheets are cut into equal number of sizes shapes and length. All are joined at an angle of 30 degrees between each metal sheets and they are then covered by a thin metal sheet circularly to prevent blades from injuring anyone.

2.6. ASSEMBLY OF PARTS

After designing and production of all parts. The transformation of individual parts into singular device takes place. All the parts are fixed according to their desired geometry and solid model design.

2.7. PLACING OF PNEUMATIC SYSTEM

The pneumatic system is placed right into the center of the plate so it will linearly displace along the y axis and cut the pizza evenly from all sides.

2.8. PLACEMENT OF GAS CYLINDER

The gas cylinder is placed after all the work is done. It is positioned into the rectangular box. And the pipes are connected to the pneumatic system. The face of the box is closed.

2.9. CLEANING AND MAINTENANCE OF BLADES

The system is designed to use a stainless-steel blade which will be nonstick. The device will be easy to handle like any other blender or general use equipment. It is recommended to wash and clean the machine after every 500 cuts. As the blades will be rust free there is no harm in washing them with a standard dishwasher.

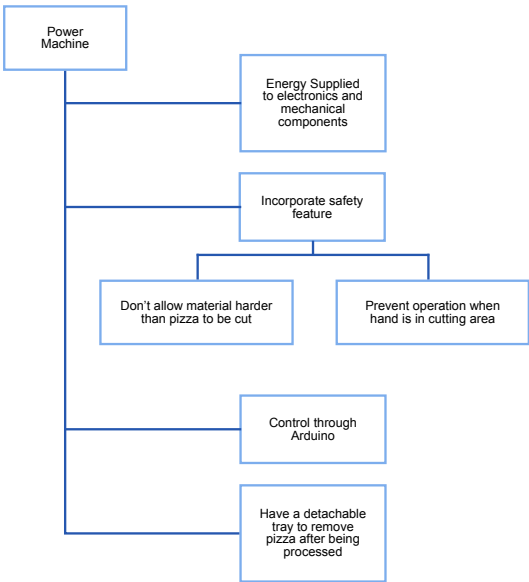The system breakdown is shown in the figure below:
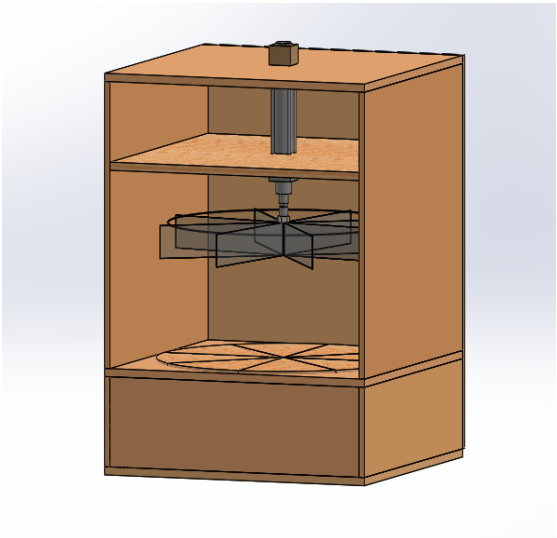

Figure 1. Project Layout.

Figure 2. Final Design.

3. RESULTS

3.1. DIMENSION AND MATERIALS

The dimension of each parts and materials used are mentioned as follows.

Table 1. Dimensions of each material

S.no	Name	Material	Dimension
1.	Pneumatic cylinder	Aluminum	40mm*150mm
2.	Wood	Balsa	8" * 4"
3.	Screw	Metal	1"
4.	Blade	Steel	11"

3.2. STRESS ANALYSIS

The stress analysis was conducted on medium sized element i.e. not too much fine or coarse. The reason of such mesh selection is the material i.e. wood in this case. The wood which will be used for the prototype is balsa that has high infill density. The load of 5lbf was applied to the pizza dish that pneumatic system will apply to cut the pizza. The yield for the material is $2x10^7$ Kpsi whereas the analysis showed the induced von-mises stress of $7x10^5$ Kpsi i.e. below our yielding point. This analysis showed that with given amount of force needed to cut the pizza, the pizza tray wouldn't go for yielding.
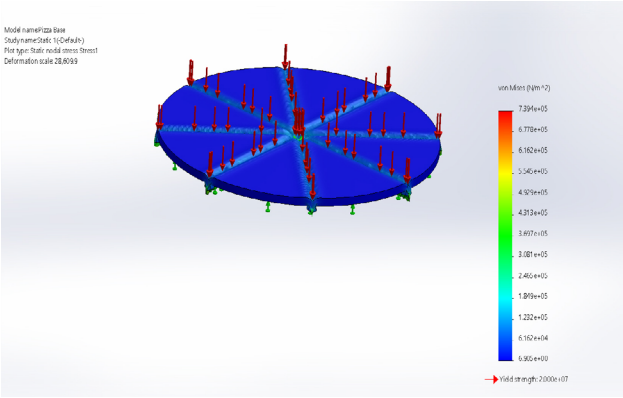
Figure 3. Stress Analysis Results.
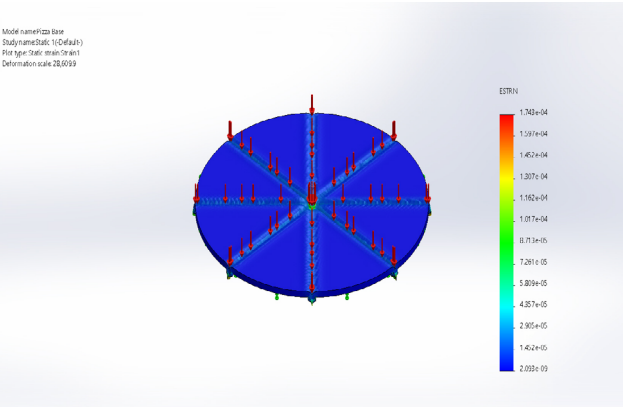
3.3. STRAIN ANALYSIS

Figure 4. Strain Analysis Results.

The maximum strain of the project is around $1.74e^{-4}$.it show that it can bear that amount of force. The factory of safety of that system is 27.

3.4. FACTOR OF SAFETY
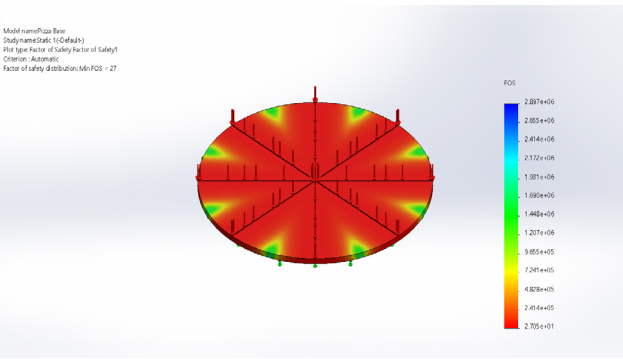
Figure 5. FOS Analysis.

The factory of safety of this system is 27. This shows it is safe because the plate will start to break when it reaches to $2.9*e^6$. It is used as a define factor or as a factor purpose.

3.5. DISPLACEMENT ANALYSIS
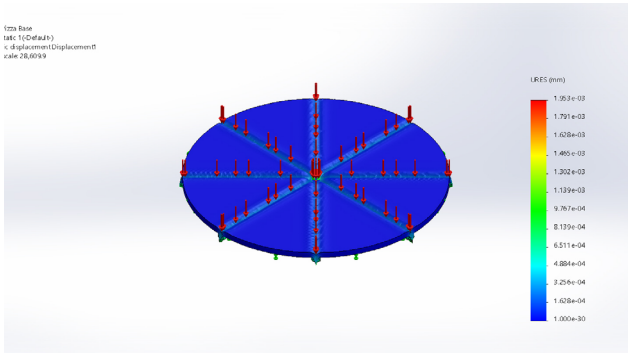
Figure 6. Deflection Analysis.

Designers are often given scenarios where there is a displacement limit in the design, but they either need to find the amount of force needed to reach that displacement or the displacement limit and force is known, but the design needs to be optimized to work within the specific requirements. The maximum displacement of this system is $1.9*e^3$.

3.6. MOTION ANALYSIS
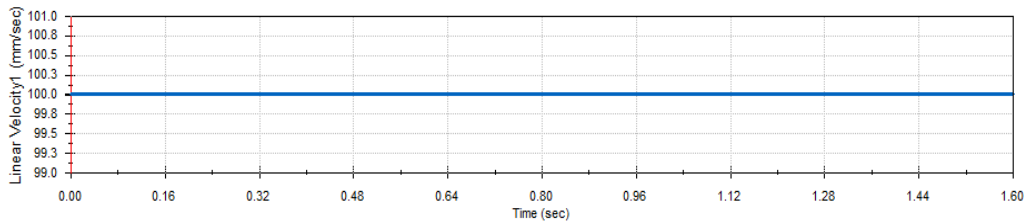
Figure 7. Velocity of cutter prior to contact with pizza.

The cutter puts stress on the plate where the pizza is placed and hence it is the most critical region in our project. The velocity of the system remain contants.

Figure 8. Velocity of cutter after contact with pizza board.

We have seen a linear displacement when we put the motor in the system and study that in motion analysis. The displcaement increases with increase in time. The pneumatic cylinder is linearily diplaced in y direction and cuts the pizza into even slices.

The system can bear more amount of weight if the material is steel or any other type. But the cost factor will also increase with that.

4. DISCUSSION

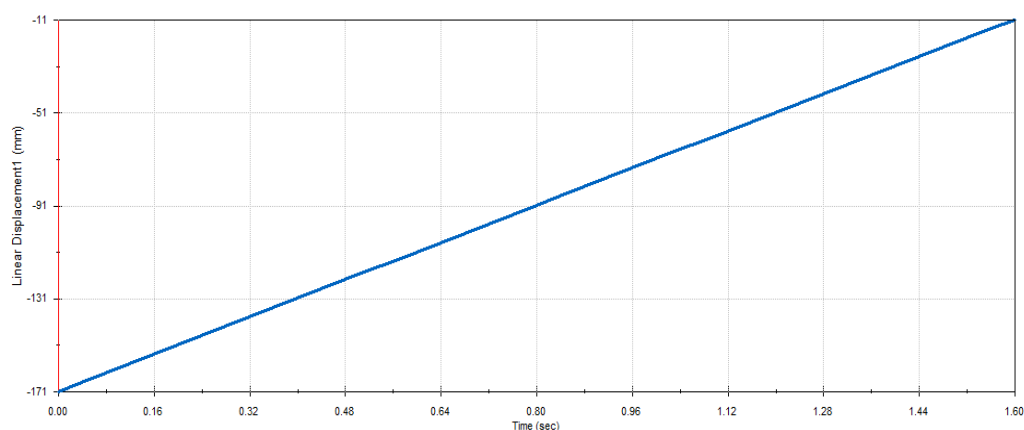This automatic pizza system can perform specific tasks with better efficiency. The results which we have obtained through our simulation analysis are very close to our expected or practical results. We have put different amounts of pressure and compared the findings with our simulation results. The pneumatic cylinder can provide 150psi pressure. We keep changing the amount of pressure and observe the result obtained. As we can see the stress, strain, displacement and factor of safety in the figures. The plate that we have used for pizza placement contains the most critical region, hence it will not break if we use the pneumatic pressure fully around 150psi. The dimensions and area of the project provide more strength to the system. The system will break if we use a heavier pneumatic system with a higher pressure. Because of this, the system will last longer and will be more efficient as compared to other available systems.

4.1. SURVEY ANALYSIS

As a part of this research, a survey was conducted so that the market need of product could be determined. The survey was forwarded to more than 20 Pizza vendors of different brands. Out of them, 20 pizza vendors responded. The survey consisted of several questions that helped us identify their requirements and expectancy towards this solution. The questions asked are given below.

- *Do you face any issues to cut pizza equally?*

- *Does the unequal pizza slices affects the quality of pizza?*

- *Do you face any difficulties to serve large number of guests for dine-in and takeway at a time?*

- *Is their any gap in market to welcome a product that would help the server cutting pizza slices into equal pieces?*

- *Do the customers complaint regarding the inconsistency of the cut?*

Mixed response to this survey were received but most of the responders agreed to the need of such product. Almost, 70% of the respondents agreed that they normally face issues in cutting the pizza slices equally while 83% of them agreed that an inconsistent cut affects the overall quality of pizza. Around 78% of the responders agreed to the fact that during festive seasons they face severe issues in serving the pizza on time that leads to a bad impact on overall companies' image. Also, on an average 73% of responders agreed that the market will welcome such product that would help the industry in serving their clients better in lesser period of time. This survey clearly yields the need of such product; hence the result of these survey motivates us to move further on to the designing phase.

5. CONCLUSION

The automatic pizza cutter can cut the slices into different sizes up to 21 inches. This will help the restaurants to perform tasks quickly and will reduce the cost and time and will add to the precision. Although this project can be considered as a luxury but once used this makes their life easy and be a major factor in reducing time hence turning it into a necessity rather than a luxury.

ACKNOWLEDGMENTS

REFERENCES

Astakhov, V., & Davim, J. (2008). Tools (geometry and material) and tool wear. In *Machining: Fundamentals and Recent Advances*. Springer, London. https://doi.org/10.1007/978-1-84800-213-5_2

Atkins, T. (2006). Optimum blade configurations for the cutting of soft solids. *Engineering Fracture Mechanics, 73*(16), 2523-2531. https://doi.org/10.1016/j.engfracmech.2006.06.006

Deokar, K., Malaviya, K., Mistry, K., Chaudhari, P., & Dutta, M. (2017). Design and Manufacturing of Coconut De-Husking, Cutting and Grating Machine. *International Journal of Engineering Science and Computing (IJESC), 7*(4). http://ijesc.org/upload/ba58739c0ff3dff6a31b8ba043180357.Design%20and%20Manufacturing%20of%20Coconut%20De-Husking,%20Cutting%20and%20Grating%20Machine.pdf

Gracia, L., Perez-Vidal, C., & Gracia-López, C. (2009). Automated cutting system to obtain the stigmas of the saffron flower. *Biosystems Engineering, 104*(1), 8-17. https://doi.org/10.1016/j.biosystemseng.2009.06.003

Jolly, J. (2019, January 29). *Domino's sells more than 500,000 pizzas in record UK trading day.* The Guardian. https://www.theguardian.com/business/2019/jan/29/dominos-pizzas-record-uk-sales-profits

Kurin, M. O., & Surdu, M. V. (2017). The Concept of the Mechanism and Kinetics of Influence of Mechanochemical Processes on Edge Cutting Machining. *Metallofizika i Noveishie Tekhnologii, 39*(3). https://doi.org/10.15407/mfint.39.03.0401

Links, Z. (2019, August 01). *How Much Pizza Does the Average American Eat in a Year?* The Sauce by Slice. https://blog.slicelife.com/how-much-pizza-average-american-eat-year/

Littman, J. (2018, December 17). *Report: North American pizza market to grow 10% in next 5 years.* Restaurant Dive. https://www.restaurantdive.com/news/report-north-american-pizza-market-to-grow-10-in-next-5-years/544523/

The Economist. (2015, February 26). *The Economist explains - Rising dough in the pizza industry.* https://www.economist.com/the-economist-explains/2015/02/26/rising-dough-in-the-pizza-industry

/11/

AN INNOVATIVE JIG TO TEST MECHANICAL BEARINGS EXPOSED TO HIGH VOLTAGE ELECTRICAL CURRENT DISCHARGES

Nicolaas Steenekamp

Gauteng Department of Infrastructure Development, Impophoma House, Johannesburg, (South Africa).

E-mail: nicolaas.steenekamp@gauteng.gov.za ORCID: http://orcid.org/0000-0001-6858-4207

Arthur James Swart

Department of Electrical, Electronic and Computer Engineering, Central University of Technology, Bloemfontein, (South Africa).

E-mail: aswart@cut.ac.za ORCID: http://orcid.org/0000-0001-5906-2896

ABSTRACT

Premature bearing failures due to Electrical Current Discharge (ECD) has been recognised for almost a century. The purpose of this paper is to present an innovative jig that may be used to expose mechanical bearings to ECD, in order to clarify its associated effects on the bearing that need to be understood before any mitigating techniques can be proposed. An experimental design is used in this study. A method is presented using an ignition coil wiring harness of a vehicle to safely induce ECD across a specific bearing. Three samples were used and analysed with an optical and electron scanning microscope. The used ball bearing exposed to ECD showed micro-cratering, a result of electric current passage. Micro arching marks on the raceway surface of this bearing was also visible, and especially near the groove of the synthetic rubber seal and steel plate slinger. Surface pits were observed which were produced by electrical arching. A few deep scratches and indentations were observed on the raceway surface. This is due to abrasive wear particles embedded in the raceway surface sliding between the major bearing components. The aspect of electrical pitting wear and debris found in the lubricating oil are unknown and deserve further research from a tribological point of view. A recommendation is made to use this innovative jig to test the impact of ECD on bearings from other suppliers.

KEYWORDS

Electrical Current Discharges, Micro Arching, Micro Cratering, Ball Bearing, LOM, SEM.

1. INTRODUCTION

The global bearings market was valued at approximately USD 92.81 billion in 2017 (Bizwit Research & Consulting LLP, 2019). Ball bearings are a common component in machinery that finds widespread use in numerous industrial applications. These include air, water and land transport, agriculture, construction, manufacturing and mining industries. Premature bearing failures is one of the main reasons for machinery down time (Jacobs *et al.*, 2016). The failure mechanisms of bearings have been well researched and documented i.e. Brinelling, Contamination, Corrosion, Fatigue, Fit, Lubrication, Misalignment and Overloading (Massi *et al.*, 2010; Bhadeshia, 2012; Upadhyay, Kumaraswamidhas, & Azam, 2013).

However, bearings may also fail due to Electrical Current Discharges (ECD) that may originate with lightning, high voltage spikes or high potential differences. The cause of bearing failure due to electric current passage has been recognised for almost a century (Liu, 2014). As a matter of fact, electric potential difference exists between shafts and bearing housings in machinery equipment due to the asymmetric effects of the magnetic fields, magnetized shaft, and electrostatic effects, etc. (Chiou, Lee, & Lin, 2009). Some practical solutions to mitigate bearing currents has worked effectively for sinusoidal alternating currents i.e. shaft grounding to bypass current, ceramic-coated bearings and hybrid insulated bearings. Some of these solutions are not as effective against the fast switching Pulse Width Modulation (PWM) inverter technology that causes high frequency non-sinusoidal bearing current (Liu, 2014). A diversity of condition monitoring techniques exist that can be used to identify developmental bearing failure.

The purpose of this paper is to present an innovative jig that may be used to expose mechanical bearings to ECD, in order to clarify its associated effects on the bearing that need to be understood before any mitigating techniques can be proposed. Firstly, an overview of the construction and operation of different types of key bearings is presented. Secondly, analysis techniques are presented to separate a single failure mechanism from the complex mechanisms. Thirdly, a method is presented using an ignition coil wiring harness of a vehicle to safely induce ECD across a specific bearing. Fourthly, the obtained results are discussed. Finally, concluding remarks and recommendations are presented.

2. MAIN BEARING CLASSIFICATIONS

An organogram outlining the classification of commonly found bearings is as shown Figure 1 (NTN Corporation, 2015). A rolling bearing consists of four major components: an inner and outer raceway, rolling elements and a cage that maintains equally spaced intervals between the rolling elements. The rolling elements are situated between the inner and outer raceways to translate motion. Rolling bearings are grouped into two main rolling element classifications, ball bearings and roller bearings. Ball bearings are classified by the raceway type: deep groove or angular contact. Roller bearings are classified by the roller type: cylindrical, needle, tapered, and spherical (NTN Corporation, 2015). Roller bearings typically have greater load carrying capacities because of the greater contact area of the roller bearings to the adjacent raceway surfaces (Bhadeshia, n.d.).

Furthermore, rolling bearings can also be classified by the load type: radial or thrust. Radial bearings support radial loads and thrust bearings support axial loads. Most roller bearings can simultaneously support radial and thrust loads (NTN Corporation, 2015). Rolling bearings are also supplied in multiples of separable and non-separable rolling rows, for example single, double and quadruplet configurations. The choice of a bearing and configuration depends on the stiffness and load requirements of the application. A brief discussion on some of these bearings now follows.

Duplex angular contact ball bearings are typically selected to increase stiffness and load carrying capacity of the support ends of upright and overhung shafts and screw drives (SKF Group, n.d.a). Angular contact ball bearings have inner and outer ring raceways that are displaced relative to each other in the direction of the bearing axis. The configurations are typically back-to-back, face-to-face and tandem. Duplex angular contact ball bearings are most commonly found in centrifugal pumps (SKF Group, 2012a).

Self-aligning ball bearings are typically selected for industrial applications where low friction is preferred over high load carrying capacity to accommodate misalignment, shaft deflections and thermal expansion (SKF Group, n.d.b). Furthermore, the self-aligning ball bearing has the lowest friction of all rolling bearings which allows them to operate at higher speeds and cooler temperatures (SKF Group, 2018). Self-aligning ball bearings have two raceways on the inner ring and has a single spherical raceway on the outer ring that can

counteract up to three degrees of misalignment. Tapered bore ball bearings induce bearing preload and are typically secured with adapter sleeves to smooth or stepped shafts. They are typically found in paper mills (SKF Group, 2018) and the textile industry (SKF Group, 2014).

Like duplex angular contact ball bearings, high-speed duplex angular contact ball bearings are typically selected for applications that demand high reliability and superior accuracy, for example a machine tool spindle in CNC turning, machining centre and milling machine (SKF Group, 2012b). High-speed duplex bearings are usually sealed to eliminate contamination to prevent premature bearing failures.

Radial needle roller bearings are typically selected for their stiffness and high load carrying capacity (SKF Group, n.d.c). The diameter of a roller element of a needle roller bearing is relatively small in relation to its length. Needle roller bearings are used in applications where space is limited. Typically, a needle roller is combined with a shaft or housing bore to serve as a raceway. They are used, for example, in the universal joint of a drive shaft and rocker-arm pivot of a vehicle (SKF Group, n.d.d).

Spherical thrust roller bearings are well suited for heavy-duty applications where axial and or combined axial and radial loads needs to be accommodated (SKF Group, 2010). Spherical thrust roller bearings are like self-aligning ball bearings and are typically found in a cooling water pump for a thermal power plant and marine thrusters ("SKF explorer spherical roller thrust bearings boost design options", 2003).
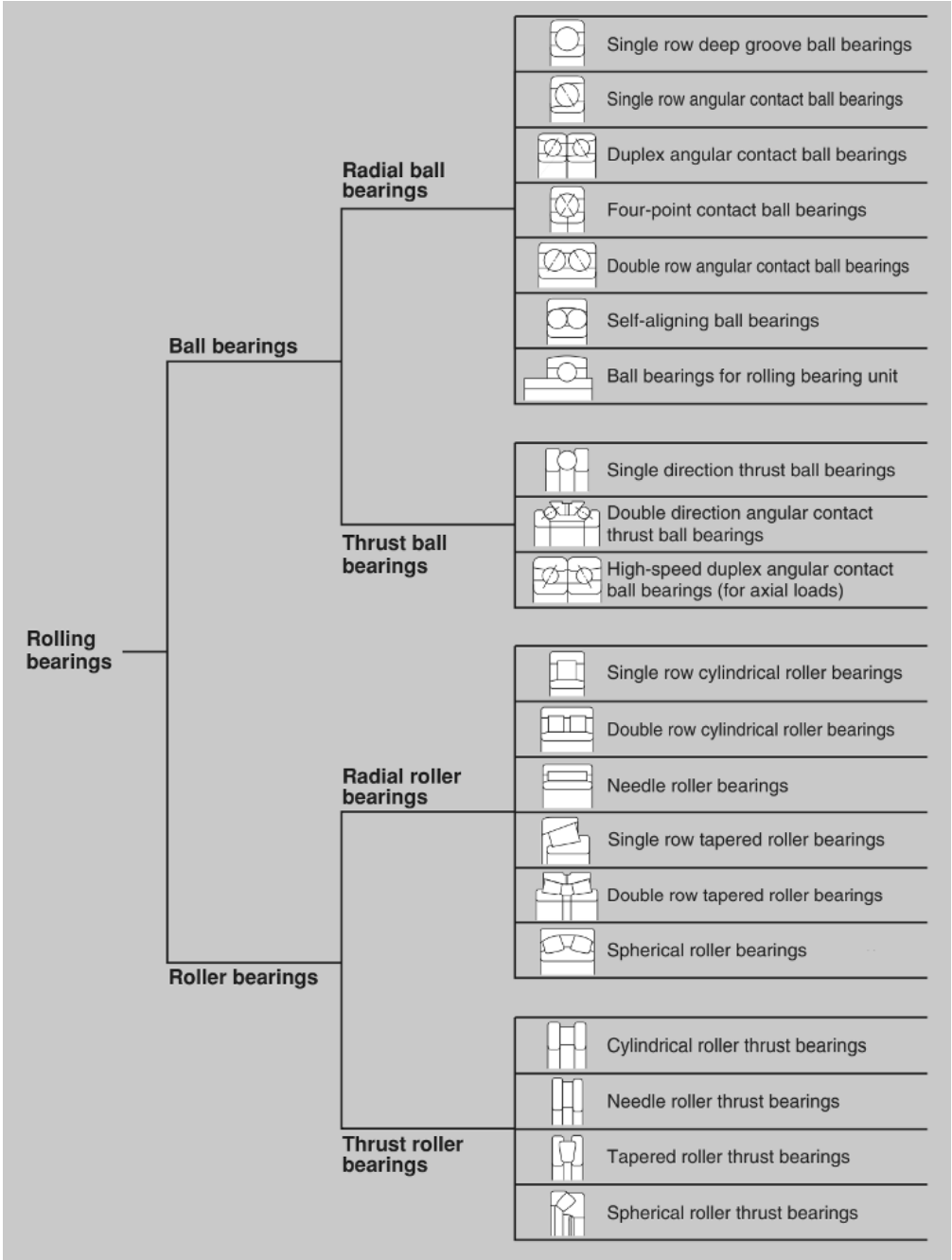
Figure 1. Classification of rolling bearings. **Source:** (NTN Corporation, 2015).

For this research work, a radial ball bearing for rolling bearing units, as shown in Figure 2, is selected as it is cost effective and has a basic mounting interface that can be used

between the surface of the jig and the pulley shaft system. This type of bearing is based on a sealed deep groove ball bearing. The ring of the outer raceway is convex to allow for shaft miss-alignment by tilting in the rolling bearing unit, and the ring of the inner raceway is extended with a locking device to enabling quick and easy mounting onto shafts (SKF Group, n.d.e). The structural diagram of the radial ball bearing for rolling bearing unit used is shown in Figure 3.

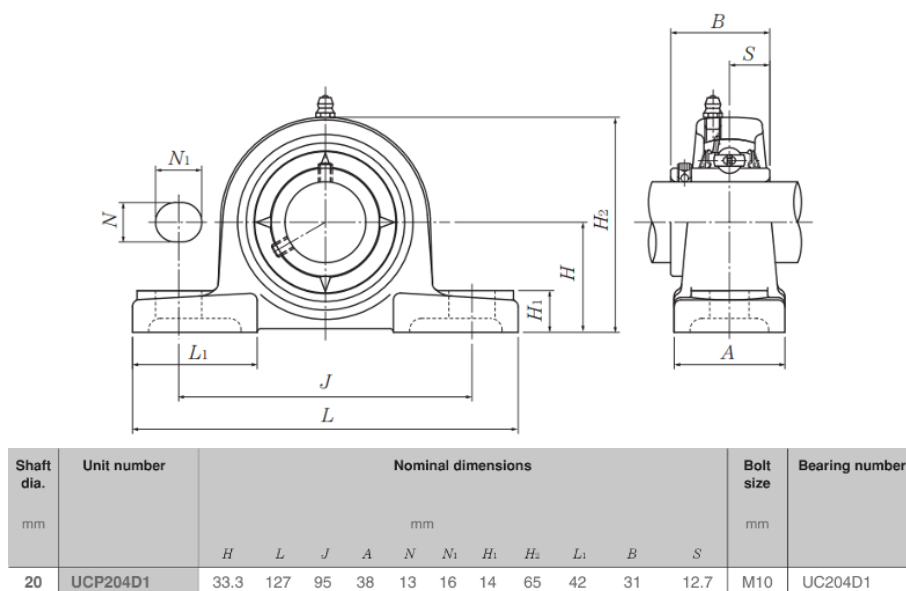| Shaft dia.	Unit number	Nominal dimensions											Bolt size	Bearing number
mm		mm											mm	
		H	L	J	A	N	N_1	H_1	H_2	L_1	B	S		
20	UCP204D1	33.3	127	95	38	13	16	14	65	42	31	12.7	M10	UC204D1

Figure 2. Radial ball bearing for rolling bearing unit. **Source:** (NTN Corporation, 2018).
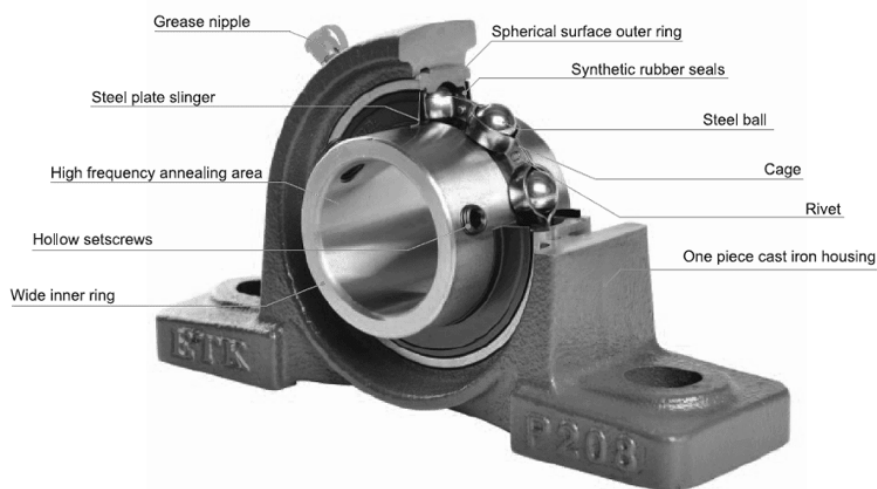

Figure 3. Structural diagram of the radial ball bearing for rolling bearing unit. **Source:** (ETK Bearing Company, n.d.).

Rolling bearings for special applications such as journal bearings, linear actuators, and linear motion products are excluded from the scope of this work, as the main objective is to initially verify the operation of the jig along with its results. Various techniques exist to analyse these bearings for damage after they have been used, as discussed in the next subsection.

3. BEARING ANALYSIS TECHNIQUES

Various techniques exist to analyse bearings after they have been damaged by ECD. Typical evaluations include Solid particle analysis, Fourier Transform Infrared Spectroscopy (FTIR), Light optical microscope (LOM), Scanning Electron Microscope (SEM) and Chemical Analysis.

Solid particle analysis is an excellent technique to analyse debris found in the lubrication of machinery. The morphological results of the wear debris of the components are key in determining commonalities. A particle separating disk is used to separate the solid debris particles from the lubrication for viewing under a microscope. Adequate magnification and lighting are required for viewing and analysis of the filter patches (Raadnui, 2012).

FTIR is used to examine the degradation of lubrication (Aditya, Amarnath, & Kankar, 2014). The FTIR analyser is used to record the transmittance spectrum of new and used lubrication. The Nitration Index and Oxidation Index are widely applied for quantifying the oil degradation in used oil analysis. Nitration products have a characteristic absorbance between the wavenumber range of 1650 cm^{-1} and 1600 cm^{-1}, the region immediately below that of the oxidation products. Oil oxidation occurs in the carbonyl ($C=O$) region between the wavenumber range of 1800 cm^{-1} and 1670 cm^{-1} (Robinson, n.d.).

LOM analysis is popular as it illuminates and magnifies small samples that are difficult to clearly observe with the naked eye. Purely digital microscopes are now available that directly display images on a computer screen (Gianfrancesco, 2017). One of the disadvantages of LOM is the relatively large resolution limit. The resolution limit is controlled by diffraction, which in turn is controlled by the numerical aperture of the optical system and the wavelength of the light used. Another disadvantage of LOM is the poor contrast produced when light is reflected off surfaces with a high degree of reflectivity (Bergström, 2015).

The SEM overcomes these challenges. The magnification power of the electron microscope is continually improving, with modern field emission scanning electron microscopy (FESEM) providing magnifications of up to 550 000 times and resolutions down to 0.5 nm (Ingham, 2013). SEM instrumentation is equipped with energy dispersive spectroscopy (EDS) system that allows for the study of the topography, morphology, chemical composition and crystallographic Information (Scimeca *et al.*, 2018). The techniques as shown in Table 1 will be applied to the used samples bearings to analyse ECD damage.

Table 1. Bearing analysis techniques.

No	Analysis technique	Equipment model number	Purpose of analysis technique
1	LOM analysis	Celestron 44302	LOM will provide initial images of any damage
2	SEM/EDS analysis	Jeol JSM 6610	SEM will verify the images and provide chemical composition

4. THE INNOVATIVE JIG

This section presents the innovative jig that may be used to expose mechanical bearings to ECD and is shown in Figure 4. The labels are presented in Table 2 with a short description and purpose.
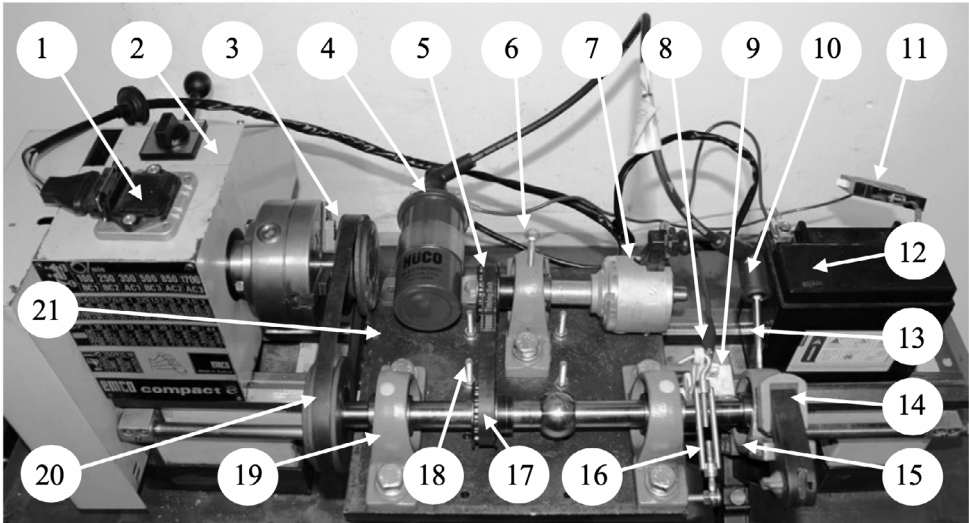

Figure 4. The innovative jig.

The innovative jig comprises readily available components in South Africa. Some of the components required minimal alterations to fit into the jig, without compromising its

functionality. The separation of the carbon brush holder from the voltage regulator of an automotive alternator was challenging due to the poor stiffness of the material and to perform workpiece clamping of the carbon brush holder. A variety of prying tools were successfully used to separate the carbon brush holder from the voltage regulator.

Another challenge encountered was in reducing the shank circumference of the ignition distributor to fit through the wide inner ring of the rolling bearing unit for rigid mounting purposes. The internal cavity of the ignition distributor seems to have been pre-cast asymmetrical, causing the tooling to rupture through the thinned wall sections along the shank. The shank circumference at the drive gear end of the ignition distributor has an internal plain bearing which offered enough clamping support for rigid mounting purposes that overcame this challenge. The overall cost of the project was approximately USD 336.

Table 2. List of components of the innovative jig and their purpose.

No	Description	Purpose
1	Ignition control module	Electronic switch to control timing between discharges of the ignition coil
2	Bench Lathe	220V electrical motor providing rotational motion to the lathe V-belt and pulley
3	Lathe V-belt and pulley	Driving pulley, providing 850 revolutions per minute (rpm)
4	12 Volt electronic ignition coil	The ignition coil steps up the 12 V input to a 30 000 V output
5	Distributor timing belt and pulley	Providing rotational motion to the Hall effect sensor of the ignition distributor
6	Clamping screw	Angular alignment of timing belt and timing pulley of the ignition distributor
7	Ignition distributor	Hall effect sensor provides an input signal to the ignition control module
8	Crocodile clip, cathode terminal	Battery cathode terminal connected to the carbon brush holder
9	Carbon brush	A spring-loaded carbon brush contact interface between the cathode terminal and the shaft mounted radial ball bearing sample
10	Ignition spark plug lead	Connecting lead to transfer high voltage pulses between the ignition coil and radial ball bearing sample; this becomes the anode terminal
11	Circuit breaker	A circuit breaker is used to switch the power supplied from the battery to the ignition coil wiring harness on or off
12	12 V 12 Ah battery	Direct current power supply to the electrical components
13	Thread cutting tap	A thread cutting tap is screwed in to the grease nipple hole to create a spark gap of two-millimetres between the outer raceway of the radial ball bearing sample and the anode terminal

No	Description	Purpose
14	Insulated G-clamp	Rotational restraint and grounding isolator for the radial ball bearing sample
15	Radial ball bearing sample	Radial ball bearing sample fixed to the shaft with two hollow set screws as shown in Figure 3
16	Turnbuckle hook to eye	A screw mechanism used to adjust the contact depth of the spring-loaded carbon brush to the linear shaft
17	Jig Timing belt and pulley	Parallel alignment of timing belt and driving timing pulley
18	Jig mounting screw	The jig attaches to the cross slide of the lathe. The V-belt is tensioned between the lathe end driving pulley and jig end driven pulley
19	Shaft bearing supports	Typical bearing support ends for the shaft to allow rotational motion
20	Jig V-belt and pulley	Driven pulley output shaft speed, 850 revolutions per minute (rpm)
21	Base plate of jig	Mounting interface for selected components

5. METHODOLOGY

This section presents the method to safely induce ECD across a radial ball bearing for rolling bearing units, in order to clarify its associated effects on the bearing that need to be understood before any mitigating techniques can be proposed. An experimental design is used which may be considered as a detailed investigational plan to obtain the maximum amount of information specific to the objectives (McIntosh & Pontius, 2017). The detailed investigational plan in this study starts with:

- Assembly procedure of the innovative jig as shown in Figure 4 and Table 2;
- The location and weather conditions of the research site as shown in Table 3;
- Test parameters for the radial ball bearing for rolling bearing unit samples as shown in Table 4;
- To cut material samples from each of the tested radial ball bearing for rolling bearing units for LOM and SEM analyses.

Table 3. The location and weather conditions of the research site.

Latitude	Longitude	Elevation	Season	Temperature	Wind	Humidity
25°47'34.74"S	28°19'5.77"E	1418m	Spring	22 °C	13 km/h	53%

Table 4. Test parameters for the radial ball bearing for rolling bearing unit samples.

Sample	Time	Shaft Speed	ECD
1	0 minutes	0 rpm	No
2	15 minutes	850 rpm	No
3	15 minutes	850 rpm	Yes

An ignition coil wiring harness of a vehicle was used to induce ECD across a radial ball bearing. This product was selected because it is widely used in the automotive industry, and readily available over the counter. The test parameters for the radial ball bearing samples are shown in Table 4. The experiment was done on 31 October 2019 at 19h00. Sample 1 was kept unused as new with the purpose of being a control sample with which to compare and evaluate the other two samples. Sample 2 and 3 were both exposed to a shaft rotational speed of 850 rpm for fifteen-minutes.

Only sample 3 was exposed to ECD. Sample 2 and 3 were rigidly mounted with two hollow set screws onto a linear shaft section of the innovative jig, as shown in Figure 4. An insulated G-clamp was mounted on each sample as a rotational restraint and grounding isolator. For sample 3, the cathode terminal was connected to the carbon brush holder. A thread cutting tap was screwed into the grease nipple hole of the bearing unit of sample 3 to create a spark gap of two millimetres between the outer raceway anode terminal. The bench lathe was switched on and brought up to a speed of 850 rpm. The power supply circuit breaker was activated, and the fifteen-minute countdown started. Samples were cut from each of the tested radial ball bearing for rolling bearing units. The samples 1, 2 and 3 were mounted for LOM and SEM to analyse for damage as shown in Table 1.

6. TEST RESULTS AND DISCUSSION

The section presents the results that were obtained by using the methodology as presented in the previous section. The results are presented as samples 1, 2 and 3. The SEM photographs of ball bearings retrieved from samples 1, 2 and 3 are as shown in Figure 5, Figure 6 and Figure 7 respectively. The Jeol JSM 6610 SEM had a magnification factor of 60 and a size scale of 200 μm.
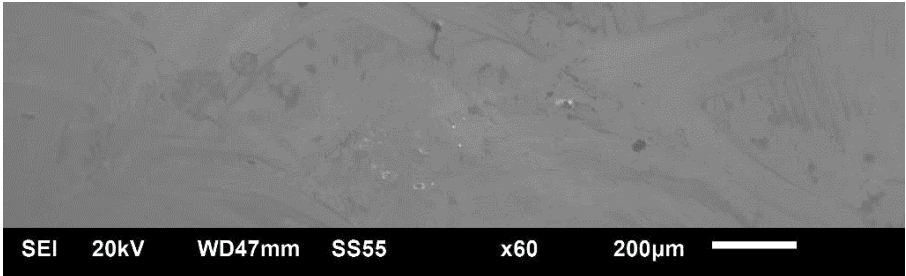

SEI　20kV　WD47mm　SS55　　　x60　　200μm

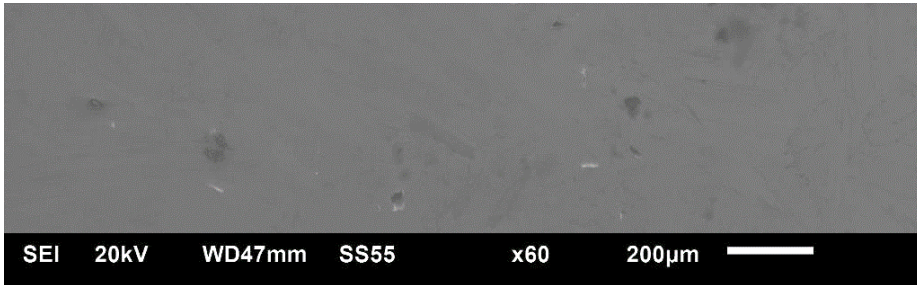**Figure 5.** SEM photograph of a ball bearing: Sample 1 – Unused bearing.

Figure 6. SEM photograph of a ball bearing: Sample 2 – Used with no ECD.
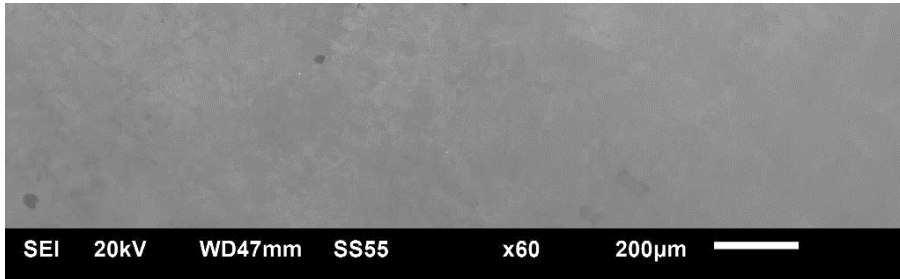

Figure 7. SEM photograph of a ball bearing: Sample 3 – Used with ECD.

Sample 1 (see Figure 5) shows the surface of an unused ball bearing which served as the control sample. Bearing manufacturers polishes rolling elements to an average surface roughness of 0.05 µm (Jacobs, 2014). The irregular scratch marks on the surface could be due the unavoidable ball to ball collisions in the polishing process (Pattabhiraman *et al.*, 2010). Sample 2 (see Figure 6) shows a polished surface of a ball bearing. During run in, a mild degree of polishing occurred between contacting asperities and were worn down that produced fine abrasive particles. The polishing results in a satisfactory contact between surfaces which is considered acceptable wear and tear ("Polishing – Bearing failure", n.d.). Sample 3 (see Figure 7) shows a dull surface appearance that is characterized by small craters of a few microns in diameter. Micro-cratering is a result of electric current passage in the bearing (SKF Group, 2006). The LOM photographs of the outer raceway of samples 1, 2 and 3 are as shown in Figure 8, Figure 9 and Figure 10 respectively. The Celestron 44302 LOM had a magnification factor of 3.
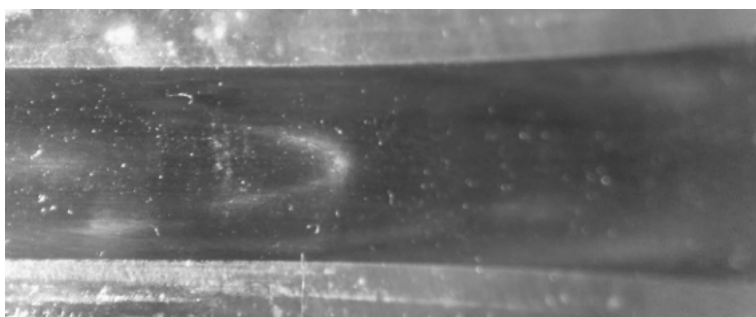
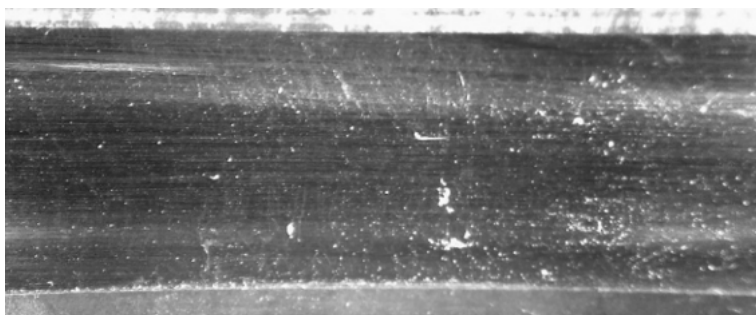**Figure 8.** LOM photograph of the outer race: Sample 1 – Unused bearing.

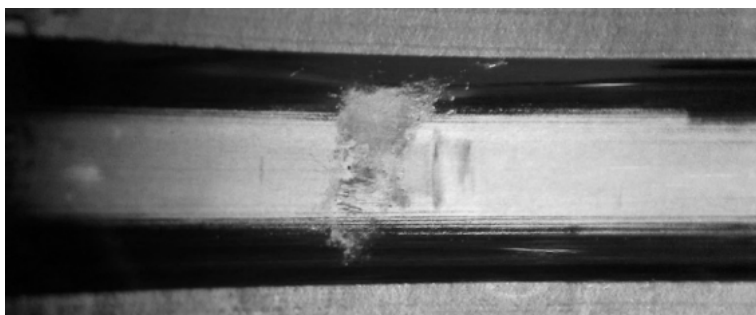**Figure 9.** LOM photograph of the outer race: Sample 2 – Used with no ECD.

Figure 10. LOM photograph of the outer race: Sample 3 – Used with ECD.

Sample 1 (see Figure 8) shows the unused surface of an outer raceway which served as the control sample. The surface showed no observable damage. Sample 2 (see Figure 9) showed scratch marks on the raceway surface, parallel to the rolling direction. A higher magnification of the localized areas of samples 1 and 2 were sought with SEM (see Figure 11 and Figure 12). The Jeol JSM 6610 SEM had a magnification factor of 130 and a size scale of 100 µm. Similar to the results obtained from the ball bearing samples 1 and 2 (see Figure 5 and Figure 6), the raceway samples 1 and 2 had a mild degree of polishing that occurred between contacting asperities that worn down that produced fine abrasive

particles. For abrasive wear to occur, the fine particles, or one of the contacting surfaces, needs to be substantially harder than the abraded surface. The abrasive wear process leads to a characteristic surface topography of long grooves running in the sliding direction (Jiménez & Bermúdez, 2011). Sample 3 (see Figure 10) showed localised damage on the outer raceway surface (circle shown in Figure 10). The damage was observed to be adjacent to the anode terminal (see Figure 4 and Table 2). A higher magnification of the localized area of samples 3 was sought with SEM (see Figure 13).
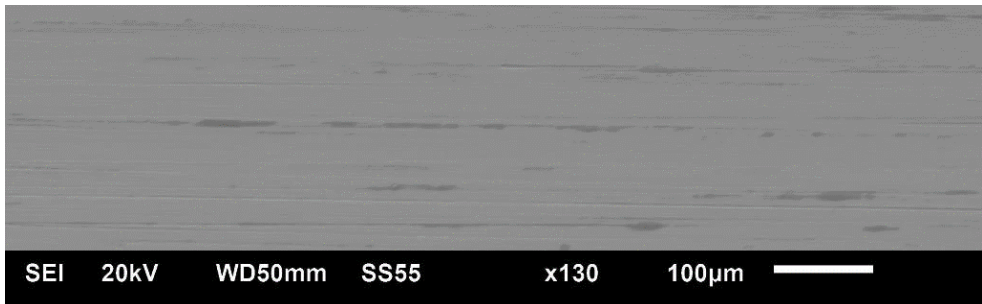

Figure 11. SEM photograph of the outer race: Sample 1 – Unused bearing.
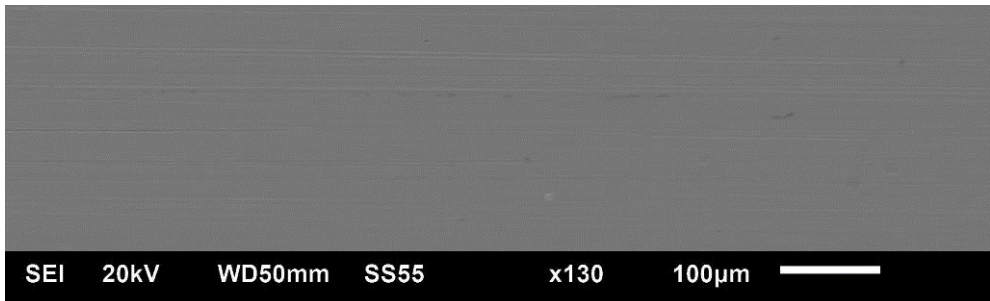
Figure 12. SEM photograph of the outer race: Sample 2 – Used with no ECD.

The SEM photograph of the outer raceway of sample 3 is as shown in Figure 13. The Jeol JSM 6610 SEM had a magnification factor of 11 and a size scale of 1 mm. Sample 3 (see Figure 13) shows micro arching marks on the raceway surface leading towards the groove of the synthetic rubber seal and steel plate slinger (see Figure 3). The arcing marks are typical proof of electric current passage in the bearing (Liu, 2014). A higher magnification of the localized area of samples 3 (circle shown in Figure 13) was sought with SEM. The Jeol JSM 6610 SEM had a magnification factor of 35 and a size scale of 500 μm was used as shown in Figure 14.
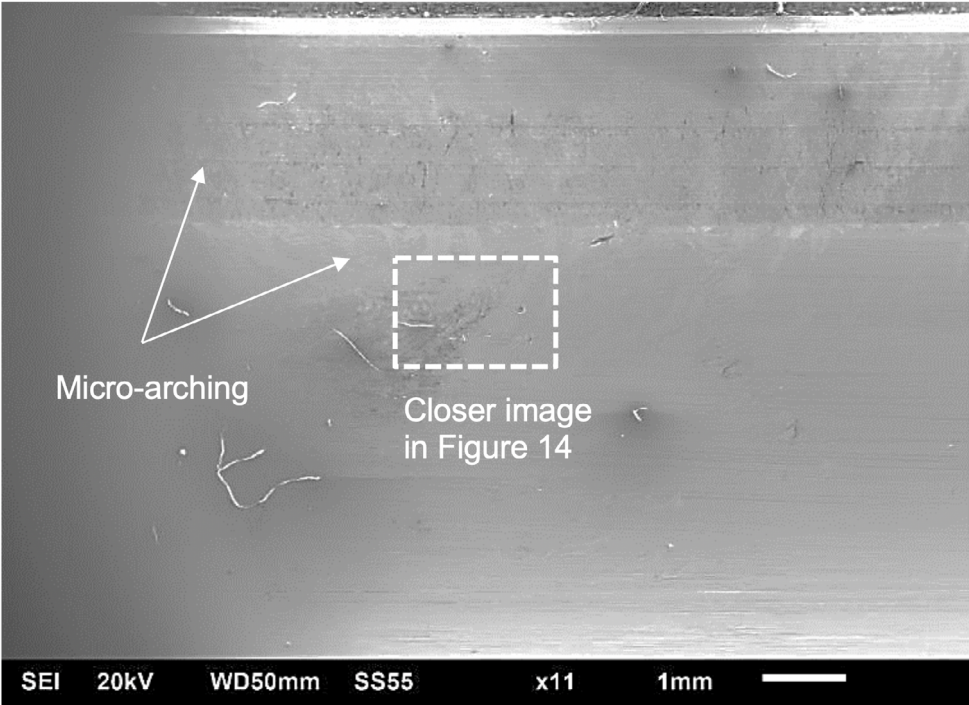
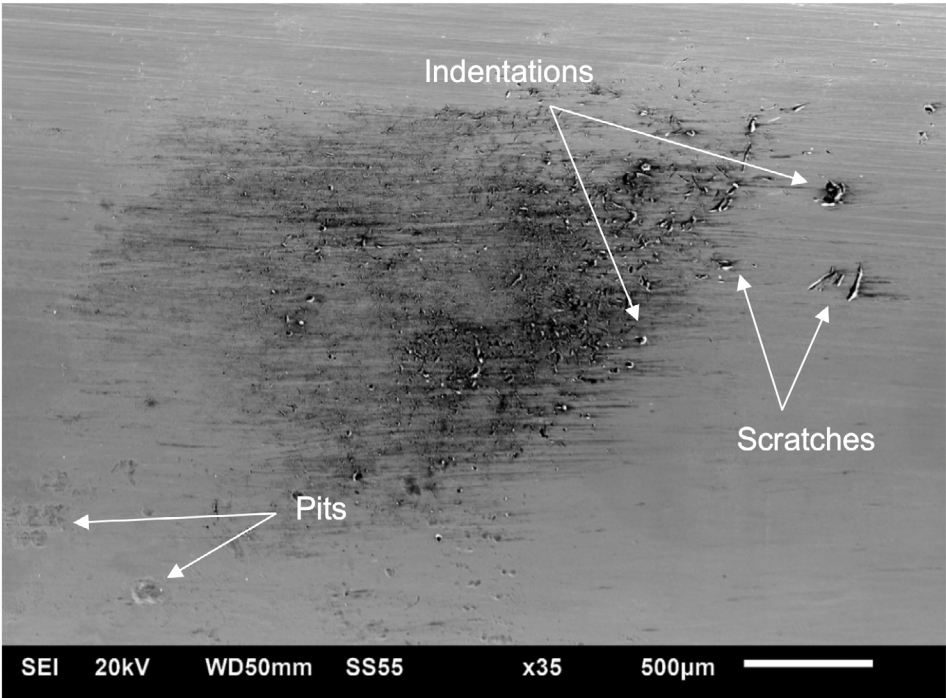**Figure 13.** SEM photograph of the outer race: Sample 3 – Used with ECD.

Figure 14. SEM photograph of the outer race: sample 3 – Used with ECD.

Sample 3 (see Figure 14) shows many surface pits which were produced by electrical arching (Raadnui, 2012). A few deep scratches and indentations are observed on the raceway surface. This is due to the abrasive wear particles embedded in the raceway surface and ploughed away (Aditya, Amarnath, & Kankar, 2014). Any rolling bearing has some degree of sliding due to the difference in the internal geometry and loading conditions of the bearing (Morales-Espejel, 2019).

7. CONCLUSION

The purpose of this paper was to present an innovative jig that may be used to expose mechanical bearings to ECD, in order to clarify its associated effects on the bearing that need to be understood before any mitigating techniques can be proposed. The ball bearing exposed to ECD showed a dull surface appearance that is characterized by small craters of a few microns in diameter. Micro-cratering is a result of electric current passage in the bearing. Micro-arching marks were observed on the outer raceway surface. The arcing marks are typical proof of electric current passage in the bearing. A few deep scratches and indentations are observed on the raceway surface. This is due to the abrasive wear particles embedded in the raceway surface and ploughed away due to the difference in the internal geometry and loading conditions of the bearing. The aspect of electrical pitting wear and debris found in the lubricating oil deserve further research from a tribological point of view. Some practical solutions to mitigate bearing currents has worked effectively for sinusoidal alternating currents. Some of the solutions are not as effective against the fast switching Pulse Width Modulation (PWM) inverter technology that causes high frequency non-sinusoidal bearing current. The foremost limitation of this article is that neither the voltage, nor the current values of ECD are known. A recommendation is made to conduct qualitative research with the innovative jig to test the impact of ECD on bearings from other suppliers. The obtained primary data will warrant similarities or differences present in used ball bearings exposed to ECD.

REFERENCES

Aditya, S., Amarnath, M., & Kankar, P. K. (2014). Failure Analysis of a Grease-Lubricated Cylindrical Roller Bearing. *Procedia Technology, 14*, 59-66. https://doi.org/10.1016/j.protcy.2014.08.009

Bergström, J. (2015). Chapter 2 - Experimental Characterization Techniques. In *Mechanics of Solid Polymers - Theory and Computational Modeling*. Elsevier, 19-114.

Bhadeshia, H. K. D. H. (2012). Steels for bearings. *Progress in Materials Science, 57*(2), 268-435. https://doi.org/10.1016/j.pmatsci.2011.06.002

Bhadeshia, H. K. D. H. (n.d.). *Mechanical Bearings*. University of Cambridge. https://www.phase-trans.msm.cam.ac.uk/2010/types/index.html

Bizwit Research & Consulting LLP. (2019, May 15). *Global Bearings Market Size study, by product (Roller Bearings, Ball Bearings and others) Application (Automotive, Agriculture, Electrical, Mining & Construction, Railway & Aerospace, Automotive Aftermarket and Others) and Regional Forecasts 2018-2025.* https://www.wiseguyreports.com/reports/4041840-global-bearings-market-size-study-by-product-roller#

Chiou, Y.-C., Lee, R.-T., & Lin, S.-M. (2009). Formation mechanism of electrical damage on sliding lubricated contacts for steel pair under DC electric field. *Wear, 266*, 110-118. https://doi.org/10.1016/j.wear.2008.06.001

ETK Bearing Company. (n.d.). *Bearing Units Introduction & Selection*. http://www.etkbearing.com/about/?72.html

Gianfrancesco, A. D. (2017). Chapter 8 - Technologies for chemical analyses, microstructural and inspection investigation. In *Materials for Ultra-Supercritical and Advanced Ultra-Supercritical Power Plants*. Elsevier, 197-245. https://doi.org/10.1016/B978-0-08-100552-1.00008-7

Ingham, J. P. (2013). Chapter 1 - Introduction. In *Geomaterials Under the Microscope*. Elsevier, 7-20.

Jacobs, W. (2014). *Experimental analysis of the dynamic characteristics and lubricant film of a ball bearing under combined static and dynamic load*. KU Leuven - Faculty of Engineering Science.

Jacobs, W., Van Hooreweder, B., Boonen, R., Sas, P., & Moens, D. (2016). The influence of external dynamic loads on the lifetime of rolling element bearings: Experimental analysis of the lubricant film and surface wear. *Mechanical Systems and Signal Processing, 74*(1), 144-164. https://doi.org/10.1016/j.ymssp.2015.04.033

Jiménez, A.-E., & Bermúdez, M.-D. (2011). Chapter 2 - Friction and wear. In *Tribology for Engineers A Practical Guide. Woodhead* Publishing Limited, 33-63.

Liu, W. (2014). The prevalent motor bearing premature failures due to the high frequency electric current passage. *Engineering Failure Analysis, 45,* 118-127. https://doi.org/10.1016/j.engfailanal.2014.06.021

Massi, F., Rocchi, J., Culla, A., & Berthier, Y. (2010). Coupling system dynamics and contact behaviour: Modelling bearings subjected to environmental induced vibrations and 'false brinelling' degradation. *Mechanical Systems and Signal Processing, 24*(4), 1068–1080. https://doi.org/10.1016/j.ymssp.2009.09.004

McIntosh, A., & Pontius, J. (2017). Chapter 1 - Tools and Skills. In *Science and the Global Environment. Case Studies Integrating Science Global Environment*. Elsevier, 514.

Morales-Espejel, G. E. (2019, June 28). *Wear and surface fatigue in rolling bearings.* http://evolution.skf.com/wear-and-surface-fatigue-in-rolling-bearings/

NTN Corporation. (2015). *Ball and Roller Bearings*. https://www.ntnglobal.com/en/products/catalog/pdf/2202E_all.pdf

NTN Corporation. (2018). *Bearing Units.* https://www.ntnglobal.com/en/products/catalog/pdf/2400E_all.pdf

Pattabhiraman, S., Levesque, G., Kim, N. H., & Arakere, N. K. (2010). Uncertainty analysis for rolling contact fatigue failure probability of silicon nitride ball bearings. *International Journal of Solids and Structures, 47*(18-19), 2543–2553. https://doi.org/10.1016/j.ijsolstr.2010.05.018

Polishing – Bearing failure. (n.d.). https://onyxinsight.com/wind-turbine-failures-encyclopedia/bearing-failures/polishing/

Raadnui, S. (2012). Between "ferrogram" and "filtergram" makers is the multiple centrifiltergram maker: a new technique for solid debris separation. *Journal of Physics: Conference Series, 364*, 1-7. https://iopscience.iop.org/article/10.1088/1742-6596/364/1/012087

Robinson, N. (n.d.). Monitoring oil degradation with infrared spectroscopy. Wearcheck Division of Set Point Technology. *Technical Bulletin*, (18). http://www.wearcheck.com/virtual_directories/Literature/Techdoc/WZA018.pdf

Scimeca, M., Bischetti, S., Lamsira, H. K., Bonfiglio, R., & Bonanno, E. (2018). Energy Dispersive X-ray (EDX) microanalysis: A powerful tool in biomedical research and diagnosis. *European Journal of Histochemistry, 62*(1), 1-10.

SKF explorer spherical roller thrust bearings boost design options. (2003, May 29). http://evolution.skf.com/skf-explorer-spherical-roller-thrust-bearings-boost-design-options

SKF Group. (2006). *Electrically insulated bearings from SKF.* https://www.skf.com/binary/tcm:12-295325/0901d1968008da41-6160-EN-Motor-Insocoat-hybrid_tcm_12-295325.pdf

SKF Group. (2010). *SKF spherical roller thrust bearings. For long lasting performance.* https://www.skf.com/binary/tcm:12-121034/0901d1968027f7c9-06104_1-EN_tcm_12-121034.pdf

SKF Group. (2012a). *Bearing in centrifugal pumps. Application handbook.* https://www.skf.com/binary/26-154513/100-955-Bearings-in-centrifugal-pumps.pdf

SKF Group. (2012b). *Super-precision angular contact ball bearings: High-speed, B design, sealed as standard S719 .. B (HB .. /S) and S70 .. B (HX .. /S) series.* https://www.skf.com/binary/30-75457/0901d196801b304f-Super-precision-angular-contact-ball-bearings-High-speed-B-design-sealed---06939_5-EN.pdf

SKF Group. (2014). *SKF self-aligning ball bearings for the textile industry.* https://www.skf.com/binary/21-161175/Self-aligning-ball-bearings-for-textile-industry.pdf

SKF Group. (2018). *Self-aligning ball bearings.* http://www.bearing.net.au/wp-content/uploads/2018/02/6000_EN_03_SABB.compressed.pdf

SKF Group. (n.d.a). *Bearing arrangements.* https://www.skf.com/africa/en/products/bearings-units-housings/super-precision-bearings/angular-contact-thrust-ball-bearings-for-screw-drives/bearingarrangementdesign/bearing_arrangements/index.html

SKF Group. (n.d.b). *Self-aligning ball bearings.* https://www.skf.com/africa/en/products/bearings-units-housings/ball-bearings/self-aligning-ball-bearings/index.html

SKF Group. (n.d.c). *Needle roller bearings.* https://www.skf.com/africa/en/products/bearings-units-housings/roller-bearings/needle-roller-bearings/index.html

SKF Group. (n.d.d). *U-joints.* https://www.skf.com/ca/en/products/vehicle-aftermarket/automotive/drivetrain/u-joints/index.html

SKF Group. (n.d.e). *Insert bearings (Y-bearings).* https://www.skf.com/uk/products/bearings-units-housings/ball-bearings/insert-bearings/index.html

Upadhyay, R. K., Kumaraswamidhas, L. A., & Azam, S. (2013). Rolling element bearing failure analysis: A case study. *Case Studies in Engineering Failure Analysis, 1*(1), 15-17. https://doi.org/10.1016/j.csefa.2012.11.003

/12/

ADHESION LEVEL IDENTIFICATION IN WHEEL-RAIL CONTACT USING DEEP NEURAL NETWORKS

Sanaullah Mehran Ujjan

ME Scholar, NCRA- Condition Monitoring Lab.

Mehran University of Engineering and Technology. Jamshoro, (Pakistan).

E-mail: mehranujjan44@gmail.com ORCID: https://orcid.org/0000-0003-1879-8754

Imtiaz Hussain Kalwar

Head of Department, Electrical Engineering.

DHA Suffa University. Karachi, (Pakistan).

E-mail: imtiaz.hussain@dsu.edu.pk ORCID: https://orcid.org/0000-0002-7947-9178

Bhawani Shankar Chowdhry

Professor Emeritus.

Mehran University of Engineering and Technology. Jamshroo, (Pakistan).

E-mail: bhawani.chowdhry@faculty.muet.edu.pk ORCID: https://orcid.org/0000-0002-4340-9602

Tayab Din Memon

Chairman, Department of Electronics.

Mehran University of Engineering and Technology. Jamshoro, (Pakistan).

E-mail: tayabdin82@gmail.com ORCID: https://orcid.org/0000-0001-8122-5647

Dileep Kumar Soother

Research Assistant, NCRA- Condition Monitoring Lab.

Mehran University of Engineering and Technology. Jamshoro, (Pakistan).

E-mail: dileepkalani1994@gmail.com ORCID: https://orcid.org/0000-0002-6211-1078

ABSTRACT

Robust and accurate adhesion level identification is crucial for proper operation of railway vehicle. It is necessary for braking and traction forces characterization, development of maintenance strategies, wheel-rail wear predictions and development of robust onboard health monitoring systems. Adhesion being the function of many uncertain parameters is difficult to model, whereas data driven algorithms such as Deep Neural networks (DNNs) are very good at mapping a nonlinear function from cause to effect. In this research a solid axle Wheel-set was modeled along with different adhesion conditions and a dataset was prepared for the training of DNNs in Python. Furthermore, it explored the potential of DNNs and various data driven algorithms on our noisy sequential dataset for classification task and achieved 91% accuracy in identification of adhesion condition with our final model.

KEYWORDS

1. INTRODUCTION

Adhesion level identification is an important task for proper operation of a railway vehicle as traction effort is a direct function of adhesion coefficient. Hence different magnitude of tracking and braking forces is required in different contact conditions, making adhesion level identification crucial for tracking and braking forces characterization (Spiryagin *et al.*, 2014). Both overestimation or under estimation can cause either derailment or rapid noise at wheel rail interface (Olofsson, 2009).

Adhesion coefficient quantitatively relates ratio of traction effort to the normal load on the wheel and qualitatively represents contact condition between wheel and rail.

Many cases of derailment have been reported in Pakistan ("A Timeline of Neglect: Train Incidents in Pakistan", 2019) due to various causes but with a suitable mechanism of adhesion level identification and adhesion control at least one factor (over/under estimation of adhesion condition) can be tackled down.

Adhesion problem has sought attention of many researchers and many solutions ranging from mathematical control theory to statistical and genetic algorithms (Bibi, Chowdry, & Shah, 2018) have been proposed and applied (Shrestha, Wu, & Spiryagin, 2019). Although, here we compare two of them, model based and data driven work on adhesion, but later being rarely applied we aim to express the potential of data driven models in railway domain.

1.1. MODEL BASED WORK

Several attempts to correctly estimate the adhesion have been reported in recent years related to model based approaches (Shrestha *et al.*, 2019; Malvezzi *et al.*, 2013; Hussain, 2012; Ward *et al.*, 2012) where a mathematical relation between excitation and response of the system is constructed. Adhesion has been expressed as a function of slip velocity and acceleration by Carl and Brook (1985), and Malvezzi *et al.* (2013). Function of longitudinal vehicle velocity and pressure in contact zone by Spiryagin *et al.* (2016), function of lateral creep force and yaw movement by Ward *et al.* (2012).

However modelling a physical phenomenon such as adhesion with too many uncertain or even unknown factors is a time taking task. As any mathematical model inherently has the tendency to ignore some parameters in the process but ignoring adhesion effective parameters for the sake of simplicity and robustness of the model can cause difficulties especially when the model is later on used for complex tasks e.g. development of a Real-time on-board health monitoring system in locomotives (Shah *et al.*, 2020).

Nonetheless, with the current state of knowledge about adhesion it remains a riddle to be solved. With the beginning of Era of Big data and Deep learning models whose implementations in many domains yielded state of the art results. In 2018 Rail safety and standards board announced 300,000 euros for encouraging the researchers to develop data driven solutions for solving the adhesion riddle.

1.2. DATA DRIVEN WORK

Only few examples of implementation of data driven solutions for solving adhesion have been reported up till now, Castillo *et al.* (2016) have used Artificial Neural Networks (ANNs) to estimate adhesion states in an ABS system. Li, Feng, and Wei (2015) have used optimized Recursive ANN with the focus on optimizing the utilization rate of adhesion available. Gajdar, Rudas, and Suda (1997) have used classical BP Neural network to estimate friction coefficient of the rail wheel which is mathematically different but closely associated with adhesion coefficient. Data is extracted through a simulated wheel rail condition. Malvezzi *et al.* (2013) have used Neural networks in combination with an adhesion model to identify adhesion coefficient. Experimental data is acquired during tracking and braking tests. Zhang *et al.* (2017) have used a deep auto sparse encoder to estimate adhesion status of a locomotive however the parameters chosen for training the Autoencoder are not directly measurable and have been acquired through an SMC estimator, so the accuracy of the data driven model heavily depends upon the SMC observer. From the above mentioned data driven approaches are experimentally verified and show viable results (Castillo *et al.*, 2016; Li *et al.*, 2015). However, very few approaches solely focus on adhesion identification and ignore the complexities associated with it, also any data driven algorithm should be able to identify adhesion conditions from directly measurable parameters rather than relying on estimated parameters (Zhang *et al.*, 2017; Gajdar *et al.*, 1997).

In this research, a data driven method based on DNNs is employed, which solely focuses on adhesion condition identification. Main objective of this study has been to produce a self-reliant data driven solution to the adhesion riddle. Data driven model should predict adhesion condition from noisy sensor data, without relying on estimation theory to get clearer data at their input. This will enhance possibility of integration of this model in an onboard condition monitoring system.

Rest of the paper proceeds as follows. Section 2 and 3 describe the simulation of the wheel-rail interaction and different adhesion conditions, Section 4 includes data recording and dataset preparation, Section 5 explains the process of implementation of DNNs, Section 6 compares and discusses the results obtained with different data driven algorithms, and Section 7 concludes the paper.

2. SIMULATING WHEEL-RAIL INTERACTION

In order to acquire data for the training of DNNs, a Wheel-rail contact model which manifests the running of a wheel on a track in different adhesion conditions was needed so a nonlinear model of a solid axle Wheel-set established in Hussain, Mei, and Ritchings (2013) was simulated in MATLAB/Simulink.

Figure 1 shows diagram of the modeled solid-axle Wheel-set, F_{xr} and F_{xl} are longitudinal creep forces, w_r and w_l are angular velocities of right and left wheel respectively and V is longitudinal velocity of the Wheelset under the effect of creep forces.
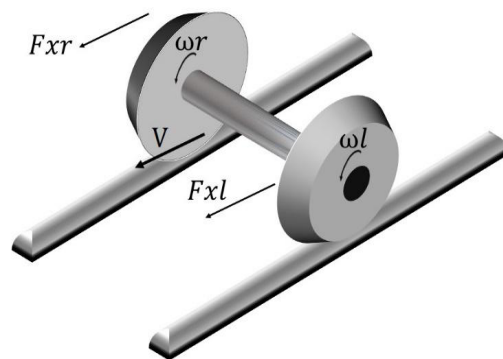

Figure 1. Solid Axle Wheel-set on a straight track.

Below are the equations of motions of this Wheel-set model.

$$V = \left(\left(\frac{1}{M_v} \right) * \int \left(F_{xr} + F_{xl} \right) dt \right) + v_0 \tag{1}$$

$$\omega_R = \left(\left(\frac{1}{I_r} \right) * \int \left(T_m - T_s - T_r \right) dt \right) + \omega_0 \tag{2}$$

$$\omega_L = \left(\left(\frac{1}{I_l} \right) * \int \left(T_s - T_l \right) dt \right) + \omega_0 \tag{3}$$

$$\theta_S = \int \left(\omega_R - \omega_L \right) dt \tag{4}$$

Here θ_s is angle of twist when both wheels have different angular velocities, where as F_{xr}, F_{xl} creep forces of both wheels and can be calculated as:

$$F_{xr} = \frac{F_r * \gamma_{xr}}{\gamma r} \tag{5}$$

$$F_{xl} = \frac{F_l * \gamma_{xl}}{\gamma l} \tag{6}$$

Where F_r and F_l are total creep forces of left and right wheel calculated from adhesion coefficient µ and normal load N.

$$F_r = \mu_r * N \tag{7}$$

$$F_l = \mu_l * N \tag{8}$$

µr and µl are adhesion coefficients representing the different adhesion levels, these coefficients are calculated by Polach model (Polach, 2005).

3. SIMULATING DIFFERENT ADHESION CONDITIONS

In order to manifest the different adhesion conditions or adhesion coefficient values in (8) (9) on which the Wheel-set model was to run, we used Polach model to generate different adhesion conditions (Polach, 2005), Figure 2 shows different adhesion conditions on which the simulations are carried out.
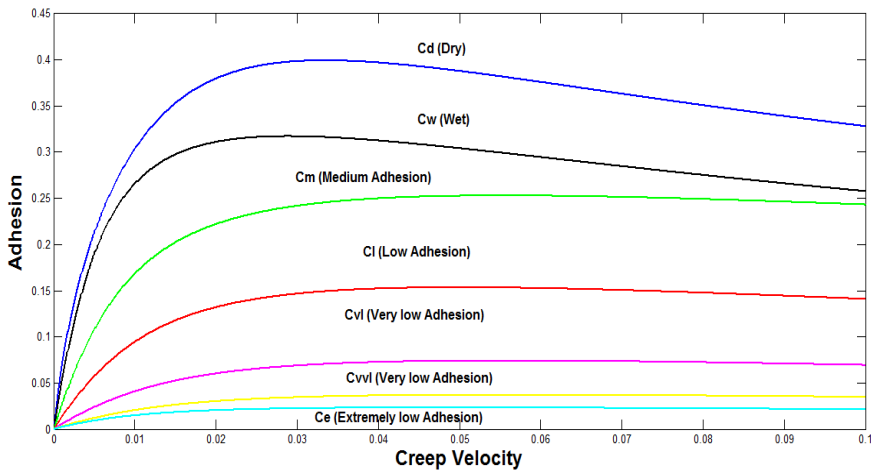
Figure 2. Adhesion curves from Polach Model.

Here are the equations used in simulating different adhesion conditions based on Polach model (Polach, 2005).

$$\mu = \mu_0 (1 - A) e^\wedge(-BVc) + A \tag{9}$$

$$F = \frac{2Q\mu}{\pi}\left(\frac{\varepsilon}{\varepsilon^2 + 1} + \arctan\varepsilon\right) \tag{10}$$

$$\varepsilon = \frac{2}{3}\frac{C\pi a^2 b}{Q\mu}S \tag{11}$$

In (9) μ is adhesion coefficient and A, B are curve tuning parameters whereas V_c is creep velocity, In (10) F is creep force, Q is wheel load, and ε is gradient of tangential stress in the area of adhesion which is calculated in (11) from a, b half axes of contact ellipses, contact sheer stiffness C, and total creep s.

4. DATA RECORDING AND PREPARTION OF DATASET

On each of the contact conditions manifested by Polach model, Wheel-set was run for 5 minutes and parameters which are practically measurable through sensors namely, longitudinal velocity V, angular velocity of both wheels and the integration of the difference between them θ_s was generated using simulations in presence of constant track disturbance.

Figure 3 shows the one sample of theta recorded during 0.63 seconds of simulation on 7 different adhesion conditions, length of the sample 0.63 seconds is chosen with a trial and error process, lower sample size being more preferable as it would increase the response time of the DNN, however 0.63 was identified as limit without deteriorating performance of the model, magnitude of θ_s seems to lower with decrease in adhesion, but frequency seems to increase. However signal's characteristics are not part of discussion here as data driven algorithms will be feed individual values of and should classify and identify them as different signals
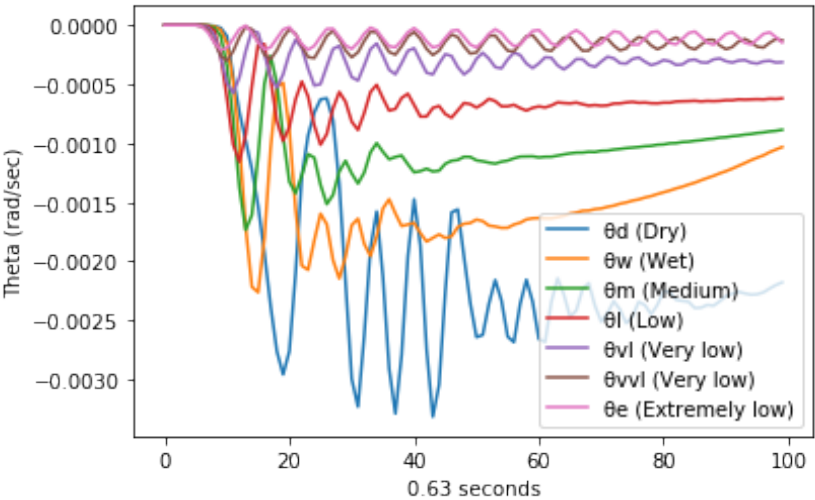

Figure 2. Single Sample of θ_s on different Adhesion conditions.

Keeping in mind the robustness required in the model, recorded parameters were analyzed and θ_s was chosen as the parameter to train the DNNs as it is a scaled and meaningful representation of angular velocities of both wheels, hence reducing the no of features and simplifying the process of convergence of DNN.

Recorded sequence data was converted into a comma separated file (CSV) and preprocessed using Python programming in order to be used for training the DNN, Sequences of θ_s recorded over different adhesion conditions were spilt on equal interval of 0.63 seconds, labeled and stacked into a matrix of n x m shape as shown below:

$$data = \begin{bmatrix} \theta_{11} & \theta_{12} & \square & \theta_{1m} \\ \theta_{21} & \theta_{22} & \square & \theta_{2m} \\ \square & \square & \square & \square \\ \theta_{n1} & \theta_{n2} & \square & \theta_{nm} \\ 0 & 1 & \square & 6 \end{bmatrix} \qquad (12)$$

Here n=100 no of features in a single sample of theta for 0.63 seconds, where m= 3290 total no of examples from all classes, 470 from each class or adhesion condition. Last row represents labels associated with each class or adhesion condition [0, 6]. Data matrix was shuffled and spilt using 70/30 rule into Train set which was to be used for training the DNN and Test set on which the validation of the trained model was done.

5. DNN IMPLEMENTATION

DNN was implemented using the Tensorflow and Keras, High End APIs of Python used for implementation of Deep learning models. We went through various Hyper parameters configurations of the DNN, no of neurons in each layer, no of layers, activation functions, loss functions, regularization parameters, and optimizers. Figure 4 shows the configuration of the model which exhibited the highest validation accuracy and less generalization error.
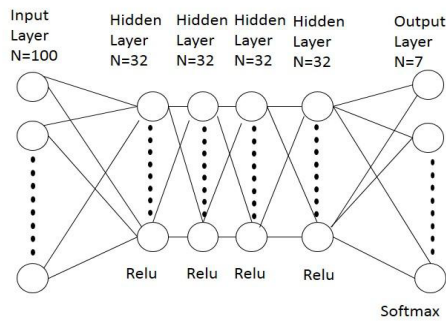
Figure 2. Block diagram of DNN.

The four densely-connected (each input is connected to every neuron in succeeding hidden layer) each with 32 neurons with a relu (rectifying linear unit) activation were used. Each neuron represents a matrix multiplication and summation operation, every neuron a_n^l superscript l representing the no of layer and n is number of neuron are calculated as in (13) and then relu activation function is applied as in (14).

$$a_n^l = \sum_{n=1}^{N} w_n \theta_n \tag{13}$$

$$f(a) = \begin{cases} 0 & if \quad a < 0 \\ a & if \quad a \geq 0 \end{cases} \tag{14}$$

In (13) w_n represents weights of the NN which are randomly initialized from Gaussian distribution and are optimized over iterations using an optimization function reported in Kingma and Ba (2015). Equation (15) shows the way Adam optimizer way of updating its weight, it can be thought of a combination between stochastic gradient descent and RMSprop (Root Mean Square proportion).

$$w_t = w_{t-1} - \eta \frac{\widehat{m_t}}{\sqrt{\widehat{v_t + \varepsilon}}} \tag{15}$$

Here η is the step size like learning rate, $\widehat{m_t}$ and $\widehat{v_t}$ are exponentials of moving averages of weights. Loss function used here is categorical cross entropy which is one of the most used ways of loss calculation in multiclass classification problems. Softmax at the output is a stack of multiple sigmoid activation functions in order to calculate the probability of each class.

6. RESULTS AND DISSCUSSION

Having formulated problem as a multiclass classification one, multiple data driven algorithms were tried, Table 1 shows validation accuracy achieved by different data driven algorithms.

Table 1. Accuracy of different data driven algorithms on our dataset.

Algorithm	Accuracy
Decision Tree	80%
Logistic Regression	19%
K-nearest Neighbours	62%
Support Vector Machine-Polynomial	71%
Support Vector Machine-Guassian	35%
Deep Neural Network (DNN/MLP)	91%

Table 1 shows that DNN outperformed traditional data driven methods by a large margin on our sequence classification task and achieved reasonable accuracy to work with. Keeping in mind the future real time implementation, and reasonable accuracy achieved on a simpler

model other Deep Models such as Convolutional and Recurrent Neural Networks are not compared here as those may be bulky and an overkill in terms of computational cost of those models.

Confusion matrix in Figure 5 shows the accuracy achieved by DNN on individual classes (adhesion conditions) and Table 2 show accuracy as well as precision and recall of the DNN achieved by model.
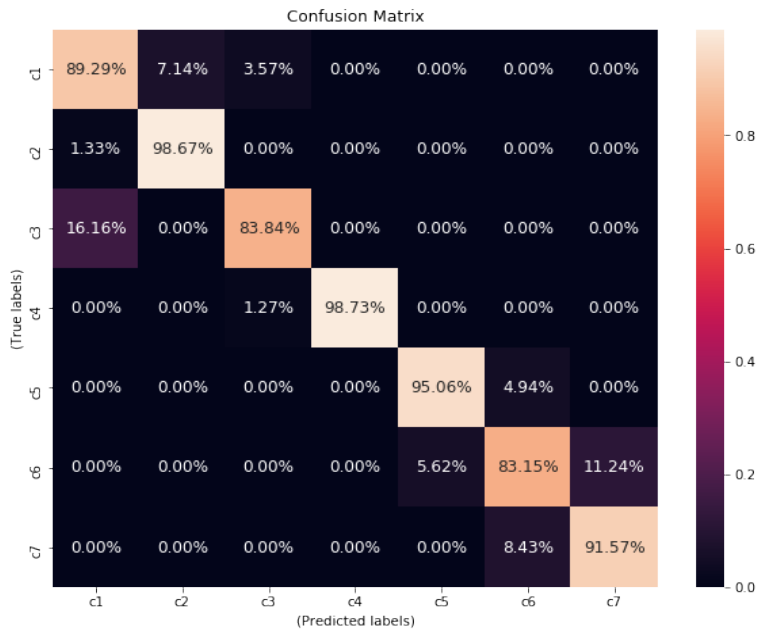

Figure 2. Confusion Matrix (DNN).

Table 1. Classification report (DNN).

	Precision	Recall	F1-score
Cd (Dry)	0.82	0.89	0.85
Cw (Wet)	0.93	0.99	0.95
Cm (Medium)	0.95	0.84	0.89
Cl (Low)	1.00	0.99	0.99
Cvl (Very low)	0.94	0.95	0.94
Cvvl (Very low)	0.87	0.83	0.85
Ce (Extremely low)	0.88	0.92	0.90
Accuracy			0.91
Macro average	0.91	0.91	0.91
Weighted average	0.91	0.91	0.91

7. CONCLUSION AND FUTURE WORK

This paper demonstrates the potential of data driven model a Deep Neural Network solely focusing on identification of contact condition or adhesion condition. It was observed in the results that deep neural networks performed well on the task of inferring adhesion condition from directly measurable parameters and achieved 91% accuracy on data. However experimental data collection in railway is expensive and open access datasets are a rarity, providing labels to that data is another problem in its entirety. Point to the future is to attempt further on adhesion riddle using data driven model that may overcome the hurdles of less availability of data and should be able to work in an unsupervised setting.

ACKNOWLEDGMENT

REFERENCES

A Timeline of Neglect: Train Incidents in Pakistan. (2019, October 31). The Express Tribune. https://tribune.com.pk/story/2090607/1-timeline-neglect-train-incidents-pakistan/?__cf_chl_jschl_tk__=67b51aba1d9fc784047d7a9762c146c04cc3533c-1580365929-0-AcF2YBpMeT3YhfRtd7XjbqIHW9ee6w56yPvQP0YDpiMvDN3xSyqEQ9ABBwqUJBVwBWTQvnuWfHkSJxYVI48aCK-CgNuuVfT1N3OQ

Bibi, R., Chowdry, B. S., & Shah, R. A. (2018). PSO Based Localization of Multiple Mobile Robots Emplying LEGO EV3. In *2018 International Conference on Computing, Mathematics and Engineering Technologies (iCoMET), Sukkur, Pakistan*. https://doi.org/10.1109/ICOMET.2018.8346452

Carl, B., & Brook, S. (1985). United States patent. *Geothermics*, *14*(4), 595–599. https://doi.org/10.1016/0375-6505(85)90011-2

Castillo, J. J., Cabrera, J. A., Guerra, A. J., & Simón, A. (2016). A Novel Electrohydraulic Brake System with Tire-Road Friction Estimation and Continuous Brake Pressure Control. *IEEE Transactions on Industrial Electronics*, *63*(3), 1863−1875. https://doi.org/10.1109/TIE.2015.2494041

Gajdar, T., Rudas, I., & Suda, Y. (1997). Neural Network based estimation of friction coefficient of wheel and rail. In *Proceedings of IEEE International Conference on Intelligent Engineering Systems, Proceedings, Budapest, Hungary,* 315−318. https://doi.org/10.1109/ines.1997.632437

Hussain, I. (2012). *Multiple model based real time estimation of wheel-rail contact conditions.* (PhD thesis). University of Salford. http://usir.salford.ac.uk/id/eprint/38094/

Hussain, I., Mei, T. X., & Ritchings, R. T. (2013). Estimation of wheel-rail contact conditions and adhesion using the multiple model approach. *Vehicle System Dynamics*, *51*(1), 32−53. https://doi.org/10.1080/00423114.2012.708759

Kingma, D. P., & Ba, J. L. (2015). Adam: A method for stochastic optimization. In *3rd International Conference on Learning Representations, ICLR 2015 - Conference Track Proceedings, San Diego, 1−15.* https://arxiv.org/abs/1412.6980

Li, N., Feng, X., & Wei, X. (2015). Optimized adhesion control of locomotive airbrake based on GSA-RNN. In *7th International Conference on Intelligent Human-Machine Systems and Cybernetics, Hangzhou, China*, *2*, *157−161.* https://doi.org/10.1109/IHMSC.2015.222

Malvezzi, M., Pugi, L., Papini, S., Rindi, A., & Toni, P. (2013). Identification of a wheel-rail adhesion coefficient from experimental data during braking tests. *Proceedings of the Institution of Mechanical Engineers, Part F: Journal of Rail and Rapid Transit*, *227*(2), 128−139. https://doi.org/10.1177/0954409712458490

Olofsson, U. (2009). Adhesion and friction modification. In *Wheel-Rail Interface Handbook*. Woodhead Publishing Limited. https://doi.org/10.1533/9781845696788.1.510

Polach, O. (2005). Creep forces in simulations of traction vehicles running on adhesion limit. *Wear*, *258*(7−8), 992−1000. https://doi.org/10.1016/j.wear.2004.03.046

Shah, A. A., Chowdhry, B. S., Memon, T. D., & Kalwar, I. H. (2020). Real Time Identification of Railway Track Surface Faults using Canny Edge Detector and 2D Discrete Wavelet Transform. *Annals of Emerging Technologies in Computing (AETiC), 4*(2), 53–60. https://doi.org/10.33166/AETiC.2020.02.005

Shrestha, S., Wu, Q., & Spiryagin, M. (2019). Review of adhesion estimation approaches for rail vehicles. *International Journal of Rail Transportation*, *7*(2), 79–102. https://doi.org/10.1080/23248378.2018.1513344

Spiryagin, M., Cole, C., Sun, Y. Q., McClanachan, M., Spiryagin, V., & McSweeney, T. (2014). *Design and simulation of rail vehicles.* CRC Press. https://doi.org/10.1201/b17029

Spiryagin, M., Wolfs, P. J., Cole, C., Spiryagin, V., Sun, Y. Q., & Mcsweeney, T. (2016). Theoretical investigation of the effect of rail cleaning by wheels on locomotive tractive effort. In *CORE 2016, Maintaining the Momentum, Conference on Railway Excellence, Melbourne, Victoria.* https://trid.trb.org/view/1468498

Ward, C. P., Goodall, R. M., Dixon, R., & Charles, G. A. (2012). Adhesion estimation at the wheel-rail interface using advanced model-based filtering. *International Journal Of Vehicle Mechanics and Mobility*, *50*(12), 1797–1816. https://doi.org/10.1080/00423114.2012.707782

Zhang, C., Sun, J., He, J., & Liu, L. (2017). Online Estimation of the Adhesion Coefficient and Its Derivative Based on the Cascading SMC Observer. *Journal of Sensors*, *2017*, Article ID 8419295. https://doi.org/10.1155/2017/8419295

/13/

COMPARATIVE ANALYSIS OF SUPERVISED MACHINE LEARNING ALGORITHMS FOR HEART DISEASE DETECTION

Hector Daniel Huapaya

Member of the artificial intelligence research group of the faculty of systems engineering, department of software engineering at the National University Mayor de San Marcos, Lima, (Perú).

E-mail: hector.huapaya@unmsm.edu.pe ORCID: https://orcid.org/0000-0003-3616-9046

Ciro Rodriguez

Professor at the School of Software Engineering at the National University Mayor de San Marcos, Lima, (Perú).

E-mail: crodriguezro@unmsm.edu.pe ORCID: https://orcid.org/0000-0003-2112-1349

Doris Esenarro

Professor at the Faculty of Environmental Engineering and Graduate School of the National University Federico Villarreal, Lima, (Perú).

E-mail: desenarro@unfv.edu.pe ORCID: https://orcid.org/0000-0002-7186-9614

ABSTRACT

This paper describes the most prominent algorithms of Supervised Machine Learning (SML), their characteristics, and comparatives in the way of treating data. The Heart Disease dataset obtained from Kaggle was used to determine and test its highest percentage of accuracy. To achieve the objective, Python sklearn libraries were used to implement the selected algorithms, evaluate and determine which algorithm is the one that obtains the best results, applying decision tree algorithms achieved the best prediction results.

KEYWORDS

Supervised machine learning, Heart disease, Decision tree algorithms, Prediction.

1. INTRODUCTION

Machine learning is one of the fastest-growing areas of computer science (Srivastava *et al.*, 2014), with long-range applications, which refers to the automatic detection of significant patterns in data with machine learning tools, which give programs the ability to learn and adapt.

Machine learning has become one of the pillars of information technology and, with that, a reasonably central, though generally hidden, part of our life. With the increasing amount of data available, there is a good reason to believe that intelligent data analysis will be even more widespread as a necessary ingredient for technological progress.

There are several applications for Machine Learning (ML), being one of the most important data mining (Bustamante, Rodríguez, & Esenarro, 2019). The handling of a large amount of data makes people more likely to make mistakes during analyzes or, possibly, when trying to establish relationships between multiple characteristics.

Data mining and machine learning go hand in hand with which several ideas can be derived through appropriate learning algorithms. There has been significant progress in data mining and machine learning as a result of the evolution of nanotechnology, which generated curiosity to find hidden patterns in the data to obtain results. The fusion of math and statistics, machine learning and artificial intelligence, information theory and big data, and hight processing computation, has created a reliable science, with a firm mathematical base and compelling tools.

This paper focuses on the classification of ML algorithms and the determination of the most efficient algorithm with the best accuracy and precision. In addition to establishing the performance of different algorithms in large and small datasets with one view, classify them correctly, and provide information on how to build supervised machine learning models.

2. CONCEPTUAL FRAMEWORK

2.1. CLASSIFICATION OF SUPERVISED LEARNING ALGORITHMS

Supervised machine learning algorithms deal more with the classification of data that includes the following algorithms: Linear Classifiers, Logistic Regression, Naive Bayes Classifier, Perceptron, Support Vector Machine; Quadratic classifiers, K-Means grouping, Reinforcement, Decision Tree, Random Forest (RF); Neural networks, Bayesian networks.

1) **Linear Classifiers**: Linear models for classification separate input vectors into classes using linear decision limits (hyperplane). The objective of linear classifiers in machine learning is to group elements that have similar characteristic values into groups (Ray, 2018). A linear classifier achieves this objective by making a classification decision based on the value of the linear combination of the characteristics. A linear classifier is often used in situations where classification speed is a problem since it is classified as the fastest classifier. Besides, linear classifiers often work very well when the number of dimensions is significant, as in the classification of documents, where each element is typically the number of counts of a word in a report. However, the rate of convergence between the variables in the data set depends on the margin. In general terms, the margin quantifies how linearly separable a collection of data is and, therefore, how easy it is to solve a given classification problem.

2) **Naive Bayesian Networks**: These are elementary Bayesian networks that are composed of acyclic graphs directed with a single parent (representing the unobserved node) and several children (corresponding to the observed nodes) with a strong assumption of independence between nodes children in the context of their father. Thus, the independence model (Naive Bayes) is based on the estimate. Bayes classifiers tend to be less accurate than other more sophisticated learning algorithms (such as Artificial Neural Networks). However, in a large-scale comparison of the Bayes naive classifier with state-of-the-art algorithms for decision tree induction, instance-based learning and rule induction in standard reference data sets, and discovered that it is sometimes superior to the other learning schemes, even in data sets with dependencies of substantial characteristics. The Bayes classifier has an attribute independence problem that was addressed with the average estimators of a dependence.

3) **Support Vector Machines**: This is the most recent supervised machine learning supervised technique. Support vector machine models (SVM) are closely related to classical multilayer perceptron neural networks. SVMs revolve around the notion of a "margin" on each side of a hyperplane that separates two kinds of data. It has been shown that maximizing the margin and, therefore, creating the most significant possible distance between the separation hyperplane and the instances on each side thereof reduces an upper limit on the expected generalization error.

4) **K-means**: It is one of the simplest unsupervised learning algorithms that solve the known clustering problem. The procedure follows a simple and straightforward way to classify a given set of data through a certain number of groups (suppose k groups) set a priori. The K-Means algorithm is used when tagged data is not available (Bhavsar & Ganatra, 2012). General method of conversion approximate general rules into a highly accurate prediction rule. Given the "weak" learning algorithm that you can consistently find classifiers ("general rules") at least slightly better than random, say 55% accuracy, with sufficient data, a reinforcing algorithm can build a single classifier with very high precision, say 99%.

5) **Decree Tree**: Decision trees (DT) are trees that classify instances by ordering them according to characteristic values. Each node in a decision tree represents a characteristic in an example that will be organized, and each branch represents a value that the node can assume. Instances are arranged from the root node and are sorted based on their characteristic values. The decision tree learning, used in data mining and machine learning, uses a decision tree as a predictive model that assigns observations on an element to conclusions about the objective value element.

6) **Neural Networks**: They can perform several regressions and classification tasks at the same time, although commonly, each network performs only one (Sethi *et al.*, 2019). Therefore, in the vast majority of cases, the network will have a single output variable. However, in the case of classification problems of many states, this may correspond to several output units (the post-processing stage is responsible for the assignment of output units to output variables) (Mureșan & Oltean, 2018).

2.2. CHARACTERISTICS OF MACHINE LEARNING ALGORITHMS

Supervised machine learning techniques are applicable in numerous domains. In general, Support Vector Machines and neural networks tend to work much better when it comes to multidimensional and continuous features (Agarwal & Sagar, 2019). On the other hand, logic-based systems tend to work better when it comes to discrete/categorical features. For neural network models and Support Vector Machines, the large sample size is required to achieve maximum prediction accuracy, while Bayesian networks may need a relatively small data set.

There is a general agreement that the K nearest neighbor algorithm is very sensitive to irrelevant characteristics: this characteristic can be explained by the way the algorithm works. Besides, the presence of irrelevant characteristics can make the training of the neural network very inefficient, even impractical. The most decision tree algorithms cannot work well with problems that require diagonal partitions (Sathya & Abraham, 2013). The division of the instance space is orthogonal to the axis of a variable and parallel to all other axes. Therefore, the resulting regions after separation are all hyper-angles. Artificial neural networks and support vector machines work well when multicollinearity is present, and there is a non-linear relationship between the input and output characteristics.

Naive Bayes (NB) requires little storage space during the training and classification stages: the strict minimum is the memory needed to store prior and conditional probabilities. The basic kNN algorithm uses a large amount of storage space for the training phase (Cao *et al.*, 2019), and its execution space is at least as ample as its training space. On the contrary, for all non-lazy learners, the execution space is usually much smaller than the training space, since the resulting classifier is often a very condensed summary of the data. Besides, Naive Bayes and CNN can easily be used as incremental learners, while rule algorithms cannot. Naive Bayes is naturally robust to missing values since these are ignored in the probabilities of calculation and, therefore, have no impact on the final decision. On the contrary, kNN and neural networks require complete records to do their job.

Finally, the decision trees and NB generally have different operational profiles, when one is very precise, and the other is not, and vice versa. In contrast, decision trees and rule classifiers have a similar operational profile. SVM and ANN also have a similar operational

profile. No single learning algorithm can uniformly outperform other algorithms in all data sets.

Different data sets with different types of variables and the number of instances determine the kind of algorithm that will work well (Manzoor & Singla, 2019). There is no single learning algorithm that exceeds other algorithms based on all data sets according to the free lunch theorem. The following table presents a comparative analysis of several learning algorithms.

3. METHODOLOGY

The methodology to determine the best-supervised algorithm applied in the heart disease dataset will begin with the interpretation of the data, the preprocessing of the data, and the application of the algorithms to determine the best accuracy.

A. Dataset

The dataset used for this research will be "Heart Disease" which was found in the Kaggle repository, this database contains 76 attributes, but all published experiments refer to the use of a subset of 14 of them. In particular, the Cleveland database is the only one that ML researchers have used to date. The "goal" field refers to the presence of heart disease in the patient. It has an integer value of 0 (no presence) to 4. Experiments with the Cleveland database have concentrated on the simple attempt to distinguish presence (values 1, 2, 3, 4) from absence (value 0) (Ray, 2018; Sethi *et al.*, 2019; Agarwal & Sagar, 2019).

B. Interpretation of the data

Next, the data extracted is interpreted from the empirically chosen database.
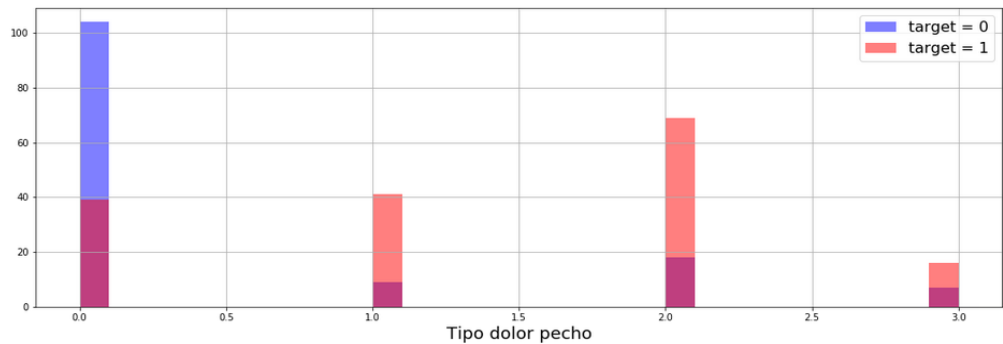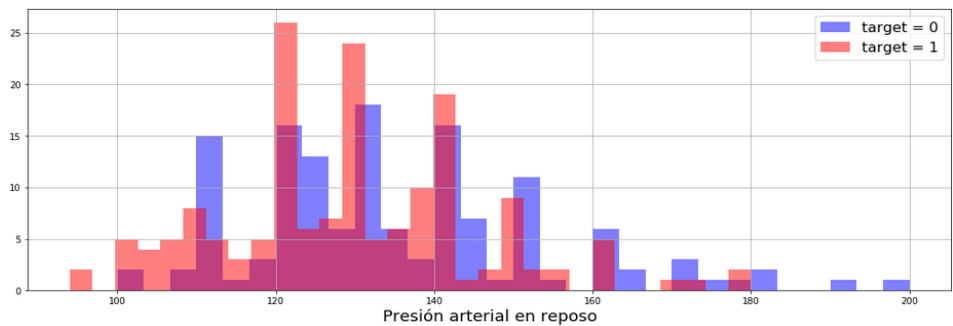

Figure 1. Type of chest pain.
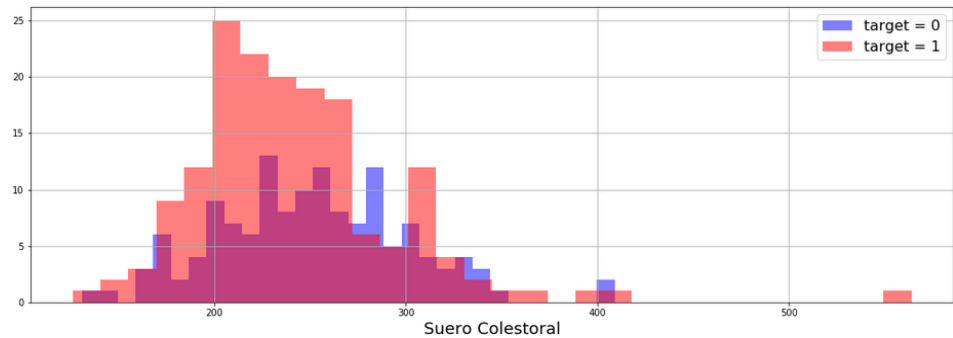
Figure 2. Resting blood pressure.
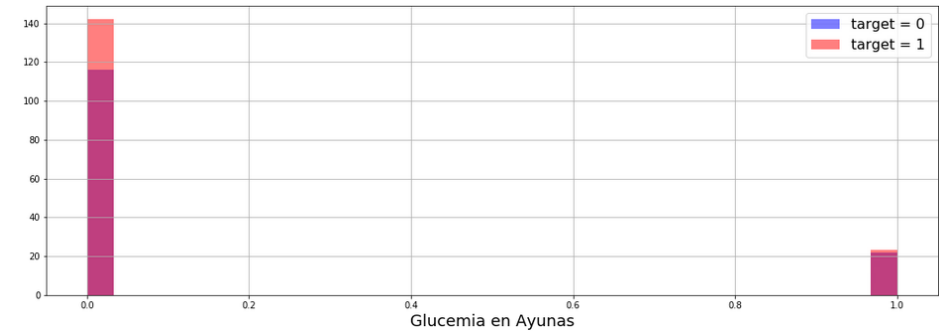

Figure 3. Serum cholesterol.
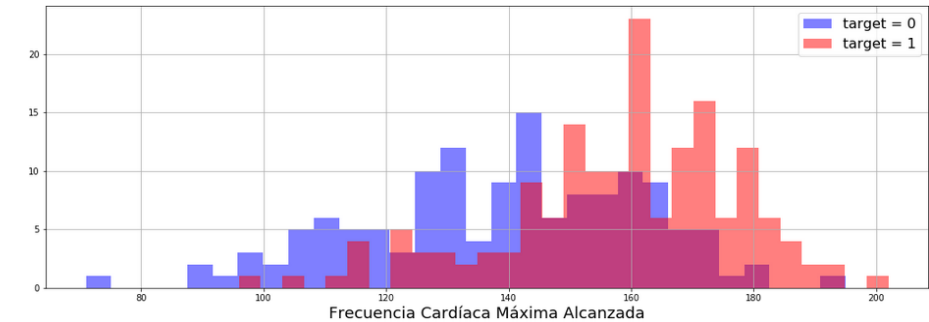

Figure 4. Fasting blood sugar.

Figure 5. Maximum heart rate reached.

From the visualization of figures 1,2,3,4, and 5 by category is possible to observe how the data are expressed, which makes it possible to detect if there is a probability of heart disease.

C. Application of algorithms

After understanding the data and interpreting the information to be generated, the following algorithms will be applied.

1. *K Nearest Neighbors (KNN)*

Because the KNN algorithm classifier predicts the class of a given test observation by identifying the observations that are closest to it, the scale of the variables is essential. Any variable that has a large scale will have a much more significant effect on the distance between the observations than the variables that are on a small scale, and therefore on the KNN classifier (Sethi *et al.*, 2019; Agarwal & Sagar, 2019; Cao *et al.*, 2019; Manzoor & Singla, 2019).

After determining the training and test data with the preprocessing processes, let's use the elbow method to choose a good value of K.
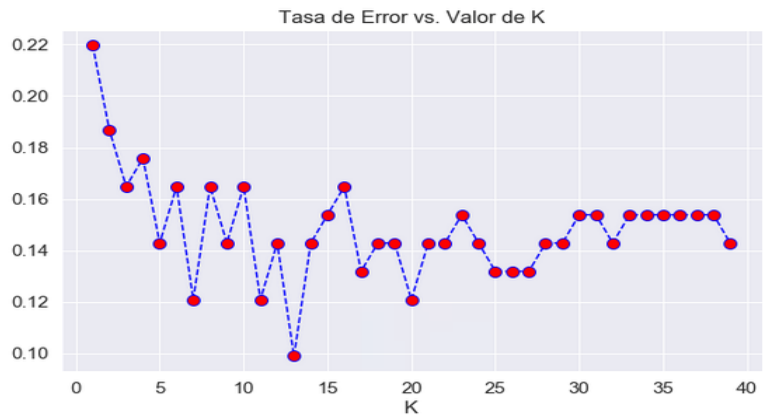

Figure 6. Error rate vs. K-value.

Here we can see the error rate after applying K = 13, let's re-enter the model with this data, and this information is reached.

1. **Decision trees:** The data is divided into a training set and a test set, then a single decision tree will be trained, using the sklearn library, to evaluate the created decision tree.

2. **Random Forest:** The data is preprocessed, and the training and test variables are separated to train the model.

3. **Neural Network:** The sklearn library will be used to preprocess the data to prepare for training.

4. **Support Vector Machines:** The data is preprocessed to apply the algorithm, the training and test variables are separated; we train the model using the sklearn library.

5. RESULTS

After applying the selected supervised learning algorithms to the dataset chosen for comparison, the following algorithm results are obtained.

A. K Nearest Neighbors (KNN)

To evaluate the model test data was used to find the confusion matrix, with which we can calculate the accuracy, precision, recall, and f1-score metrics, the following information is available:

Table 1. Result of applying the KNN algorithm.

	precision	recall	f1-score	support
0	0.95	0.84	0.89	44
1	0.87	0.96	0.91	47
micro avg	0.90	0.90	0.90	91
macro avg	0.91	0.90	0.90	91
weighted avg	0.91	0.90	0.90	91

Table 1 shows the average weight as 0.91, and the accuracy formula that is the sum of the real positives with the true negatives among the total population is applied, an accuracy of 45,614 is reached, and confusion matrix as :

```
[[37  7]
 [ 2 45]]
```

B. Decision Trees

Applying the decision tree, we get the following results.

Table 2. Result of applying the Decision Trees algorithm.

	precision	recall	f1-score	support
0	0.94	0.68	0.79	44
1	0.76	0.96	0.85	47
micro avg	0.82	0.82	0.82	91
macro avg	0.85	0.82	0.82	91
weighted avg	0.85	0.82	0.82	91

Table 2 shows the average weight as 0.85, and confusion matrix as:

```
print(confusion_matrix(y_test,predictions))

[[102   5]
 [  8  56]]
```

C. Random Forest

We evaluate the random forest model according to the data already preprocessed and trained with several estimates of 100.

Table 3. Result of applying the Random Forest algorithm.

	precision	recall	f1-score	support
0	0.84	0.73	0.78	44
1	0.77	0.87	0.82	47
micro avg	0.80	0.80	0.80	91
macro avg	0.81	0.80	0.80	91
weighted avg	0.81	0.80	0.80	91

It has an average weight of 0.81, and the confusion matrix as:

```
print(confusion_matrix(y_test,rfc_pred))

[[32 12]
 [ 6 41]]
```

D. Neural Network

Training and test data are separated, to train the model using Keras dataset, then the model will be evaluated. Figures 7 and 8 show the models.
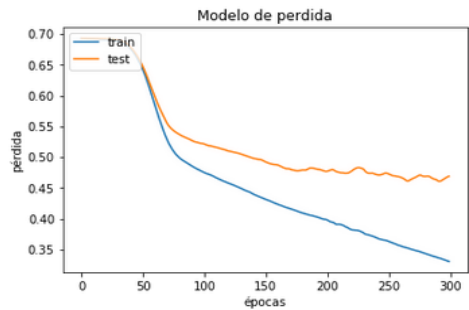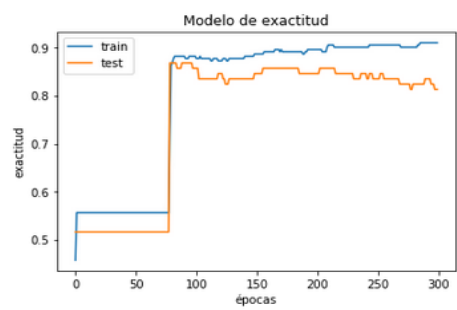

Figure 7. Loss model.

Figure 8. Accuracy model.

Table 4. Result of applying Neural Network algorithm.

```
               precision   recall  f1-score   support

           0        0.79     0.84      0.81        44
           1        0.84     0.79      0.81        47

   micro avg        0.81     0.81      0.81        91
   macro avg        0.81     0.81      0.81        91
weighted avg        0.81     0.81      0.81        91
```

Table 4 shows the weight average accuracy obtained of 0.81.

The following confusion and information matrix are obtained:

```
array([[37,  7],
       [10, 37]], dtype=int64)

print (classification_report(y_test,y_pred))
```

E. Support Vector Machines (SVM)

The model will be evaluated according to the preprocessed data, and the following is obtained, and the report classification and matrix are:

```
[[35  9]
 [ 5 42]]
```

```
print (classification_report(y_test,predictions))
```

Table 5. Result of applying Support Vector Machines algorithm.

```
                   precision    recall  f1-score   support

             0       0.88      0.80      0.83        44
             1       0.82      0.89      0.86        47

   micro avg       0.85      0.85      0.85        91
   macro avg       0.85      0.84      0.85        91
weighted avg       0.85      0.85      0.85        91
```

Table 5 shows the weighted average accuracy of 0.85.

6. CONCLUSION

As was observed in the results, the model of k nearest neighbors has obtained better results in precision with an average accuracy of 0.91 for the heart disease dataset. For future work, other types of classification or segmentation can be applied to achieve a better prediction of the chosen dataset.

ACKNOWLEDGMENTS

REFERENCES

Agarwal, R., & Sagar, P. (2019). A Comparative Study of Supervised Machine Learning Algorithms for Fruit Prediction. *Journal of Web Development and Web Designing, 4*(1), 14-18. https://zenodo.org/record/2621205#.XoRZtYgzZPY

Bhavsar, H., & Ganatra, A. (2012). A Comparative Study of Training Algorithms for Supervised Machine Learning. *International Journal of Soft Computing and Engineering (IJSCE),* *2*(4), 74-81. http://www.ijsce.org/wp-content/uploads/papers/v2i4/D0887072412.pdf

Bustamante, J. C., Rodríguez, C., & Esenarro, D. (2019). Real Time Facial Expression Recognition System Based on Deep Learning. International Journal of Recent Technology and Engineering (IJRTE), 8(2S11), 4047-4051. https://www.ijrte.org/wp-content/uploads/papers/v8i2S11/B15910982S1119.pdf

Cao, Y., Fang, X., Ottosson, J., Näslund, E., & Stenberg, E. (2019). A Comparative Study of Machine Learning Algorithms in Predicting Severe Complications after Bariatric Surgery. *Journal of Clinical Medicine, 8*(5), 668. https://doi.org/10.3390/jcm8050668

Manzoor, S. I., & Singla, J. (2019). A Comparative Analysis of Machine Learning Techniques for Spam Detection. *International Journal of Advanced Trends in Computer Science and Engineering, 8*(3), 810-814. http://www.warse.org/IJATCSE/static/pdf/file/ijatcse73832019.pdf

Mureșan, H., & Oltean, M. (2018). Fruit recognition from images using deep learning. *Acta Universitatis Sapientiae, Informatica, 10*(1), 26-42. https://www.researchgate.net/publication/321475443_Fruit_recognition_from_images_using_deep_learning

Osisanwo, F. Y., Akinsola, J. E. T., Awodele, O., Hinmikaiye, J. O., Olakanmi, O., & Akinjobi, J. (2017). Supervised Machine Learning Algorithms: Classification and Comparison. *International Journal of Computer Trends and Technology (IJCTT), 48*(3), 128-138. https://doi.org/10.14445/22312803/IJCTT-V48P126

Ray, S. (2018). *A Comparative Analysis and Testing of Supervised Machine Learning Algorithm*s. https://doi.org/10.13140/RG.2.2.16803.60967

Sathya, R., & Abraham, A. (2013). Comparison of Supervised and Unsupervised Learning Algorithms for Pattern Classification. *International Journal of Advanced Research in Artificial Intelligence (IJARAI), 2*(2). http://dx.doi.org/10.14569/IJARAI.2013.020206

Sethi, K., Gupta, A., Gupta, G., & Jaiswal, V. (2019). Comparative Analysis of Machine Learning Algorithms on Different Datasets. In *Circulation in Computer Science International Conference on Innovations in Computing (ICIC 2017), 87-91.* https://www. researchgate.net/publication/332223901_Comparative_Analysis_of_Machine_ Learning_Algorithms_on_Different_Datasets

Srivastava, N., Hinton, G., Krizhevsky, A., Sutskever, I., & Salakhutdinov, R. (2014). Dropout: A Simple Way to Prevent Neural Networks from Overfitting. *Journal of Machine Learning Research, 15*(1), 1929-1958. https://www.researchgate.net/ publication/286794765_Dropout_A_Simple_Way_to_Prevent_Neural_Networks_ from_Overfitting

/14/

EFFECT OF COVID-19 EPIDEMIC ON RESEARCH ACTIVITY OF RESEARCHER IN PAKISTAN ENGINEERING UNIVERSITY AND ITS SOLUTION VIA TECHNOLOGY

Shafiq-ur-Rehman Massan

QEC and Co-ordination

Mohammad Ali Jinnah University

Karachi, (Pakistan).

E-mail: srmassan@hotmail.com ORCID: https://orcid.org/0000-0001-6548-6513

Muhammad Mujtaba Shaikh

Department of Basic Sciences and Related Studies

Mehran University of Engineering and Technology

Jamshoro, (Pakistan).

E-mail: mujtaba.shaikh@faculty.muet.edu.pk ORCID: https://orcid.org/0000-0002-1471-822X

Abdul Samad Dahri

Business Administration and Social Sciences

Mohammad Ali Jinnah University

Karachi, (Pakistan).

E-mail: dahriabdulsamad@gmail.com ORCID: https://orcid.org/0000-0003-4517-3493

ABSTRACT

This work focuses on taking the research from impact factor to impact which means that it would propose the best interventions required at both public and private sector universities to improve the research scenario in times of emergency. The timing of this work coincides with the current corona virus pandemic and it encompasses the best practices for such an era in modern times. It proposes the requisite revamping and careful reworking of the university towards becoming a research enabler for the students at a time of crisis.

This article analyzes the effects of the Coronavirus disease on the researchers who must maintain social distance during confinement at the university and yet be able to carry out meaningful research by utilizing videoconferencing and other facilities.

KEYWORDS

Novel Coronavirus-19 (2019-NCoV) or (COVID-19), Severe Acute Respiratory Syndrome Coronavirus 2 (SARS-CoV-2), Research, Private Sector University (PRV), Public Sector University (PSU), Higher Education Commission (HEC), National Academy for Higher Education (NAHE), Research goals (RG), Video conferencing (VF), WhatsApp (WA).

1. INTRODUCTION

The corona pandemic was declared in January 2020 by the World Health Organization (WHO) (Bastola *et al.*, 2020; Li *et al.*, 2020). The WHO also shared the guidelines for meeting the requirements posed by this pandemic (World Health Organization, n.d.-a), the procedures for overcoming the overwhelming efficient human transmission of this disease are discussed in Huang *et al.* (2020China, was caused by a novel betacoronavirus, the 2019 novel coronavirus (2019-nCoV), and Lee & Hsueh (2020). The day-by-day details, situation reports and advice is enlisted in Chiodini (2020).

We have never been more prepared yet so indecisive in dealing with the corona pandemic. It pertinent that the entire humanity does not lock down all of its intellect over a single problem, we must continue to evolve in all spheres of life if we are to move ahead. Let the biologists do their job while the rest of the humanity prepares itself for many such a challenge in all other spheres of life.

Knowledge has become the cornerstone and the most important aspect of any organization (Numprasertchai & Igel, 2005). The question of producing high impact research has never been so profound as we must face such a magnanimous disease. According to international reports about 54 academic papers in English language were published about COVID-19 by 30th January 2020 and by 3rd February 2020, just 23 Chinese-language papers were contributed. When faced with such looming figures of developed nations, the response of Pakistani and South Asian countries is still far from adequate (Siddique, 2020).

The focus of research is to inculcate effective, critical, analytical and communication skills for the changing global paradigm. The current issue has placed new constraints on all sectors that must now evolve to overcome the barriers to effective mitigation. Whilst, the job sectors have to evolve with traditional jobs giving way to new and non-traditional forms of work. The manager-subordinate paradigm is also under skepticism with more direct forms of hierarchy being placed. Hence, many an employee may find himself directly reporting to the Group head or the CEO without any intermediaries. This has been possible due to the extreme specialization required at some levels of the newly evolving job structures. The depletion of the traditional manager-subordinate model the graduates have to arm themselves with new techniques and methods of being useful in the pandemic infused

millennial economy. The importance of being able to carry out work independently or to improve a certain segment of the work has never been greater.

Presently, Pakistan is undergoing the second resurgence of its education sector. The first influx of researchers from abroad has contributed to a secondary, yet meaningful second influx of local researchers. This second pool of researchers shall form the next broad base for the local proliferation of the technologies in the country. This is the time when this pool of researchers shall be tested for their worth and contribution. This work focuses on the best practices for adherence to gear-up the graduates of today and tomorrow towards meeting the challenges of facing such a pandemic and the subsequent job paradigm change.

The impact of research on government policies has never been greater as it formulates the foundations of policy. The 177 universities of Pakistan have more than 12,000 faculty members with PhD degrees and annually about 1500 PhD scholars are added to the research stream (Siddique, 2020). However, the need for external knowledge and knowledge sharing is key towards removing insular adaptations to acquire, integrate and share knowledge (Numprasertchai & Igel, 2005).

The universities must now increase productivity and efficiency through strategy and tacit knowledge (Numprasertchai & Igel, 2005). The success of today's academia shall be tested on how well they have adapted to the changing times. The interventions shall be required at the development, process, transfer, utilization, and validation of knowledge (Numprasertchai & Igel, 2005). Online teaching shall be new standard and the academia shall have to invariably change forever in this new paradigm. While the research paradigm has to shift from quantity to quality and from student grades to actual service towards humanity. Hence, the important role of ICT is stressed for knowledge proliferation and attainment of research goals (Numprasertchai & Igel, 2005).

It is all too evident that job descriptions have changed in this era of emergency, we must now work from home and at home, interaction is digital. So in this era of technology, where will the daily wage laborer go? One answer is that personification of tasks is individual while their execution is to be ensured by manual labor.

The objective of this work is to take a view point of a university's situation and formulate the areas that need improvement. This work underlines the importance and the interventions undertaken throughout Pakistan to meet the situation arising out of the Corona epidemic. This work enumerates the best practices for managing research and its timelines.

The data is analyzed for only one department and faculty. This data is not the final word on this chapter as it pertains to evaluation before the mid-semester research presentations. The situation is improving with more students opting for online methods of communication with their supervisors and for research.

A good number of recommendations have been enumerated for improving the research scenario in the present circumstances and an avid conclusion is drawn.

2. FROM IMPACT FACTOR TO IMPACT

This paper focuses on the specific aspect of creating high value research in a developing country like Pakistan where there are many financial limitations towards meaningful research. There is a general concept that the universities of Pakistan are not as well developed or have not been able to produce credible science. However, this is not true as some examples quoted here show the resilient efforts of our scientists.

The first National Center for Virology is has been envisaged at the University of Karachi at its prestigious International Center for Chemical and Biological Sciences with the collaboration of Wuhan Institute of Virology and three institutions from Germany namely Medidiagnost, Tuebingen University, and Eberhard Karls-University of Tuebingen (Siddique).

Researchers from the Mehran University of Engineering and Technology have designed a fully automated ventilator. Whereas the UET Lahore is also pursuing this cause of designing ventilators with great fervor and zeal through the Higher Education Commission's RAPID Research and Innovation grant (Siddique, 2020).

The National University of Science and Technology has developed coronavirus diagnostic KITS at cost effective prices with high accuracy and sensitivity. The price of this kit is deemed to be one-fourth as compared to a foreign kit. The NUST Atta-ur-Rahman School

of Applied Biosciences (ASAB) has successfully developed Molecular Diagnostic Assays for the detection of (2019-nCoV). These kits have been developed in collaboration with Armed Forces Institute of Pathology (AFIP) Rawalpindi, in collaboration with Columbia University USA, DZIF Germany, and Wuhan Institute of Virology China. These kits are field tested and reliable (Siddique, 2020).

In another recent development, the Punjab University has also a low-price kit for Coronavirus diagnosis at its center of Excellence in Molecular Biology. The price of conducting the test on this kit is a mere 5 USD or 800 PKR only. The university plans to develop thousands of kits within a week for the benefit of the masses (Siddique, 2020).

The universities of Pakistan have adapted well to the changing paradigm of 'flipping the classes'; this term was coined by Salman Khan of the world renowned Khan academy. The online classes paradigm has been accepted countrywide and high quality instruction is being carried out at all major universities around the country (Siddique, 2020).

The role of the Higher Education Commission as the catalyst and benefactor of many funded researches going on in the country cannot be denied. The HEC Rapid research initiative is one such method that has been devised to meet the urgent needs of the country (Higher Education Comission, 2020b).

The HEC has also put forward its guidelines for the universities for online teaching and these are available at (Higher Education Comission, 2020a). However, the modus operandi for conducting and orchestrating research remotely has still to be formulated.

The HEC has defined two methods to meet the present situation either ("HEC asks universities to start online teaching", 2020),

1) The universities must remain closed till May 31 and treat this period as summer vacation or,

2) The universities must resort to online teaching and utilize the publicly available platforms such as Teams etc.

The HEC has stressed that the quality of instruction must not be compromised in these online interactions ("HEC asks universities to start online teaching", 2020). The HEC

is also establishing an National Knowledge Bank (NKB) for providing online access to a range of materials and lectures etc. ("HEC asks universities to start online teaching", 2020). Moreover, the best online tutorials and materials shall be gathered by the National Academy for Higher Education (NAHE) ("HEC asks universities to start online teaching", 2020).

3. MANAGING RESEARCH

3.1. OBJECTIVES

The work describes the best practices for proliferation of research geared towards meaningful output in times of pandemic or emergency.

From the literature at hand and from the experience gained it is evident that the universities need to react fast in these times to take the research to world-class standards. A research policy that has to be thought out and implemented by letter and spirit.

From the experience of the research work submitted it can be concluded that most of the research work shows that short term measures have taken precedence over long term gains. Past projects show that definite goals have not been set and lip service has been done on the completion of short term research projects. Research is not the top priority of the students who must understand that improving the current scenario at every level is the key to success in every challenge that they must face in life.

The economic costs of indecisiveness and short term tenures of previous research team will culminate into unstructured and below standard publications unless corrected at this juncture.

The universities with semester system have mainly three types of research credits i.e.,

1) 3 credits that must be completed in one semester for the undergraduate students

2) 6 credits which must be completed in one or two semesters for the graduate students and

3) 30 credits for PhD students that must be completed in chunks of 6 credits.

Thus the universities have the burden to minimize the human contact while conducting meaningful research in these times.

3.2. RESEARCH FRAMEWORK FOR UNIVERSITIES

There are three distinct levels or layers of work involved in managing a university wide research network and are described as under,

A. Policy framework layer

All the requirements of policy level and the setting out of the goals under the university vision and mission are the responsibility at this layer. The Director of the Research Division reports and sets out the goals for his department to be attained during the course of the year in the Academic Council held earlier. These goals have to be tracked, met and the reasons for any shortfall defined in the upcoming AC meeting.

The primary objective of this layer is to ensure that the deadlines are endorsed by the relevant AC meeting at the beginning of the year. This is because a wide disparity is seen in department's perspectives on when to collect the research works and when to conduct the viva etc.

B. Management framework layer

All the management tasks and adherence to the timelines are to be ensured at this level. This is to be managed by the Deputy Director/Manager of research at the university level.

C. Human layer

All the human interaction tasks and contacts with the relevant departments are to be performed at the is layer This layer may be headed by an Assistant Manager who would ensure that the human side of things are amicably managed.

4. MANAGING THE TIMELINES

It is proposed to adhere to the following timelines in principle,

1) Registration of research credits should be done normally at the beginning of the semester.

2) Research meeting should be held at the beginning of the first week, preferable first Sunday after the commencement of the classes.

3) Selection of research supervisors should be completed at the end of the third week.

4) Selection of research titles and the students should stick to this title till the end of the semester. This should be ideally completed by the end of the third week.

5) Submission of Chapters 1, 2 and 3 should be completed by early seventh week.

6) Mid-term evaluation should be conducted by the end of the seventh week.

7) Preview copy or spiral copy should be submitted by fourteenth week.

8) Final presentation should be held online by the end of the sixteenth week.

9) Hardbound copies should be submitted by the end of the seventeenth week.

5. METHODOLOGY

This study emanates from the authors knowledge and experience and encompasses all the best practices for the promulgation of a research centered mindset at the university level.

For the prevention of bias in this research, the recommendations and the results were peer-reviewed by a senior researcher. The recommendations for the research units pertain to Bio-Sciences, Business Administration, Computer Science and Engineering.

To also remove the bias the evaluation levels for the Supervisor, Externals and Internals should be set with the following recommendations,

1) Timely submission on deadlines – 20% marks allocated by the research unit

2) Midterm – Internal 10%, Supervisor 10%

3) Final term – Supervisor 30%, External 30%

It is also recommended to have two layers of corrections, one at the content level by the internals and the other to view the formatting of the final thesis to be done by the respective library division.

Minimal human to human interaction should be observed with all manual submissions handled with proper care or through mail. Sanitization of all surfaces and contacts are to be ensured.

6. DATA ANALYSIS

The data was analyzed for one faculty at a prominent university and it was found that initially out of 18 research faculty, almost 16% have been successful in developing contact with research candidates without any compromise on the time lapse in the time university was off. On the other hand, out of 17 students registered to these 16% supervisors, 41% have successfully kept the project on track and have been completing assignments and progressing in their research work, whereas 59% are yet to maintain facilities to continue their work.
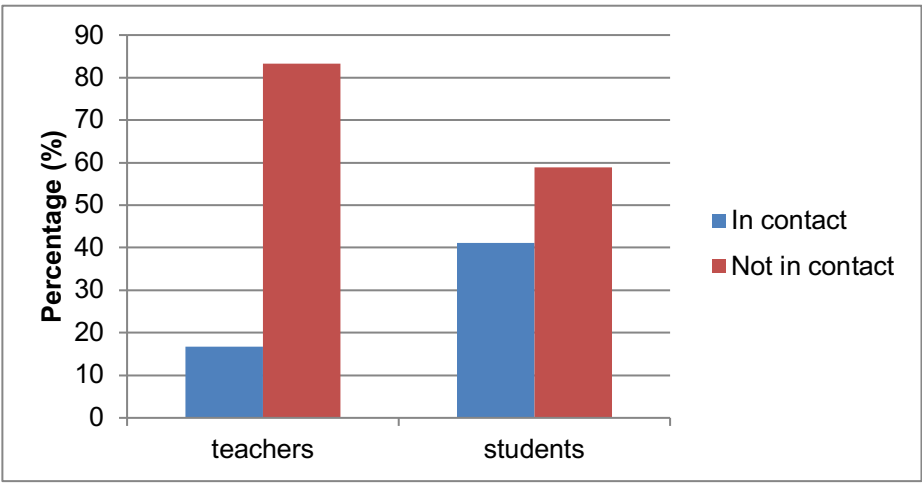
Figure 1. The percentage of supervisors and research candidates whether in active contact or not from March 07, 2020 to April 06, 2020.

In the event of successful contact of supervisors with the candidates, so far 28 active contacts have been reported online. The mode of contact was mostly through WhatsApp and mobile calls since the research projects of masters and doctorate level have one candidate registered per topic. 89% of the established online meetings have been through WhatsApp and calls, whereas 11% of the times zoom meetings were used for detailed discussion and analysis of results.

However, the situation is yet to improve following a very strict follow-up by the university authorities so that each and every student is able to complete his research on time. In this regard the mid-term presentations are to be held online and the record maintained on a google sheet. The video presentations shall be saved for assessment and regulatory authorities.
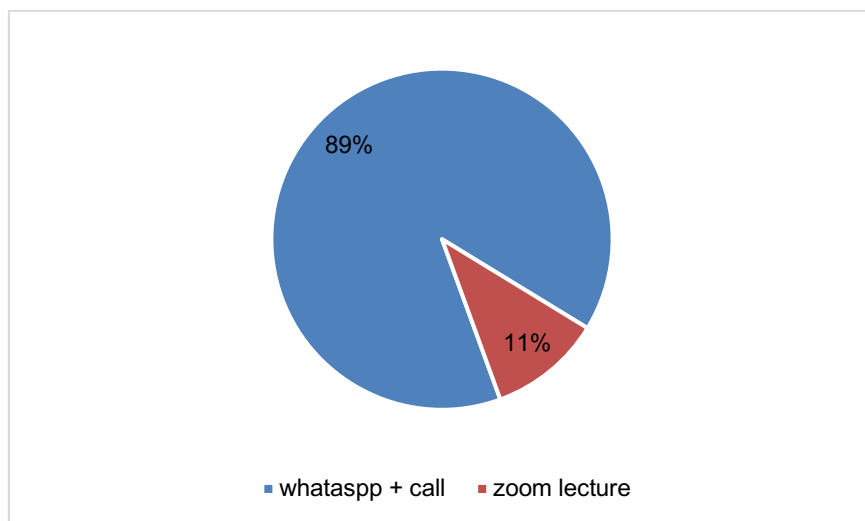

Figure 2. Mode of contact in the active online meetings.

It was noticed that the predominant mode of contact was through Telecom and WhatsApp and a minority of students were approached through Zoom software.

7. RECOMMENDATIONS

There are many recommendations that can be submitted in view of this pandemic. However, the main outlines are as follows. In principle the research entity / institution is geared up towards these guidelines,

1) Appointment of a focal person to guide and manage all research related activities at the university level.

2) All people entering the university premises must wear masks, apply sanitizer and be screened for body temperature (Chen, Pradhan, & Xue, 2020) with a focus on early screening and detection (Alburikan & Abuelizz, 2020).

3) All infected people are advised rest, medical care or appropriate home care (Zhang *et al.*, 2020) and need to recover before attempting to undertake research at the university.

4) To apply safety and health guidelines that have been proposed by the World Health Organization (World Health Organization, n.d.-b; Ronco, Navalesi, & Vincent, 2020; Jansson, Liao, & Rello, 2020).

5) Gain experience of professional management of research activities particularly assessment methods.

6) To reduce academic losses due to lack of focus and co-ordination amongst the students. To particularly manage the chaos and un-certainty of the Coronavirus era.

7) Integrated software and platform for managing the student information and various complex interactions such as change of supervisor and change of thesis title.

8) Formulation of standard SOP's and formats for establishment of clear chain of command.

9) Grade visibility to the student at different levels.

10) Availability of standard templates for assessment of various theses.

11) Marks distribution to be well known to the students in advance.

12) To initiate online presentations for creating industry exposure and linkages.

13) To invite current research from the industry and on the Coronavirus pandemic through forward looking office of industrial liaison.

14) Enactment of an online students' rights council on WhatsApp for paper writing.

15) Online thesis formatting help to be extended to the students during the semester.

16) Online workshops and presentations on different software packages that are utilized in research such as reference managers and SPSS, SmartPLS, MATLAB, Minitab etc.

17) Online Workshops and sessions known as work-at-homes to be held to help the students finish their theses in time and with collaboration.

18) To manage and mitigate the effects of any panic like situation or eventuality and to ensure emergency readiness at all quarters.

19) And the last but not the least to improve the one to one interaction between the students and the supervisors through online modes of interaction.

8. CONCLUSION

It has been concluded in various studies that more invasive quarantines and adept social distancing will be required to mitigate the effects of the Coronavirus COVID-19 pandemic (Elmousalami & Hassanien, n.d.). Hence, the value of the above recommendations is pertinent with an end to overcome the present global pandemic.

Continuity of good practices, effective command, clear and lucid communication of instructions is to be ensured at all levels. The validity and reliability of all results and examination methods also have to be ensured since most interaction is online. The standard of evaluation has to rise at a higher level to meet this situation.

ACKNOWLEDGEMENT

REFERENCES

Alburikan, K. A., & Abuelizz, H. A. (2020). Identifying factors and target preventive therapies for Middle East Respiratory Syndrome sucsibtable patients. *Saudi Pharmaceutical Journal, 28*(2), 161–164. https://doi.org/10.1016/J.JSPS.2019.11.016

Bastola, A., Sah, R., Rodriguez-Morales, A. J., Lal, B. K., Jha, R., Ojha, H. C., Shrestha, B., Chu, D. K. W., Poon, L. L. M., Costello, A., Morita, K., & Pandey, B. D. (2020). The first 2019 novel coronavirus case in Nepal. *The Lancet Infectious Diseases, 20*(3), 279–280. https://doi.org/10.1016/S1473-3099(20)30067-0

Chen, Y., Pradhan, S., & Xue, S. (2020). What are we doing in the dermatology outpatient department amidst the raging of the 2019 novel coronavirus? *Journal of the American Academy of Dermatology, 82*(4), 1034. https://doi.org/10.1016/J.JAAD.2020.02.030

Chiodini, J. (2020). Maps, masks and media − Traveller and practitioner resources for 2019 novel coronavirus (2019-nCoV) acute respiratory virus. *Travel Medicine and Infectious Disease, 33,* 101574. https://doi.org/10.1016/J.TMAID.2020.101574

Elmousalami, H. H., & Hassanien, A. E. (n.d.). *Day Level Forecasting for Coronavirus Disease (COVID-19) Spread: Analysis, Modeling and Recommendations.* Cornell University. arXiv:2003.07778.

HEC asks universities to start online teaching. (2020, March 30). The News International. https://www.thenews.com.pk/print/636738-hec-asks-universities-to-start-online-teaching

Higher Education Comission. (2020a). *HEC Covid-19 guidance* 1-4. https://hec.gov.pk/english/Pages/Covid-19-Guidance.aspx

Higher Education Comission. (2020b). *RAPID Research and Innovation Initiative (RRII).* https://www.hec.gov.pk/english/services/RnD/RRIF/Pages/default.aspx

Huang, C., Wang, Y., Li, X., Ren, L., Zhao, J., Hu, Y., Zhang, L., Fan, G., Xu, J., Gu, X., Cheng, Z., Yu, T., Xia, J., Wei, Y., Wu, W., Xie, X., Yin, W., Li, H., Liu, M., … & Cao, B. (2020). Clinical features of patients infected with 2019 novel coronavirus in Wuhan, China. *The Lancet, 395*(10223), 497−506. https://doi.org/10.1016/S0140-6736(20)30183-5

Jansson, M., Liao, X., & Rello, J. (2020). Strengthening ICU health security for a coronavirus epidemic. *Intensive and Critical Care Nursing, 57,* 102812. https://doi.org/10.1016/J.ICCN.2020.102812

Lee, P.-I., & Hsueh, P.-R. (2020). Emerging threats from zoonotic coronaviruses-from SARS and MERS to 2019-nCoV. *Journal of Microbiology, Immunology and Infection.* https://doi.org/10.1016/J.JMII.2020.02.001

Li, J., Li, J. (Justin), Xie, X., Cai, X., Huang, J., Tian, X., & Zhu, H. (2020). Game consumption and the 2019 novel coronavirus. *The Lancet Infectious Diseases, 20*(3), 275−276. https://doi.org/10.1016/S1473-3099(20)30063-3

Numprasertchai, S., & Igel, B. (2005). Managing knowledge through collaboration: multiple case studies of managing research in university laboratories in Thailand. *Technovation, 25*(10), 1173–1182. https://doi.org/10.1016/j.technovation.2004.03.001

Ronco, C., Navalesi, P., & Vincent, J. L. (2020). Coronavirus epidemic: preparing for extracorporeal organ support in intensive care. *The Lancet Respiratory Medicine, 8*(3), 240–241. https://doi.org/10.1016/S2213-2600(20)30060-6

Siddique, M. A. (2020, April 1). *Where Pakistani universities stand.* Daily Times. https://dailytimes.com.pk/586590/where-pakistani-universities-stand/

World Health Organization. (n.d.-a). *Infection prevention and control during health care when COVID-19 is suspected.* https://www.who.int/emergencies/diseases/novel-coronavirus-2019/technical-guidance/infection-prevention-and-control

World Health Organization. (n.d.-b). *WHO guidelines on hand hygiene in health care: first global patient safety challenge – clean care is safer care.* Geneva. https://www.who.int/gpsc/5may/tools/who_guidelines-handhygiene_summary.pdf

Zhang, J., Zhou, L., Yang, Y., Peng, W., Wang, W., & Chen, X. (2020). Therapeutic and triage strategies for 2019 novel coronavirus disease in fever clinics. *The Lancet Respiratory Medicine, 8*(3), e11–e12. https://doi.org/10.1016/S2213-2600(20)30071-0

/15/

USABILITY OF EGOVERNANCE APPLICATION FOR CITIZENS OF PAKISTAN

Abdul Samad Dahri

Business Administration and Social Sciences

Mohammad Ali Jinnah University, Karachi, (Pakistan).

E-mail: dahriabdulsamad@gmail.com ORCID: https://orcid.org/0000-0003-4517-3493

Shafiq-ur-Rehman Massan

QEC and Co-ordination

Mohammad Ali Jinnah University, Karachi, (Pakistan).

E-mail: srmassan@hotmail.com ORCID: https://orcid.org/0000-0001-6548-6513

Ayaz Ali Maitlo

Department of Business Administration,

University of Sindh, Larkana Campus, (Pakistan).

E-mail: ayazalimaitlo@gmail.com ORCID: https://orcid.org/0000-0001-9831-8380

ABSTRACT

eGovernance is a vital component of any nations' modern governmental structure and suitable for mass-scale adaptation. Pakistan has also established an eGovernance council for mitigation of the problems of the common man. One big step in this direction is the establishment of Pakistan Citizens' Portal (PCP) that facilitates eGovernance. Through the PCP app, citizens can directly lodge complaints and report their issues for immediate resolution.

This study looks at the important aspect of mobile usability through field tests to determine the viability of the PCP app in Pakistan. This study is vital towards determining the main factors for large scale adaptation of the PCP app and underlines the weaknesses of the present system.

Hence, the PCP app was evaluated in terms of efficiency and effectiveness according to ISO 92421-11. And the user satisfaction was measured through system usability satisfaction (SUS) on five-point Likert scale. The evaluation method included more than a dozen citizens of Sindh and findings showed that overall application enriched the user experience. However, the few areas of PCP were identified as needing improvements. The main areas that the PCP application needs to improve are the areas of registration and 'findability' which would further improve user satisfaction and experience.

KEYWORDS

1. INTRODUCTION

eGovernance is the most recent trend of governance worldwide. Proper implementation of eGovernance requires SMART (Simple, Moral, Accountable, Responsive and Transparent) work ethic (Mehra & Prabhu, 2013). The advent of information communication technology (ICT) has infused a new sphere of governmental intervention. The issues of the citizens are now being handled by eGovernance.

UNESCO defines eGovernance as the application of ICT towards participatory decision making hence improving information and service delivery (Obi, 2007). Similarly, with the advent of time the quality and type of services required by the common man in Pakistan is changing. Presently, the government is facing a challenge to manage the vast requirements of health, education travel, credit, security and documentation (Javaid & Arfeen, 2017).

eGovernance process is a fairly recent trend globally. It helps improve interaction within the civil society by improving the processes of the government, interconnecting the citizens, and building viable interactions within society (Brown, *et al.* 2013). Though, literature reveals misconception regarding the difference between traditional and eGovernance, where, eGovernance appears to simply add more electronic devices to governance rather than cumbersome paper based work. Therefore, to change perception and practices, government needs to integrate technology with feasible policy change in the system (Arfeen, Khan, & Amanullah, 2012).

According to united nations eGovernance survey, Pakistan was placed at 137 in 2003 out of 139 countries which declined to 146 in the year 2010 and further to 156 in 2012. There could be many factors to this decline, but the problem of Pakistan is not the lack of resources but bad governance (Rais, 2019). Even though, from layman of Asia to future tiger of Asia, needs bold steps by the government of Pakistan (Ministry of Planning, Development & Reform Government of Pakistan, 2020). Yet, lethargic bureaucracy and lack of accountability left government helpless and leads inefficiencies in the system towards implementation of solutions to citizen problems and complaints.

Effective eGovernance implementation utilizes internet to provide of value added public services to civil society as per OECD (Ubaldi, 2009). eGovernance therefore needs

connectivity of digital devices to deliver solutions and improve citizen lives (United Nations Conference on Trade and Development, 2009). Mobile devices have become more user friendly and useful and allow the users greater flexibility to perform more tasks. Another advantage is that mobile network signals cover 85% of the international population and 80% of these are smartphones users (Chaffey, 2016). Similarly, in Pakistan 2G mobile covers nearly 90% of population (PTA annual report 2014-2015). While, 57% of rural and urban population have smartphones (Rizvi, 2018). This highlights penetration of mobile technology and indicates untapped eGovernance intervention potential in Pakistan. Therefore, eGovernance through mobile application holds the future for efficient and quality solutions of mitigation of citizen complaints.

Capitalizing over mobile access, current government tapped true potential and launched eGovernance Pakistan Citizens' Portal (PCP) mobile application 2018. This initiative is first of its kind in the history of Pakistan. This app providing access of 70,000 government offices to citizens at a single click and was recognized as 2nd best app in Global Summit held in Dubai February 2019. Moreover, 1.173 million users including overseas, and local citizens got registered. 553,125 complaints were lodged, and 509,153 complaints were resolved making rate of 92% including the provinces of Khyber Pakhtunkhwa, Sindh, Islamabad, Baluchistan and Azad Kashmir. While, Sindh provincial government was worst at 40% in terms of complaint resolution and even worse at 84% for complaints pending rate (News Desk, 2019).

On contrary, according to Furlow (2012), 95% of mobile applications are not field tested. Since PCP mobile application is a new phenomenon in Pakistan, its independent field testing is essential for upgrades by product developers. Similarly, the past literature on mobile application usability comprises of surveys or literature reviews rather field evaluation (Dahri, Al-Athwari, & Hussain, 2019). This study serves the purpose of field evaluation of PCP mobile application usability evaluation tests. Indeed, mobile usability evaluation test reveals the quality of how users adapt and utilize it and assess its actual field performance.

According to Coursaris and Kim (2011), mobile usability evaluation test is vital for smartphone users enabling the design of user friendly applications and determines success of the product (Baharuddin, Singh, & Razali, 2013). In simple words, mobile usability

evaluation test facilitates users of the technology to achieve their specific tasks with ease (Coursaris & Kim, 2011).

2. USER ASSESSMENT

The participants were requested to perform a few simple tasks enlisted below:

1) Registering themselves with the system (Figure 1),

2) Application home screen usability (Figure 2)

3) Searching for relevant department (Figure 3)

4) Lodging a complaint (Figure 4),

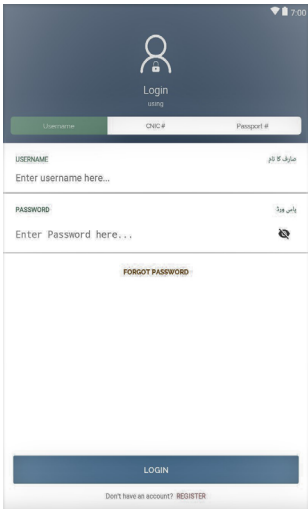5) Feedback (Figure 5),

6) ISO 9241-11 Usability framework (Figure 6)

Figure 1. Registering themselves with the system.
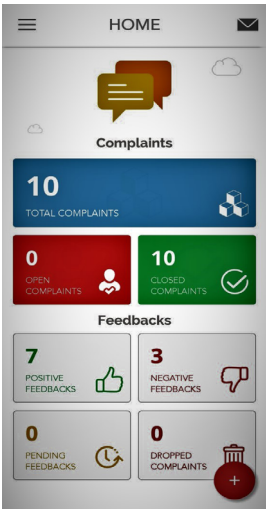
Figure 2. Application home screen usability.
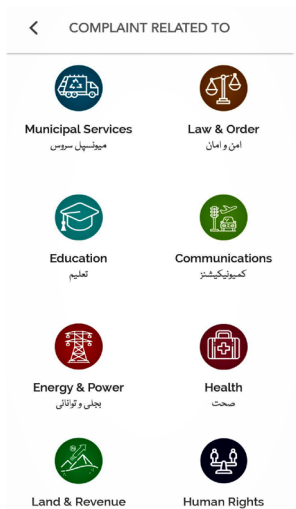
Figure 3. Searching for relevant department.
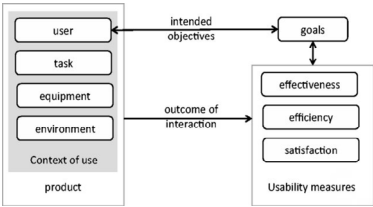
Figure 5. Feedback

Figure 6. ISO 9241-11 Usability framework.

3. MEASURES AND METHODS

Quantitative usability design is provided by ISO-9241-11 (see Figure 6) that outlines user metrics with step by step implementation (UCD). The most common usability test is the typical task performance to measure effectiveness of the application, i.e. to what extent the user is able to achieve his desired goals. While efficiency is the level of resources and the amount of effort required by the user to attain accuracy and completeness of his desired goal. And last but not the least satisfaction or discontent is measurable by experiencing his acceptable usability level during the performance of a task.

Effectiveness as well as efficiency during interaction with the application may be measured by evaluating the completion of the given tasks and by counting the number of errors in user's attempt. Efficiency is to be measured by the resources and the efforts undertaken to achieve the desired task. Likewise, for general assessment of PCP, satisfaction is measured with system usability scale (SUS) which was developed and designed by Brooke in 1996 consist of 10 items on a Likert scale of 0-4 during the experience of the user interaction with the mobile application. We have utilized SUS in this study for validity, reliability and sensitivity scores that range from a mere 0 to about 100. The SUS score of 50 or below is

considered to be poor, above 70 to be in the good range and while 85 or greater score is considered to be excellent (Bangor, Kortum, & Miller, 2009).

The statistical methods used in this paper may be referenced from Shaikh, Massan and Wagan (2015), Memon and Shaikh (2016), Shaikh, Memon and Hussain (2016), Arain, Shaikh and Shaikh (2017), Khowaja *et al.* (2019), Shaikh, Massan and Wagan (2019), Soomro *et al.* (2019) and Sultan, Shaikh and Chowdhry (2020).

4. RESULTS

The number of participants were 15 from Hyderabad city of Sindh province as complaint resolution was the lowest from Sindh province of Pakistan. Most (70%) of the participants were middle aged adults (30-40), 30% of the participants ranged between 20-29 years of age, 70% of them had attained some education at college level and all used smartphones.

4.1. EFFECTIVENESS

Task 1 and 3 were recorded difficult having a total of 35% and 46% failure rates respectively. Task 4 and 5 were completed in the absence of any errors. Task 2 accumulated largest errors by participants and took more time. The kinds of error were:

1) Difficulty to remember steps of the procedure.

2) Department options and typically.

3) Complaint resolution information was repeated.

4.2. EFFICIENCY

Table 1 reveals that task 1 (Getting registered with the system), 2 (Application home screen usability), and 3 (Searching for relevant department) consumed more time due to expected difficulty and errors as well as had higher mean time. On the other hand, task 4 (Lodging a complaint) and 5 (Feed Back) consumed less mean time as that of task 1, 2, and 3.

Table 1. Time taken for each task per task.

S.No	Task 1	Task 2	Task 3	Task 4	Task 5
Mean	4.21	3.95	4.01	2.58	1.89
(SD)	(0.97)	(0.55)	(0.69)	(1.09)	(1.91)

4.3. SATISFACTION

The average SUS scores for the group was recorded at 85. This score indicates a sound satisfaction level across these PCP users. However, is a quite wide variation in scores of satisfaction that ranged from 62 to as high as 92 (at 30- point range). It was observed that 60 to 74 is a good rating and higher was excellent and under acceptable region where most of the participants' satisfaction scores were noticed.
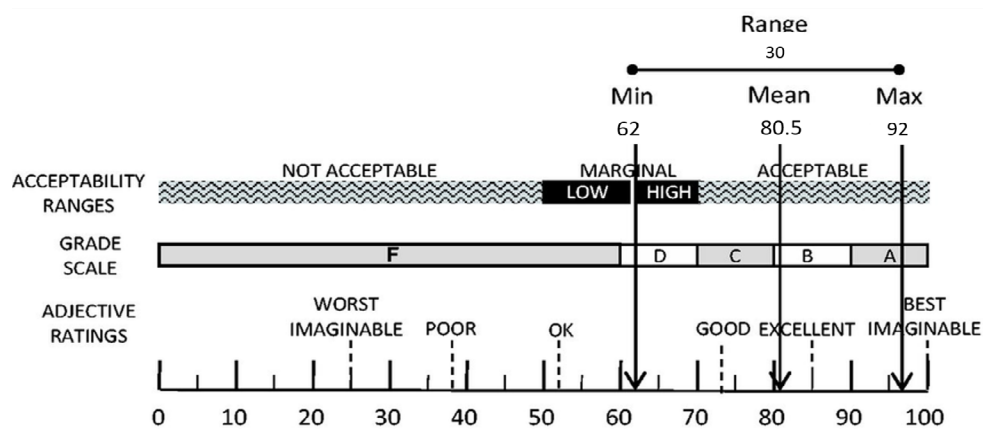

Figure 7. Variation in scores of satisfaction.

The tasks were based on the given guidelines of ISO for real time citizen interaction with application and validation. An error was reported whenever any user failed to complete any given task. The efficiency was estimated by measuring the average time utilized by a user towards the completion of each task from beginning to the successful completion. The evaluation of satisfaction score was done by measuring the SUS and the scores calculated by the use of guidelines of Brooke. The descriptive statistical data was obtained by the use of SPSS version 25.

5. INTERPRETATION

The interpretation of Task Performance, results, satisfaction and demographic trends show that task 1 (getting registered) and 3 (searching for relevant department) had most errors, was considered difficult and time consuming. These issues might arise due to lack of application comprehensiveness as, even task 1 (getting registered) took time of users though over several portals getting registered is routine task. However, overall user satisfaction was

excellent. The results also indicate areas of improvement. Such as, multiple registration options, over informed grid on home screen and repetition of information regarding complaint resolution.

The demography of participants revealed that male participants were slightly more informed and performed better than female participants on SUS scores. Similarly, younger participants took less time and made few errors in task 1 and 3.

6. RECOMMENDATIONS

The study results tender some recommendations that might advance the experience and enhance the user satisfaction as follows:

1) User menu must be in list format.

2) Icon must illustrate departments included.

3) Registration process should follow less steps.

4) Application home screen should be user friendly.

5) Illiterate portion of citizens should also be considered.

6) Colors should be vivid and should match with actual logo of each department.

7. CONTRIBUTIONS TO LITERATURE

This is one of the foremost usability studies on the PCP application in the province of Sindh in Pakistan. It has addressed the issues of effectiveness, efficiency, and satisfaction by using validated scores are recommended by (Lyles, Sarkar, & Osborn, 2014). This study utilizes and validates ISO designed usability standards of the SUS instrument towards the comparison of usability metrics and performance. This study bridges the present gap within the literatures of usability and helps identifying eGovernance improvement criteria of government of Pakistan. Following (Coursaris & Kim, 2011) this study also contributes to understanding of demography and technology interaction in Pakistan's society and its influence on usability performance. The scores may be utilized to design future interventions

for capturing the target population quickly and effectively. Hence, this study highlights main issued in the PCP application that must be removed to make it a successful and viable tool.

8. CONCLUSION

The study findings show that most of the users had good perceived usability satisfaction and only one-third of the users were rated as possessing little or poor usability. The results can be utilized by the developers objectively to design the necessary corrections in the PCP application. The objectivity of the results indicates the mismatch between the developer perception and the user experience which must be bridged.

ACKNOWLEDGEMENT

REFERENCES

Arain, S., Shaikh, F., & Shaikh, M. M. (2017). Problem of Traffic Congestion and Correlation Analysis of Driving behaviors in Qasimabad, Hyderabad. *Mehran University Research Journal of Engineering and Technology*, *36*(1), 139–148. https://trid.trb.org/view/1442479

Arfeen, M. I., Khan, N., & Amanullah, M. (2012). Public Sector Innovation through e-Governance in Pakistan. *Life Science*, *9*(3), 1226–1233. http://www.lifesciencesite.com/lsj/life0903/174_9492life0903_1226_1233.pdf

Baharuddin, R., Singh, D., & Razali, R. (2013). Usability dimensions for mobile applications-a review. *Research Journal of Applied Sciences, Engineering and Technology*, *5*(6), 2225–2231. https://doi.org/10.19026/rjaset.5.4776

Bangor, A., Kortum, P., & Miller, J. (2009). Determining what individual SUS scores mean: Adding an adjective rating scale. *Journal of Usability Studies*, *4*(3), 114–123. http://citeseerx.ist.psu.edu/viewdoc/download?doi=10.1.1.177.1240&rep=rep1&type=pdf

Brown, W., Yen, P.-Y., Rojas, M., & Schnall, R. (2013). Assessment of the Health IT Usability Evaluation Model (Health-ITUEM) for evaluating mobile health (mHealth) technology. *Journal of Biomedical Informatics*, *46*(6), 1080–1087. https://doi.org/10.1016/J.JBI.2013.08.001

Chaffey, D. (2016). *Mobile marketing statistics compilation*. https://doi.org/10.15358/9783800653140-121

Coursaris, C. K., & Kim, D. J. (2011). A meta-analytical review of empirical mobile usability studies. *Journal of Usability Studies*, *6*(3), 117–171. http://uxpajournal.org/wp-content/uploads/sites/8/pdf/JUS_Coursaris_May_2011.pdf

Dahri, A. S., Al-Athwari, A., & Hussain, A. (2019). Usability Evaluation of Mobile Health Application from AI Perspective in Rural Areas of Pakistan. *International Journal of Interactive Mobile Technologies*, *13*(11), 213–225. https://doi.org/10.3991/ijim.v13i11.11513

Furlow, B. (2012, November 2). *mHealth apps may make chronic disease management easier*. Clinical Advisor. https://www.clinicaladvisor.com/home/features/mhealth-apps-may-make-chronic-disease-management-easier/

Javaid, M., & Arfeen, M. (2017). *Impact of eGovernment on Citizen Satisfaction: A Case of Federal Government Agencies in Pakistan*, 221–237. https://doi.org/10.1007/978-3-319-65930-5_19

Khowaja, A., Mahar, M. H., Lashari, H. N., Wasi, S., & Massan, S.-R. (2019). Personality Evaluation of Student Community using Sentiment Analysis. *Nternational Journal of Computer Science & Network Security (IJCSNS)*, *19*(3), 167–180. https://www.researchgate.net/publication/332395067_Personality_Evaluation_of_Student_Community_using_Sentiment_Analysis

Lyles, C. R., Sarkar, U., & Osborn, C. Y. (2014). Getting a technology-based diabetes intervention ready for prime time: a review of usability testing studies. *Current Diabetes Reports*, *14*(10), 534. https://doi.org/10.1007/s11892-014-0534-9

Mehra, K., & Prabhu, C. S. R. (2013). *E-Governance: Concepts and Case Studies* : ix. PHI Learning Private Limited.

Memon, A. J., & Shaikh, M. M. (2016). Confidence bounds for energy conservation in electric motors: An economical solution using statistical techniques. *Energy*, *109*, 592–601. https://doi.org/10.1016/J.ENERGY.2016.05.014

Ministry of Planning, Development & Reform Government of Pakistan. (2020). *Pakistan 2025. One Nation - One Vision.* https://www.pc.gov.pk/uploads/vision2025/Pakistan-Vision-2025.pdf

News Desk. (2019, October 3). *PTI govt takes lead in citizens' complaint resolution*. The Express Tribune. https://tribune.com.pk/story/2071030/1-pti-govt-takes-lead-citizens-complaint-resolution/

Obi, T. (2007). *E-governance: A Global Perspective on a New Paradigm* (p. 27). IOS Press.

Rais, R. B. (2019). Citizens Portal: Improving governance through technology. Retrieved November 21, 2019, from http://arabnews.pk/node/1587581

Rizvi, J. (2018, November 9). *Pakistan's urban-rural mobile ownership divide set to close soon, study shows.* The News. https://www.thenews.com.pk/print/391338-pakistan-s-urban-rural-mobile-ownership-divide-set-to-close-soon-study-shows

Shaikh, M. M., Massan, S.-R., & Wagan, A. I. (2015). A new explicit approximation to Colebrook's friction factor in rough pipes under highly turbulent cases. *International Journal of Heat and Mass Transfer*, *88*, 538–543. https://doi.org/10.1016/j.ijheatmasstransfer.2015.05.006

Shaikh, M. M., Massan, S.-R., & Wagan, A. I. (2019). A sixteen decimal places' accurate Darcy friction factor database using non-linear Colebrook's equation with a million nodes: A way forward to the soft computing techniques. *Data in Brief*, *27*, 104733. https://doi.org/10.1016/J.DIB.2019.104733

Shaikh, M. M., Memon, A. J., & Hussain, M. (2016). Data on electrical energy conservation using high efficiency motors for the confidence bounds using statistical techniques. *Data in Brief*, *8*, 529–535. https://doi.org/10.1016/J.DIB.2016.06.004

Soomro, M. A., Memon, S. A., Shaikh, M. M., & Channa, A. (2019). Indoor air CO2 assessment of classrooms of educational institutes of hyderabad city and its comparison with other countries. In *AIP Conference Proceedings*, *2119*(1), 020014. AIP Publishing LLC. https://doi.org/10.1063/1.5115373

Sultan, M., Shaikh, M. M., & Chowdhry, N. P. (2020). Comparative Analysis of Knee Joint Replacement and Stem Cells Therapy Treatment for Knee Osteoarthritis Using Statistical Techniques. *Research in Medical and Engineering Sciences*, *8*(4), 887–897. https://crimsonpublishers.com/rmes/pdf/RMES.000693.pdf

Ubaldi, B. (2009). *OECD e-Government Studies: Rethinking e-Government Services; User-Centred Approaches.* www.oecd.org/gov/egov/services

United Nations Conference on Trade and Development. (2009). *Information Economy Report 2009, Trends and Outlook in Turbulent Times*. United Nations. https://unctad.org/en/Docs/ier2009_en.pdf

/16/

EXTENDED KALMAN FILTER FOR ESTIMATION OF CONTACT FORCES AT WHEEL-RAIL INTERFACE

Khakoo Mal

PhD Scholar, Department of Electronic Engineering,
Mehran University of Engineering and Technology, Jamshoro, (Pakistan).
E-mail: 17phdiict05@students.muet.edu.pk ORCID: https://orcid.org/0000-0002-5754-0441

Imtiaz Hussain

Associate Professor, Electrical Engineering.
DHA Suffa University. Karachi, (Pakistan).
E-mail: imtiaz.hussain@dsu.edu.pk ORCID: https://orcid.org/0000-0002-7947-9178

Bhawani Shankar Chowdhry

Professor Emeritus.
Mehran University of Engineering and Technology. Jamshroo, (Pakistan).
E-mail: bhawani.chowdhry@faculty.muet.edu.pk ORCID: https://orcid.org/0000-0002-4340-9602

Tayab Din Memon

Associate Professor, Department of Electronics.
Mehran University of Engineering and Technology. Jamshoro, (Pakistan).
E-mail: tayabdin82@gmail.com ORCID: https://orcid.org/0000-0001-8122-5647

ABSTRACT

The wheel-track interface is the most significant part in the railway dynamics because the forces produced at wheel-track interface governs the dynamic behavior of entire vehicle. This contact force is complex and highly non-linear function of creep and affected with other railway vehicle parameters. The real knowledge of creep force is necessary for reliable and safe railway vehicle operation. This paper proposed model-based estimation technique to estimate non-linear wheelset dynamics. In this paper, non-linear railway wheelset is modeled and estimated using Extended Kalman Filter (EKF). Both wheelset model and EKF are developed and simulated in Simulink/MATLAB.

KEYWORDS

Railway dynamics, Wheel-rail interface, Model-based estimation, Extended Kalman Filter.

1. INTRODUCTION

The main element of any study of rolling stock behavior is the wheel-track interaction patch (Simon, 2006). All the forces which help and direct the railway vehicle transmit via this narrow area of contact and knowing of the nature of these forces is most important for any investigation of the generic railway vehicle behavior (Melnik & Koziak, 2017).

The Wheel-track condition information can be detected in real time to provide traction and braking control schemes for re-adhesion. For example, in Charles, Goodall and Dixon (2008) an indirect technique based on Kalman Filter (KF) is proposed for the estimation of low adhesion with wheel-track profile by using conicity and wheel-rail contact forces. A method using Kalman filter has also been introduced in Mei, Yu and Wilson (2008) and Hussain and Mei (2009) to identify the slip after evaluating the torsional frequencies in the axle of wheelset. Two indirect monitoring schemes using a bank of Kalman filters are proposed for (i) wheel slip detection and, (ii) real time contact condition and adhesion estimation in Hussain and Mei (2010, 2011). In Hussain, Mei and Ritchings (2013) and Ward, Goodall and Dixon (2011), the development of techniques based on Kalman-Bucy filter proposed for the estimation of wheel-track interface conditions in real time to predict the track and wheel wear, the development of rolling contact fatigue and any regions of adhesion variations or low adhesion.

However, due to nonlinear nature of wheel-rail dynamic behavior, Kalman-Bucy filter is difficult to use for entire operating conditions. A method using Heuristic non-linear contact model and Kalker's linear theory is proposed in Anyakwo, Pislaru and Ball (2012) for modeling and simulation of dynamic behavior of wheel-track interaction in order to discover the shape of interaction patch and for obtaining the tangential interaction forces generated in wheel-rail interaction area. On the basis of measurement of traction motor's parameters, (i) creep forces can be predicted by means of Kalman filter between roller and wheel (Zhao, Liang & Iwnicki, 2012) and (ii) slip-slide is detected and estimated by using Extended Kalman Filter (EKF) (Zhao & Liang, 2013).

A system based on two different processing methods, i.e., model-based approach using Kalman-Bucy filter and non-model based using direct data analysis, is presented for on-board indirect detection of low adhesion condition in Hubbard *et al.* (2013a, 2013b).

However, the technique using yaw acceleration as a normalization method provides only a rough estimate and introduces a huge delay to obtain an estimate. A model-based technique using Unscented Kalman Filter (UKF) is proposed by Zhao *et al.* (2014) for estimation of creep, creep forces as well as friction coefficient from the behavior of traction motor. However estimators seem unreliable in some critical track conditions, hence still work is needed to monitor these wheel-rail parameters more effectively in real time.

A system based on the principles of synergetic control theory is proposed in Radionov and Mushenko (2015) to estimate adhesion moment in wheel-track contact point. Two-dimensional inverse wagon model based on acceleration is developed in Sun, Cole and Spiryagin (2015) for evaluation and monitoring of wheel-rail contact dynamics forces. The results at higher speed are agreeable, however improvement in the model is further needed to reduce the error at all expected speeds. Another technique using multi-rate EKF state identification is presented in Wang *et al.* (2016) for detection of slip velocity by merging the multi-rate technique and Extended Kalman filter technique to identify the load torque of traction motor. On the basis of fitting non-linear model, EKF can also be applied to identify the wheel-track interaction forces and moments that takes into account the interface nonlinearities (Strano & Terzo, 2018).

After reviewing the literature on condition monitoring of railway wheelset dynamics, it is observed that the problem to analyze wheelset conditions and update them to desired situation still needs to be improved in order to accomplish the expectation of railway vehicle to be really high speed, high comfort, more safer and economical means of transport across the world.

In this paper, Extended Kalman filter is designed for non-linear railway wheelset model to estimate lateral velocity and yaw rate of wheelset as well as creep and creep force. Polach formulae for creep force and friction coefficient are used in modeling of non-linear wheelset. Both modeling of non-linear wheelset and designing of EKF are done in Simulink/MATLAB.

2. MODELING OF NON-LINEAR WHEELSET

The motion of a railway vehicle is directed by interaction forces produced at wheel-track contact, which change non linearly with respect to creepage and are affected by the unpredictable variations in the adhesion conditions (Hussain, 2012). A single solid-axle wheelset shown in Figure 1 is taken for modeling and estimation of wheel-rail conditions.

Figure 1. Railway wheelset [captured by author during field visit].

The creepages (the relative speed of the wheel to rail) of right and left wheels of wheels in longitudinal direction are expressed in following equations.

$$\gamma_{xR} = \frac{(r_0\omega_R - v)}{v} - \frac{L_g\Psi'}{v} - \frac{\omega_R\lambda_w(y - y_t)}{v} \tag{1}$$

$$\gamma_{xL} = \frac{(r_0\omega_L - v)}{v} - \frac{L_g\Psi'}{v} - \frac{\omega_L\lambda_w(y - y_t)}{v} \tag{2}$$

The main objective of this paper is to develop a state of art technique to detect the changes in wheel-rail contact conditions. The term $\frac{(r_0\omega_R - v)}{v}$ in equations (1) and (2) does not involve lateral and yaw dynamics, hence can be excluded in simplified longitudinal creep equations because only yaw and lateral dynamics are sufficient for detecting these changes. Further , so the simplified creep equations used in above model become as:

$$\gamma_{xR} = -\frac{L_g\Psi'}{v} - \frac{\lambda_w(y - y_t)}{r_0} \tag{3}$$

$$\gamma_{xL} = -\gamma_{xR} = \frac{L_g\Psi'}{v} + \frac{\lambda_w(y - y_t)}{r_0} \tag{4}$$

The creepages in lateral direction are expressed as:

$$\gamma_{yR} = \gamma_{yL} = \gamma_y = \frac{y'}{v} - \Psi \tag{5}$$

While in equations (6) total creep of the wheels is depicted.

$$\gamma_{i = \sqrt{\gamma_{ji}^2 + \gamma_{ji}^2}} \tag{6}$$

As the wheel-rail contact forces govern railway vehicle's dynamics are creep forces and are the function of creeps. The adhesion coefficient is the ratio of tangential force that is creep force to normal force and hence is also a function of creep. Figure 2 illustrates a classic nonlinear change of the adhesion coefficient with respect to creepage for all track conditions i.e. dry, wet, poor and worst conditions.
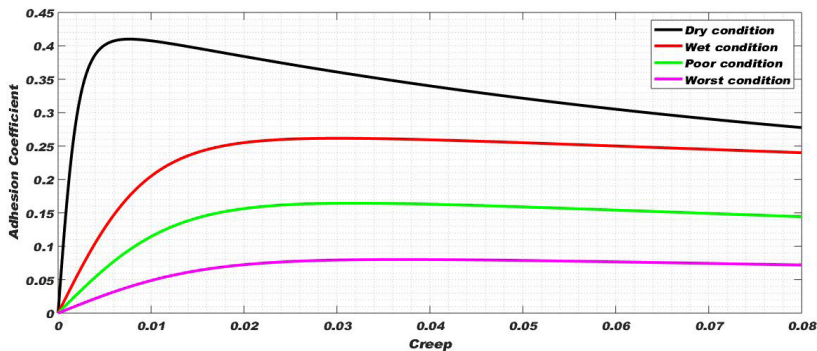
Figure 2. Creep v/s Adhesion Coefficient for all conditions of wheel-rail interface.

Following equations illustrate creep forces and adhesion coefficient.

$$F_{ji} = \frac{F_i \gamma_{ji}}{\gamma_i} \tag{7}$$

i = Right and left wheels, j = longitudinal and lateral directions

F_i is the total creep force and can be calculated by Polach formula (Polach, 2005).

$$F = \frac{2NU}{}\left[\frac{k_A}{1+(k_A)^2} + \arctan(k_S)\right] \tag{8}$$

Where U is friction coefficient, is gradient of the tangential stress in area of adhesion, k_A is reduction factor in the area of adhesion and is the reduction factor in slip. Both U and are illustrated as:

$$U = u_0\left[(1-A)e^{(-B\gamma v)} + A\right] \tag{9}$$

Where u_0 is maximum friction coefficient at zero creep velocity, A is ratio of friction coefficient at infinity creep velocity to u_0 and B is coefficient of exponential friction decrease.

$$= \frac{2}{3}\frac{a^2bc}{NU}\gamma \tag{10}$$

While a and b are half-axes of contact ellipse and c is coefficient of contact shear stiffness in N/m³.

$$\mu = \frac{F}{N} \tag{11}$$

The equations of motion of railway wheelset at any point of creep curve of Figure 2 are expressed as (Hussain and Mei, 2009):

$$M_v x'' = F_{xR} + F_{xL} \tag{12}$$

$$m_w y'' = -F_{yR} - F_{yL} + F_C \tag{13}$$

$$I_w \Psi'' = F_{xR}L_g - F_{xL}L_g - K_w\Psi \tag{14}$$

$$T_s = K_s\theta_s + C_S(\omega_R - \omega_L) \tag{15}$$

$$I_L\omega'_L = T_s - T_L \tag{16}$$

$$I_R\omega'_R = T_m - T_s - T_R \tag{17}$$

Where $\theta_s = \int(\omega_R - \omega_L)dt$

F_C is centripetal force component and can be neglected when vehicle does not run in curves and C_S is material damping of shaft which is normally very small. Hence both terms are not considered in this research.

In Table 1 detailed information of all parameters used in simulated wheelset model is given.

Table 1. Parameters used in modeling on non-linear wheelset.

No.	Symbol	Parameter	Value	Unit
1	γ_{xR}	Right wheel creep in longitudinal direction	calculated	ratio
2	γ_{xL}	Left wheel creep in longitudinal direction	calculated	ratio
3	γ_{yR}	Right wheel creep in lateral direction	calculated	ratio
4	γ_{yL}	Left wheel creep in lateral direction	calculated	ratio
5	γ_R	Total creep of right wheel	calculated	ratio
6	γ_L	Total creep of left wheel	calculated	ratio
7	r_0	Wheel radius	0.5 (constant)	m
8	L_g	Half gauge of track	0.75 (constant)	m
9	λ_w	Wheel conicity	0.15 (constant)	rad
10	ω_L	Angular velocity of left wheel	calculated	rad/sec
11	ω_R	Angular velocity of right wheel	calculated	rad/sec
12	v	Vehicle's forward velocity	calculated	m/sec
13	y	Lateral displacement	Output	m
14	y_t	Track disturbance in lateral direction	input	m
15	Ψ	Yaw angle	output	rad
16	F_{xR}	Right wheel creep force in longitudinal direction	calculated	Newton
17	F_{xL}	Left wheel creep force in longitudinal direction	calculated	Newton
18	F_{yR}	Right wheel creep force in lateral direction	calculated	Newton
19	F_{yL}	Left wheel creep force in lateral direction	calculated	Newton
20	F_R	Total creep force of right wheel	calculated	Newton
21	F_L	Total creep force of left wheel	calculated	Newton
22	μ	Adhesion coefficient between track and wheel	calculated	ratio
23	N	Normal load on wheel	constant	Newton
24	M_v	Vehicle mass	15000 (constant)	Kg
25	I_w	Yaw moment of inertia of wheelset	700 (constant)	Kgm^2
26	K_w	Yaw stiffness	5×10^6 (constant)	N//rad
27	m_w	Wheel weight with induction motor	1250 (constant)	Kg
28	v_0	Vehicle's forward velocity at initial	input	m/sec
29	ω_0	Angular velocity of wheelset at initial	input	Rad/sec
30	T_m	Torque of traction motor	input	Nm
31	T_s	Torsional torque	calculated	Nm
32	T_R	Traction torque on right wheel	calculated	Nm

No.	Symbol	Parameter	Value	Unit
33	T_L	Traction torque on left wheel	calculated	Nm
34	I_R	Right wheel inertia	134 (constant)	Kgm^2
35	I_L	Left wheel inertia	64 (constant)	Kgm^2
36	K_s	Torsional stiffness	6063260 (constant)	N/m
37	θ_s	Twist angle	calculated	rad

3. DESIGNING OF EXTENDED KALMAN FILTER FOR ESTIMATING NON-LINEAR WHEELSET MODEL

Being non-linear nature of railway wheelset model, it is difficult to estimate the wheelset dynamics with ordinary estimation techniques. Therefore Extended Kalman filter is used to estimate wheelset dynamics and contact force in all adhesion conditions. Kalman filter utilizes measurements associated to the state and error covariance matrices to produce a gain known as Kalman gain. Figure 3 shows the block diagram of Kalman filter with generic scheme.
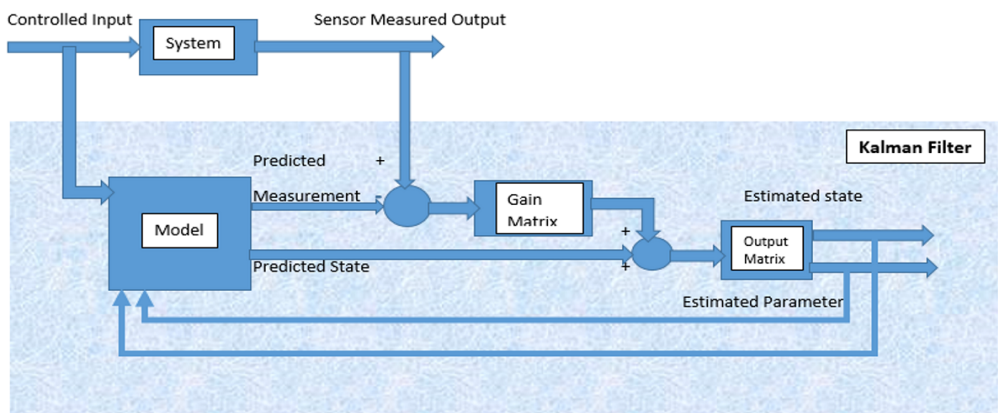
Figure 3. Block diagram of the Kalman filter with generic scheme.

Extended Kalman filter (the extension form of Kalman filter) linearizes the current mean and covariance by assessing Jacobian matrices and their partial derivatives (Ngigi *et al.*, 2012)

From non-linear model of railway wheelset, single equation (18) in matrix form is furnished after putting the values of F_{xR}, F_{xL}, F_{yR} and F_{yL} in equations (13) and (14).

$$
\begin{bmatrix} y' \\ \Psi' \\ y'' \\ \Psi'' \end{bmatrix} = \begin{bmatrix} 0 & 0 & 1 & 0 \\ 0 & 0 & 0 & 1 \\ 0 & \dfrac{1}{m_w}\left(\dfrac{F_R}{\gamma_R}+\dfrac{F_L}{\gamma_L}\right) & -\dfrac{1}{m_w v}\left(\dfrac{F_R}{\gamma_R}+\dfrac{F_L}{\gamma_L}\right) & 0 \\ -\dfrac{L_g \lambda_w}{I_w r_0}\left(\dfrac{F_R}{\gamma_R}+\dfrac{F_L}{\gamma_L}\right) & -\dfrac{k_w}{I_w} & 0 & -\dfrac{L_g^{\,2}}{I_w v}\left(\dfrac{F_R}{\gamma_R}+\dfrac{F_L}{\gamma_L}\right) \end{bmatrix} \begin{bmatrix} y \\ \Psi \\ y' \\ \Psi' \end{bmatrix} + \begin{bmatrix} 0 \\ 0 \\ 0 \\ \dfrac{L_g}{I_w r_0}\left(\dfrac{F_R}{\gamma_R}+\dfrac{F_L}{\gamma_L}\right) \end{bmatrix} y_t \quad (18)
$$

If left and right wheel creep are same ($\gamma_R = \gamma_L = \gamma$ and $F_R = F_L = F$) then

$$
\begin{bmatrix} y' \\ \Psi' \\ y'' \\ \Psi'' \end{bmatrix} = \begin{bmatrix} 0 & 0 & 1 & 0 \\ 0 & 0 & 0 & 1 \\ 0 & \dfrac{2}{m_w}\dfrac{F}{\gamma} & -\dfrac{2}{m_w v}\dfrac{F}{\gamma} & 0 \\ -\dfrac{2L_g \lambda_w}{I_w r_0}\dfrac{F}{\gamma} & -\dfrac{k_w}{I_w} & 0 & -\dfrac{2L_g^{\,2}}{I_w v}\dfrac{F}{\gamma} \end{bmatrix} \begin{bmatrix} y \\ \Psi \\ y' \\ \Psi' \end{bmatrix} + \begin{bmatrix} 0 \\ 0 \\ 0 \\ \dfrac{2L_g}{I_w r_0}\dfrac{F}{\gamma} \end{bmatrix} y_t \quad (19)
$$

Here are state variables of wheelset model i.e y'(lateral velocity), Ψ' (Yaw rate) γ (Creep or slip), U (friction coefficient) and F (Creep force) taken for EKF algorithm. Lateral acceleration (y'') and yaw rate (Ψ'') can be measured along noise with accelerometer and gyroscope. From equation (19):

$$
y'' = \left(y'\right)' = \frac{2}{m_w}\left(\Psi\frac{F}{\gamma} - \frac{y'}{v}\frac{F}{\gamma}\right) \tag{20}
$$

$$
\Psi'' = \left(\Psi'\right)' = \frac{1}{I_w}\left(\frac{2y_t L_g}{r_0}\frac{F}{\gamma} - \frac{2y L_g \lambda_w}{r_0}\frac{F}{\gamma} - \frac{2\Psi' L_g^{\,2}}{v}\frac{F}{\gamma} - K_w\Psi\right) \tag{21}
$$

$$
\gamma = \sqrt{\left(\frac{L_g \Psi'}{v} + \frac{\lambda_w\left(y - y_t\right)}{r_0}\right)^2 + \left(\frac{y'}{v} - \Psi\right)^2} \tag{22}
$$

$$
U_k = u_0[(1-A)e^{(-B\gamma v)} + A] \tag{23}
$$

$$
F = \frac{2NU}{}\left[\frac{k_A}{1+(k_A)^2} + \arctan\left(k_S\right)\right] \tag{24}
$$

Now it is required to discretize equations (20)-(24) by using Forward Euler (FE) method in order to design Extended Kalman filter for estimation.

$$y'_k = y'_{k-1} + \frac{2\tau}{m_w}\left(\Psi \frac{F_{k-1}}{\gamma_{k-1}} - \frac{y'_{k-1}}{v}\frac{F_{k-1}}{\gamma_{k-1}}\right) \tag{25}$$

$$\Psi'_k = \Psi'_{k-1} + \frac{\tau}{I_w}\left(\frac{2y_t L_g}{r_0}\frac{F_{k-1}}{\gamma_{k-1}} - \frac{2yL_g\lambda_w}{r_0}\frac{F_{k-1}}{\gamma_{k-1}} - \frac{2\Psi'_{k-1}L_g^2}{r_0}\frac{F_{k-1}}{\gamma_{k-1}} - K_w\Psi\right) \tag{26}$$

$$\gamma_k = \sqrt{\left(\frac{L_g\Psi'_{k-1}}{v} + \frac{\lambda_w(y-y_t)}{r_0}\right)^2 + \left(\frac{y'_{k-1}}{v} - \Psi\right)^2} \tag{27}$$

$$U_k = u_0[(1-A)e^{(-B\gamma_{k-1}v)} + A] \tag{28}$$

$$F_k = \frac{2NU_{k-1}}{}\left[\frac{k_A\frac{2}{3}\frac{a^2bc}{NU_{k-1}}\gamma_{k-1}}{1+(k_A\frac{2}{3}\frac{a^2bc}{NU_{k-1}}\gamma_{k-1})^2} + \arctan\left(k_S\frac{2}{3}\frac{a^2bc}{NU_{k-1}}\gamma_{k-1}\right)\right] \tag{29}$$

As the Extended Kalman filter uses a 2 step predictor-corrector algorithm (Welch & Bishop, 2001). The predictor step is given by

$$\hat{x}_k^- = f\left(\hat{x}_{k-1}, u_k, k\right) \tag{30}$$

$$P_k^- = F_{k-1}P_{k-1}F_{k-1}^T + Q_k \tag{31}$$

And the equations of corrector step are,

$$K_k = P_k^- H_k^T\left(H_k P_k^- H_k^T + R_k\right)^{-1} \tag{32}$$

$$\hat{x}_k = \hat{x}_k^- + K_k\left(\tilde{y}_k - h\left(x^{\hat{}-}_k, u_k, k\right)\right) \tag{33}$$

$$P_k = \left(I - K_k H_k\right)P_k^- \tag{34}$$

Where f and h are non-linear functions relating to process and measurement states, while:

$$F_k = \frac{\partial f}{\partial x}\Big|\hat{x}_k, u_k, k \ \text{ and } \ H_k = \frac{\partial h}{\partial x}\Big|\hat{x}_k, u_k, k$$

Nomenclature of EKF algorithm is given in below table.

Table 2. Nomenclature of EKF algorithm.

Symbol	Description
x⁻k	discretized a-priori estimated process
x⁻k	discretized a-postriori estimated process
Pk-	a-priori estimate of the covariance of process error
Pk	estimate of the covariance of measurement error
Fk	Jacobian matrix of process
Hk	Jacobian matrix of measurement
Qk	process noise covariance
Rk	measurement noise covariance
Kk	Kalman gain
ỹk	measured output

The Jacobean matrix of process matrix:

$$x_k = \begin{bmatrix} y'_k \\ \Psi'_k \\ \gamma_k \\ U_k \\ F_k \end{bmatrix} \ \text{is}$$

$$F_k = \begin{bmatrix}
\dfrac{\partial y'_k}{\partial y'_k} & \dfrac{\partial y'_k}{\partial \psi'_k} & \dfrac{\partial y'_k}{\partial \gamma_k} & \dfrac{\partial y'_k}{\partial U_k} & \dfrac{\partial y'_k}{\partial F_k} \\[2ex]
\dfrac{\partial \psi'_k}{\partial y'_k} & \dfrac{\partial \psi'_k}{\partial \psi'_k} & \dfrac{\partial \psi'_k}{\partial \gamma_k} & \dfrac{\partial \psi'_k}{\partial U_k} & \dfrac{\partial \psi'_k}{\partial F_k} \\[2ex]
\dfrac{\partial \gamma_k}{\partial y'_k} & \dfrac{\partial \gamma_k}{\partial \psi'_k} & \dfrac{\partial \gamma_k}{\partial \gamma_k} & \dfrac{\partial \gamma_k}{\partial U_k} & \dfrac{\partial \gamma_k}{\partial F_k} \\[2ex]
\dfrac{\partial U_k}{\partial y'_k} & \dfrac{\partial U_k}{\partial \psi'_k} & \dfrac{\partial U_k}{\partial \gamma_k} & \dfrac{\partial U_k}{\partial U_k} & \dfrac{\partial U_k}{\partial F_k} \\[2ex]
\dfrac{\partial F_k}{\partial y'_k} & \dfrac{\partial F_k}{\partial \psi'_k} & \dfrac{\partial F_k}{\partial \gamma_k} & \dfrac{\partial F_k}{\partial U_k} & \dfrac{\partial F_k}{\partial F_k}
\end{bmatrix} \qquad (35)$$

And the Jacobian matrix of measurement matrix $m_k = \begin{bmatrix} y''_k \\ \Psi'_k \end{bmatrix}$ is

$$H_k = \begin{bmatrix} \dfrac{\partial y''_k}{\partial y'_k} & \dfrac{\partial y''_k}{\partial \Psi'_k} & \dfrac{\partial y''_k}{\partial \gamma_k} & \dfrac{\partial y''_k}{\partial U_k} & \dfrac{\partial y''_k}{\partial F_k} \\ \dfrac{\partial \Psi'_k}{\partial y'_k} & \dfrac{\partial \Psi'_k}{\partial \Psi'_k} & \dfrac{\partial \Psi'_k}{\partial \gamma_k} & \dfrac{\partial \Psi'_k}{\partial U_k} & \dfrac{\partial \Psi'_k}{\partial F_k} \end{bmatrix} \tag{36}$$

4. SIMULATION RESULTS

The simulation models of non-linear railway wheelset and EKF are developed in Simulink/ MATLAB and are simulated 50 microseconds step size. As the vehicle is kept on constant velocity i.e. motor torque is applied zero, only random track disturbance of ±7mm magnitude in lateral direction is applied as input to the model for exciting lateral dynamics. Curves of Figure 2 are tuned with Polach parameters k_A, k_S, u_0, A and B. Table 3 contains the values which are used to tune these creep curves. Along with Kalman gain and Jacobian matrices, the other EKF tuning parameters are measurement noise covariance of inertial sensors and process noise covariance for entire range of track conditions which are set in equation (37)-(40). The measurement noise covariance matrix in equation (37) is calculated by adding noise power for accelerometer and gyro sensor, while the process noise matrices of equations (38)-(40) are calculated based on fine tuning of results.

$$R = [1x10^{-7} \ 1x10^{-13}] \tag{37}$$

$$Q1 = [5x10^{-14} \ 1x10^{-14} \ 1x10^{-14} \ 1x10^{-14} \ 1x10^{-14}] \text{ for dry condition} \tag{38}$$

$$Q2 = [0.5x10^{-12} \ 9x10^{-17} \ 1x10^{-12} \ 1x10^{-12} \ 1x10^{-12}] \text{ for wet condition} \tag{39}$$

$$Q3 = Q4 = [1x10^{-13} \ 9x10^{-17} \ 1x10^{-12} \ 1x10^{-12} \ 1x10^{-12}] \text{ for poor and worst condition} \tag{40}$$

Table 3. Polach parameters.

Parameter	Dry condition	Wet condition	Poor condition	Worst condition
kA	1	1	1	1
kS	1	1	1	1
u0	0.46	0.3	0.2	0.1
A	0.4	0.4	0.1	0.1
B	0.6	0.2	0.2	0.2

Following tests are performed on wheelset with EKF algorithm.

(i) Dry condition, (ii) Wet condition, (iii) Poor condition, (iv) Worst condition and (v) Transition from dry condition to worst condition.

4.1. DRY CONDITION TEST

The lateral velocity and yaw rate of wheelset as well as creep and creep force are computed along with error on dry condition curve (Dry curve of Figure 2) and shown in Figure 4 to 7.
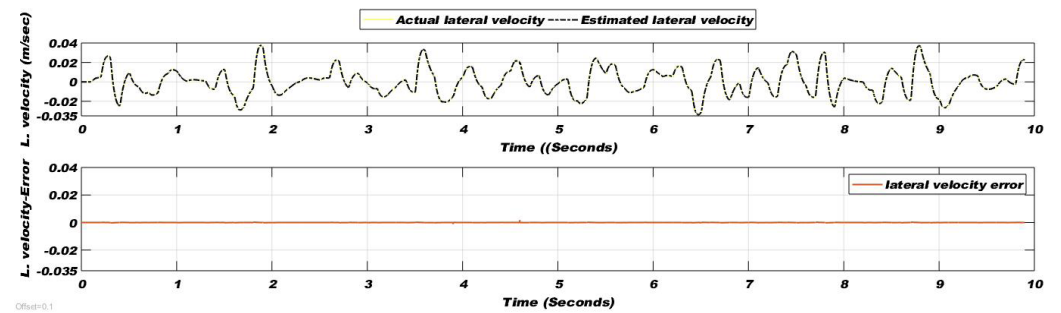
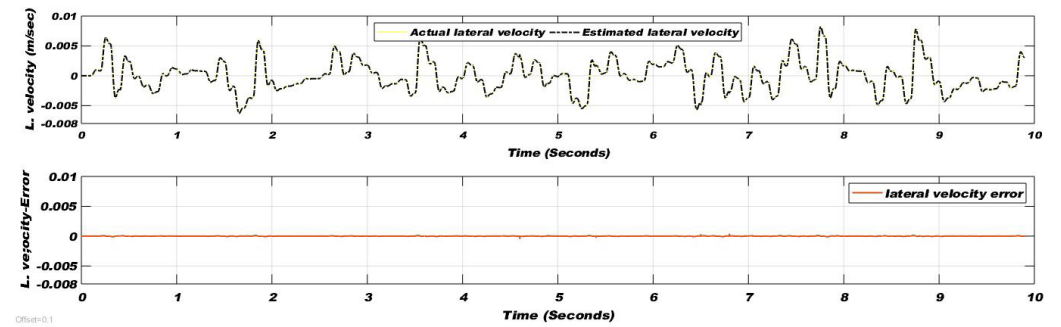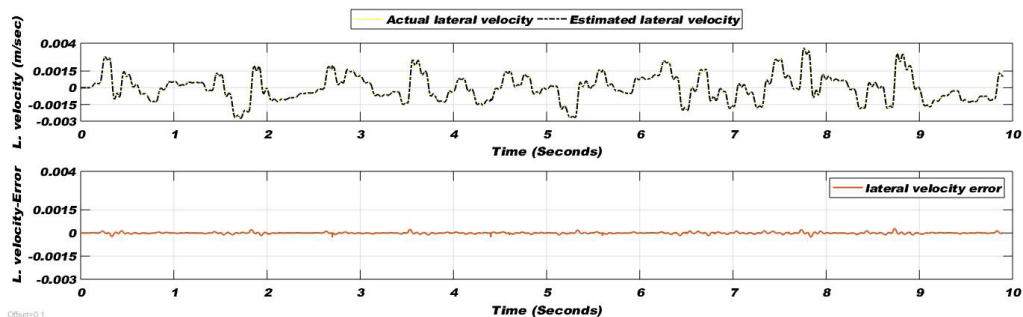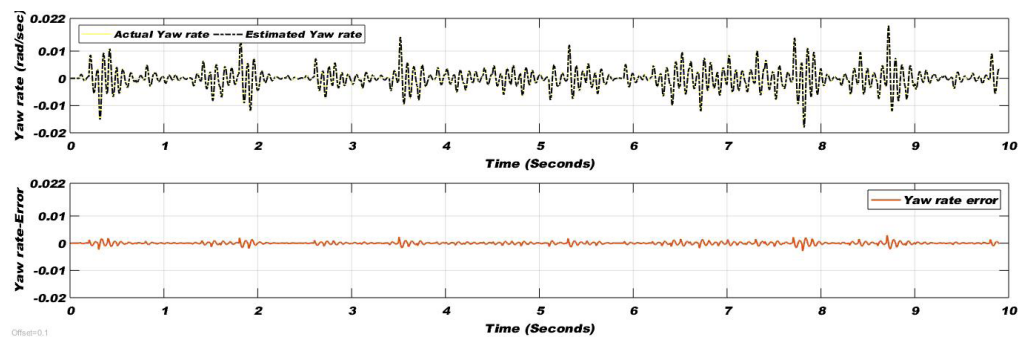**Figure 4.** lateral velocity comparison (top) and Error (bottom) for dry condition of wheel-rail interface.
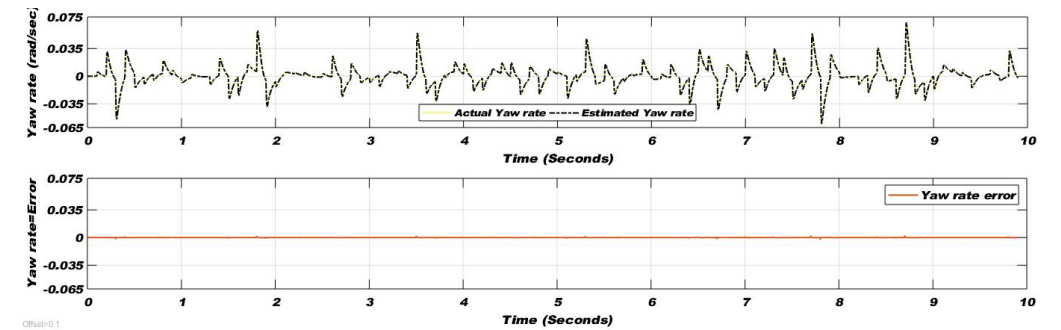
Figure 5. Yaw rate comparison (top) and Error (bottom) for dry condition of wheel-rail interface.
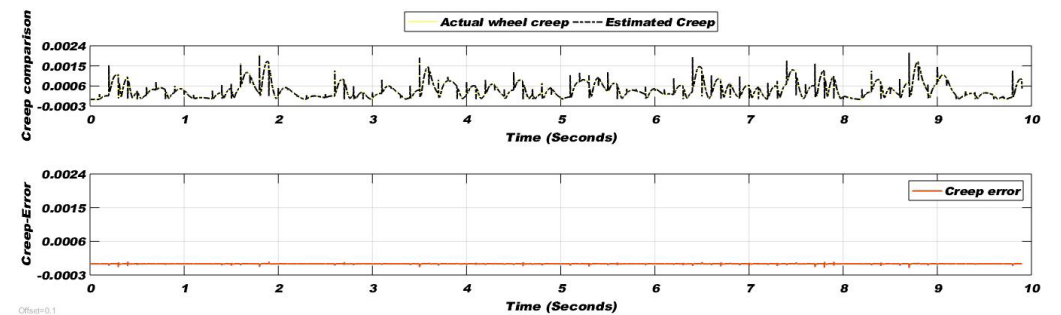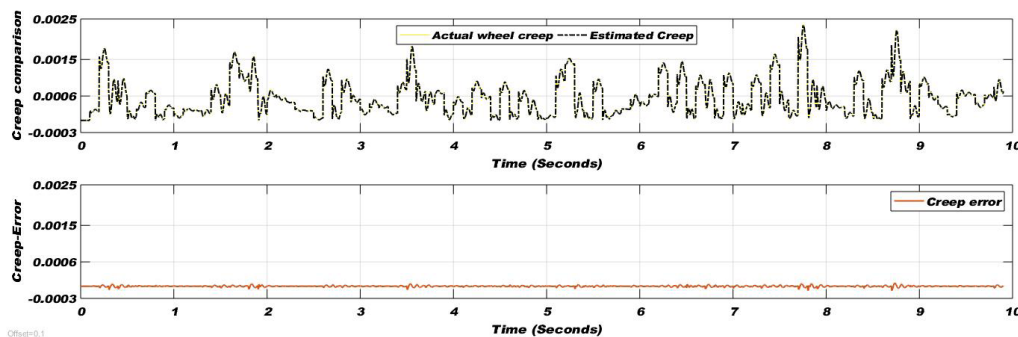

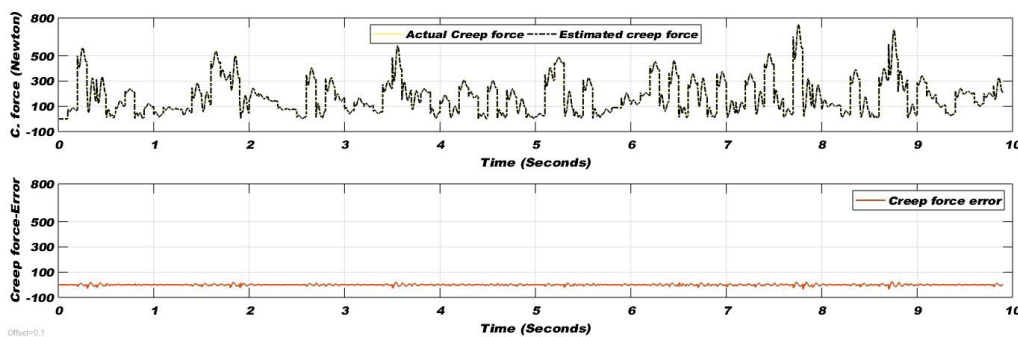**Figure 6.** Creep comparison (top) and Error (bottom) for dry condition of wheel-rail interface.
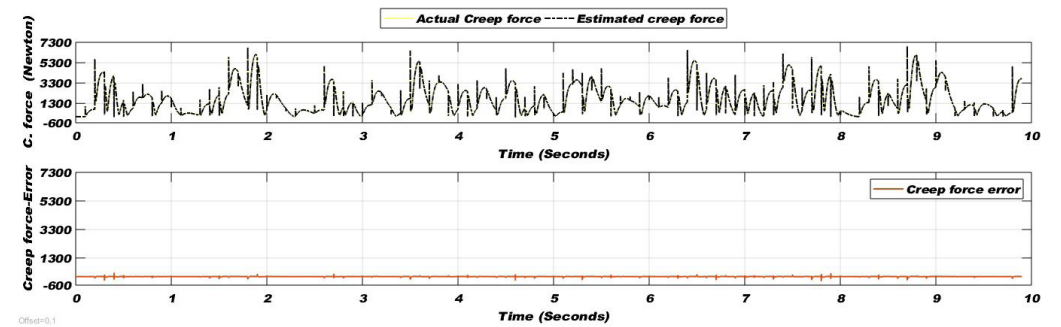
Figure 7. Creep force comparison (top) and Error (bottom) for dry condition of wheel-rail interface.

4.2. WET CONDITION TEST

The lateral velocity and yaw rate of wheelset as well as creep and creep force are computed along with error on wet track condition curve (Wet curve of Figure 2) and shown in Figure 8 to 11.
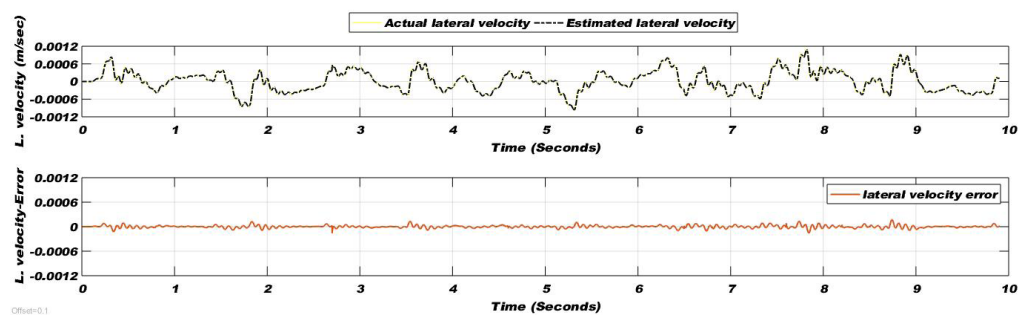

Figure 8. Lateral velocity comparison (top) and Error (bottom) for wet condition of wheel-rail interface.
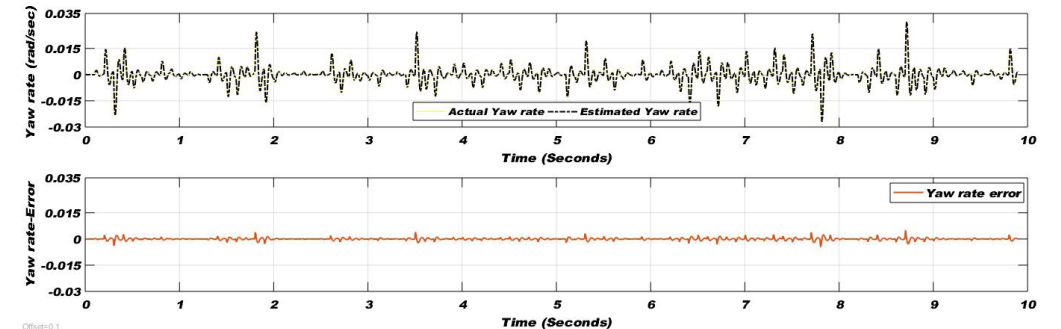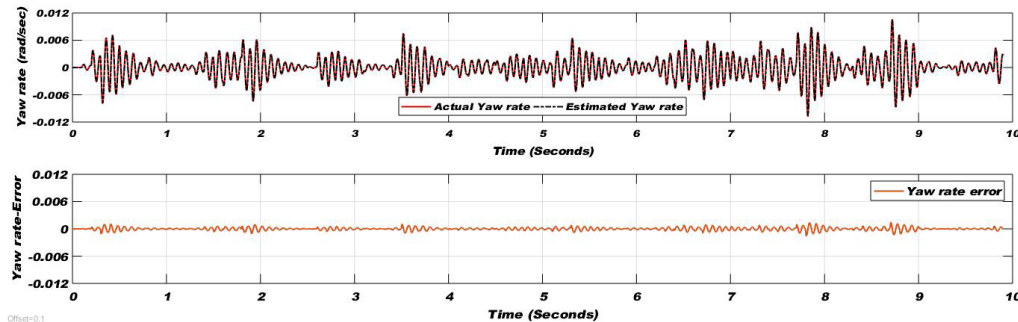

Figure 9. Yaw rate comparison (top) and Error (bottom) for wet condition of wheel-rail interface.
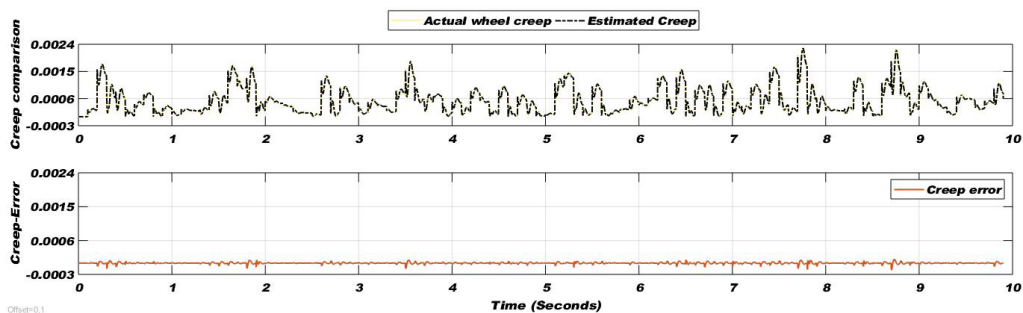
Figure 10. Creep comparison (top) and Error (bottom) for wet condition of wheel-rail interface.
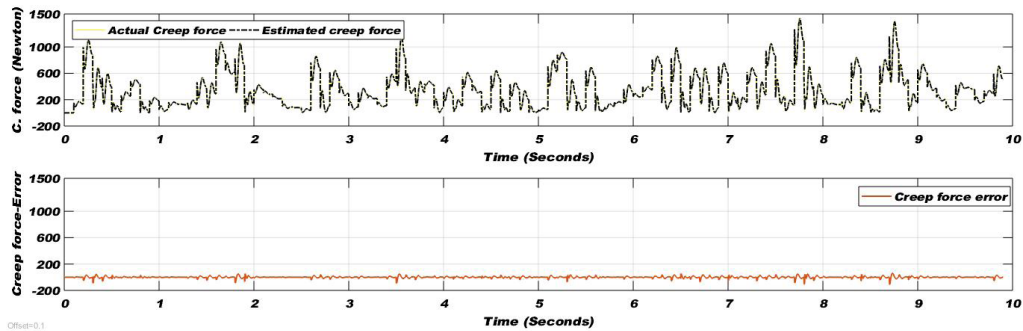
Figure 11. Creep force comparison (top) and Error (bottom) for wet condition of wheel-rail interface.

4.3. POOR CONDITION TEST

The lateral velocity and yaw rate of wheelset as well as creep and creep force are computed along with error on poor track condition curve (Poor curve of Figure 2) and shown in Figure 12 to 15.

Figure 12. Lateral velocity comparison (top) and Error (bottom) for poor condition of wheel-rail interface.

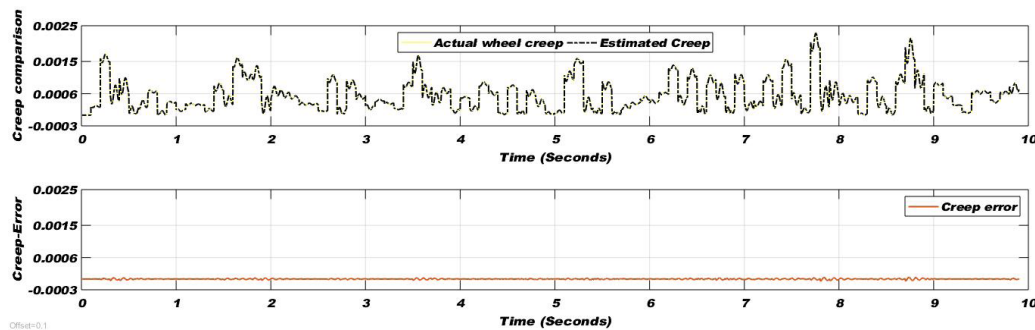**Figure 13.** Yaw rate comparison (top) and Error (bottom) for poor condition of wheel-rail interface.

Figure 14. Creep comparison (top) and Error (bottom) for poor condition of wheel-rail interface.
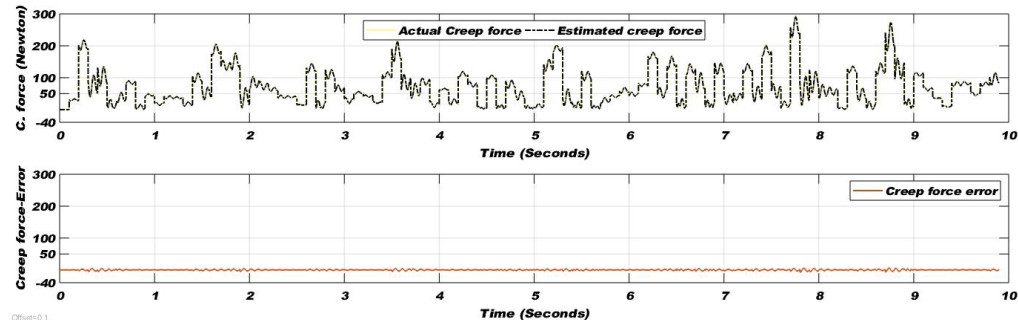

Figure 15. Creep force comparison (top) and Error (bottom) for poor condition of wheel-rail interface.

4.4. WORST CONDITION TEST

The lateral velocity and yaw rate of wheelset as well as creep and creep force are computed along with error on worst track condition curve (Worst curve of Figure 2) and shown in Figure 16 to 19.
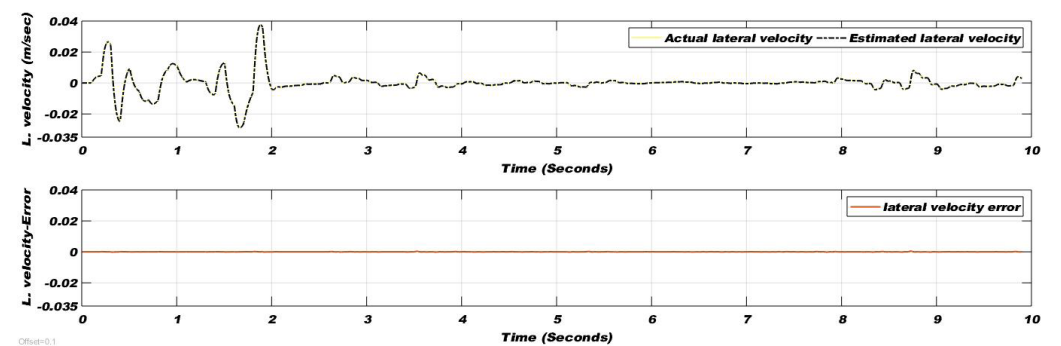
Figure 16. Lateral velocity comparison (top) and Error (bottom) for worst condition of wheel-rail interface.

Figure 17. Yaw rate comparison (top) and Error (bottom) for worst condition of wheel-rail interface.

Figure 18. Creep comparison (top) and Error (bottom) for worst condition of wheel-rail interface.

Figure 19. Creep force comparison (top) and Error (bottom) for worst condition of wheel-rail interface.

4.5. TRANSITION TEST FROM DRY CONDITION TO WORST CONDITION

The lateral velocity and yaw rate of wheelset as well as creep and creep force are computed along with error on all adhesion condition curves (Dry to worst curves of Figure 2) and shown in Figure 20 to 23. During simulation adhesion condition changed at every 2 seconds from dry to worst adhesion conditions in 8 seconds of simulation time and then the condition again changed from worst to wet. The graphs show the changings of adhesion conditions and match estimated results with actual results.

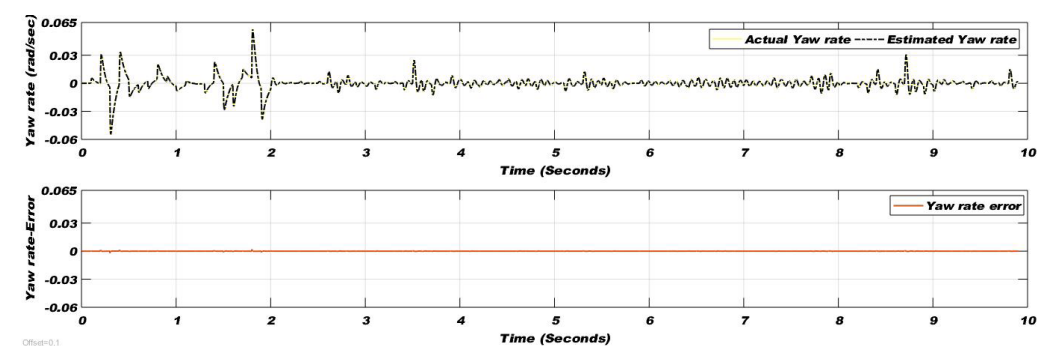**Figure 20.** Lateral velocity comparison (top) and Error (bottom) for all track conditions of wheel-rail interface.

Figure 21. Yaw rate comparison (top) and Error (bottom) for all adhesion condition of wheel-rail interface.
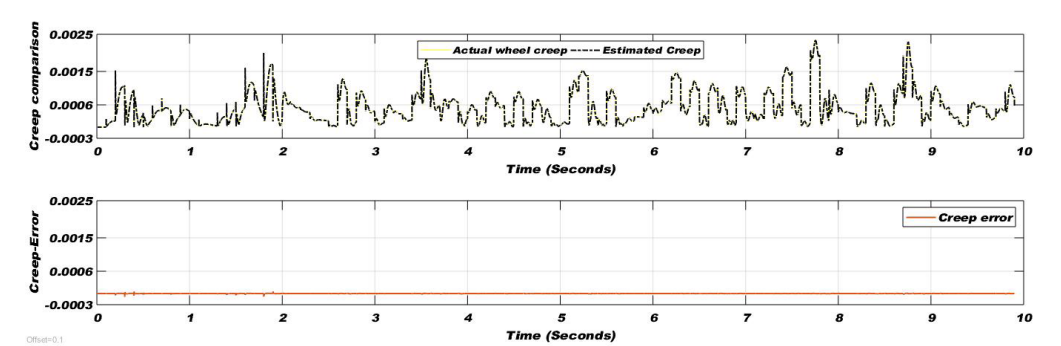

Figure 22. Creep comparison (top) and Error (bottom) for all adhesion condition of wheel-rail interface.
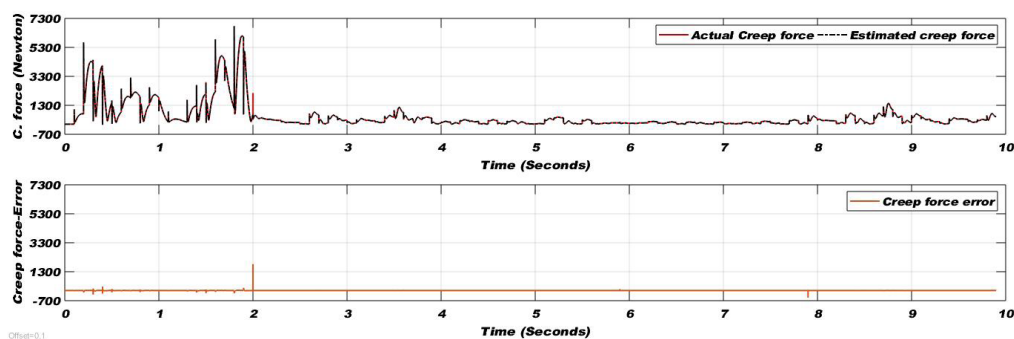
Figure 23. Creep force comparison (top) and Error (bottom) for all adhesion condition of wheel-rail interface.

4.5. ERROR ANALYSIS

It is shown from Figure 4 to 23 that the Extended Kalman filter is a valid estimation technique to estimate wheelset dynamics with authenticity. However, estimated creep force error in Figure 23 became high for few moments during simulation (a spike seen at 2 seconds) due to sudden change of adhesion condition from dry to wet.

Overall, EKF estimates the wheelset dynamics perfectly for dry, wet, poor and worst adhesion conditions and can be used for condition monitoring of rolling stock.

5. CONCLUSION

As wheel-rail contact force is complex and non-linear function of slip and affected with other vehicle parameters, therefore it is difficult to estimate by simple estimating techniques. In this paper, the Extended Kalman filter is used to estimated lateral velocity and yaw rate of railway wheelset as well as creep and creep force of wheel-rail interface and validated through Simulink/MATLAB. EKF estimates not only wheelset dynamics for dry, wet, poor and worst adhesion conditions but perfectly estimates for transition of all track conditions during simulation.

Further, research is going to estimate wheel-rail dynamics in traction and braking modes, also work is going on to implement the simulation work on FPGA platform.

ACKNOWLEDGEMENT

REFERENCES

Anyakwo, A., Pislaru, C., & Ball, A. (2012). A new method for modelling and simulation of the dynamic behaviour of the wheel-rail contact. *International Journal of Automation and Computing*, *9*(3), 237–247. https://doi.org/10.1007/s11633-012-0640-6

Charles, G., Goodall, R., & Dixon, R. (2008). Model-based condition monitoring at the wheel-rail interface. *Vehicle System Dynamics*, *46*(SUPPL.1), 415–430. https://doi.org/10.1080/00423110801979259.

Hubbard, P. D., Ward, C., Dixon, R., & Goodall, R. (2013a). Real time detection of low adhesion in the wheel/rail contact. *Proceedings of the Institution of Mechanical Engineers, Part F: Journal of Rail and Rapid Transit*, *227*(6), 623–634. https://doi.org/10.1177/0954409713503634

Hubbard, P. D., Ward, C., Dixon, R., & Goodall, R. (2013b). Verification of model-based adhesion estimation in the wheel-rail interface. *Chemical Engineering Transactions*, *33*, 757–762. https://doi.org/10.3303/CET1333127

Hussain, I. (2012). *Multiple Model Based Real Time Estimation of Wheel-Rail Contact Conditions* (PhD thesis). University of Salford. http://usir.salford.ac.uk/id/eprint/38094/

Hussain, I., & Mei, T. X. (2010). Multi Kalman filtering approach for estimation of wheel-rail contact conditions. *In UKACC International Conference on CONTROL 2010*. https://doi.org/10.1049/ic.2010.0326

Hussain, I., & Mei, T. X. (2011). Identification of the wheel-rail contact condition for traction and braking control. *Proceedings of the 22nd International Symposium on Dynamics of Vehicles on Roads and Tracks*, *Manchester, United Kingdom,* pp. 14–19. https://www.researchgate.net/publication/261672525_Identification_of_the_Wheel-Rail_Contact_Conditions_for_Traction_and_Braking_control

Hussain, I., Mei, T. X., & Jones, A. H. (2009). Modeling and estimation of non-linear wheel-rail contact mechanics. In *20th International Conference on Systems Engineering (ICSE2009)*, 219–223. https://www.researchgate.net/publication/261633475_Modeling_and_Estimation_of_Non-linear_Wheel-Rail_Contact_Mechanics

Hussain, I., Mei, T. X., & Ritchings, R. T. (2013). Estimation of wheel-rail contact conditions and adhesion using the multiple model approach. *Vehicle System Dynamics*, *51*(1), 32–53. https://doi.org/10.1080/00423114.2012.708759

Mei, T., Yu, J., & Wilson, D. (2008). A mechatronic approach for anti-slip control in railway traction. *IFAC Proceedings Volumes*, *41*(2), 8275-8280. https://doi.org/10.3182/20080706-5-KR-1001.01399

Melnik, R., & Koziak, S. (2017). Rail vehicle suspension condition monitoring - approach and implementation. *Journal of Vibroengineering*, *19*(1), 487–501. https://doi.org/10.21595/jve.2016.17072

Ngigi, R. W., Pislaru, C., Ball, A., & Gu, F. (2012). Modern techniques for condition monitoring of railway vehicle dynamics. *Journal of Physics: Conference Series*, *364*(1). https://iopscience.iop.org/article/10.1088/1742-6596/364/1/012016/meta

Polach, O. (2005). Creep forces in simulations of traction vehicles running on adhesion limit. *Wear, 258*(7-8), 992–1000. https://doi.org/10.1016/j.wear.2004.03.046

Radionov, I. A., & Mushenko, A. S. (2015). The method of estimation of adhesion at "wheel-railway" contact point. In *2015 International Siberian Conference on Control and Communications (SIBCON)*, pp. 1–5. https://doi.org/10.1109/SIBCON.2015.7147156

Simon, I. (2006). *Handbook of Railway Vehicle Dynamics*, *Handbook of Railway Vehicle Dynamics*. CRC Press.

Strano, S., & Terzo, M. (2018). On the real-time estimation of the wheel-rail contact force by means of a new nonlinear estimator design model. *Mechanical Systems and Signal Processing*, 105, pp. 391–403. https://doi.org/10.1016/j.ymssp.2017.12.024

Sun, Y. Q., Cole, C., & Spiryagin, M. (2015). Monitoring vertical wheel-rail contact forces based on freight wagon inverse modelling. *Advances in Mechanical Engineering*, *7*(5), 1–11. https://www.researchgate.net/publication/277910673_Monitoring_vertical_wheel-rail_contact_forces_based_on_freight_wagon_inverse_modelling

Wang, S., Xiao, J., Huang, J., & Sheng, H. (2016). Locomotive wheel slip detection based on multi-rate state identification of motor load torque. *Journal of the Franklin Institute*, *353*(2), 521–540. https://doi.org/10.1016/j.jfranklin.2015.11.012

Ward, C. P., Goodall, R. M., & Dixon, R. (2011). Contact force estimation in the railway vehicle wheel-rail interface. *IFAC Proceedings Volumes*, *44*(1), 4398–4403. https://doi.org/10.3182/20110828-6-IT-1002.02904

Welch, G., & Bishop, G. (2001). *An Introduction to the Kalman Filter*. University of North Carolina at Chapel Hill Department of Computer Science Chapel Hill, NC 27599-3175. https://www.cs.unc.edu/~welch/media/pdf/kalman_intro.pdf

Zhao, Y., & Liang, B. (2013). Re-adhesion control for a railway single wheelset test rig based on the behaviour of the traction motor. *International Journal of Vehicle Mechanics and Mobility*, *51*(8), 1173–1185. https://doi.org/10.1080/00423114.2013.788194

Zhao, Y., Liang, B., & Iwnicki, S. (2012). Estimation of the friction coefficient between wheel and rail surface using traction motor behaviour. *Journal of Physics: Conference Series*, *364*(1). https://iopscience.iop.org/article/10.1088/1742-6596/364/1/012004

Zhao, Y., Liang, B., & Iwnicki, S. (2014). Friction coefficient estimation using an unscented Kalman filter. *International Journal of Vehicle Mechanics and Mobility*, *52*(suppl. 1), 220–234. https://doi.org/10.1080/00423114.2014.891757

/17/

ADVANCES IN AUGMENTED REALITY (AR) FOR MEDICAL SIMULATION AND TRAINING

Vladimir Ivanov

Herzen State Pedagogical University of Russia
Saint-Petersburg, (Russia).
E-mail: voliva@rambler.ru ORCID: https://orcid.org/0000-0001-8194-2718

Alexander Klygach

Herzen State Pedagogical University of Russia
Saint-Petersburg, (Russia).
E-mail: voolf00@yandex.ru ORCID: https://orcid.org/0000-0002-2984-0201

Sam Shterenberg

Pavlov First Saint-Petersburg State Medical University
Saint-Petersburg, (Russia).
E-mail: sam.d.s@mail.ru ORCID: https://orcid.org/0000-0002-6428-8328

Sergey Strelkov

Herzen State Pedagogical University of Russia,
Saint-Petersburg, (Russia).
E-mail: sergin3d2d@gmail.com ORCID: https://orcid.org/0000-0002-4830-5407

Jason Levy

University of Hawaii,
Honolulu, (USA).
E-mail: jlevy@hawaii.edu ORCID: https://orcid.org/0000-0002-9978-5412

ABSTRACT

Digital technologies are transforming the field of medical training, simulation and mode-
ling. Advances in the field of virtual Augmented Reality (AR) and virtual simulation are
described in detail, particularly as they relate to medical education and training. An over-
view of key medical simulation tools is provided in order provide foundational knowledge
about this rapidly growing field. A timely and valuable original Augmented Realty system
is put forward. The key components of this original system for medical training and simu-
lation include the following three dimensions: advances in open surgery, realistic visualiza-
tions and innovative haptic was used. Each component of this Augmented Reality system is
described in detail. First, the open surgery module emphasized appendectomies (the most
common surgical procedures used in our model). Second, three different approaches for
creating realistic and accurate 3D medical models were put forth. Third, haptic feedback
involved the use of an enhanced Novint Falcon system in which a custom grip provides
additional degrees of freedom. Finally, advances in game simulation, modeling and role
playing are discussed for the field of emergency medicine.

KEYWORDS

Surgical Simulator, Virtual Reality, Real-time Rendering, 3D Visualization, Haptic Feed-
back, Open Surgery, Laparoscopy, Emergency Medicine, Simulations.

1. INTRODUCTION

Medical simulations, modeling and visualizations have undergone a rapid shift the beginning of 20th century due to a number of reasons (Kron *et al.*, 2010). First, modern approaches for less invasive surgery have redefined surgical procedures such as endoscopy and robotics surgery. Second, the dramatic rise of computing power has provided an opportunity to implement complex simulations in real-time. Finally, more accurate algorithms for rigid and soft body simulations, realistic 3d visualizations, haptic controllers, and virtual reality have allowed medical simulation to be used for digital gaming rather than simply physical modeling.

Specific approaches and technologies for medical simulations for medical simulations have grown by leaps and bounds. For example, innovative research has occurred dealing with the generation of textures of irregular objects from models and photo sequences (Chen *et al.*, 2003). The role of medical simulations has rapidly expanded throughout the healthcare field (Kunkler, 2006). This paper involves a case study of medical simulations for lap.

2. MODERN MEDICAL SIMULATION MARKET

2.1. MARKET OVERVIEW

According to Prescient & Strategic Intelligence data, the global surgical simulation market was valued at $254.7 million in 2017 with a growing trend. The value of this field is forecasted to increase to twice its value in 2023 (Figure 1). Another notable trend is that augmented reality (AR) and virtual reality (VR) are being used to enhance the quality and efficiency of medical training. Thus, it is expected that this market will continue to grow, and digital technologies will continue to have a major impact on the medical simulation field.
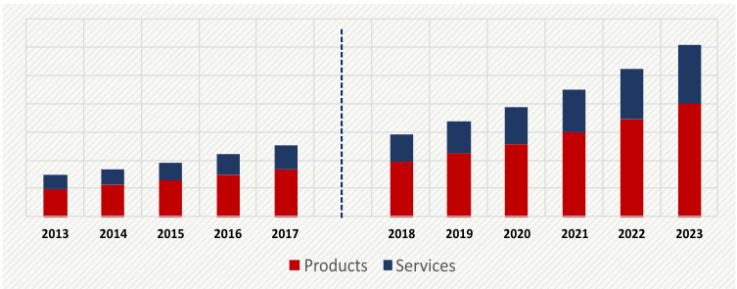

Figure 1. Worldwide surgical simulation market by offering (2013-2023).

2.2. MEDICAL SIMULATORS

VirtaMed is a company primarily focused on simulator development for orthopedics, genecology and urology. The company develops surgical simulators which are designed on a single flexible plat-form with the ability to expand and add additional procedures. All simulators are combined with an anatomical model to provide the optimal tactile feedback and real-world manipulations. In addition, for better efficiency each virtual procedure allows for guided training: specific colored hints and ghost tools show trainees how to perform different tasks (Figure 2).
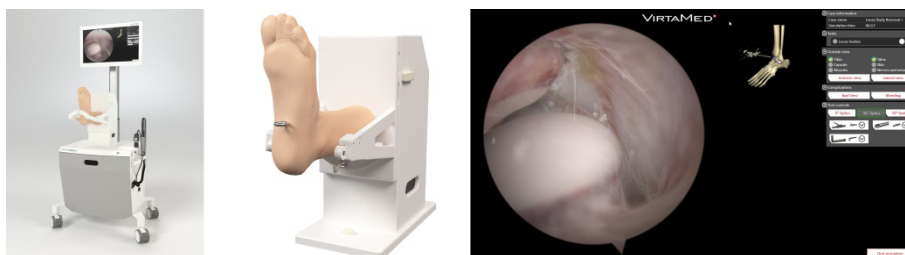

Figure 2. ArthroS Ankle by VirtaMed AG.

NeuroVR is a platform for neurological training that enables neurosurgeons to practice skills with the help of virtual reality (Figure 3). Such a system does not depend on real life models but uses haptic controllers for VR manipulations. The range of allowed exercises are derived from actual patient images, which provides more realistic and accurate images of surgical procedures. The system also captures objective metrics and measures the proficiency of procedures in order to track educational progress.

Figure 3. NeuroVR system with stereoscopic microscopic view.

SurgicalScience is a company which develops various simulation products, mostly for laparoscopy and endoscopy. The LapSim product is designed to improve psychomotor

skills using virtual reality with haptic feedback (Figure 4). It features different modules for laparoscopic exercises that arrange from navigation to suturing. This system also has a portable version known as "LapSim essence".
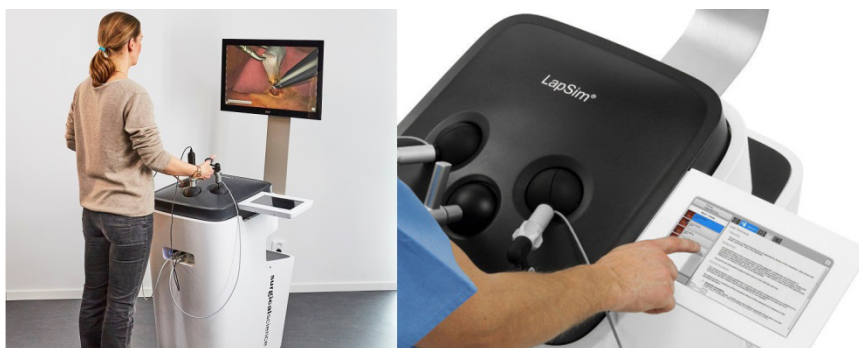

Figure 4. LapSim with in-house developed haptic system.

3. AN ORIGINAL APPROACH TO THE DEVELOPMENT OF MEDICAL SIMULATION

3.1. KEY ASPECTS

Most surgical simulators that are currently available on the market have weaknesses ranging from simplified 3D visualizations to a limited ability to perform open surgery. Most existing modeling tools are also limited because they have been designed primarily for specific surgical approaches, like endoscopy. For this reasons we develop an open surgery simulator for carried out an appendectomy with realistic visualizations using haptic feedback (Figure 5).
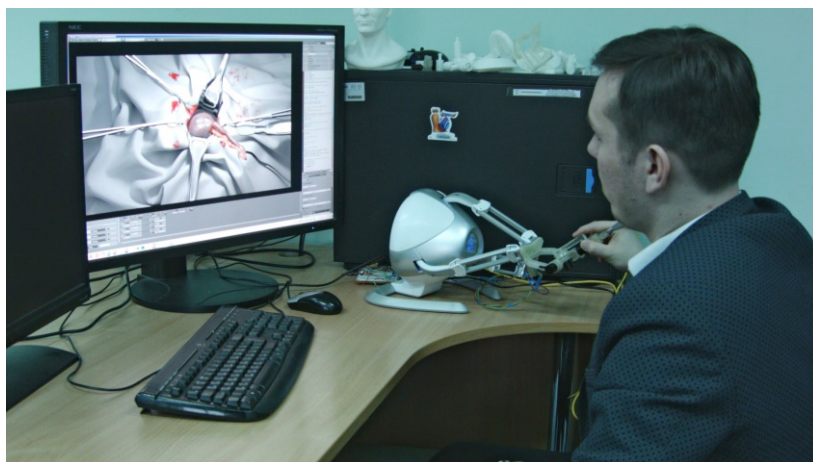

Figure 5. Surgery simulator based on open appendectomy with haptic feedback.

3.2. REALISTIC VISUALIZATION

Despite advanced real-time rendering solutions that are currently available, it is still difficult to produce realistic images in a surgical simulator due to a software limitations. For example it is difficult to incorporate graphics solutions onto a complex modeling engine (that captures the physics of the system). To overcome this challenge the developed system is based on a modern game engine which allows for the use of physically based shader models and enhances it with a customized physics engine to work with soft tissue (Figure 6).
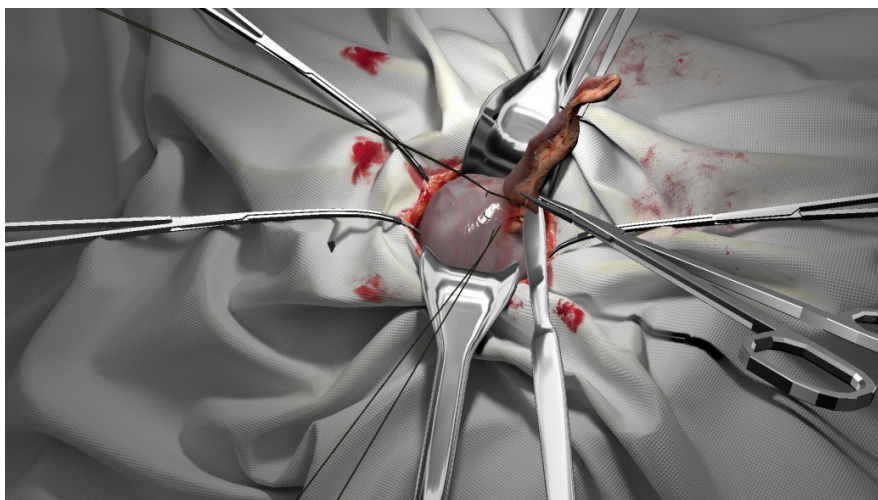

Figure 6. The stage, where the mesoappendix is dissected.

3.3. CREATING MODELS BASED ON PATIENT'S DATA AND ANATOMICAL ATLASES

More accurate modeling results may be obtained by a number of approaches. One method involves taking photos from an actual surgical procedure and extracting textures from these images (Figure 7). It is also possible to build models based on a sequence of photos using photogrammetry solutions.
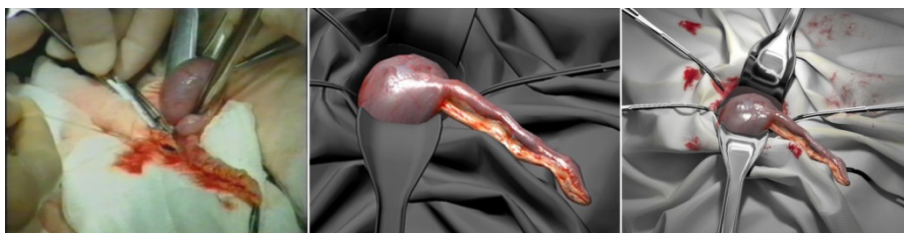

Figure 7. Photo from surgery procedure (left), appendix model with textures (center), overall view in surgical simulator (right).

Another method involves building models based on MRI or CT data. For instance, a heart model with specific pathologies can be recreated with the help of MRI and contouring data. This is achieved through multiple stages (Figure 8). At first, we built model of ventricles from countering data and then projected a master heart model onto them and finally added textures based on real-life heart images.
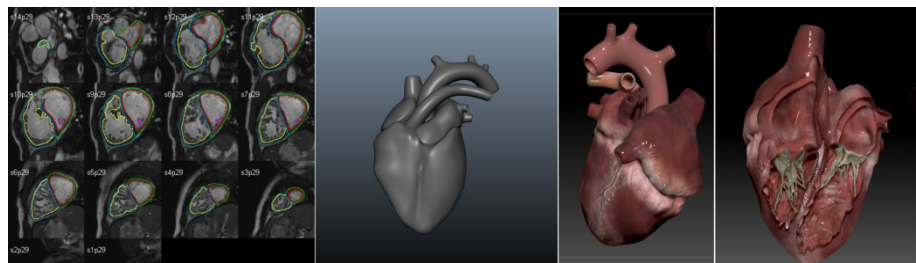

Figure 8. MRI with contouring data (left), reconstructed heart 3d model (center), heart 3d model with textures and internal structures (right).

In complex cases, where photography or tomography is not enough to build a full model, anatomical atlases are used: knowledge and data from multiple atlases like Gray's anatomy and 3d atlas of human body were combined to reveal the position of the larynx. This helped accurately showcase the location of the larynx in comparison other anatomical structures like skull, and muscles (Figure 9).
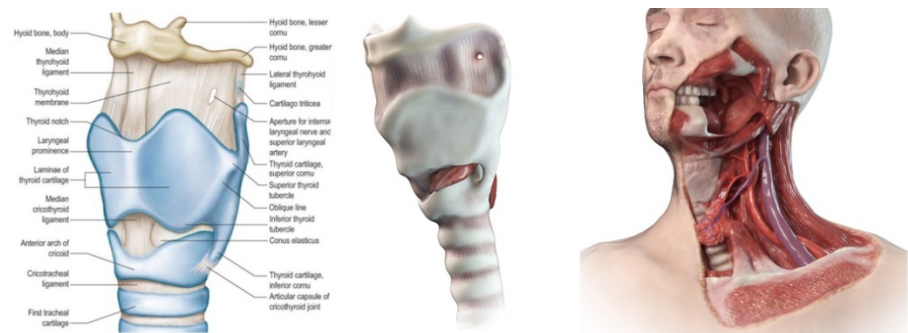

Figure 9. Larynx image from Gray's anatomy atlas (left), 3d model of larynx (center), neck section with larynx (right).

3.4. HAPTIC FEEDBACK

In order to achieve fully realistic visualization our system is supplemented with haptic feedback. This helps to sense virtual 3D objects and allows the development of proper psychomotor skills for surgeons. The Novint Falcon Haptic device was used as the foundation to implement this haptic feedback technology. While this tool is designed primary for games,

it also provides accurate haptic feed-back with three degrees of freedom (DOF). This device is also the cheapest haptic system on the market, thereby reducing the overall cost of simulator significantly.

In order to use this device as a tool for surgical simulations the system was redesigned in several ways. For example a custom designed grip was developed with extra three DOF to allow for the creation of a tilting surgical tool (Figure 10). This tool is based on absolute hall encoders and transmits data as separate stream through a digital-to-analog converter. In addition, it has a slot for swapping different surgical instruments.

Figure 10. Custom designed grip to provide extra 3-degree of freedom.

3.5. LAPROSCOPIC SURGICAL SIMULATORS

There are a number of laparoscopic surgical simulators available on the market. Laparoscopic training simulators have been used effectively to enhance laparoscopic surgery training scenarios. For example, Sauerland, Jaschinski and Neugebauer (2010) examined the use of laparoscopic versus open surgery for suspected appendicitis. Our proposed Laparoscopic Surgery Simulator can demonstrate virtually all major abdominal surgical procedures and assist surgeons in learning a range of surgical methodologies. Our open surgery simulator constitutes a timely, complex and important niche simulator tool. The aforementioned solutions for creating 3d models and haptic feedback can help to achieve more realistic laparoscopic surgery visualization and modeling in a cost-efficient way.

4. GAMES, ROLE PLAYING AND SIMULATIONS FOR EMERGENCY PHYSICIANS AND THE COVID-19 PANDEMIC

There is a need for better-trained emergency physicians in the COVID-19 era. Emergency physicians and other educational, research, and practitioners in the health field must in-

creasingly have simulation experience to make crucial decisions within a highly politicized, volatile and pressurized context. The education of future generations of emergency physicians and emergency management professionals must draw across the boundaries of physical/social science, technology, engineering, and mathematics. The COVID-19 pandemic has shown that traditional approaches to responding to health disasters, reducing risk and mitigating losses are inadequate. Starting in the 1950s, the emphasis was on the disciplines of civil defense and humanitarian relief.

Role play, scenario methods and game simulations have been successfully used across a wide variety of learning environments ranging from military training, high school driver's education to the diplomatic art of negotiation. Role play and game simulation provide a learning-by-doing experience and thus have been shown to increase emergency management effectiveness in various application ranging from hospital disaster planning and public health to the mental and social aspects of health emergencies. Modeling and simulation tools have been shown to build higher cognitive skills for emergency management training and education and to help with individual and group learning in crisis simulations. There are a number of emergency medicine fields where role play and game simulations are used successfully in improving graduate and undergraduate learning outcomes. Despite the successes of role play and game simulations across a wide range of educational environments, there is a need for more such learning tools within in emergency healthcare education.

Our ongoing research seeks provide a bridge between the emergency response focus generally filled by community and technical colleges and theoretical focus of graduate level courses. Future work seeks to develop prototype simulations for undergraduate emergency medical curricula. A further outcome of the project will be a framework and workplan to leverage the lessons learned in this paper for complete development, implementation and faculty support materials of emergency medicine simulations.

REFERENCES

Chen, R., Lu, D., & Pan, Y. (2003). Generating Textures of Irregular Objects from Models and Photo Sequences. *Journal of Image and Graphics*, 8.

Kron, F. W., Gjerde, C. L., Sen, A., & Fetters, M. D. (2010). Medical student attitudes toward video games and related new media technologies in medical education. *BMC Medical Education*, *10*(50), 1–10. https://doi.org/10.1186/1472-6920-10-50

Kunkler, K. (2006) The role of medical simulation. *The International Journal of Medical Robotics and Computer Assisted Surgery, 2*(3), 203–210. https://onlinelibrary.wiley.com/doi/10.1002/rcs.101

McDermott, W. (2018). *The PBR guide. Part 1*. Allegorithmic. https://academy.substance3d.com/courses/the-pbr-guide-part-1

Sauerland, S., Jaschinski, T., & Neugebauer, E. A. (2010). Laparoscopic versus open surgery for sus-pected appendicitis. *Cochrane Database of Systematic Reviews*, (10). https://doi.org/10.1002/14651858.CD001546.pub3

tecnología

Glosas de innovacion aplicadas a la pyme